

THE MECHANICAL DESIGN  
OF AN ELECTRIC TOWN CAR

A thesis  
submitted in fulfilment  
of the requirements for the Degree of  
Master of Engineering (Mechanical)  
in the  
University of Canterbury  
Christchurch  
New Zealand.

by

Edgar Vandendungen, B.E. (Hons)

University of Canterbury

September, 1982

#### ACKNOWLEDGEMENTS

Sincere thanks to Mr R.T.C.Harman who has supervised this project, offering guidance and encouragement throughout.

The support of Professor D.C.Stevenson and the staff of the Department of Mechanical Engineering is gratefully acknowledged. Particular thanks to Dr J.Astley and Dr K.Whybrew, as well as Mr E.D.Retallick, Mr B.Taylor and Mr R.Tinker.

Thanks to Todd Motor Industries Ltd. for providing a Todd Motors Scholarship.

Special thanks to those friends and relatives whose encouragement has helped make this thesis possible.

## SUMMARY

This report examines the mechanical design of the University of Canterbury Mark II Electric Town Car. An interconnected suspension system is proposed and analysed in some detail. The selection of suspension geometry to incorporate anti-dive and to restrict body roll is discussed and the rear suspension trailing arms are analysed. The general layout features a backbone chassis with batteries between the front wheels and beneath the front passengers, with the electric motors and rear suspension beneath the rearward facing rear passengers. Two alternative methods of construction are proposed and discussed, including the adaption of the A40 Farina bodywork.

## CONTENTS

	<u>PAGE</u>
1 INTRODUCTION	1
2. INTERCONNECTED SUSPENSION	3
2.1 HISTORY	3
2.2 INTERCONNECTED SUSPENSION THEORY	5
2.2.1 General Principles	5
2.2.2 Vibrations	7
2.2.3 Pitch Angle Deflections	10
2.3 APPLICATION OF AN INTERCONNECTED SUSPENSION SYSTEM	13
2.3.1 Previous Work	13
2.3.2 Suspension as Built	17
2.3.3 Comparison of Systems	22
2.4 SUSPENSION ANALYSIS ON A DIGITAL COMPUTER	24
2.4.1 The Interconnected Suspension Program INTERSUSP.	24
2.4.2 Discussion of Results	30
3. SUSPENSION GEOMETRY	34
3.1 PITCH CHARACTERISTICS	34
3.2 ROLL CHARACTERISTICS	40
4. REAR SUSPENSION TRAILING ARM	47
4.1 DRIVE SYSTEM	47
4.2 SUSPENSION ARM	47
5. CHASSIS LAYOUT AND DESIGN	52
5.1 LAYOUT	52
5.2 METHODS OF CONSTRUCTION	54
5.3 ADAPTION OF A40 FARINA BODYWORK	58
5.4 GRP-FOAM SANDWICH ANALYSIS AND CONSTRUCTION	58
6. CONCLUSION	61

	<u>PAGE</u>
REFERENCES	62
APPENDIX 2.4.1    Interconnected Suspension Program, Data Input and Answer Code Handbook	67
APPENDIX 2.4.2    Interconnected Suspension Analysis Program, INTERSUSP.	80
APPENDIX 3.2       Wishbone Analysis Program, WISHANAL.	132
APPENDIX 4.1       Correspondence between the University of Canterbury and Uniroyal Ltd.	158
APPENDIX 4.2       Finite Element Analysis Using PAFEC 75 on a B6700 Computer Applicable to the Rear Suspension Arm of an Electric Town Car.	172
APPENDIX 6.1       Engineering Workshop Drawings for the Manufacture of an Electric Town Car.	195

## CHAPTER 1

### INTRODUCTION

The requirement for an Electric Town Car has arisen as a result of the development, by Mr. D. J. Byers of the Electrical Engineering Department, of an electronic control system, using static inverters, and powering AC induction motors (Byers and Harman, 1975 and Byers, 1977).

At present an interim vehicle exists, which has been used as an electric test-bed vehicle and has proven the electric drive system to be satisfactory (Harman and Byers, 1980).

A practical saleable electric town car, to replace the interim vehicle and to confirm the performance of the electric drive system was required. Such a vehicle must have a practical minimum weight, a body design of low aerodynamic resistance, a comfortable ride and an efficient drive system. The concept therefore is a full four seater saloon car, aimed at the second car market. It should be comfortable and have no distracting features that would detract from the electric vehicle capacity.

The original object was that the vehicle be built from scratch, rather than be based on an existing internal combustion engine car. This allows for the proper location of batteries for easy access and/or quick exchange and allows the body to be designed to minimise rolling and windage losses.

It was envisaged that this vehicle might be a production prototype, so that methods of construction and other design considerations should keep this in mind.

The requirements of low mechanical rolling resistance and low aerodynamic drag for any vehicle and particularly electric vehicles has been documented (Byers and Harman, 1975, and Harman, 1977).

The use of toothed belt or chain drive, direct from the motors to the rear wheels eliminates mechanical losses that would otherwise exist in the differential, drive-shaft bearings etc. The differential effect is achieved electrically.

Special locally made 145-SR-13 radial ply tyres are utilized, incorporating features that decrease the energy losses and hence the rolling resistance. The tyres have two circumferential steel belts, one radial ply and lighter than normal sidewall construction.

Wind tunnel tests were conducted (MacDonald, 1978) aimed at reducing the drag coefficient of the electric town car. This was done by modifying a one-fifth scale model of a proposed body shape designed by the Wellington Polytechnic in collaboration with the University of Canterbury. A number of these proposed modifications were incorporated in the town car, when alterations to the A40 Farina body structure were carried out.

As a town car, the requirement of passenger comfort is important, as is the need for a compact car able to accommodate four adults. This report examines an interconnected suspension used to achieve big-car ride comfort in a small/medium sized car, it examines the suspension geometry used to control pitch and roll, it covers the analysis of the rear suspension arms incorporating the drive motors and discusses the chassis layout based on an earlier report and methods of chassis construction. No attempt has been made to discuss the detail component design, although reductions of some 20 A1-size workshop drawings is included in Appendix 6.1.

## CHAPTER 2

### INTERCONNECTED SUSPENSION

#### 2.1 HISTORY

Interconnected suspension - sometimes called Equalizing Suspension or Coupled Suspension - it is generally agreed, provides an improved ride compared to conventional suspension.

This agreement comes from both practical considerations of suspension design (Giles, 1960; Baker, 1973; Givens, 1975); and from mathematical analysis (Pevsner, 1957; Ellis, 1973; Bulman, 1976; Bastow, 1980).

The Citroen 2CV in 1949 was the first commercial application of interconnected suspension, followed by Packard in 1955. The Hydrolastic and Hydrogas cars from British Leyland are more recent examples.

A soft ride is traditionally synonymous with poor handling. Improve the handling and a harsh ride results. Interconnected suspension provides a means to reconcile this conflict, by reducing the natural frequency of pitching.

Reduction of pitching is the main advantage of interconnected suspension. Pitching is particularly unpleasant to passengers. Lowering this frequency reduces the angular acceleration and improves the ride qualities. However, the closer the exciting frequency is to the natural frequency of the vehicle suspension the greater is the amplitude of oscillation. The use of interconnecting suspensions enables the natural frequency to be reduced to a value at which resonance is not normally encountered. In these circumstances the vibration due to road irregularities is purely vertical.

In an earlier report, Vandendungen (1976) a comparison was made between three cars to illustrate the effect of interconnected suspension. The cars approximate the Electric Town Car, and are identical to each other except for the suspension springing.

Car A has interconnected suspension, with the interconnection stiffness one-half that of the front or rear suspension. Car B has conventional suspension (interconnection stiffness zero) with the front and rear stiffness the same as car A. Car C has conventional suspension with the front and rear stiffness altered to produce the same bounce frequency as car A.



The results are as follows:

	<u>Calculated Resonant Frequencies</u>	
	<u>Pitch</u>	<u>Bounce</u>
Car A (Interconnected)	45 cpm	77 cpm
Car B (Conventional)	59 cpm	65 cpm
Car C (Conventional)	72 cpm	77 cpm

For the same bounce frequency, the pitch frequency for the interconnected car, might be expected to decrease by 27 cpm relative to the conventional car, depending on the interconnection stiffness used.

Similar results were achieved for the Austin Allegro with the Hydrogas Interconnected Suspension System, Baker (1973).

	<u>Measured Resonant Frequencies</u>	
	<u>Pitch</u>	<u>Bounce</u>
Hydrogas Interconnected Suspension	78 cpm	67 cpm
Typical continental small car with conventional suspension and good handling	104 cpm	85 cpm
	<u>26 cpm difference.</u>	

Packard cars in 1956 were using a bounce frequency of 54 cpm and a pitch frequency of 40 cpm, (Pevsner, 1957). With such low frequencies, the Packard required self-levelling, anti-dive, anti-squat and anti-roll bars. The Allegro with its high frequencies does not require these. As a comparison, the Rover 3500 and BMW 728, (Hartley, 1978) have the following nominal frequencies:

	<u>Pitch</u>	<u>Bounce</u>
Rover 3500	64 cpm	69 cpm
BMW 728	65 cpm	71 cpm

The BMW 728, for example, has anti-roll bars front and rear and anti-dive geometry incorporated at the front.

## 2.2 INTERCONNECTED SUSPENSION THEORY

### 2.2.1 General Principles

Figure 2.1 illustrates a simple interconnected suspension system. Between the body and the front and rear wheel assemblies on each side of the vehicle are springs  $C_3$  and  $C_4$  respectively. An interconnecting beam couples the front wheel assembly to the rear wheel assembly. Between each end of the beam and the respective wheel assemblies are additional springs  $C_1$  and  $C_2$  respectively. A pivot, distance  $d$  from the front wheel assembly and distance  $e$  from the rear secures the beam to the body on each side.

When the front wheel hits a bump, it rises and compresses  $C_1$  and  $C_3$ . The reaction of  $C_1$  is transmitted through the interconnecting beam to  $C_2$  and hence to the rear wheel. Thus when either front wheel hits a bump, there is an increased reaction at both the front and rear wheels, causing that side of the vehicle to rise. If both front wheels hit a bump at the same time, the whole vehicle will rise. There is considerably less pitching compared to conventional suspension, and this is found to increase passenger ride comfort. Springs  $C_3$  and  $C_4$  are required to maintain pitch stability.

Where  $f_1$  and  $f_2$  are the front and rear wheel displacements relative to the body, and assuming linear springrates, then the front and rear wheel reactions  $P_1$  and  $P_2$  respectively can be expressed as follows:

$$\left. \begin{aligned} P_1 &= C_{11}f_1 + C_{12}f_2 \\ P_2 &= C_{21}f_1 + C_{22}f_2 \end{aligned} \right\} \quad (2.2.1)$$

where  $C_{11}$ ,  $C_{12}$ ,  $C_{21}$  and  $C_{22}$  are relative stiffness values and are expressed in terms of  $C_1$ ,  $C_2$ ,  $C_3$ ,  $C_4$ ,  $d$  and  $e$ .

The stiffness  $C_{11}$  is the springrate at the front wheel due to the displacement of the front wheel and  $C_{21}$  is the springrate or stiffness at the rearwheel due to the displacement of the front wheels and so on.  $C_{11}$  and  $C_{22}$  are therefore basic stiffnesses, while  $C_{12}$  and  $C_{21}$  are inter-connecting stiffnesses.

Where  $G_1$  and  $G_2$  are static front and rear wheel loads and  $f_{01}$  and  $f_{02}$  are static front and rear wheel displacements, equation (2.2.1) can be written as:

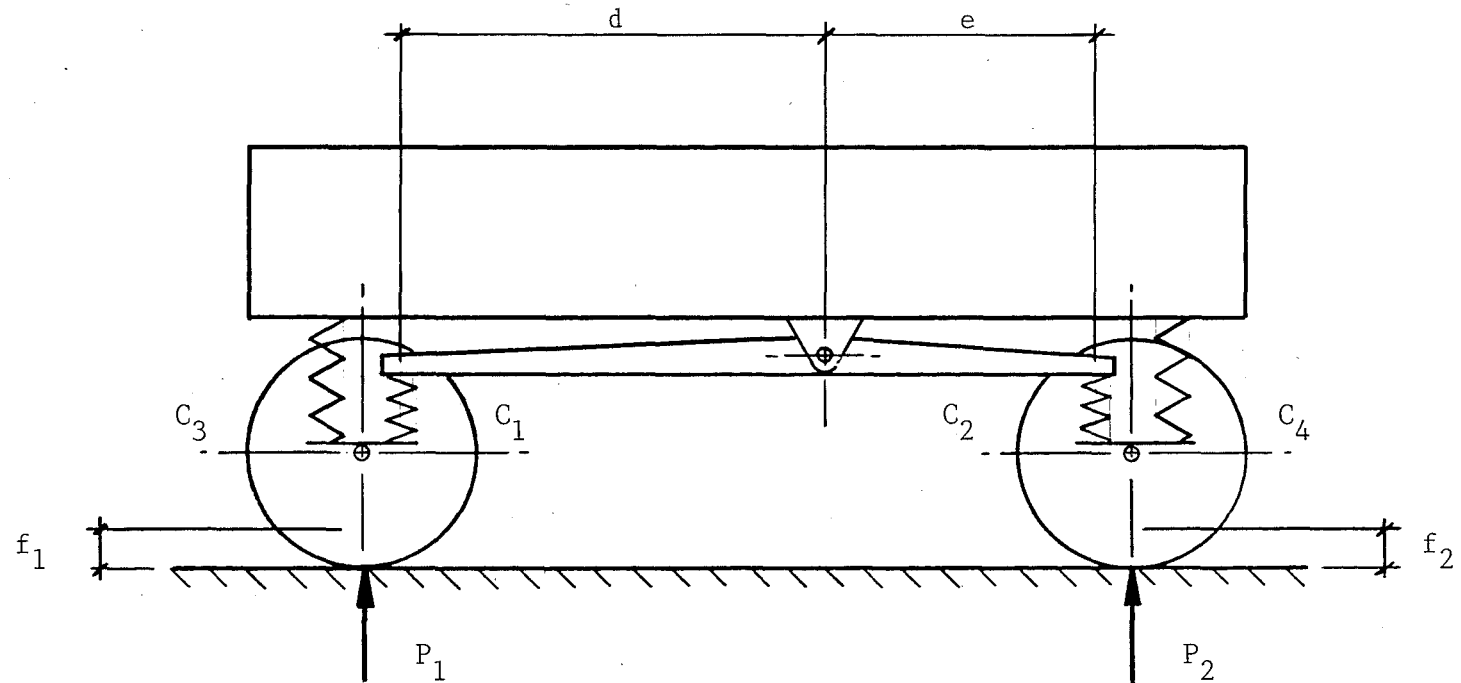


Figure 2.1. Simple Interconnected Suspension System.

$$G_1 = C_{11}f_{01} + C_{12}f_{02}$$

$$G_2 = C_{21}f_{01} + C_{22}f_{02}$$

Solving for  $f_{01}$  and  $f_{02}$ :

$$\left. \begin{aligned} f_{01} &= \frac{C_{22} G_1 - C_{12} G_2}{C_{11} C_{22} - C_{12} C_{21}} \\ f_{02} &= \frac{C_{11} G_2 - C_{21} G_1}{C_{11} C_{22} - C_{12} C_{21}} \end{aligned} \right\} \quad (2.2.2)$$

### 2.2.2 Vibrations

Ignoring unsprung masses, the tyre stiffness, friction and viscous damping and with reference to figure 2.2.2 the equations of motion are;

$$\left. \begin{aligned} M\ddot{Z} - P_{g1} - P_{g2} &= 0 \\ I_O \ddot{\psi} - P_{g1}a + P_{g2}b &= 0 \end{aligned} \right\} \quad (2.2.3)$$

where  $M$  is the mass of the body,  $I_O = MK^2$  the moment of inertia of the body relative to the lateral or transverse axis through the centre of gravity;  $K$  the radius of gyration;  $a$  and  $b$  the distances from the centre of gravity to the front and rear axles respectively, and  $P_{g1}$  and  $P_{g2}$  the dynamic load.

According to equation (2.2.1)

$$P_{g1} = C_{11}f_{g1} + C_{12}f_{g2}$$

$$P_{g2} = C_{21}f_{g1} + C_{22}f_{g2}$$

where  $f_{g1}$  and  $f_{g2}$  are the deflections of the front and rear springs under the dynamic load. Since

$$f_{g1} = q_1 - Z - a\psi$$

$$f_{g2} = q_2 - Z + b\psi$$

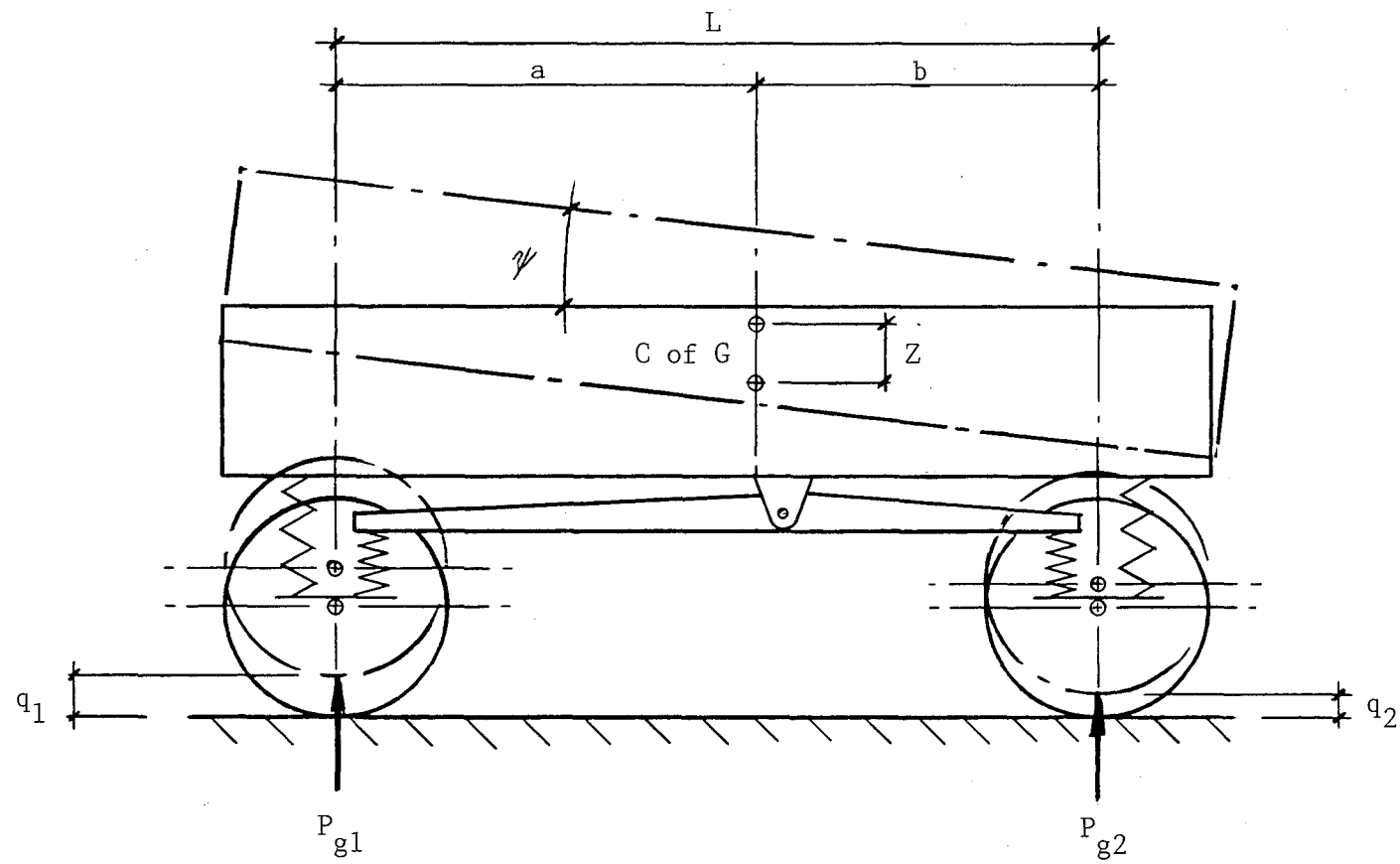


Figure 2.2.2. Bump Conditions.

Equation (2.2.3) becomes:

$$\begin{aligned}
 M\ddot{Z} + (C_{11} + C_{22} + C_{12} + C_{21})\dot{Z} + [a(C_{11} + C_{21}) - b(C_{22} + C_{12})]\dot{\psi} \\
 = q_1(C_{11} + C_{21}) + q_2(C_{22} + C_{12}) \\
 I_o\ddot{\psi} + [a^2C_{11} + b^2C_{22} - ab(C_{12} + C_{21})]\dot{\psi} + [a(C_{11} + C_{12}) - b(C_{22} + C_{21})]Z \\
 = q_1(aC_{11} - bC_{21}) - q_2(bC_{22} - aC_{12})
 \end{aligned} \tag{2.2.4}$$

The left-hand sides of equations (2.2.4) are the free vibrations of the system, while the right-hand sides are time dependent as  $q_1, q_2$  are functions of time and represent the road irregularities.

The equations for free vibration are:

$$\left. \begin{aligned} \ddot{Z} + \omega_z^2 Z + \eta_{C1}\dot{\psi} &= 0 \\ \ddot{\psi} + \omega_\alpha^2 \psi + \eta_{C2}\dot{Z} &= 0 \end{aligned} \right\} \tag{2.2.5}$$

$$\text{where } \omega_z^2 = (C_{11} + C_{22} + C_{12} + C_{21})/M \tag{2.2.6}$$

$$\omega_\alpha^2 = [a^2C_{11} + b^2C_{22} - ab(C_{12} + C_{21})]/MK^2 \tag{2.2.7}$$

$$\eta_{C1} = [a(C_{11} + C_{21}) - b(C_{22} + C_{12})]/M \tag{2.2.8}$$

$$\eta_{C2} = [a(C_{11} + C_{12}) - b(C_{22} + C_{21})]/MK^2 \tag{2.2.9}$$

The magnitudes  $\omega_z$  and  $\omega_\alpha$  are the partial frequencies of the system, that is, the frequencies which would apply if one of the coordinates  $Z$  or  $\psi$  is constant while the other is variable. If the coupling factors  $\eta_{C1}$  and  $\eta_{C2}$  are zero then the vertical and angular oscillations are independent, in which case the partial frequencies are the frequencies of the system.

Equations 2.2.5 can be shown to have the following solutions:

$$\begin{aligned}
 \psi &= B_1 \sin(\Omega_1 t + a_1) + B_2 \sin(\Omega_2 t + a_2) \\
 Z &= B_1 \frac{\Omega_1^2 - \omega_\alpha^2}{\eta_{C2}} \sin(\Omega_1 t + a_1) \\
 &\quad + B_2 \frac{\Omega_2^2 - \omega_\alpha^2}{\eta_{C2}} \sin(\Omega_2 t + a_2)
 \end{aligned} \tag{2.2.10}$$

The natural frequencies are given by

$$\Omega^2 = \frac{1}{2} \left( \omega_z^2 + \omega_\alpha^2 \pm \sqrt{(\omega_\alpha^2 - \omega_z^2)^2 + 4\eta_{C1} \eta_{C2}} \right) \quad (2.2.11)$$

Equations (2.2.5), (2.2.10) and (2.2.11) apply equally well to conventional suspensions where there is no interconnection. Equations (2.2.6) and (2.2.7) show that the presence of the interconnection stiffness  $C_{12}$  and  $C_{21}$  between front and rear, increases the frequency of vertical vibration  $\omega_z$  and decreases that of pitching  $\omega_\alpha$ . The reduction of pitching is of particular importance.

It can be seen from equation (2.2.7) that it is possible to reduce the pitching frequency to any required value. If  $a^2 C_{11} + b^2 C_{22} = ab(C_{12} + C_{21})$ , then the frequency would be zero and the system unstable owing to the absence of pitch stiffness in the suspension.

### 2.2.3 Pitch Angle Deflections

Application of a braking or acceleration load or a variation in the static load causes the body to assume a new position, both with regard to height and to angle.

If the load on the front wheels is increased by  $\Delta G_1$ , then from equation (2.2.2) the static deflections will be increased thus:

$$\left. \begin{aligned} \Delta f_{01} &= \frac{C_{22} \Delta G_1}{C_{11}C_{22} - C_{12}C_{21}} \\ \Delta f_{02} &= - \frac{C_{21} \Delta G_1}{C_{11}C_{22} - C_{12}C_{21}} \end{aligned} \right\} \quad (2.2.12)$$

The minus sign indicating that the deflection of the rear suspension is reduced as the load on the front wheels is increased. The corresponding angular displacement is:

$$\begin{aligned} \Delta \psi &= \frac{\Delta f_{02} - \Delta f_{01}}{L} \\ &= - \frac{C_{22} + C_{21}}{C_{11}C_{22} - C_{12}C_{21}} \frac{\Delta G_1}{L} \end{aligned} \quad (2.2.13)$$

where  $L$  is the vehicle wheelbase ( $= a + b$ ).

Similarly for  $G_2$  on the rear wheels:

$$\left. \begin{aligned} \Delta f_{01} &= \frac{-C_{12} \Delta G_2}{C_{11}C_{22} - C_{12}C_{21}} \\ \Delta f_{02} &= \frac{C_{11} \Delta G_2}{C_{11}C_{22} - C_{12}C_{21}} \end{aligned} \right\} \quad (2.2.14)$$

$$\begin{aligned} \Delta \psi &= \frac{f_{02} - f_{01}}{L} \\ &= \frac{C_{11} + C_{12}}{C_{11}C_{22} - C_{12}C_{21}} \frac{\Delta G_2}{L} \end{aligned} \quad (2.2.15)$$

These equations show that the additional deflections  $\Delta f_{01}$  and  $\Delta f_{02}$  and the angular displacement  $\Delta \psi$  depend to a large extent on the stiffness of the interconnection system  $C_{12}$  and  $C_{21}$ ; increasing the stiffness results in an increase in  $\Delta f_{01}$  and  $\Delta f_{02}$  and a considerable increase of the angle  $\Delta \psi$ . With a conventional suspension system in which  $C_{12} = C_{21} = 0$ , the additional deflection and angular displacement of the body due to a change in the front to rear weight distribution is less than with an interconnected suspension system.

For the three cars cited in section 2.1, the deflections and angular displacements due to the addition of a  $\Delta G_2 = 750$  N load at the rear wheels with  $L = 2.4$  m are as follows:

		$\Delta f_{01}$	$\Delta f_{02}$	$\Delta \psi$
Car A:	Interconnected	- 22 mm	49 mm	1 deg. 41 min.
Car B:	Conventional	0 mm	38 mm	0 deg. 54 min.
Car C:	Conventional	0 mm	26 mm	0 deg. 37 min.

Car B has the same front and rear spring rate  $C_{11}$  and  $C_{22}$  as car A, the angle of tilt is half that of car A. Car C has the same bounce frequency, but higher pitch frequency than car A, and the angle of tilt is a little over one-third that of the car with interconnected suspension, car A.



The sensitivity of interconnected suspension systems to the load distribution between front and rear wheels constitutes its main disadvantage and limits the possibility of increasing the coupling stiffness  $C_{12}$  and  $C_{21}$ . If these stiffness values are of a similar order to the stiffnesses  $C_{11}$  and  $C_{22}$ , then even a slight alteration of the load distribution between front and rear wheels leads to a substantial deflection of the suspension and pitching of the body. The example considered above has the coupling stiffnesses  $C_{12}$  and  $C_{21}$  as half the value of the stiffnesses  $C_{11}$  and  $C_{22}$ .

When a car is braked its front wheels are subjected to an additional vertical loading, while the loading on the rear wheels is reduced. For a constant braking effort  $T$  at the wheels, the change in vertical reactions at the front and rear wheels can be expressed approximately as follows:

$$\Delta P_1 = \frac{Th}{L}$$

$$\Delta P_2 = -\frac{Th}{L}$$

where  $h$  is the vehicle centre of gravity height and  $L$  the vehicle wheelbase.

Substituting  $P_1$  and  $P_2$  into equations (2.2.13) and (2.2.15) yields the angle of tilt due to braking effort  $T$

$$\Delta \psi_T = -\frac{C_{11} + C_{22} + C_{12} + C_{21}}{C_{11}C_{22} - C_{12}C_{21}} \cdot \frac{Th}{L^2} \quad (2.2.16)$$

Comparing the three cars again, at a deceleration rate of 0.6 g, assuming no anti-dive or anti-squat geometry, wheelbase  $L = 2.4$  m,  $h = 0.6$  m and  $M = 1000$  kg:

Body Pitch Angle Due to Braking

Car A:	Interconnected	6 deg.	24 min.
Car B:	Conventional	3 deg.	21 min.
Car C:	Conventional	2 deg.	20 min.

As was the case with the uneven load distribution, the angle of pitch of the body with interconnected suspension is considerably greater than that of the cars with conventional suspension. In order to reduce the angle to an acceptable level during braking and accelerating, anti-dive and anti-squat geometry needs to be incorporated into the suspension design.

## 2.3 APPLICATION OF AN INTERCONNECTED SUSPENSION SYSTEM

### 2.3.1 Previous Work

In an earlier report, Vandendungen (1976), an interconnected suspension system was proposed. This is shown in figure 2.3.1 which illustrates the lefthand side of a vehicle. The front, rear and auxiliary torsion cars are necessarily less than one-half of the vehicle width.

When the front wheel hits a bump, this causes the front torsion car to wind up (1) and apply additional tension in the cable (3). This additional tension causes the rear torsion car to wind up (4) and apply additional load at the rear wheels (2). Hitting a bump with one front wheel causes an increased reaction at both the front and rear wheels causing that side of the car to rise. Pitching is thus reduced.

If the pitch arms which connect the torsion cars via the cable are inclined towards each other as in figures 2.3.2a and 2.3.2b, the springrates become non-linear and some pitch stability is induced. In case this effect was insufficient, an appropriate, auxiliary torsion car, fixed to the chassis at the inner end and acting like spring  $C_4$  in figure 2.2.1, would increase the pitch stiffness to the desired level. It might also be used to adjust the static pitch angle by rotation of its anchored end.

The proposed suspension was analysed in 1976 and the springrates deduced, using the nomenclature from figures 2.3.2 and 3.

$$C_{11} = \frac{C_1 C_2}{\ell_1^2 (C_2 + C_1/R)} \quad (2.3.1)$$

$$C_{22} = \frac{(C_1 C_2 + C_3 C_1 + C_2 C_3 R)}{\ell_2^2 (C_1 + C_2 R)} \quad (2.3.2)$$

$$C_{12} = \frac{\ell_3}{\ell_4} \frac{C_1 C_2}{\ell_1 \ell_2 (C_1 + C_2 R)} \quad (2.3.3)$$

$$C_{21} = \frac{\ell_4}{\ell_3} \frac{C_1 C_2}{\ell_1 \ell_2 (C_2 + C_1/R)} \quad (2.3.4)$$

A computer program was written later, as part of this M.E. project (see section 2.4), to investigate the suspension system. This showed that in practice insufficient pitch stability could be achieved from the

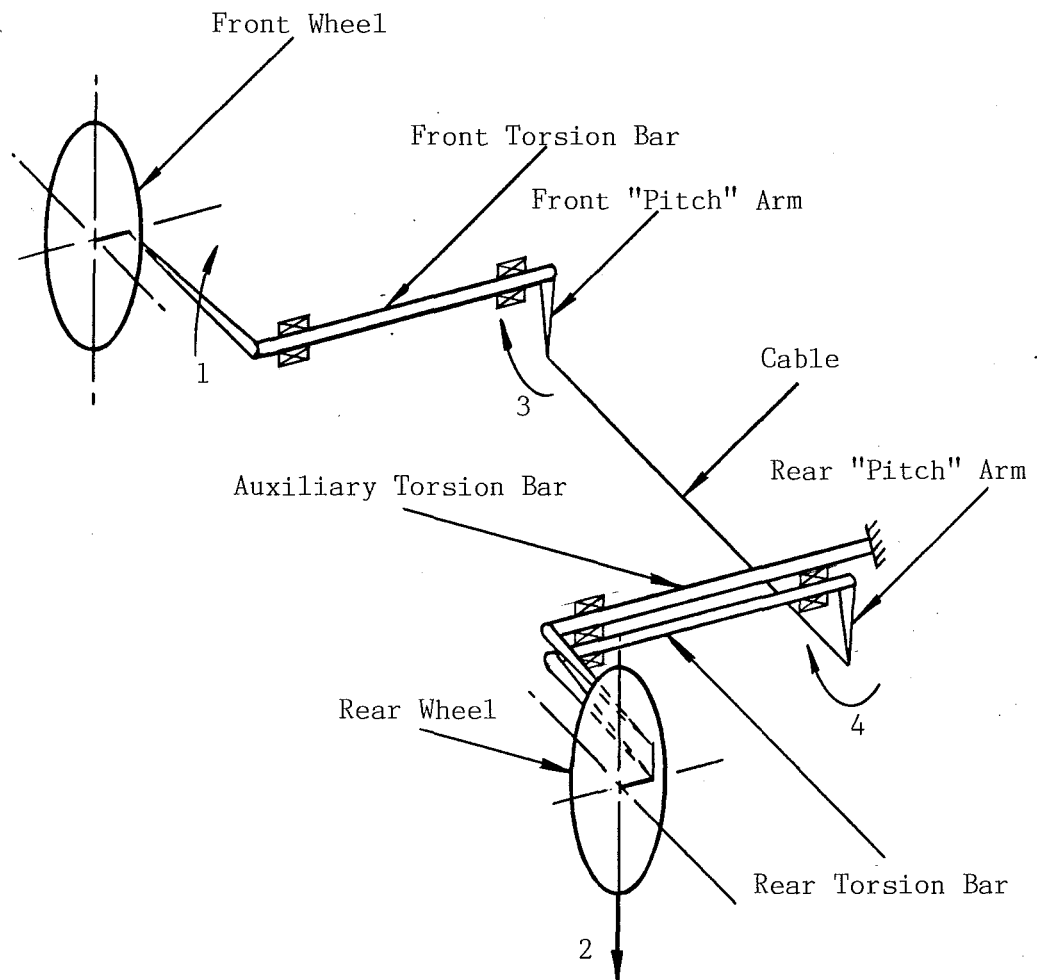


Figure 2.3.1. Original Proposed Design of Interconnected Suspension

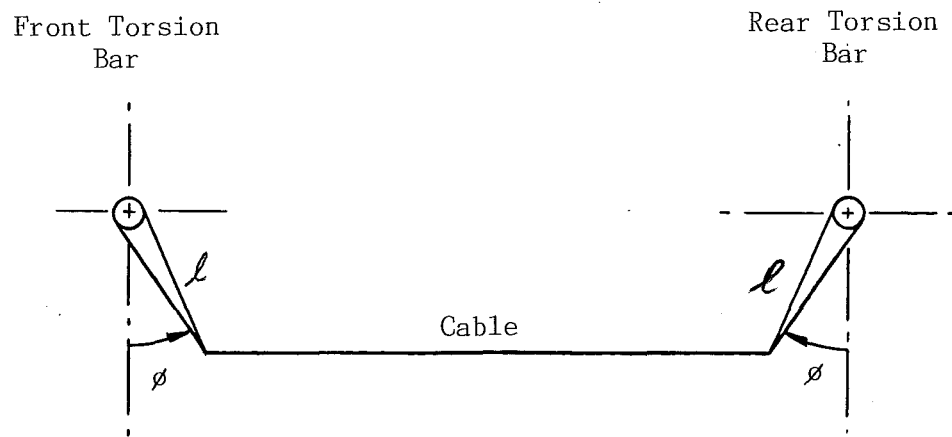


Figure 2.3.2.a. Pitch Arms in Undeflected Position.

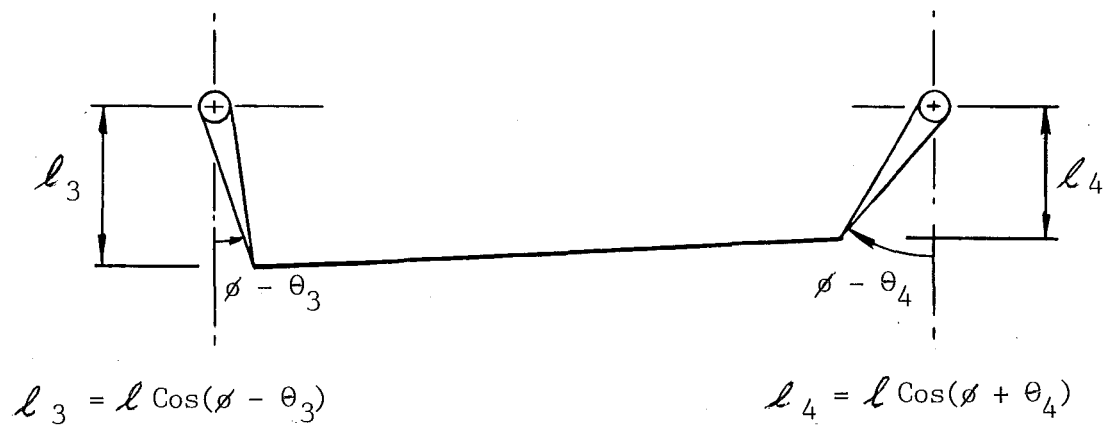


Figure 2.3.2.b. Pitch Arms in Deflected Position.

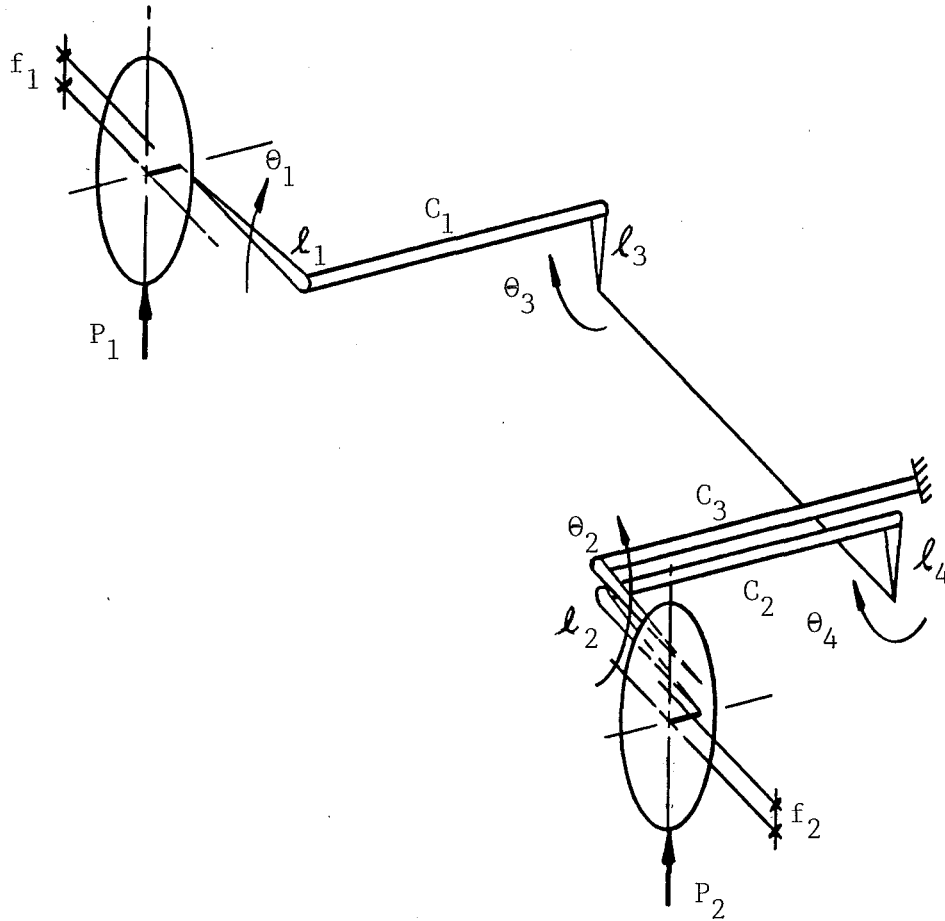


Figure 2.3.3. Nomenclature.

$f_1$  Front wheel displacement relative to body.

$f_2$  Rear wheel displacement relative to body.

$P_1$  Reaction on front wheels.

$P_2$  Reaction on rear wheels.

$l_1$  Effective length of front leading arm.

$l_2$  Effective length of rear trailing arm.

$l_3$  Effective length of front pitch arm.

$l_4$  Effective length of rear pitch arm.

$C_1$  Stiffness of front torsion bar.

$C_2$  Stiffness of rear torsion bar.

$C_3$  Stiffness of auxiliary torsion bar.

$\theta_1$  Angle deviation from static for arm  $l_1$ .

$\theta_2$  Angle deviation from static for arm  $l_2$ .

$\theta_3$  Angle deviation from static for arm  $l_3$ .

$\theta_4$  Angle deviation from static for arm  $l_4$ .

R Ratio  $l_3\theta_4/l_4\theta_3$ .

inclined pitch arms alone, as the angular deflection was too small to gain the required effect. The auxiliary torsion bar would therefore be required, but it could better be used to control the motion of the interconnecting cable.

### 2.3.2 Suspension as Built

The suspension as built utilizes three torsion bars on each side of the vehicle. The auxiliary torsion bar has one end connected to the rear pitch arm, rather than the rear suspension arm, and the other end fixed to the chassis as in figure 2.3.4. Using the nomenclature as previously,  $\theta_4$  is common to both the rear torsion bar  $C_2$  and the auxiliary torsion bar  $C_3$ .

Assume that the front wheels have been displaced by an amount  $f_1$ , relative to the body, figure 2.3.4. Torsion bar  $C_1$  will twist by an angle  $\theta_1 - \theta_3$  and the tension  $T$  in the cable will increase. Torsion bar  $C_2$  will twist by an angle  $\theta_4 - \theta_2$  and torsion bar  $C_3$  will twist by an angle  $\theta_4$ . The reaction  $P_1$  on the front wheels will increase, as will the reaction  $P_2$  on the rear wheels and the car will rise vertically. The reaction of torsion bar  $C_3$  on the vehicle body maintains the pitch stability.

From equations (2.2.1), the vehicle springrates are derived as follows:

- (a) Fix the rear wheels relative to the body, so that  $f_2 = 0$ , and equations (2.2.1) become,

$$P_1 = C_{11} f_1$$

$$P_2 = C_{21} f_1$$

thus  $C_{11}$  and  $C_{21}$  are derived.

- (b) Fix the front wheels relative to the body so that  $f_1 = 0$  and equations (2.2.1) become,

$$P_2 = C_{22} f_2$$

$$P_1 = C_{12} f_2$$

thus  $C_{22}$  and  $C_{12}$  are derived.

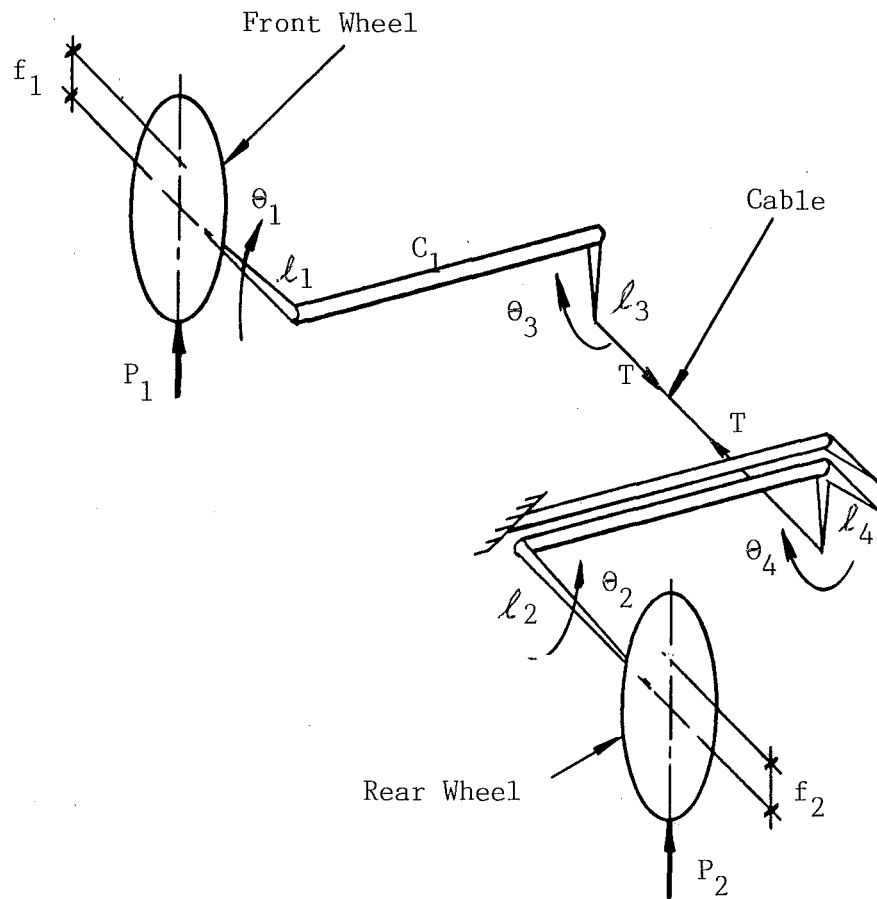
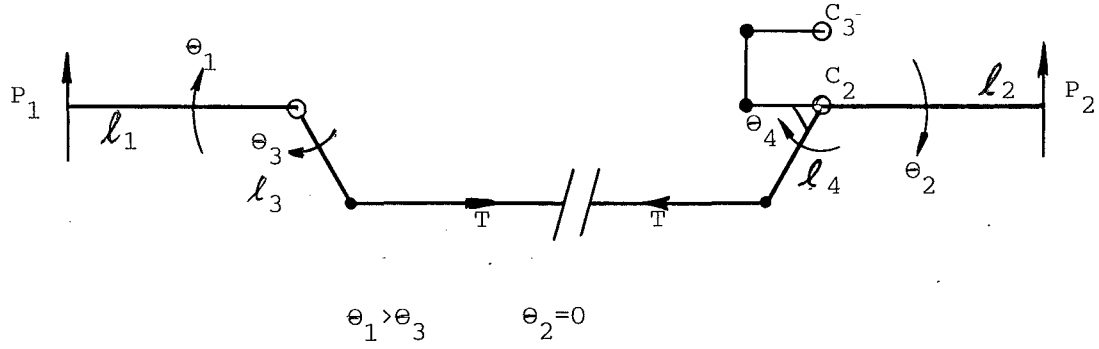


Figure 2.3.4. Torsion Bar Interconnected Suspension.



Take moments about torsion bars  $C_1$  and  $C_2$ .

$$(1) \quad P_1 l_1 = T l_3 \Rightarrow T = P_1 l_1 / l_3$$

$$(2) \quad P_2 l_2 = T l_4 - C_3 \theta_4$$

Torsion bar moments.

$$(3) \quad P_1 l_1 = C_1 (\theta_1 - \theta_3) = (C_1 l_1 / l_1 - C_1 \theta_3)$$

$$(4) \quad P_2 l_2 = C_2 \theta_4.$$

Substitute (2) into (4)

$$C_2 \theta_4 = T l_4 - C_3 \theta_4$$

Substitute (1)

$$C_2 \theta_4 = \frac{P_1 l_1 l_4}{l_3} - C_3 \theta_4$$

$$\Rightarrow \theta_4 (C_2 + C_3) = P_1 l_1 l_4 / l_3.$$

$$(5) \quad \theta_4 = \frac{P_1 l_1}{(C_2 + C_3)} \frac{l_4}{l_3}$$

Substitute (5) into (3)

$$P_1 l_1 = \frac{C_1 l_1}{l_1} - \frac{C_1 \theta_3}{\theta_4} \cdot \theta_4 = \frac{C_1 l_1}{l_1} - C_1 \frac{\theta_3}{\theta_4} \frac{P_1 l_1}{(C_2 + C_3)} \frac{l_4}{l_3}$$

and if 
$$R = \frac{l_3}{l_4} \frac{\theta_4}{\theta_3}$$



$$P_1 \ell_1 \left( 1 + \frac{C_1}{(C_2+C_3)} \cdot \frac{1}{R} \right) = \frac{C_1 f_1}{\ell_1}$$

$$(6) \quad P_1 = \frac{C_1 (C_2+C_3)}{\ell_1^2 (C_2+C_3+C_1/R)} f_1$$

so that

$$C_1 = \frac{C_1 (C_2+C_3)}{\ell_1^2 (C_2+C_3+C_1/R)} \quad (2.3.5)$$

For  $C_{21}$ , substitute (1) and (5) into

$$P_2 \ell_2 = P_1 \ell_1 \frac{\ell_4}{\ell_3} - \frac{C_3}{C_2+C_3} \frac{\ell_4}{\ell_3} P_1 \ell_1$$

$$(7) \quad P_2 = \frac{P_1 \ell_1}{\ell_2} \frac{\ell_4}{\ell_3} \left( 1 - \frac{C_3}{(C_2+C_3)} \right)$$

substitute (6) into (7)

$$P_2 = \frac{\ell_4}{\ell_3} \frac{C_1 C_2}{\ell_1 \ell_2 (C_2+C_3+C_1/R)} f_1$$

so that

$$C_{21} = \frac{\ell_4}{\ell_3} \frac{C_1 C_2}{\ell_1 \ell_2 (C_2+C_3+C_1/R)} \quad (2.3.6)$$

(b) Rear wheel displacement.

$$\theta_2 > \theta_4, \quad \theta_1 = 0.$$

Take moments about torsion bars  $C_1$  and  $C_2$

$$(1) \quad P_1 \ell_1 = T \ell_3$$

$$(2) \quad P_2 \ell_2 = T \ell_4 + C_3 \theta_4 \Rightarrow T = \frac{P_2 \ell_2}{\ell_4} - \frac{C_3 \theta_4}{\ell_4}$$

Torsion bar moments

$$(3) \quad P_1 \ell_1 = C_1 \theta_3$$

$$(4) \quad P_2 \ell_2 = C_2 (\theta_2 - \theta_4) = C_2 f_2 / \ell_2 - C_2 \theta_4$$

substitute (1) into (3)

$$C_1 \theta_3 = T \ell_3$$

substitute (2)

$$C_1 \theta_3 = P_2 \ell_2 \frac{\ell_3}{\ell_4} - C_3 \theta_4 \frac{\ell_3}{\ell_4}$$

$$\Rightarrow C_1 \frac{\theta_3}{\theta_4} \cdot \theta_4 = P_2 \ell_2 \frac{\ell_3}{\ell_4} - C_3 \theta_4 \frac{\ell_3}{\ell_4}$$

$$(5) \quad \theta_4 = \frac{P_2 \ell_2 R}{(C_1 + C_3 R)}$$

substitute (5) into (4)

$$P_2 \ell_2 = \frac{C_2 f_2}{\ell_2} - \frac{C_2 P_2 \ell_2 R}{(C_1 + C_3 R)}$$

$$(6) \quad P_2 = \frac{C_2 (C_1 + C_3 R)}{\ell_2^2 (C_1 + C_2 R + C_3 R)} f_2$$

$$\text{so that} \quad C_{22} = \frac{C_2 (C_1 + C_3 R)}{\ell_2^2 (C_1 + C_2 R + C_3 R)} \quad (2.3.7)$$

substitute (2) and (5) into (1)

$$P_1 \ell_1 = P_2 \ell_2 \frac{\ell_3}{\ell_4} - P_2 \ell_2 \frac{\ell_3}{\ell_4} \frac{C_3 R}{(C_1 + C_3 R)}$$

$$= P_2 \ell_2 \frac{\ell_3}{\ell_4} \left( 1 - \frac{C_3 R}{(C_1 + C_3 R)} \right)$$

$$(7) \quad P_1 = P_2 \frac{\ell_2}{\ell_1} \frac{\ell_3}{\ell_4} \left( 1 - \frac{C_3 R}{(C_1 + C_3 R)} \right)$$

substitute (6) into (7)

$$P_1 = \frac{\ell_3}{\ell_4} \frac{C_2 (C_1 + C_3 R)}{\ell_1 \ell_2 (C_1 + C_2 R + C_3 R)} \cdot \frac{C_1}{(C_1 + C_3 R)} f_2$$

$$(8) \quad P_1 = \frac{\ell_3}{\ell_4} \frac{C_1 C_2}{\ell_1 \ell_2 (C_1 + C_2 R + C_3 R)} f_2$$

$$\text{so that} \quad C_{12} = \frac{\ell_3}{\ell_4} \frac{C_1 C_2}{\ell_1 \ell_2 (C_1 + C_2 R + C_3 R)} \quad (2.3.8)$$

Assuming linear springrates, the suspension is unstable if  $a^2 C_{11} + b_2 C_{22} = ab(C_{12} + C_{21})$ . (See section 2.2.2). In the case where  $a = b$ , then  $C_{11} + C_{22} = C_{12} + C_{21}$ . Substituting in  $C_{11}$ ,  $C_{22}$ ,  $C_{21}$  and  $C_{21}$  we have

$$\frac{C_1 (C_2 + C_3)}{\ell_1^2 (C_2 + C_3 + C_1/R)} + \frac{C_2 (C_1 + C_3 R)}{\ell_2^2 (C_1 + C_2 R + C_3 R)} = \frac{\ell_4}{\ell_3} \frac{C_1 C_2}{\ell_1 \ell_2 (C_2 + C_3 + C_1/R)} + \frac{\ell_3}{\ell_4} \frac{C_1 C_2}{\ell_1 \ell_2 (C_1 + C_2 R + C_3 R)}$$

In this case where  $a = b$ , then  $P_1 = P_2$  and  $P_1 = \frac{T \ell_3}{\ell_1} = P_2 = \frac{T \ell_4}{\ell_2}$

$$\text{Hence} \quad \frac{\ell_3}{\ell_4} = \frac{\ell_1}{\ell_2}$$

Substituting  $\ell_3/\ell_4 = \ell_1/\ell_2$  and manipulating R:

$$\frac{R C_1 (C_2 + C_3)}{\ell_1^2 (C_2 R + C_3 R + C_1)} + \frac{C_2 (C_1 + C_3 R)}{\ell_2^2 (C_1 + C_2 R + C_3 R)} = \frac{C_1 C_2 R}{\ell_1^2 (C_1 + C_2 R + C_3 R)} + \frac{C_1 C_2}{\ell_2^2 (C_1 + C_2 R + C_3 R)}$$

Multiply through by  $(C_1 + C_2 R + C_3 R) \ell_1^2 \ell_2^2$  so that  $\ell_2^2 R_1 C_1 (C_2 + C_3) + \ell_1^2 C_2 (C_1 + C_3 R) =$

$$\ell_2^2 C_1 C_2 R + \ell_1^2 C_1 C_2 \text{ which leads to } \ell_2^2 (C_1 C_2 R - C_1 C_2 R - C_1 C_3 R) + \ell_1^2 (C_1 C_2 - C_1 C_2 - C_2 C_3 R) = 0$$

and hence  $C_3 (C_1 \ell_2^2 + C_2 \ell_1^2) = 0$  for instability. Thus the system is unstable if  $C_3 = 0$ , that is, if the third or auxiliary torsion bar is not present.

### 2.3.3 Comparison of Systems

The springrates of the two proposed torsion bar systems are summarized as follows:

<u>Auxiliary torsion bar position:</u>	<u>on suspension arm</u>	<u>on pitch arm</u>
$C_{11}$	$\frac{C_1 C_2}{\ell_1^2 (C_2 + C_1/R)}$	$\frac{C_1 (C_2 + C_3)}{\ell_1^2 (C_2 + C_3 + C_1/R)}$
$C_{22}$	$\frac{(C_1 C_2 + C_1 C_3 + C_2 C_3 R)}{\ell_2^2 (C_1 + C_2 R)}$	$\frac{C_2 (C_1 + C_3 R)}{\ell_2^2 (C_1 + C_2 R + C_3 R)}$
$C_{12}$	$\frac{\ell_3}{\ell_4} \frac{C_1 C_2}{\ell_1 \ell_2 (C_1 + C_2 R)}$	$\frac{\ell_3}{\ell_4} \frac{C_1 C_4}{\ell_1 \ell_2 (C_1 + C_2 R + C_3 R)}$
$C_{21}$	$\frac{\ell_4}{\ell_3} \frac{C_1 C_2}{\ell_1 \ell_2 (C_2 + C_1/R)}$	$\frac{\ell_4}{\ell_3} \frac{C_1 C_2}{\ell_1 \ell_2 (C_2 + C_3 + C_1/R)}$

With the auxiliary torsion bar  $C_3$  connected to the rear suspension arm,  $C_3$  affects and increases only  $C_{22}$ . With the auxiliary torsion bar  $C_3$  connected to the pitch arms,  $C_3$  affects all the springrates, increasing the basic stiffnesses  $C_{11}$  and  $C_{22}$  and decreasing the interconnecting stiffnesses  $C_{12}$  and  $C_{21}$ . This system is versatile, enabling  $C_{11}$ ,  $C_{22}$  and the coupling stiffnesses as a pair, to be altered separately, by using different combinations of  $C_1$ ,  $C_2$  and  $C_3$ .

Consider a numerical example for a vehicle which approximates the Electric Town Car, with  $M = 1050$  kg,  $K = 0.49$  L,  $a = 0.449$  L,  $b = 0.551$  L,  $\ell_1 = 0.45$ ,  $\ell_2 = 0.51$  and  $L = 2.23$ . From these  $K^2/ab = 0.97$  which is possibly a little too large. For ease of calculation assume  $R=1$  and  $\ell_3/\ell_4 = 1$ .

	<u><math>C_3</math> on pitch arm</u>	<u><math>C_3</math> on rear arm case 1</u>	<u><math>C_3</math> on rear arm case 2</u>
$C_1$	3638	3638	1500
$C_2$	3638	3638	1500
$C_3$	3181	3181	3181
$C_{11}$	23430	17966	7407
$C_{22}$	18242	38446	30227
$C_{21}$	11030	15852	6536
$C_{12}$	11030	15852	6536

	<u>C<sub>3</sub> on pitch arm</u>	<u>C<sub>3</sub> on rear arm</u> <u>case 1</u>	<u>C<sub>3</sub> on rear arm</u> <u>case 2</u>
$w_z^2$	60.698	83.920	48.292
$w_\alpha^2$	19.046	29.552	29.494
$\eta_{c1}$	-1.410	-31.314	-29.737
$\eta_{c2}$	-1.180	-26.212	-24.892
Bounce Hz	1.24	1.56	1.31
Pitch Hz	0.694	0.661	0.506
Bounce cpm	74	94	79
Pitch cpm	42	40	30
Body tilt 750 N rear luggage	2.2°	1.5°	1.5°
Body tilt 0.6 g braking	-7.3°	-7.0°	-9.8°

With the torsion car  $C_3$  attached to the rear suspension arm, the difference between bounce and pitch frequencies was limited to approximately 50 cpm and the ratio of bounce to pitch did not go below 2.3 for all the different spring combinations of  $C_1$ ,  $C_2$  and  $C_3$  tried. This layout proved to be limited.

## 2.4 SUSPENSION ANALYSIS ON A DIGITAL COMPUTER

### 2.4.1 The Interconnected Suspension Program "Intersusp"

The object of writing this program was to establish the pitch characteristics of the inclined arms which interconnect the main tension bars via cables and more importantly to calculate the position and condition of each suspension component for every front and rear, bump and rebound permutation and hence the vehicle's suspension characteristics and vibration responses at each permutation.

As discussed in section 2.3.1 the inclined pitch arms alone do not contribute sufficient pitch stability and a third torsion bar is required. These so-called pitch arms are retained inclined towards each other (rather than parallel) as they produce a non-linear rising-springrate effect.

The program analyses the suspension proposed in section 2.3.2 and uses equations (2.3.5) to (2.3.8) inclusive for  $C_{11}$ ,  $C_{21}$ ,  $C_{22}$  and  $C_{12}$ . For every permutation of bounce and rebound of  $F_1$  and  $F_2$  analysed, the instantaneous values of  $\theta_1$ ,  $\theta_2$ ,  $\theta_3$ ,  $\theta_4$ ,  $\ell_1$ ,  $\ell_2$ ,  $\ell_3$ ,  $\ell_4$  and  $R$  are calculated. The angles  $\theta_3$  and  $\theta_4$  and lengths  $\ell_3$  and  $\ell_4$  are not independent and a Modified Newton-Raphson Iteration Method is employed. Using the analysis in section 2.2.2 the corresponding partial bounce and pitch frequencies and coupling coefficients are calculated and hence the bounce and pitch frequencies.

In addition to the dynamic wheel loadings  $P_1$  and  $P_2$ , the ratio of dynamic to static wheel loadings are calculated. To aid the mechanical design, at every permutation of  $F_1$  and  $F_2$ , the cable tension and the windup angles and stresses for all three torsion bars is also calculated.

The computer printout lists the vehicle data, some static condition suspension properties and finally the bump and rebound analysis. A guide on how to input the data cards is given in the booklet "Interconnected Suspension Program, Data Input and Answer Code Handbook", Appendix 2.4.1.

With reference to the sample printout, the "Program Control Integers" comprise the first data card. The value of the integers control a subroutine DATALIST which, in this example sets up the program to expect circular rather than rectangular front and rear torsion bars, no Load-Brake-Acceleration Data, a rectangular auxiliary torsion bar and so on. Separate cards are then read for the data on the front torsion bar, rear torsion bar, arm lengths, initial angles, vehicle geometry and auxiliary torsion bar. This data is echoed on the printout.

The springrate and stressrate for the three torsion bars is calculated, SAE (1947) and printed.

A subroutine ARMLTH is called to calculate the required effective armlength of the rear pitch arm  $L_4$ , based on the vehicle geometry. Armlengths  $AL_3$  and  $AL_4$  are the required physical centre to centre lengths of the front and rear pitch arms, while  $AL_6$  is the corresponding centre to centre length of the cables. The locked pitch angles refers to the condition when the four-car-linkage system comprising front and rear pitch arms and the cable becomes locked, forming a triangle such that the cable and one arm are in line.

The static deflections front and rear are calculated in subroutine STDEFL, assuming that the inboard ends of the front and rear torsion bars are fixed. Equations (2.2.2) were not used, as these assume  $C_{11}$ ,  $C_{22}$ ,

# PROGRAM CONTROL INTEGERS

```

ITF * 1 FRONT TORSION BAR (1=CIRCULAR,2=RECTANGULAR)
ITR * 1 REAR TORSION BAR (1=CIRCULAR,2=RECTANGULAR)
IAL * 1 ARM LENGTH DATA
IAD * 1 INITIAL ANGLE DATA
IVG * 1 VEHICLE GEOMETRY DATA
LBA * 0 LOAD-BRAKE-ACCELERATION DATA
ITA * 2 AUX TORSION BAR (1=CIRCULAR,2=RECTANGULAR)
0

```

```

FRONT TORSION BAR * * CIRCULAR * * ITF = 1
G L B
.78453E+11 0.4960 0.0220 0.0000 0.0000 0.0000 0.0000 0.0000

```

```

REAR TORSION BAR * * CIRCULAR * * ITR = 1
G L B
.78453E+11 0.4960 0.0220 0.0000 0.0000 0.0000 0.0000 0.0000

```

```

ARM LENGTH DATA * * IAL = 1
AL1 AL2 AL3 AL4 AL5 AL6 L3
0.4500 0.5099 0.0000 0.0000 1.3500 0.0000 0.0700 0.0000

```

```

INITIAL ANGLE DATA * * IAD = 1
A1 A2 A3 A4 A5 A6
0.0000 0.0196 1.0472 1.0472 0.0000 0.0000 0.0000 0.0000

```

```

VEHICLE GEOMETRY DATA * * IVG = 1
WB A B H M K
2.2300 0.4499 0.5510 0.2200 1049.6000 0.4900 0.0000 0.0000

```

```

AUXILIARY TORSION BAR * * RECTANGULAR * * ITA = 2
G L A B N2 N3
.78453E+11 0.4560 0.0190 0.0190 0.2100 0.1400 0.0000 0.0000

```

```

EACH FRONT TORSION BAR * TORSION RATE C1 = 3.638 KNM/RAD
* STRESS RATE = 1739.885 MPA/RAD

```

```

EACH REAR TORSION BAR * TORSION RATE C2 = 3.638 KNM/RAD
* STRESS RATE = 1739.885 MPA/RAD

```

```

EACH AUXILIARY TOR BAR * TORSION RATE C3 = 3.181 KNM/RAD
* STRESS RATE = 2208.307 MPA/RAD

```

SUBROUTINE \* ARMLTH \* HAS BEEN CALLED

```

EFFECTIVE LENGTH L4 = 0.0646
ARM LENGTHS * AL3 = 0.0806 AND AL4 = 0.0748 METRES
CABLE LENGTH AL6 = 1.2723 AND INITIAL CABLE ANGLE A6 = -0.0040 RADIAN

```

```

FRONT BUMP * LOCKED PITCH ANGLES ARE * FRONT = 1.5048 AND REAR = 0.0598 RADIAN
REAR BUMP * LOCKED PITCH ANGLES ARE * FRONT = 0.0553 AND REAR = 1.5824 RADIAN

```

SUBROUTINE \* SDEFI \* HAS BEEN CALLED

```

* F1 F2 P1 P2 THT1 THT2 THT3 THT4 P/G1 P/G2 RATIO T ITS
0.0000 0.0000 2.8357 2.3108 0.0000 0.0000 0.0000 0.0000 1.0000 1.0000 1.0832 18.2297 0
INITIAL THT1 = -0.3508 * INITIAL THT2 = 0.3239
STATIC DEFLECTIONS * FRONT = -0.1546 * REAR = -0.1617 M

```

SUBROUTINE \* BUMP \* HAS BEEN CALLED

SUBROUTINE \* BUMP \* HAS BEEN CALLED

F1	F2	P1	P2	THT1	THT2	THT3	THT4	P/G1	P/G2	RATIO	T	ITS
-0.1000	-0.1000	1.0784	0.8942	-0.2241	0.1978	-0.0034	-0.0036	0.3803	0.3869	1.1658	6.7734	8
CORRES WHEEL RATES ARE * C11	12.9642 * C22	9.3031 * C12	5.6386	1.2727 HZ	0.7292 HZ	C COEFFS =	0.5322	0.4026				
CORRES FREQS ARE * PITCH	0.1291 * BOUNCE	1.2626 HZ	0.7146 HZ	STRESS * S1 =	226.3136 * S2 =	-212.9384 * S3 =	-8.0358 MPA					
CORRES ANGLES * PH11 =	0.1301 * PH12 =	-0.1224 RAD AND										
-0.1000	-0.0500	1.3858	1.3133	-0.2241	0.0983	-0.0034	-0.0427	0.4887	0.5683	1.0872	8.9135	6
CORRES WHEEL RATES ARE * C11	12.6763 * C22	9.1100 * C12	5.5490	1.2626 HZ	0.7146 HZ	C COEFFS =	0.7232	0.0974				
CORRES FREQS ARE * PITCH	0.1146 * BOUNCE	1.2626 HZ	0.7146 HZ	STRESS * S1 =	290.8228 * S2 =	-318.0702 * S3 =	-94.3138 MPA					
CORRES ANGLES * PH11 =	0.1972 * PH12 =	-0.1828 RAD AND										
-0.1000	0.0000	1.6902	1.7424	-0.2241	0.0000	-0.0772	-0.0797	0.5960	0.7540	1.0160	11.1538	6
CORRES WHEEL RATES ARE * C11	12.3904 * C22	9.1003 * C12	5.5100	1.2578 HZ	0.7043 HZ	C COEFFS =	0.4625	-0.5784				
CORRES FREQS ARE * PITCH	0.7044 * BOUNCE	1.2578 HZ	0.7043 HZ	STRESS * S1 =	354.7019 * S2 =	-424.8568 * S3 =	-175.9211 MPA					
CORRES ANGLES * PH11 =	0.2039 * PH12 =	-0.2442 RAD AND										
-0.1000	0.0500	1.9938	2.1975	-0.2241	-0.0981	-0.1138	-0.1149	0.7031	0.9510	0.9503	13.5278	8
CORRES WHEEL RATES ARE * C11	12.1025 * C22	9.2676 * C12	5.5183	1.2585 HZ	0.6979 HZ	C COEFFS =	-0.2288	-1.6296				
CORRES FREQS ARE * PITCH	0.6978 * BOUNCE	1.2585 HZ	0.6979 HZ	STRESS * S1 =	418.4131 * S2 =	-534.2985 * S3 =	-253.7389 MPA					
CORRES ANGLES * PH11 =	0.2405 * PH12 =	-0.3071 RAD AND										
-0.1000	0.1000	2.2987	2.6973	-0.2241	-0.1970	-0.1505	-0.1487	0.8106	1.1673	0.8888	16.0748	8
CORRES WHEEL RATES ARE * C11	11.8089 * C22	9.6265 * C12	5.5743	1.2646 HZ	0.6960 HZ	C COEFFS =	-1.3802	-3.1040				
CORRES FREQS ARE * PITCH	0.6942 * BOUNCE	1.2646 HZ	0.6960 HZ	STRESS * S1 =	462.3903 * S2 =	-647.5152 * S3 =	-328.4595 MPA					
CORRES ANGLES * PH11 =	0.2473 * PH12 =	-0.3722 RAD AND										
-0.0500	-0.1000	1.6744	1.1925	-0.1113	0.1978	0.0336	0.0372	0.5905	0.5161	1.2526	10.4898	8
CORRES WHEEL RATES ARE * C11	12.7555 * C22	9.1836 * C12	5.5213	1.2599 HZ	0.7309 HZ	C COEFFS =	0.2137	0.6037				
CORRES FREQS ARE * PITCH	0.7308 * BOUNCE	1.2599 HZ	0.7309 HZ	STRESS * S1 =	358.1680 * S2 =	-283.9918 * S3 =	82.1470 MPA					
CORRES ANGLES * PH11 =	0.2059 * PH12 =	-0.1632 RAD AND										
-0.0500	-0.0500	1.9606	1.6078	-0.1113	0.0983	-0.0016	-0.0017	0.6914	0.6958	1.1698	12.5379	6
CORRES WHEEL RATES ARE * C11	12.4914 * C22	8.9891 * C12	5.4331	1.2499 HZ	0.7166 HZ	C COEFFS =	0.4390	0.3482				
CORRES FREQS ARE * PITCH	0.7166 * BOUNCE	1.2499 HZ	0.7166 HZ	STRESS * S1 =	419.3796 * S2 =	-389.4050 * S3 =	-3.7739 MPA					
CORRES ANGLES * PH11 =	0.2410 * PH12 =	-0.2238 RAD AND										
-0.0500	0.0000	2.2444	2.0353	-0.1113	0.0000	-0.0365	-0.0386	0.7915	0.8808	1.0953	14.6753	4
CORRES WHEEL RATES ARE * C11	12.2307 * C22	8.9751 * C12	5.4070	1.2456 HZ	0.7067 HZ	C COEFFS =	0.2171	-0.2647				
CORRES FREQS ARE * PITCH	0.7067 * BOUNCE	1.2456 HZ	0.7067 HZ	STRESS * S1 =	480.0846 * S2 =	-496.2892 * S3 =	-85.2572 MPA					
CORRES ANGLES * PH11 =	0.2459 * PH12 =	-0.2852 RAD AND										
-0.0500	0.0500	2.5279	2.4910	-0.1113	-0.0981	-0.0713	-0.0739	0.8914	1.0780	1.0269	16.9317	6
CORRES WHEEL RATES ARE * C11	11.9696 * C22	9.1351 * C12	5.4220	1.2467 HZ	0.7007 HZ	C COEFFS =	-0.4307	-1.2384				
CORRES FREQS ARE * PITCH	0.7005 * BOUNCE	1.2467 HZ	0.7007 HZ	STRESS * S1 =	540.7238 * S2 =	-605.6371 * S3 =	-163.1943 MPA					
CORRES ANGLES * PH11 =	0.3108 * PH12 =	-0.3481 RAD AND										
-0.0500	0.1000	2.8131	2.9932	-0.1113	-0.1970	-0.1064	-0.1079	0.9920	1.2953	0.9632	19.3420	6
CORRES WHEEL RATES ARE * C11	11.7049 * C22	9.4829 * C12	5.4853	1.2540 HZ	0.6992 HZ	C COEFFS =	-1.5332	-2.6178				
CORRES FREQS ARE * PITCH	0.6975 * BOUNCE	1.2540 HZ	0.6992 HZ	STRESS * S1 =	601.7220 * S2 =	-718.5466 * S3 =	-238.3021 MPA					
CORRES ANGLES * PH11 =	0.3458 * PH12 =	-0.4130 RAD AND										
0.0000	-0.1000	2.2967	1.4721	0.0000	0.1978	0.0667	0.0755	0.8099	0.6371	1.3392	14.2229	6
CORRES WHEEL RATES ARE * C11	12.8460 * C22	9.0756 * C12	5.4727	1.2551 HZ	0.7362 HZ	C COEFFS =	0.4345	1.2099				
CORRES FREQS ARE * PITCH	0.7360 * BOUNCE	1.2551 HZ	0.7362 HZ	STRESS * S1 =	494.3321 * S2 =	-350.5829 * S3 =	166.6661 MPA					
CORRES ANGLES * PH11 =	0.2441 * PH12 =	-0.2015 RAD AND										
0.0000	-0.0500	2.5671	1.8843	0.0000	0.0983	0.1332	0.0366	0.9053	0.8155	1.2517	16.1854	4
CORRES WHEEL RATES ARE * C11	12.5953 * C22	8.8804 * C12	5.5955	1.2459 HZ	0.7221 HZ	C COEFFS =	0.6802	0.9801				
CORRES FREQS ARE * PITCH	0.7219 * BOUNCE	1.2459 HZ	0.7221 HZ	STRESS * S1 =	552.5301 * S2 =	-456.3748 * S3 =	81.2259 MPA					
CORRES ANGLES * PH11 =	0.3176 * PH12 =	-0.2623 RAD AND										



* F1	F2	P1	P2	THT1	THT2	THT3	THT4	P/G1	P/G2	RATIO	T	ITS
0.0000	0.0000	2.8357	2.3108	0.0000	0.0000	0.0000	0.0000	1.0000	1.0000	1.0832	18.2297	0
CORRES WHEEL RATES ARE * C11	12.0358	* C22	8.9934	* C12	5.6679	* C21	5.2324	KN/M				
CORRES FREQS ARE * PITCH	0.7035	* BOUNCE	1.2413	HZ	PFB =	1.2414	PFP =	0.7032	HZ	C COEFFS =	-1.3806	0.3934
CORRES ANGLES * PH11 =	0.3208	* PH12 =	-0.3239	RAD AND	STRESS * S1 =	610.3524	* S2 =	-563.4618	* S3 =	0.0000	MPA	
* F1	F2	P1	P2	THT1	THT2	THT3	THT4	P/G1	P/G2	RATIO	T	ITS
0.0000	0.0500	3.1046	2.7673	0.0000	-0.0981	-0.0333	-0.0353	1.0948	1.1976	1.1019	20.3828	4
CORRES WHEEL RATES ARE * C11	12.1034	* C22	9.0174	* C12	5.3889	* C21	5.5029	KN/M				
CORRES FREQS ARE * PITCH	0.7065	* BOUNCE	1.2431	HZ	PFB =	1.2430	PFP =	0.7065	HZ	C COEFFS =	-0.1385	-0.5219
CORRES ANGLES * PH11 =	0.3841	* PH12 =	-0.3867	RAD AND	STRESS * S1 =	668.2158	* S2 =	-672.8367	* S3 =	-77.9028	MPA	
* F1	F2	P1	P2	THT1	THT2	THT3	THT4	P/G1	P/G2	RATIO	T	ITS
0.0000	0.1000	3.3755	3.2725	0.0000	-0.1970	-0.0668	-0.0694	1.1903	1.4162	1.0355	22.6760	6
CORRES WHEEL RATES ARE * C11	11.8556	* C22	9.3563	* C12	5.4579	* C21	5.6902	KN/M				
CORRES FREQS ARE * PITCH	0.7041	* BOUNCE	1.2503	HZ	PFB =	1.2498	PFP =	0.7050	HZ	C COEFFS =	-1.2093	-1.8395
CORRES ANGLES * PH11 =	0.4176	* PH12 =	-0.4515	RAD AND	STRESS * S1 =	726.5310	* S2 =	-785.5893	* S3 =	-153.2123	MPA	
* F1	F2	P1	P2	THT1	THT2	THT3	THT4	P/G1	P/G2	RATIO	T	ITS
0.0500	-0.1000	2.9719	1.7378	0.1113	0.1978	0.0968	0.1118	1.0480	0.7520	1.4270	18.0211	10
CORRES WHEEL RATES ARE * C11	13.2387	* C22	8.9757	* C12	5.4893	* C21	5.1377	KN/M				
CORRES FREQS ARE * PITCH	0.7444	* BOUNCE	1.2597	HZ	PFB =	1.2590	PFP =	0.7455	HZ	C COEFFS =	1.1932	2.2506
CORRES ANGLES * PH11 =	0.3854	* PH12 =	-0.2379	RAD AND	STRESS * S1 =	635.7050	* S2 =	-413.8493	* S3 =	246.9655	MPA	
* F1	F2	P1	P2	THT1	THT2	THT3	THT4	P/G1	P/G2	RATIO	T	ITS
0.0500	-0.0500	3.2307	2.1476	0.1113	0.0983	0.0650	0.0734	1.1393	0.9294	1.3344	19.9011	8
CORRES WHEEL RATES ARE * C11	12.9933	* C22	8.7802	* C12	5.4156	* C21	5.1867	KN/M				
CORRES FREQS ARE * PITCH	0.7303	* BOUNCE	1.2508	HZ	PFB =	1.2501	PFP =	0.7316	HZ	C COEFFS =	1.4486	2.0280
CORRES ANGLES * PH11 =	0.3872	* PH12 =	-0.2989	RAD AND	STRESS * S1 =	691.0655	* S2 =	-520.1309	* S3 =	162.1469	MPA	
* F1	F2	P1	P2	THT1	THT2	THT3	THT4	P/G1	P/G2	RATIO	T	ITS
0.0500	0.0000	3.4684	2.5736	0.1113	0.0000	0.0333	0.0368	1.2302	1.1137	1.2518	21.8577	8
CORRES WHEEL RATES ARE * C11	12.7530	* C22	8.7607	* C12	5.3925	* C21	5.2771	KN/M				
CORRES FREQS ARE * PITCH	0.7209	* BOUNCE	1.2468	HZ	PFB =	1.2463	PFP =	0.7217	HZ	C COEFFS =	1.2626	1.4681
CORRES ANGLES * PH11 =	0.4289	* PH12 =	-0.3607	RAD AND	STRESS * S1 =	746.1840	* S2 =	-627.5337	* S3 =	81.3216	MPA	
* F1	F2	P1	P2	THT1	THT2	THT3	THT4	P/G1	P/G2	RATIO	T	ITS
0.0500	0.0500	3.7468	3.0315	0.1113	-0.0981	0.0013	0.0016	1.3213	1.3119	1.1768	23.9155	6
CORRES WHEEL RATES ARE * C11	12.5145	* C22	8.9101	* C12	5.4173	* C21	5.4121	KN/M				
CORRES FREQS ARE * PITCH	0.7157	* BOUNCE	1.2478	HZ	PFB =	1.2477	PFP =	0.7158	HZ	C COEFFS =	0.6572	0.5690
CORRES ANGLES * PH11 =	0.4806	* PH12 =	-0.4236	RAD AND	STRESS * S1 =	801.4523	* S2 =	-737.0504	* S3 =	3.6066	MPA	
* F1	F2	P1	P2	THT1	THT2	THT3	THT4	P/G1	P/G2	RATIO	T	ITS
0.0500	0.1000	4.0077	3.5399	0.1113	-0.1970	-0.0306	-0.0325	1.4133	1.5319	1.1074	26.1033	6
CORRES WHEEL RATES ARE * C11	12.2747	* C22	9.2416	* C12	5.4917	* C21	5.5986	KN/M				
CORRES FREQS ARE * PITCH	0.7140	* BOUNCE	1.2546	HZ	PFB =	1.2545	PFP =	0.7141	HZ	C COEFFS =	-0.3949	-0.7110
CORRES ANGLES * PH11 =	0.4927	* PH12 =	-0.4884	RAD AND	STRESS * S1 =	857.2642	* S2 =	-849.7857	* S3 =	-71.7326	MPA	
* F1	F2	P1	P2	THT1	THT2	THT3	THT4	P/G1	P/G2	RATIO	T	ITS
0.1000	-0.1000	3.7340	1.9934	0.2241	0.1978	0.1245	0.1468	1.3168	0.8626	1.5176	21.9352	14
CORRES WHEEL RATES ARE * C11	13.9816	* C22	8.8816	* C12	5.5749	* C21	5.1067	KN/M				
CORRES FREQS ARE * PITCH	0.7559	* BOUNCE	1.2748	HZ	PFB =	1.2724	PFP =	0.7599	HZ	C COEFFS =	2.5714	3.8198
CORRES ANGLES * PH11 =	0.4504	* PH12 =	-0.2728	RAD AND	STRESS * S1 =	783.6026	* S2 =	-474.7049	* S3 =	324.2049	MPA	
* F1	F2	P1	P2	THT1	THT2	THT3	THT4	P/G1	P/G2	RATIO	T	ITS
0.1000	-0.0500	3.9848	2.4014	0.2241	0.0983	0.0943	0.1088	1.4052	1.0392	1.4193	23.7337	12
CORRES WHEEL RATES ARE * C11	13.7343	* C22	8.6862	* C12	5.5033	* C21	5.1604	KN/M				
CORRES FREQS ARE * PITCH	0.7417	* BOUNCE	1.2661	HZ	PFB =	1.2637	PFP =	0.7459	HZ	C COEFFS =	2.8270	3.5879
CORRES ANGLES * PH11 =	0.4806	* PH12 =	-0.3343	RAD AND	STRESS * S1 =	836.2288	* S2 =	-581.5987	* S3 =	240.1634	MPA	
* F1	F2	P1	P2	THT1	THT2	THT3	THT4	P/G1	P/G2	RATIO	T	ITS
0.1000	0.0000	4.2351	2.8274	0.2241	0.0000	0.0641	0.0724	1.4935	1.2230	1.3320	25.6053	10
CORRES WHEEL RATES ARE * C11	13.4927	* C22	8.6647	* C12	5.4833	* C21	5.2546	KN/M				
CORRES FREQS ARE * PITCH	0.7326	* BOUNCE	1.2620	HZ	PFB =	1.2601	PFP =	0.7359	HZ	C COEFFS =	2.6431	3.0273
CORRES ANGLES * PH11 =	0.5108	* PH12 =	-0.3963	RAD AND	STRESS * S1 =	888.7469	* S2 =	-689.4381	* S3 =	159.8924	MPA	
* F1	F2	P1	P2	THT1	THT2	THT3	THT4	P/G1	P/G2	RATIO	T	ITS
0.1000	0.0500	4.4866	3.2872	0.2241	-0.0981	0.0338	0.0374	1.5821	1.4225	1.2530	27.5723	10
CORRES WHEEL RATES ARE * C11	13.2537	* C22	8.8101	* C12	5.5123	* C21	5.3926	KN/M				
CORRES FREQS ARE * PITCH	0.7279	* BOUNCE	1.2625	HZ	PFB =	1.2615	PFP =	0.7297	HZ	C COEFFS =	2.0420	2.1362
CORRES ANGLES * PH11 =	0.5411	* PH12 =	-0.4594	RAD AND	STRESS * S1 =	941.5234	* S2 =	-799.2329	* S3 =	82.5225	MPA	

* F1	F2	P1	P2	THT1	THT2	THT3	THT4	P/G1	P/G2	RATIO	T	ITS
0.0500	0.0500	3.7468	3.0315	0.1113	-0.0981	0.0015	0.0016	1.3213	1.3119	1.1768	23.9155	6
CORRES WHEEL RATES ARE * C11 = 12.5145 * C22 = 8.9101 * C12 = 1.2478 HZ												
CORRES FREQS ARE * PITCH = 0.7157 * BOUNCE = 1.2546 HZ												
CORRES ANGLES * PH11 = 0.4006 * PH12 = -0.4236 RAD AND STRESS * S1 = 801.4523 * S2 = -737.0564 * S3 = 3.6066 MPA												
* F1	F2	P1	P2	THT1	THT2	THT3	THT4	P/G1	P/G2	RATIO	T	ITS
0.0500	0.1000	4.0077	3.5399	0.1113	-0.1970	-0.0306	-0.0325	1.4133	1.5319	1.1074	26.1033	6
CORRES WHEEL RATES ARE * C11 = 12.2747 * C22 = 9.2416 * C12 = 1.2546 HZ												
CORRES FREQS ARE * PITCH = 0.7140 * BOUNCE = 1.2546 HZ												
CORRES ANGLES * PH11 = 0.4927 * PH12 = -0.4884 RAD AND STRESS * S1 = 857.2642 * S2 = -849.7857 * S3 = -71.7326 MPA												
* F1	F2	P1	P2	THT1	THT2	THT3	THT4	P/G1	P/G2	RATIO	T	ITS
0.1000	-0.1000	3.7340	1.9934	0.2241	0.1978	0.1245	0.1468	1.3168	0.8626	1.5176	21.9352	14
CORRES WHEEL RATES ARE * C11 = 13.9816 * C22 = 8.8816 * C12 = 1.2748 HZ												
CORRES FREQS ARE * PITCH = 0.7559 * BOUNCE = 1.2748 HZ												
CORRES ANGLES * PH11 = 0.4504 * PH12 = -0.2728 RAD AND STRESS * S1 = 783.6026 * S2 = -474.7049 * S3 = 324.2049 MPA												
* F1	F2	P1	P2	THT1	THT2	THT3	THT4	P/G1	P/G2	RATIO	T	ITS
0.1000	-0.0500	3.9848	2.4014	0.2241	0.0983	0.0943	0.1088	1.4052	1.0392	1.4193	23.7337	12
CORRES WHEEL RATES ARE * C11 = 13.7343 * C22 = 8.6862 * C12 = 1.2661 HZ												
CORRES FREQS ARE * PITCH = 0.7417 * BOUNCE = 1.2661 HZ												
CORRES ANGLES * PH11 = 0.4806 * PH12 = -0.3343 RAD AND STRESS * S1 = 836.2288 * S2 = -581.5987 * S3 = 240.1634 MPA												
* F1	F2	P1	P2	THT1	THT2	THT3	THT4	P/G1	P/G2	RATIO	T	ITS
0.1000	0.0000	4.2351	2.8274	0.2241	0.0000	0.0641	0.0724	1.4935	1.2236	1.3320	25.6053	10
CORRES WHEEL RATES ARE * C11 = 13.4927 * C22 = 8.6647 * C12 = 1.2620 HZ												
CORRES FREQS ARE * PITCH = 0.7326 * BOUNCE = 1.2620 HZ												
CORRES ANGLES * PH11 = 0.5108 * PH12 = -0.3963 RAD AND STRESS * S1 = 888.7469 * S2 = -689.4381 * S3 = 159.8924 MPA												
* F1	F2	P1	P2	THT1	THT2	THT3	THT4	P/G1	P/G2	RATIO	T	ITS
0.1000	0.0500	4.4866	3.2872	0.2241	-0.0981	0.0338	0.0374	1.5821	1.4225	1.2530	27.5723	10
CORRES WHEEL RATES ARE * C11 = 13.2537 * C22 = 8.8101 * C12 = 1.2625 HZ												
CORRES FREQS ARE * PITCH = 0.7279 * BOUNCE = 1.2625 HZ												
CORRES ANGLES * PH11 = 0.5411 * PH12 = -0.4594 RAD AND STRESS * S1 = 941.5234 * S2 = -799.2329 * S3 = 82.5225 MPA												
* F1	F2	P1	P2	THT1	THT2	THT3	THT4	P/G1	P/G2	RATIO	T	ITS
0.1000	0.1000	4.7411	3.7994	0.2241	-0.1970	0.0031	0.0033	1.6719	1.6442	1.1803	29.6613	8
CORRES WHEEL RATES ARE * C11 = 13.0141 * C22 = 9.1351 * C12 = 1.2684 HZ												
CORRES FREQS ARE * PITCH = 0.7271 * BOUNCE = 1.2684 HZ												
CORRES ANGLES * PH11 = 0.5718 * PH12 = -0.5242 RAD AND STRESS * S1 = 994.9341 * S2 = -912.0706 * S3 = 7.3209 MPA												

$C_{12}$  and  $C_{21}$  are linear, which is not the case. The difference is less than 2%.

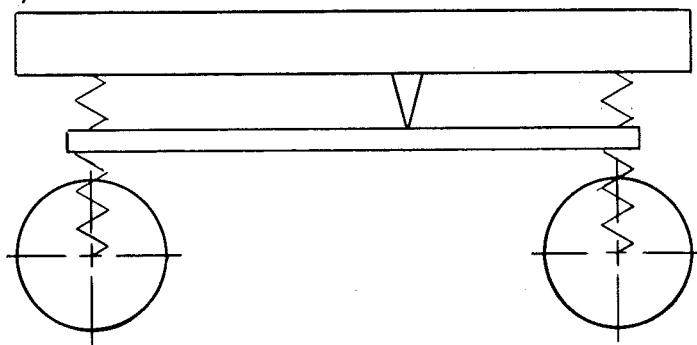
The front and rear wheel displacements relative to the vehicle body  $F_1$  and  $F_2$  are now iterated, from -100 to 100 mm in steps of 50 mm for this printout. For each of these 25 permutations all the suspension, vehicle and mechanical details discussed above are calculated and printed out.

A complete printout of the program with flowcharts and a brief description thereof is included in Appendix 2.4.2.

#### 2.4.2 Discussion of Results

Table 2.4.1 lists selected results extracted from the computer printout. The springrates  $C_{11}$ ,  $C_{22}$ ,  $C_{12}$  and  $C_{21}$  are those referred to in equation (2.2.1).

From table 2.4.1 the rising springrate effect (section 2.4.1) is apparent. For a conventional car, for which  $C_{12} = C_{21} = 0$ , with rising rate suspension, using for example a coil spring made from tapered coil wire, the maximum values of  $C_{11}$  would occur at 100, 0 and 100,000 and for  $C_{22}$  at 0, 100 and 100,100. For the interconnected suspension systems shown in figures 2.2.1 and 2.3.1 as well as for the Packard system, maximum  $C_{11}$  and  $C_{22}$  would occur at the double bump condition of 100, 100. For this interconnected suspension, maximum  $C_{11}$  occurs at 100, -100 and maximum  $C_{22}$  at -100, 100, a feature it shares in common with the Citroen 2CV. With reference to figure 2.2.1, this suspension system would be represented as,



For a car with conventional suspension the ratio of dynamic to static wheel loadings is a maximum at both single and double bump conditions. For example, the Porsche 928 has maximum values of 1.48 and 1.62 for the front and rear respectively. For this car, with interconnected suspension, the maximum wheel loading ratios of 1.67 and 1.64 front and rear respectively, occur at the double bump condition of 100,100,

TABLE 2.4.1 Selected Printout Results

Wheel Displacement Front, Rear		0, 0	100, 100	100, -100	-100, 100	0, 100	100, 0
C <sub>11</sub>	kN/m	12.04	13.01	13.98	11.81	11.86	13.49
C <sub>22</sub>	kN/m	8.99	9.14	8.88	9.63	9.36	8.66
C <sub>12</sub>	kN/m	5.67	5.59	5.57	5.57	5.46	5.48
C <sub>21</sub>	kN/m	5.23	5.58	5.12	6.12	5.69	5.25
P <sub>1</sub> /G <sub>1</sub>		1.0	1.67	1.32	0.811	1.19	1.49
P <sub>2</sub> /G <sub>2</sub>		1.0	1.64	0.863	1.17	1.42	1.22
Bounce Frequency	cpm	74.5	76.1	76.5	75.9	75.0	75.7
Pitch Frequency	cpm	42.2	43.6	45.4	41.7	42.2	44.0
Cable T	kN	18.2	29.7	21.9	16.1	22.7	25.6
C <sub>1</sub> Stress S <sub>1</sub>	MPa	610	995	784	482	727	889
C <sub>2</sub> Stress S <sub>2</sub>	MPa	-563	-912	-475	-648	-786	-689
C <sub>3</sub> Stress S <sub>3</sub>	MPa	0	7	324	-328	-153	160

in common with the conventional suspension. However, in contrast to the conventional suspension, these reduce for the single bump conditions of 100, 0 and 0, 100 and then reduce even further for the one wheel bump and other wheel rebound conditions of 100, -100 and -100, 100, illustrating clearly the mechanism for reduced pitching.

It should be observed, that, although the springrates of  $C_{11}$  and  $C_{22}$  are a maximum at 100, -100 and -100, 100 respectively, the effect of interconnection reduces the actual wheel loading of the wheel in bounce and increases the actual wheel loading of the wheel in rebound compared to a car with conventional suspension and thus reduces the pitching.

The object of this interconnected suspension is to give large car ride quality to what is basically a short car. With a wheelbase of 2230 mm the Fiat 127 at 2223 is shorter, while others like the 2CV, VW Golf and Beetle at 2400, the Escort at 2407, the Allegro at 2438, the Fiat 128 at 2448 and the Avenger at 2489 are all longer.

The frequencies of cars like the Rover 3500 and the BMW 728 were used as a guide, while those of the Allegro were considered too high. With anti-dive and self-levelling, frequencies as low as those used by Packard cars in 1956 could be considered (see section 2.1).

Self-levelling and anti-dive (Chapter 3) are incorporated. The self-levelling is achieved by using an air-spring/damper unit between the rear suspension arm and the body. This augments the suspension system, when additional loads are placed in the rear of the vehicle, by increasing  $C_{22}$ .

Early analysis had shown, that, given the geometric restrictions of the vehicle, namely the relatively narrow track and the relatively long rear trailing arm required to accommodate the motor and pulleys and the matching long effective front leading arm, that the torsion bars would be highly stressed. The torsion bars would require through hardening, shot-peening and presetting (or scragging), SAE(1947), which would allow 965 - 1035 MPa maximum working stress, depending on the amount of settling of the vehicle that would be acceptable.

Analysis of torsion bars on a number of production cars that use torsion bar suspension was then carried out. It was found that the short-series torsion bars used on the rear of certain VW Beetles would not only fit into the Electric Town Car, but had an acceptable torsion bar spring-rate and worked at similar stresses to that required in the Electric Town Car. It made economic sense to use these bars.

The computer program was altered to analyse a series of different auxiliary torsion bars on one printout, in combination with the VW torsion bars. The resultant series of pitch and bounce frequencies was examined, and with due consideration for the dynamic to static wheel loadings, the actual pitch and bounce frequencies, the brake dive angles, the self-levelling facility, the torsion bar stresses and so on, a pitch and bounce frequency combination of 42 and 75 cycles per minute respectively was chosen.

A German reference, Gross (1966) was used for the torsion moduli of the VW bars. A maximum stress of 980 MPa was also recommended for the pure torsion condition.

Torsion bars are normally loaded in one direction. The auxiliary torsion bar is loaded in both directions, the maximum recommended stress for which is 340 to 390 MPa, Gross (1966). From table 2.4.1 it can be seen that the maximum working stress is 328 MPa. It was not therefore considered prudent to use this auxiliary torsion bar as a method of self-levelling.

The steel used for the auxiliary torsion bar was XK92631 which is nominally equivalent to En45A. After machining, the bars were oil quenched at between 920 and 930°C and tempered at 500°C as recommended in "The Mechanical and Physical Properties of the British En Steels".

The cable tension has a maximum value of 29.7 kN at the double bump configuration of 100, 100. This tension was then used to select the cable size and to design the Glacier DU suspension pivot bearings. The chassis load for the two cables is 59.4 kN.

## CHAPTER 3

### SUSPENSION GEOMETRY

#### 3.1 PITCH CHARACTERISTICS

While interconnected suspension can improve ride quality by reducing the pitch frequency and hence pitch acceleration, it can, depending on the choice of basic and interconnecting stiffnesses, produce the need for self-levelling and anti-dive geometry.

The choice of frequencies and related springrates for this vehicle are such that both self-levelling and anti-dive geometry are required. From section 2.2.2, the body tilt for the placing of 750 N over the rear axle is approximately  $2.2^\circ$  without self-levelling and for a 0.6 g braking deceleration  $-7.3^\circ$  without anti-dive geometry.

Self-levelling is achieved by using air-springs at the rear as discussed in section 2.4.2. The control for levelling is manual, using an indicator attached to one pitch control torsion bar and a small electric air compressor.

With reference to figure 3.1.1,  $pT$  is the braking force on the front wheels and  $(1-p)T$  on the rear wheels, where  $T$  is the total braking force. With outboard brakes front and rear and with the suspension geometry such that these forces are purely horizontal, then the braking moment is  $(pT + (1-p)T)h = Th$ , where  $h$  is the height of the centre of gravity above ground level. This is the condition of zero anti-dive and the body tilt is given by equation 2.2.16.

If the suspension geometry were such that the front and rear braking forces acted through the transverse axis of the centre of gravity, figure 3.1.2, then the moment would be zero and the body would not tilt. This is the condition of 100% anti-dive. If the braking forces front and rear intersected the vertical line through the centre of gravity at  $0.3 h$ , figure 3.1.3, the braking moment would be  $0.7 Th$ . This is the condition of 30% anti-dive. The percentage of anti-dive front and rear are not necessarily the same.

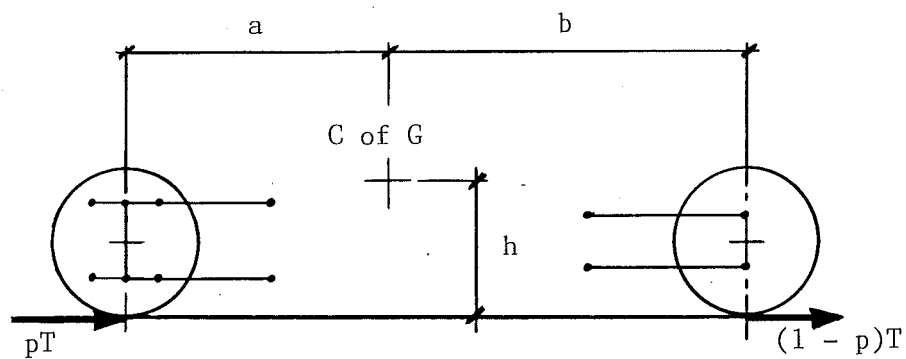


Figure 3.1.1. No Anti-Dive.

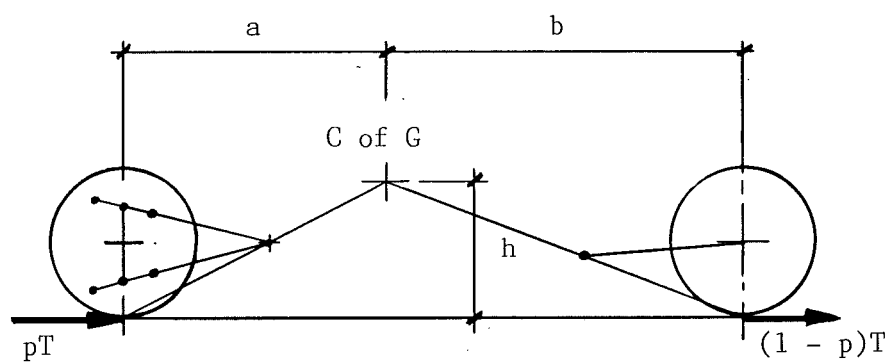


Figure 3.1.2. 100 % Anti-Dive.

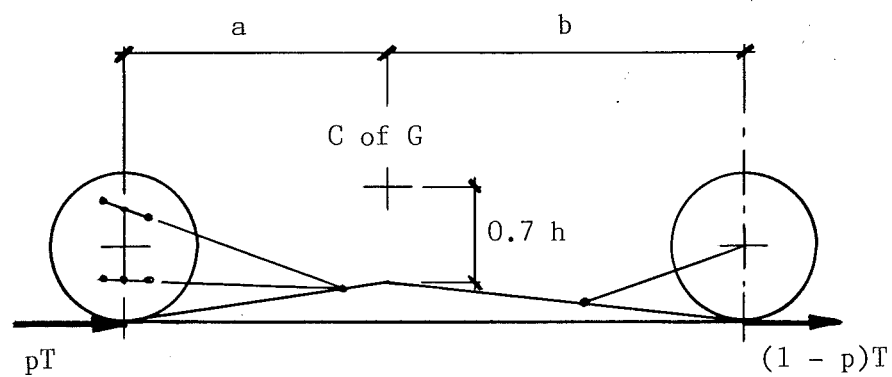


Figure 3.1.3. 30 % Anti-Dive.



Consider the front suspension geometry, figure 3.1.4, where  $a$  is the distance of the centre of gravity behind the front axle centreline, and the angle of the line of the front braking force is  $\theta_f$ . The moment due to the front wheels braking force is

$$M_f = pT(h - a \tan \theta_f) \quad (3.1.1)$$

which can be written

$$M_f = pTh \left( 1 - \frac{a \tan \theta_f}{h} \right)$$

so that if  $\frac{a \tan \theta_f}{h} = 0.3$ , then  $M_f = 0.7 pTh$  and there exists 30% anti-dive at the front.

Similarly for the rear, where  $b$  is the distance from the centre of gravity to the rear axle centre line

$$M_r = (1-p) T (h - b \tan \theta_r) \quad (3.1.2)$$

Combining 3.1.1 and 3.1.2 to give the total moment

$$M = T(h - pa \tan \theta_f - (1-p) b \tan \theta_r) \quad (3.1.3)$$

Substituting equation (3.1.3) for  $Th$  in equation (2.2.16), the body tilt angle becomes

$$\Delta\psi = - \frac{C_{11} + C_{22} + C_{12} + C_{21}}{C_{11} C_{22} - C_{12} C_{21}} \frac{T(h - pa \tan \theta_f - (1-p) b \tan \theta_r)}{L^2} \quad (3.1.4)$$

If  $\theta_f = \theta_r = 0$ , the conditions for zero anti-dive, then equation (3.1.4) reduces to equation (2.2.16).

From figure 3.1.5, the angle of the line of the front braking force  $\theta_f$  is  $8.6^\circ$ . With  $a = 1.001$  m and  $h = 0.491$  m, figure 3.1.7, this corresponds to 31% anti-dive. Nominally 30% front anti-dive is the largest percentage used. Above this, variations in castor angle with wheel displacement can become a problem.

From figure 3.1.6, the angle of the line of the rear braking force  $\theta_r = 27.9^\circ$ . With  $b = 1.229$  m and  $h = 0.491$  m, figure 3.1.7, this corresponds to 133% anti-dive. This rear suspension is such that a rear wheel braking force will produce a negative rear pitch moment and hence squatting, a feature shared with the Leyland Hydrolastic and Hydragas cars and most easily demonstrated by applying the handbrake while travelling slowly in

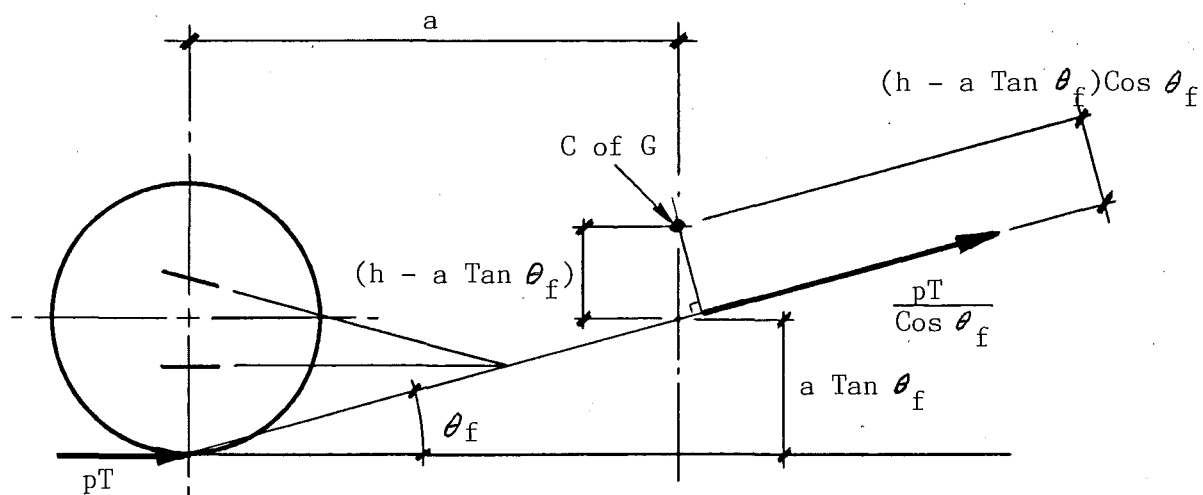


Figure 3.1.4. Side Elevation of Front Suspension Geometry.

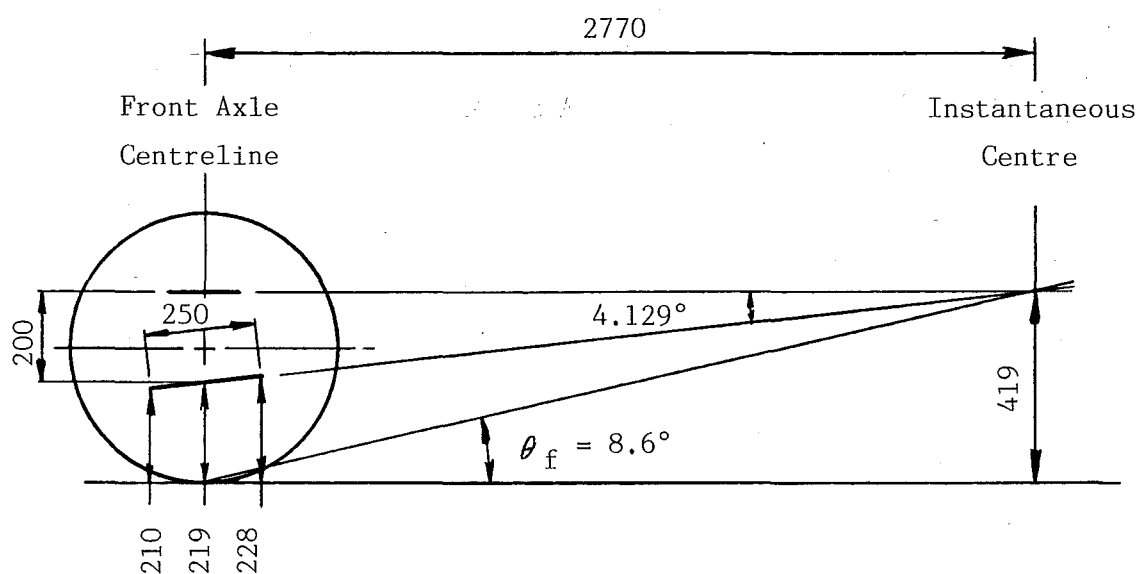


Figure 3.1.5. As Built Front Wishbone Side Elevation Geometry.  
Based on Drawing 8802 of Appendix 6.1.

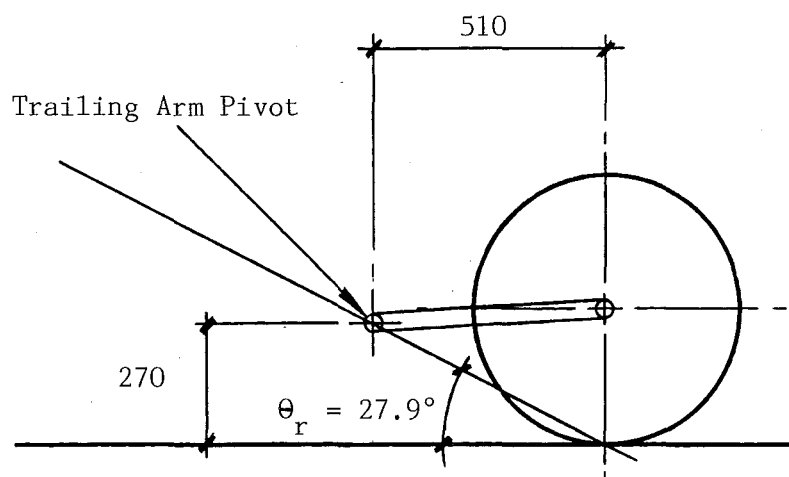


Figure 3.1.6. Rear Suspension Trailing Arm, Side Elevation.

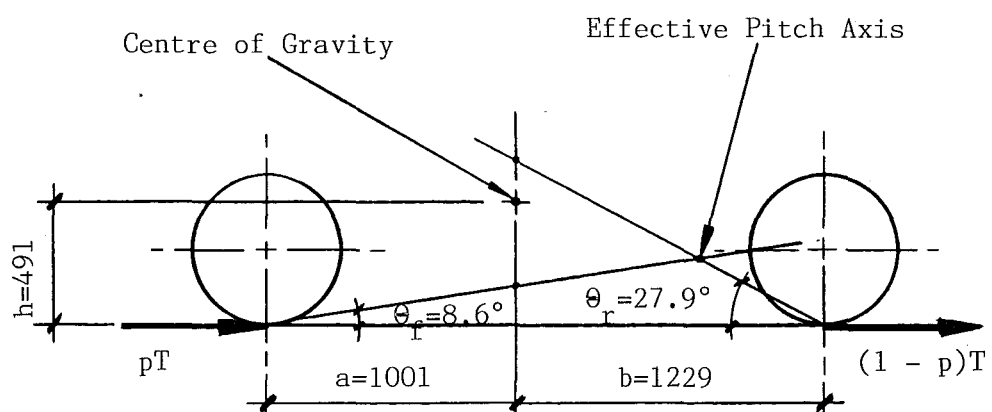


Figure 3.1.7. Vehicle Side Elevation Showing the Line of Action of Braking Forces.

either direction. Due to the short trailing arm length, the percentage anti-dive varies with wheel displacement, for example at 100,100 front, rear wheel displacement conditions,  $\theta_r$  is  $18.43^\circ$  which corresponds to 105% anti-dive.

Substituting values for  $C_{11}$ ,  $C_{22}$ ,  $C_{12}$  and  $C_{21}$  for the 0,0 position from table 2.4.1, but doubling them to convert from single wheelrates to vehicle rates, and a, b and h from figure 3.1.7, equation (3.1.4) becomes,

$$\Delta\psi = -2.341(10)^{-3} T(0.4993p - 0.1597) \text{ degrees} \quad (3.1.5)$$

The Electric Town Car has regenerative braking on the rear drive wheels only and no other rear wheel braking except the handbrake. The electrical system is set up such that initial depression of the brake pedal produces regenerative rear wheel braking only, hence  $p = 0$  for small braking values. Depressing the pedal further, brings in the conventional front disc brakes in addition to the rear wheel regenerative braking. The proportion of braking effort from the front wheels,  $p$ , will increase from zero to perhaps 0.8. From equation (3.1.5), at  $p = 0.32$   $\Delta\psi = 0$ , so that below  $p = 0.32$  the car will exhibit a tail down attitude and above  $p = 0.32$  a nose down attitude. If the electric circuit breaker were to trip under heavy braking, there would be no rear wheel braking and  $p = 1$ . Table 3.1.1 lists body tilt angles for different values of  $T$  and  $p$ .

TABLE 3.1.1 Body Tilt Angle (degrees)

$\begin{array}{c} T/Mg \\ p \end{array}$	0.1	0.2	0.3	0.4	0.5	0.6	0.7
0	0.39	0.77	1.16	1.54			
0.5	-0.22	-0.43	-0.65	-0.87	-1.08	-1.3	-1.52
0.8	-0.58	-1.16	-1.73	-2.31	-2.89	-3.47	-4.05
1.0	-0.82	-1.64	-2.46	-3.28	-4.09	-4.91	-5.73

The angle of -3.47 degrees at  $T = 0.6$  Mg and  $p = 0.8$  is on the upper limit of being acceptable for body tilt of a conventional car. The emergency condition of  $p = 1$  produces excessive body tilt angle, reduced by applying the handbrake during the said emergency. Should the body tilt angles be uncomfortably excessive in practice, the rear drum brakes can be connected into the hydraulic brake in the conventional manner.

With the electric motor on the rear suspension trailing arm (Chapter 4), tractive forces are transmitted through the trailing arm pivots, and the same theory applies for anti-squat as it did for anti-dive. Equation (3.1.4) applies, with  $p=0$  for rear wheel drive and the tractive force  $F = -T$ , so that

$$\Delta\psi = \frac{C_{11} + C_{22} + C_{12} + C_{21}}{C_{11} C_{22} - C_{12} C_{21}} \frac{F(h - b \tan \theta_r)}{L^2} \quad (3.1.6)$$

Acceleration tests with the Mk 1 Electric Car in its final state of tune in May 1978, produced an acceleration force of 1287 N. The same drive system is to be used for this vehicle. An acceleration force of 1340 N would produce an acceleration of 0.13 g and the body tilt would be -0.5 degrees.

### 3.2 ROLL CHARACTERISTICS

Just as the vehicle body exhibited pitching about an effective pitch axis (figure 3.1.7) or transverse roll axis (Steeds, 1958) due to braking forces, so too will it exhibit roll about a longitudinal roll axis due to cornering forces. While the effective pitch axis is horizontal, that is, the same height on both sides of the vehicle, the longitudinal roll axis generally is inclined to the ground, and is found by joining the individual front and rear suspension roll centres. The position of these roll centres is established from the linkage geometry in the same way as the effective pitch axis in figure 3.1.7, but by considering the suspension geometry in end elevation. The geometry left and right is generally symmetrical, so that, unlike the pitch axis, the roll centre is on the vehicle centreline.

The rear suspension comprises a pair of independent trailing arms, the pivot axis for which is horizontal with the vehicle body in end elevation and perpendicular with the body centreline in planview. The rear wheels move vertically on a single wheel bump, the roll centre is therefore at ground level. The camber angle of both rear wheels is equal in magnitude to the body roll angle at all times.

The front suspension comprises a conventional wishbone layout, chosen because: 1) anti-dive geometry can be incorporated; 2) the roll-centre height can be positioned where desirable; 3) the layout gives clearance to store the front batteries and to incorporate the interconnected

suspension leading arm; 4) dampers and anti-roll bars can be fitted easily and 5) the steering connections can be made to minimise toe-in and toe-out effects with wheel movement.

The total lateral weight transfer from the inside tyres to the outside tyres, regardless of suspension design, is  $Fh/t$ , where  $F$  is the cornering force,  $h$  the height of the centre of gravity above groundlevel and  $t$  the average track width. This total weight transfer comprises weight transfer due to the unsprung weight, front and rear, weight transfer due to the sprung weight acting at the roll centres and weight transfer due to body roll of the sprung weight.

With a nominal front weight bias, the handling characteristics of slight understeer will be produced if the weight transfer is made proportional to the front and rear weight distribution. The front and rear wheelrates are proportioned to match the weight distribution with the interconnected suspension design. From section 2.2.1, the front and rear wheel reactions are:

$$\left. \begin{aligned} P_1 &= C_{11}f_1 + C_{12}f_2 \\ P_2 &= C_{21}f_1 + C_{22}f_2 \end{aligned} \right\} \quad (2.2.1)$$

For roll conditions, with no pitching,  $f_1 = f_2$  and equations (2.2.1) become

$$P_1 = (C_{11} + C_{12})f_1$$

$$P_2 = (C_{21} + C_{22})f_2$$

so that  $(C_{11} + C_{12})$  and  $(C_{21} + C_{22})$  become the effective wheelrates, front and rear respectively.

The roll stiffness for the front is

$$\frac{\pi}{180} \cdot \frac{t_f^2 (C_{11} + C_{12})}{2} = 254 \text{ Nm/degree}$$

and for the rear

$$\frac{\pi}{180} \cdot \frac{t_r^2 (C_{21} + C_{22})}{2} = 191 \text{ Nm/degree}$$

where  $t_f = 1.282 \text{ m}$  and  $t_r = 1.240 \text{ m}$  are the respective vehicle tracks. Wheelrates  $C_{11}$ ,  $C_{12}$ ,  $C_{21}$  and  $C_{22}$  are obtained from table 2.4.1 using the 0,0 bounce condition. The front roll stiffness is further increased by

the installation of an anti-roll bar. The front suspension has the higher roll stiffness, so that it will receive the larger portion of weight transfer due to body roll.

The weight transfer due to the unsprung weight is greater at the rear. The motor and steel trailing arm have an unsprung weight of approximately 50 kg per side, compared to 15 kg per side at the front.

Weight transfer due to the sprung weight acting through the rear roll centre is zero as the roll centre height is at ground level. The roll centre at the front needs to be approximately at ground level also, to retain the balance. If the front roll centre height is increased a little above ground level, this increases the weight transfer due to the sprung weight acting at the roll centre, but decreases the weight transfer due to body roll, which would be beneficial as the front roll stiffness is greater than the rear. A front roll centre height of 35 mm above ground level was chosen as being consistent with the above and producing acceptable camber variation with bump and roll, without deviating too much from the characteristics of the rear suspension. The chosen layout fits well into the confined space of the front of the body used for the Electric Town Car.

The roll axis is therefore inclined to the ground, being 35 mm above ground at the front and at ground level at the rear. Normally the axis would be higher at the rear. The height of the roll axis at the centre of gravity position is 19.5 mm. The weight transfer due to body roll for a 0.5 Mg cornering force, with  $h = 0.491$  m and  $M = 1050$  kg, is 2428 Nm, and with a combined front plus rear roll stiffness, ignoring the front anti-roll bar, of 445 Nm/degree, the body roll is an acceptable 5.46 degrees.

In order to ascertain the roll centre height and camber variation of the front wishbone suspension for all bounce and rebound conditions a computer program WISHANAL, standing for "Wishbone Analysis", was written. The coordinates of the suspension are inputted as a set of seven coordinates, figure 3.2.1, together with the bounce and rebound limits required to be analysed. The program calculates and prints all the relevant lengths and angles, specifically isolating the length of the upper and lower suspension arms as well as the kingpin angle. A sample output printout is included here, while a complete printout of the program with flowcharts and a brief description thereof is included in Appendix 3.2.

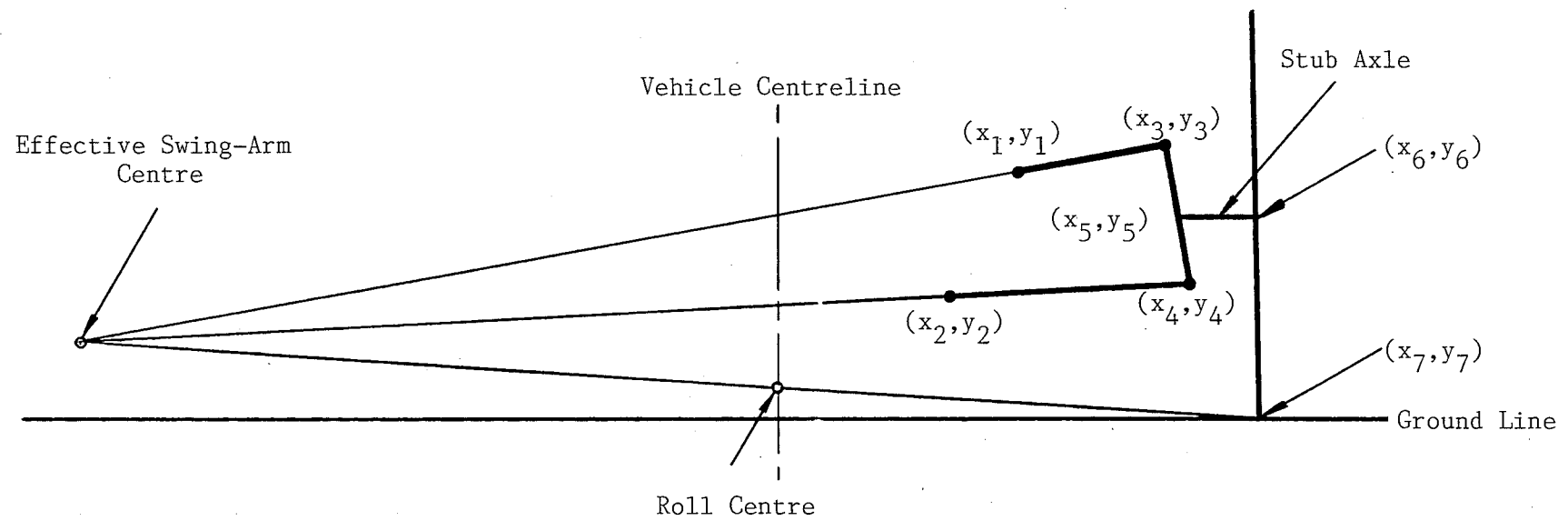


Figure 3.2.1. Wishbone Suspension, Front Elevation.



# PRELIMINARY ANALYSIS OF WISHBONE SUSPENSION GEOMETRY

	X-COORD	Y-COORD
1	330.0	419.0
2	262.0	219.0
3	522.0	414.0
4	555.0	207.0
5	0.0	0.0
6	632.0	240.0
7	637.0	0.0

TO CALCULATE FOR BOUNCE AND REBOUND  
100 100

LENGTH OF UPPER ARM IS 192.065

LENGTH OF LOWER ARM IS 293.246

LENGTHS	L12	L13	L24	L34	L35	L36	L37
	211.244	192.065	293.246	209.614	666.243	173.367	429.675
ANGLES	AX12	AX13	AX24	AX34	AX35	AX36	AX37
	-1.899	-0.026	-0.041	-1.413	-2.471	-0.883	-1.300
ANGLES	A435	A436	A437				
	-1.058	0.529	0.113				

KINGPIN ANGLE = 4.035

SCRUB IS POSITIVE OUTWARDS

	K	Y7	RY	RY-Y7	CAMBER	SCRUB	SARM	RATIO
*	0	0.000	35.418	35.418	-1.023	0.000	13887.968	10.901
*	25	25.921	34.152	8.631	-1.280	0.880	3598.710	2.825
*	50	51.705	34.223	-17.483	-1.851	0.691	2067.577	1.623
*	75	78.701	37.287	-41.413	-2.771	-0.571	1413.204	1.109
*	100	106.821	45.553	-61.268	-4.221	-2.866	1031.493	0.810
*	0	0.000	35.418	35.418	-1.023	0.000	13887.968	10.901
*	-25	-24.890	36.360	61.250	-1.078	-1.896	6399.862	5.023
*	-50	-49.068	34.557	83.625	-1.481	-4.674	2258.269	1.773
*	-75	-72.290	25.026	97.315	-2.321	-8.043	1459.415	0.910
*	-100	-93.974	-6.404	87.570	-3.786	-11.351	616.642	0.484

For each bump and rebound condition specified, the following is calculated and printed.

- K, the deviation in y-coordinate of the upper-outboard balljoint  $(x_3, y_3)$  from its static condition. The upper balljoint was chosen rather than the more logical bottom balljoint because the program has the facility for the lower arm, defined by  $(x_2, y_2)$  and  $(x_4, y_4)$ , to be horizontal or any other fixed angle, in all conditions. The lower arm can physically be a leading arm. Bounce is positive, rebound is negative.
- Y7, the y-coordinate of the tyre/ground contact point.
- RY, the instantaneous roll-centre height relative to the vehicle.
- RY-Y7, the instantaneous roll-centre height relative to the tyre/ground contact point.
- CAMBER, the camber angle of the tyre, that is the angle the wheel centreline makes to the vertical. Negative camber is the top of the tyre leaning towards the centre of the vehicle. CAMBER assumes no body roll.
- SCRUB, the lateral (sideways) displacement of the bottom of the tyre (road interface) from its static position. Scrub is positive outwards.
- SARM, the instantaneous swingarm length, that is the length of the line, parallel to the stub axle, from the instantaneous swingarm centre (where the top and bottom suspension arms geometrically intersect) to the wheel centreline.

$$\text{RATIO} = \frac{\text{SARM}}{\text{TRACK}} = \frac{\text{swing-arm length}}{\text{distance between front wheel centres}}$$

The camber variation with bounce is deliberately small for the outside more highly loaded wheel, so as to match closely the characteristics of the rear outside wheel, where there is no camber variation with bounce. For the 0.5 Mg corner, where the body roll is approximately 5.46 degrees, the outer rear wheel has a positive camber of 5.46 degrees and the inner rear wheel has a negative camber of 5.46 degrees, while the outer front wheel, with an effective wheel displacement of 61 mm, will have a positive camber of 3.3 degrees and the inner front wheel a negative camber of 7.4

degrees. The values of scrub, effective swing arm length and its ratio to the vehicle track, complete the picture of how the particular suspension geometry is working.

It is possible to carry out a more complete analysis of weight transfer and body roll, (Bastow, 1980), and steady-state cornering behaviour, (Radt and Pacejka, 1963), (Pacejka, 1973), but these would require more detailed information on individual front and rear centre of gravity positions, roll moments of inertia, tyre characteristics (Gough, 1954), (Setright 1972) and so on. The economics of using the existing anti-roll bar and some as built suspense tuning and development, if necessary, provides the solution.

## CHAPTER 4

### REAR SUSPENSION TRAILING ARM

#### 4.1 DRIVE SYSTEM

It had been proposed, Vandendungen (1976), to use a single Synchro-belt drive for each of the two driven rear wheels, with the motor and pulleys attached to the rear suspension trailing arm. A double-reduction belt drive had been successfully used on the earlier Electric Car prototype, with occasional belt-tooth jumping during regenerative braking.

The existing system was analysed, working backwards to establish the appropriate belt tensions and service factors actually being used. These tensions and factors were applied to the single belt drive system indicating unacceptable belt widths of between 76 and 90 mm depending on the actual ratio chosen. It was known that stronger belts were available, Hartley 1976. Powergrip HTD Belts from Uniroyal were investigated indicating a width of 50 mm might be possible if non-standard tensions and service factors were used. Technical correspondence was entered into with Uniroyal in England, concerning the proposed 50 mm belt and is included in Appendix 4.1. From the correspondence of Powergrip Industries in Australia, 17 July 78, it can be seen that the cheapest option, with duty excluded, was \$970.84 for a set of steel pulleys and a pair of 1280 mm belts. The equivalent using three-strand chain and standard steel and cast iron pulleys was \$190, chain was subsequently used.

#### 4.2 SUSPENSION ARM

The rear suspension arm as originally proposed, (Vandendungen, 1976), was to comprise an aluminium mounting plate with a cast or fabricated aluminium or steel beam structure around the back of the motor, extending from the stub axle to the inner end of the torsion bar mounting tube. With the restriction of the body used for this vehicle, with its narrow rear track, plus the need for the provision of wider belts (although chains were subsequently chosen), a small increase in tunnel/backbone width and optional use of the more powerful but longer MAl12M electric motor (standard motor is MAl00L) as well as a preference to be able to remove the motors from the

car without partially dismantling the suspension arm, all meant that there was insufficient space between the back of the motor and the chassis for such a beam. This led to the development of an all-plate type rear suspension trailing-arm, drawings 7937/1 and 7956 of Appendix 6.1, made from steel for ease of manufacture and for stiffness, and of minimum depth to allow the arm, complete with motor, to fit under the rear seats in the maximum bump configuration.

With a rear track for this vehicle, of 1240 mm, all the cars used for comparison in section 2.4.2 have a wider rear track. The Citroen 2CV at 1260 mm is only 20 mm wider, while the Escort, Fiat 127, Avenger, Fiat 128, VW Golf, VW Beetle and Allegro in ascending order, are wider, the Allegro with a rear track of 1391 mm is 151 mm wider.

As the diameter of the driven pulley is approximately the same as the wheel diameter, the side plate of the rear suspension arm was extended to protect the belt and pulley and form part of the belt guard.

The use of the Uniroyal Powergrip HTD Toothed Belts, or any other toothed belt, meant that the alignment of the driver and driven-pulleys was critical, as too much misalignment would cause the belt to run off. The object then was to design the rear suspension arm so that the angular misalignment between the shaft of the electric motor and the rear wheel stub axle, was, under all load conditions, within the tolerance allowable for the toothed belt drive. Finite Element Analysis provides a means of determining this misalignment.

The author had used the Finite Element Program PAFEC 70+ previously but, in collaboration with Dr. J. Astley of the University, it was decided that the more sophisticated PAFEC 75 would be more suitable for this task. It was also intended to analyse the chassis structure using Finite Element Analysis. PAFEC 75 has the facility to prepare element data rapidly, using Pafblocks to analyse anisotropic materials and reinforced plastics, and has other advantages over PAFEC 70+. The program PAFEC 75, although available, had not been run on the B6700 at the University of Canterbury before. The debugging process took a considerable amount of time and eventually precluded the analysis of the chassis using Finite Element Methods.

Figure 4.1 illustrates the output from phase 3 of the PAFEC 75 program, showing a plot of the input data, produced to confirm that the geometrical data has been inputted correctly. Figure 4.2 illustrates the output from phase 8 showing a plot of the displaced shape of the suspension arm. Appendix 4.2 gives a brief description of the phases of the PAFEC 75

0.33673  
1

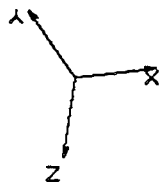
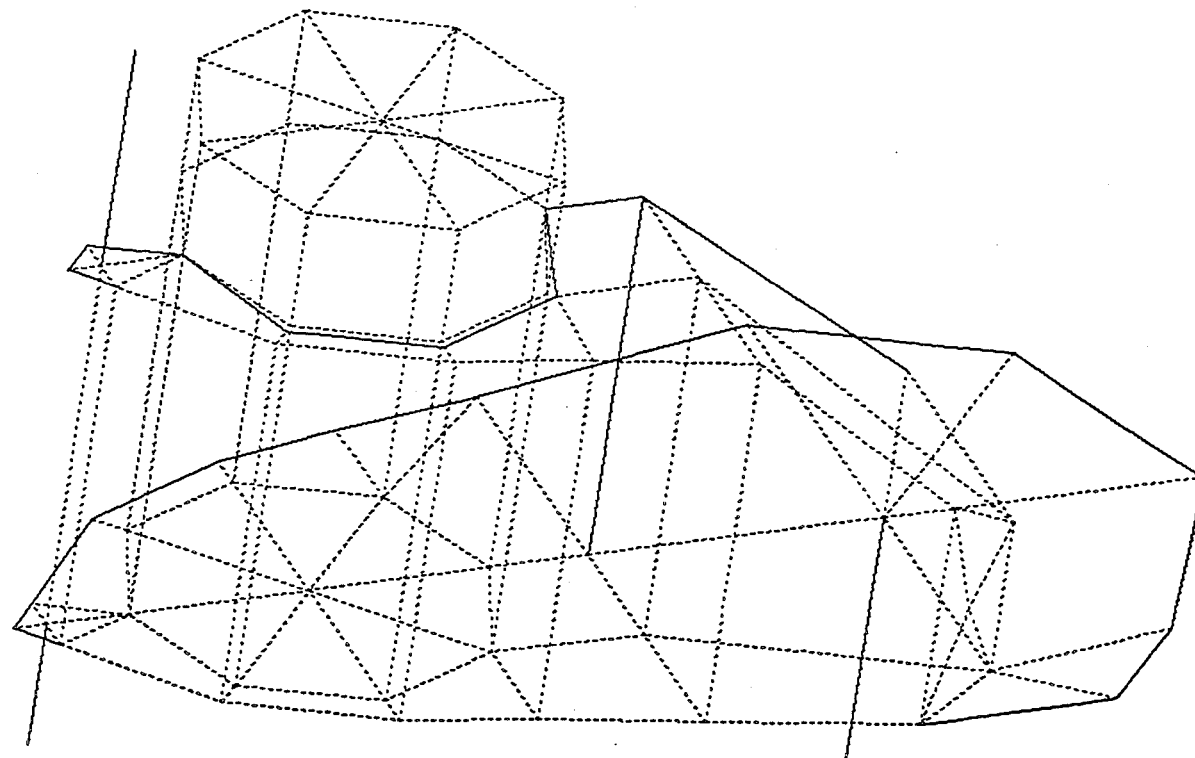


Figure 4.1. Output from Phase Three.  
Drawing of input data to visually confirm  
data has been inputted correctly.

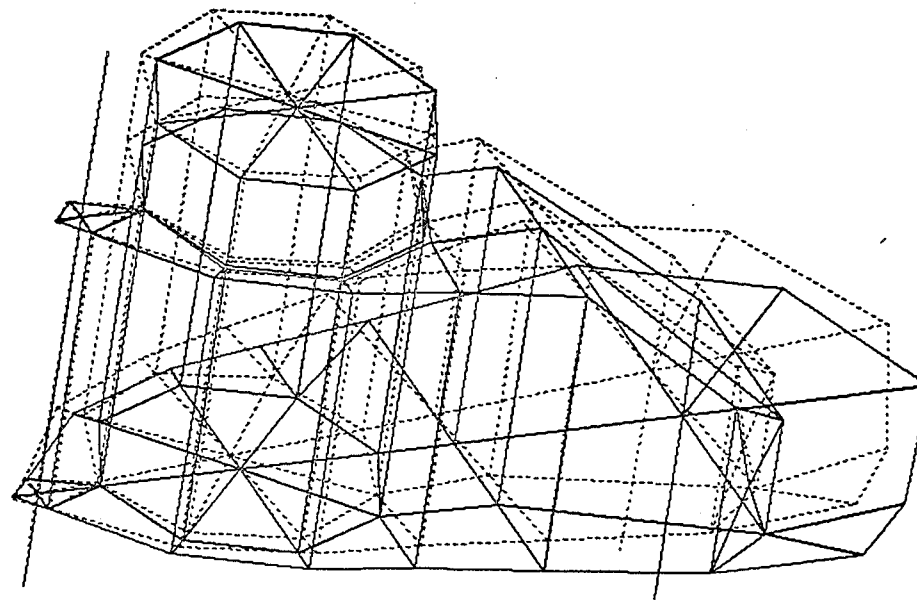


Figure 4.2. Output from Phase Eight.  
Drawing of displaced shape.

0.25928  
Z

0.007070

program, summarizes how the data is prepared and lists the input data used.

Three load cases are considered, the actual forces for which are detailed in Appendix 4.2. Load case 1 is the static 1 g condition. Case 2 is an effective 4.5 g vertical wheel loading. It is agreed that between 2.4 g and 3 g is a safe total wheel load (static plus dynamic overload) (Andrew and Whittaker, 1969 ; Sharman, 1976), but a 50% overload is considered to design purposes to account for fatigue and provide durability, (Costin and Phipps, 1961 ; Skattum, Harris and Howell, 1975); hence a 4.5 g loading. Load case 3, allows for a 3 g vertical wheel loading, combined with a 2 g lateral loading and a 2 g braking load which will cover cornering and braking on a rough road (Skattum, Harris and Howell, 1975).

From the displacement/rotation output, phase 7, illustrated in Appendix 4.2, the misalignment of the driver and driven pulleys was found to be an acceptable 1.7 degrees for load case 2. The subsequent use of chain drive meant that this misalignment was not so critical. The portion of the arm rearward and nominally above the stub axle to protect the belt and pulley was no longer as important, and could be removed to reduce unsprung weight as discussed in Appendix 4.2.



## CHAPTER 5

### CHASSIS LAYOUT AND DESIGN

#### 5.1 LAYOUT

The general layout, Figure 5.1.1, features a backbone chassis with eight batteries located between the front wheels and six beneath each of the front seats. The rear suspension trailing arms (Chapters 3 and 4) incorporating the electric motors are located beneath the rearward facing rear passengers. The front suspension is a conventional double wishbone suspension and incorporates anti-dive geometry (Chapter 3). The inverters are located under the rear seat between the trailing arm suspension units.

By considering the plan area of the car and comparing it with the combined plan area of wheels and suspension, passengers, batteries, motors and inverters it is apparent that some overlap is required. Having the front passengers sitting above six batteries each and the rear passengers above the rear suspension motors and inverter provides the solution. With all four passengers facing forward, it is normally necessary for the feet of the rear passengers to extend beneath the rear portion of the front seat, however, with this space occupied by batteries, other things being equal, the wheelbase needs to be increased. For safety reasons the batteries should not extend significantly beyond the front line of the front tyres. The front interconnecting torsion bar must fit between the rear of the front batteries and the front passengers, producing a further increase in wheelbase.

Different orientations, layouts and seating arrangements were then postulated, drawn and analysed. Although it is commonly found (Grylls), that the conventional seating arrangement takes up the least space, in this instance it was found that a more compact car could be designed with the two rear passengers facing backwards. This layout was adopted, with the rear seats nominally designed for a 50% male. It was subsequently reported that a proposed (Guess, Nial and Pocobello, 1977) and subsequently built (Shacket, 1979), General Electric Current Technology Electric Vehicle also utilized rear passengers facing backwards.

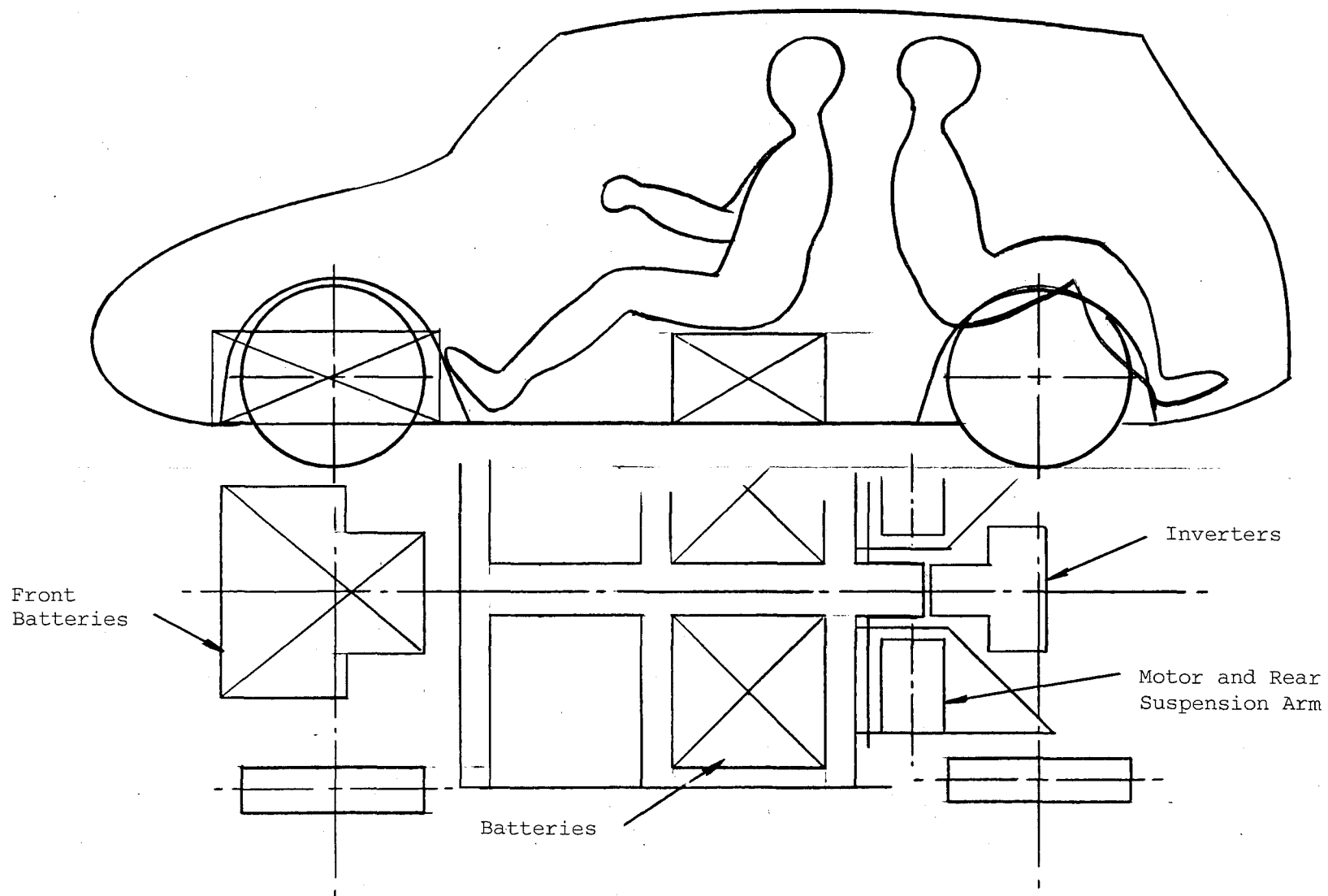


Figure 5.1.1. General Layout.

The backbone chassis is I-shaped in planview, and while the rear suspension is mounted directly to, and behind the rear cross-piece, with side batteries in front of the rear cross-piece, the front suspension and front batteries were to be cantilevered off the front cross-piece. The front batteries and suspension would be supported using a sub-assembly, incorporating progressive crushing and designed to deflect the batteries downward and the main chassis upward in a major front collision, thus preventing battery intrusion into the passenger compartment and protecting passengers from acid. Energy is absorbed in stopping the 131 kg eight battery pack at the front of the car, by the progressive crushing mechanism and by the work done in lifting or deflecting the main chassis structure upward. SAE 740040 gives information on the axial impact crushing (as opposed to buckling) of closed hat structures when loaded axially. The size and thickness is chosen so as to crush at particular impact conditions. The use of the A40 Farina (section 5.3) body meant that the energy absorbing front sub-assembly could not be incorporated, for although the complete floor structure was removed from the Farina body and replaced with a grp-foam sandwich structure, the existing front wheelarch structure which incorporated the suspension mounts and original engine mounts was not changed.

## 5.2 METHODS OF CONSTRUCTION

For vehicles in limited volume production and with the layout as described in section 5.1, two of the more obvious methods of construction are,

- (1) a steel backbone chassis with suspension components attached thereto with a separate glass reinforced plastic (grp) body, and
- (2) a complete grp-foam sandwich structure combining the function of body and chassis. The final choice of which may well depend on the design and the production facilities available when manufacture proceeds.

For a complete car a torsional stiffness of 6780 Nm/degree ( $\pm 50\%$ ) and a deflection of 1.3 mm ( $\pm 50\%$ ) under a centrally applied load of 6.67 kN is considered acceptable (Boden). Over a wheelbase of 2.23 m, for the Electric Town Car, this implies a torsional rigidity of 15119 Nm<sup>2</sup>/degree ( $\pm 50\%$ ). The steel I-shaped backbone chassis is readily able to be analysed using normal solid mechanics, (Benham and Warnock, 1973) where for example a steel backbone of outside dimensions 300 mm x 150 mm and a thickness of 0.914 mm has a torsional rigidity of 10933 Nm<sup>2</sup>/degree, without

bodywork. The steel-backbone would take the suspension loads directly, leaving the moulded grp body structure to support the batteries, inverters, passengers etc. The battery loads are such that extensive use of grp - foam - sandwich would be required. This body could be rubber mounted to the backbone chassis thus reducing the transmission of road noise and the like. The complete mechanical system, comprising chassis, front suspension, rear drive-unit suspension, with appropriate interconnection could be built up and then mated to the body, a practical arrangement for limited volume production.

The steel backbone would normally be chosen because of the combined effects of heat, vibration and concentrated loading due to the internal combustion engine on a grp structure. The Electric Town Car has no such combination of problems. The effect of concentrated suspension loads can be reduced by using a wide load base, by feeding large inertia loads directly into the suspension and by appropriate detail design and development.

While the tensile strength of certain grp composites is comparable to, and the specific strength in excess of steel and aluminium, grp composites have a modulus of elasticity approximately an order of magnitude below that of aluminium and steel (Warring, 1971). The properties of grp composites are dependent on the choice of resin and the type and form of glass reinforcement, and are well documented (for example Parkyn, 1970). Further, the reproducibility of the properties is also dependent on moulding and layup techniques and the glass/resin content, so reduced mechanical properties should be used (Oleesky and Möhr, 1964). For a more technical treatise on the subject of reinforced plastics MIL-HDBK-17A (1971) should be consulted.

In order to overcome the problems associated with the relatively low elastic modulus, it is necessary to incorporate curvature or stiffening ribs into the mouldings or to use sandwich construction (Parkin). The use of sandwich construction and in particular sandwich construction using a foam core is of interest. The grp facings provide the strength and the foam, acting rather like the web on an I-beam, produces the separation and thus the mechanism for the increased rigidity. The grp facings are considerably thinner than in the non-sandwich construction and therefore are susceptible to buckling or wrinkling if unsupported. The foam core must therefore support the compression facing against wrinkling and buckling, allowing it to develop its full compressive strength.

Of the three most common rigid plastic foams available, polyurethane is the most practical for this application, pvc the best structurally and polystyrene the least suitable. Polystyrenes are somewhat limited to mass-production techniques, they are not adaptable to in-situ application, are chemically attacked by polyester resins (though not by epoxies) and are susceptible to static creep, (Ferrigno, 1967). A cross-linked, fluoro-carbon-gas-filled PVC foam was developed by a French Company, Kleber Colombus S.A. and first used for military purposes in 1950. It exhibits higher strength/weight values than most rigid polyurethane foams and is ideally suited for a foam core in a grp-foam sandwich panel, however it is considerably more expensive than polyurethane rigid foams and cannot be foamed in-situ, (Harper, 1975). Rigid Polyurethane foam has been used in a number of diverse applications, its choice in most cases being dependent on four characteristics that distinguish it from similar materials, (Backus and Geinhardt, 1973).

- (1) Urethane foams are easily prepared from liquid raw materials.
- (2) Properties can be changed by appropriate selection of raw materials and foam density.
- (3) Thermal conductivity is the lowest among the common insulating materials.
- (4) Mechanical strength is high at low density.

An Experimental Plastic Car, developed by Bayer in Düsseldorf (October 1967) demonstrated the versatility of urethane foam. The car used a load-bearing base unit, that completely replaced the conventional chassis. The base unit and front fenders are a sandwich construction with outer skins or shells of epoxy-fibreglass and the cavity filled with rigid urethane foam ( $96 \text{ kg/m}^3$ ). The rear fenders are rigid urethane foam-core sandwich construction, with thermoplastic facings. The bonnet and boot are made from a special high density rigid urethane foam using a technique called Reaction Injection Moulding (RIM). The Citroen-Mahari (a specialized off-road vehicle) used a self-supporting floor assembly consisting of two shells of glass reinforced polyester, with urethane foam injected between them, resulting in a very stiff sandwich structure, (Hablitzel, 1973). Under conditions of extreme stress, a  $64 \text{ kg/m}^3$  urethane has been found to provide excellent durability, the foam has been used as a core for helicopter blades, upon which the leading edge spar and trailing edge skin are bonded, (Ferrigno, 1967).

It was proposed that the first vehicle to this electric town car design be made by glassing over a foam buck, rather like making a surf-board. That is, the chassis would be made into the final shape in foam and the glass reinforced plastic applied to that. For any subsequent but identical cars, the original would be used to make a pair of moulds. The skins produced from these moulds would be bolted or bonded together and the foam moulded between them in-situ, producing the sandwich structure. This method of construction restricts the foam to the thermosetting polyurethane foam, which forms a strong adhesive bond with a wide range of substrates including metals, glass and wood (Beadle) and with both polyester and epoxy grp laminates (Giles) provided they are free of grease. It would be necessary to use epoxy resin for the first vehicle as this would provide the necessary adhesion to the foam, in the first instance, whereas polyester resin would not (Beale, 1962).

The use of reinforced plastic-polyurethane core sandwich construction is extremely versatile, whether used as a unitary body/chassis construction or in combination with a steel backbone chassis. The mechanical properties of polyurethane foam are approximately proportional to the foam density (Ferrigno, 1967), so that the shear strength and modulus (bending) and compressive strength (buckling and wrinkling of the facings) can be tailored to the particular application. The resins can be chosen for chemical resistance and/or fire retardation properties in the polyesters and can be used adjacent to each other in the same lay-up. Epoxies are self-extinguishing and offer excellent chemical resistance, they are stronger though more expensive than the polyesters. The thickness of the facings can be varied to suit stress levels and can be locally thickened at points of load application or inserts can be utilized. The choice and orientation of rovings and cloth, (chopped strand mat is not normally used for such structural applications), can produce a facing that is orthotropic or quasi-isotropic or anywhere in between, so that the directional strength of the facings can be aligned with the principal stress directions. While glass fibres are the most common reinforcement, aramid fibres such as Kevlar 49 can also be considered for selected reinforcement in this application, (Anon, 1974; Jarrell, 1977; Clements and Chiao, 1977).

In order to establish accurately the principal stress directions in, and the rigidity of, the unitary chassis/body structure, it was planned to analyse the structure using the finite element method. Although this was not done (section 4.2), literature research had been completed to determine the location of different types (beam, plate, etc.) of

elements to produce the most computer cost effective and yet realistic results (Horvath, 1975; Hedges, Norville and Gurdogen, 1971; Radaaj, Zunmer and Geissler, 1970 ; Hessel and Lammers 1971; Alaylioglu and Ali, 1977), and the type of analysis, static and dynamic, (Peterson, 1971 ; Ali, Hedges and Mills, 1971).

### 5.3 ADAPTION OF A40 FARINA BODYWORK

The Electric Town Car as built utilizes conventional steel bodywork with a grp-foam sandwich floor and backbone structure. The car body is based on an Austin A40 Farina with extensive modifications so that only the side panels, side doors, side windows, windscreen, roof and front suspension support structure remain. The decision to utilize an existing body to provide the outer skin, doors and windscreen was made as an economy and time saving measure. The Farina was chosen because it had a wheelbase consistent with the Electric Town Car requirements and it was known to have a good aerodynamic shape, (White, 1967).

The modifications to the body included removing the front fenders above an existing longitudinal horizontal seam and welding in a replacement internal panel, replacing and lowering the front headlights to the minimum regulation 600 mm, attaching a grp nose to the front of the car and an appropriate grp bonnet, as well as fabricating a large gas strut assisted lift-up rear door. The floor was completely removed, some steel structure was added for mounting suspension components and to provide an interface for the grp-foam sandwich floor. These structural modifications are detailed on the drawings in Appendix 6.1.

### 5.4 GRP FOAM SANDWICH ANALYSIS AND CONSTRUCTION

The use of the A40 Farina bodywork provides a considerable amount of stiffness both in bending and in torsion to the extent that the grp. sandwich structure will not be fully tested. The grp sandwich floor panels were designed to withstand the 3 g battery inertia loading, and the backbone checked for deflection. The floor panel was made by foaming polyurethane rigid foam in-situ between two glass reinforced polyester panels thus simulating the production situation, while the front and rear crosspieces and the battery surround were made by glassing over rigid polyurethane foam using epoxy resin. Because of creep characteristics, at a sustained

loading generally only 50% of the tensile strength of thermoplastics and 70% in the case of thermosetting materials is usable (Hablitzel, 1973). Experiments on the creep of rigid urethane foam in shear (Hartsock, 1967), indicate that the creep deflection tends to level off after a period, dependent on the foam density and level of stress. Experiments indicate that foamed in-situ urethane foam is anisotropic, though it is far from orthotropic in the same sense that a honeycomb is orthotropic, (Sayigh, 1966). The strength properties across the rise are generally 60% to 80% of those in the direction of foam rise (Beadle). It has been suggested (Hartsock, 1966) that the shear strength (though not shear modulus) of in-situ foam mouldings could be as low as one-third that of free rise foams of similar density if care is not taken to minimise flow during foaming.

The side batteries and five of the front batteries are supported directly by the floor panels. The side batteries are the worst case, with a uniformly distributed loading of  $q = 4.45$  kPa in the static case, on a panel size of 472 x 420 mm. Using ECK-12 glass woven roving, 363 gm/m<sup>3</sup>, nominal thickness 0.46 mm with a warp x weft count (per inch) of 10 x 9, and orientating this in three layers at 0°/45°/90° will produce a quasi-isotropic grp facing, which for design purposes may be considered as isotropic. While the foam is anisotropic, it is at least continuous (honeycomb cores for example are not) and it is suggested (Allen, 1969) that it be considered isotropic for design purposes. The problem simplifies considerably to one of an isotropic face and an isotropic core. Further, if the facings are considered as membranes, the central deflection of a panel of any aspect ratio can be obtained (Erickson, 1950) using the formula

$$W_{\max} = \frac{qa^4 \lambda_f}{IE_f} \alpha_1 (1 + S\alpha_2)$$

where  $a = 0.42$  m (the short side) and  $b = 0.472$  m and for  $a/b = 0.89$ ,  $\alpha_1 = 0.0051$  and  $\alpha_2 = 1.65$ . Where  $\nu$  is Poissons ratio,  $\lambda_f = 1 - \nu^2 = 0.947$ .

$$S = \frac{ct\pi^2 E_f}{2a^2 \lambda_f G_c} = 1.59$$

Using the appropriate reduced mechanical properties for ECK-12,  $\sigma_f = 152$  MPa and  $E_f = 14$  GPa in polyester resin, and for 96 kg/m<sup>3</sup> polyurethane  $G_c = 8$  MPa and  $\tau_c = 706$  kPa (not reduced). For an overall panel thickness of 25 mm, and individual facing thicknesses  $t = 1.38$  mm each, the core thickness  $C = 22.24$  mm, then



$$I = \frac{t_f}{2} (C + t_f)^2 = 3.85 (10)^{-7}$$

and maximum deflection is 0.45 mm ( $w/a = 1/935$ ) in the static condition and maximum deflection is 1.35 mm ( $w/a = 1/312$ ) in the 3 g inertia load condition.

The maximum bending moment is  $M = \beta \cdot q \cdot a^2$  (Oleesky and Mohr, 1964), where for  $a/b = 0.89$ ,  $\beta_a = 0.0570$ ,  $\beta_b = 0.0493$  and  $\gamma = 0.4417$ , so that  $M = 134.3$  Nm (using 3 g inertia load). The maximum facing stress  $\sigma_f = M/t_c \cdot t_f$  where  $t_c = C = 22.24$  mm and  $t_f = t = 1.38$  mm is 4.38 MPa. The maximum core shear stress  $\tau_c = 2 \gamma q a / (t + t_c)$ , with  $t = 25$  mm is 105 kPa. The sandwich panel is therefore satisfactory, and with a static core shear stress of 35 kPa, creep will not be a problem, although the static deflection 0.45 mm will be expected to increase, perhaps doubling to approximately 1 mm (Ferrigno, 1967).

The deflection of the central backbone tunnel made up of the same 25 mm sandwich panel as above, was found to be 0.08 mm under the 6.67 kN centrally applied load as discussed in section 5.2.

The panels as built, in error, by the grp subcontractor had chopped strand mat between the woven rovings which effectively doubled the thickness of the facings. This will not double the strength or stiffness, as chopped strand mat is not as strong or stiff as woven rovings. An increase in stiffness of 50% might be expected, (Waring, 1971).

## CHAPTER 6

### CONCLUSION

The proposed Electric Town Car is being built. It has been possible to accommodate four adults in this small car by having the rear passengers facing rearwards, above the rear suspension drive unit and each of the front passengers above six batteries.

Low rolling resistance and low aerodynamic drag has been achieved by using a simple but efficient drive system utilizing a single reduction chain drive to each of the rear wheels and by aerodynamic modifications to improve the drag coefficient of the bodywork, which was based on an A40 Farina bodyshell, itself recognized to have low drag coefficient. Special low energy-loss tyres are used.

The requirements of comfortable vehicle ride are met by the use of a torsion-bar interconnected suspension, allowing the pitch frequency to be reduced to nominally 42 c.p.m., and the bounce frequency maintained at nominally 75 c.p.m. The suspension geometry has been chosen to maintain body pitch and roll angles at acceptable levels during braking and cornering. Self-levelling is required to compensate for static load variation.

An electric motor and chain drive is incorporated in each rear suspension arm. Toothed belt drive was originally proposed, and the rear arm was designed to minimise deflections during severe loading, to avoid belt run-off, resulting in suspension arms of excessive weight.

Two methods of body/chassis construction are proposed and discussed. The use of a steel backbone chassis and fibreglass body will require less development time before manufacture can commence, whereas the unitary fibre-glass-foam sandwich construction method is likely to be more economical to manufacture, as the separate chassis is eliminated but requires more design and development time. The electric town car as built incorporates features from both methods of construction.

REFERENCES

- ALAYLIOGLU, H. and ALI, R., (1977) "Body Shell Analysis by Hybrid Stress Finite Elements", Automobile Engineer, Vol.2, No.1, Feb/Mar. 1977.
- ALI, R., HEDGES, J. L., and MILLS, B., (1971), "Static Analysis on an Automobile Chassis Frame, from The Application of Finite Element Techniques to the Analysis of an Automobile Structure, I. Mech. E. Proceedings - Automobile Division; Proc. 1970-71, Vol. 184, 44/71.
- ALI, R., HEDGES, J. L., AND MILL, B., (1971) Dynamic Analysis of an Automobile Chassis Frame, I. Mech. E. Proceedings - Automobile Division, Proc. 1970-71, Vol.184, 44/71.
- ALLEN, H. G., (1969) Analysis and Design of Structural Sandwich Panels, Pergamon Press, 1969.
- ANDREW, S. and WHITTAKER, M. W., (1969) Vehicle Service Loads - Suspension Component Loads in Four Passenger Cars. MIRA Report 1969/10.
- ANON, (1977) Machine Design, June 9, 1977.
- ANON, (1974) Properties and Uses of Kevlar 49 Aramid Fibre and of Reinforced Plastics of Kevlar 49. Technical Information Bulletin No. K-1, Du Pont De Nemaours International S.A., Geneva, June 1974.
- BACKUS, J. K., and GEINHARDT, P. G., (1973) Rigid Urethane Foam, Chapter 9 of Plastic Foams Part 2, edited by Frisch, K. C., and Saunders, J. H., Marcel Dekker Inc., N.Y., 1973.
- BAKER, A., (1973) From Hydrolastic to Hydrogas. Journal of Automotive Engineering 4, 3 (copy Dec. 1973, Vol.81, No.3), (June 1973).
- BASTOW, DONALD (1974) Vehicle Attitude Changes Due to Acceleration and Braking. The Journal of Automotive Engineering, Feb. 1974.
- BASTOW, DONALD, (1980) Car Suspension and Handling, Pentech Press (1981).
- BEADLE, J. D., Processing Plastics, MacMillan Engineering Evaluations.

- BEALE, R. F., (1962). Glass Reinforced Plastics, Draughtsmen's and Allied Technicians Association, Surrey, England, 1961-1962 session.
- BENHAM, P. P., and WARNOCK, F. V., (1973). Mechanics of Solids and Structures, Pitman Publishing 1973.
- BODEN, E. E., Some Aspects of Vehicle Ride.
- BULMAN, D. N., (1976). Mathematical Suspension Modelling. Automotive Engineer, Feb. 1976.
- BYERS, D. J. and HARMAN, R. T. C. (1975). "A novel means of control of AC motors in a new concept of electric town car". The Institution of Engineers (Australia) Conference of Electrical Transportation, Adelaide, October 30-31, NCP No. 75/8, pp 13-7.
- BYERS, D. J., (1977). "The University of Canterbury electric car, Part 1, The electric town car - a viable alternative". Proceedings of Electrotechnical Group, NZIE, Vol.4, issue 1(E), 1977, pp 79-98.
- CLEMENTS, L. L., and CHIAO, T. T., (1977). Engineering Design Data for an Organic Fibre/Epoxy Composite. Composites, April 1977.
- COSTIN, MICHAEL and PHIPPS, DAVID (1961). Racing and Sports Car Chassis Design, B. T. Batsford Ltd, 1961.
- ELLIS, J. R., (1973). Effects of Suspension Design on the Attitudes of a Car During Braking and Acceleration. Proc. Instn. Mech. Engrs. 1973, Vol.187 58/73.
- ERICKSEN, W. S., (1950). Effects of Shear Deformation in the core of a Flat Rectangular Sandwich Panel. Deflection under uniform load of sandwich panels having faces of unequal thickness, U.S. Forest Products Laboratory Report 1583-C, Dec. 1950.
- FERRIGNO, T. H., (1967). Rigid Foam Plastics. Reinhold Publishing Corp. 2nd Edition, 1967.
- GILES, G. J., Body Construction and Design. Automobile Technology Series. Iliff Books, London.
- GILES, J. G., (1968). Steering Suspension and Tyres. Iliffe Books Ltd, Automotive Technology Series, Volume 1.
- GIVENS, LARRY, (1975). Packard Torsion-level Suspension. Automotive Engineering, July 1975.

- GOUGH, V. E., (1954). Cornering Characteristics of Tyres. Automobile Engineer, April 1954.
- GROSS, SIEGFRIED (1966). Calculation and Design of Metal Springs. German edition 1960, English edition edited by R. Haynes 1966.
- GRYLLS, S. H., Passenger Car Comfort. The Private Car, Institute of Mechanical Engineers, London.
- GUESS, R. H., NIAL, W. R., and POCOBELLO, M. A., (1977). Design of a Current Technology Electric Vehicle. General Electric Corporate Research and Development Report No. 77CRD124, May 1977.
- HABLITZEL, H., (1973). The Plastic Car, SAE 730465.
- HARMAN, R. T. C. (1977). "The University of Canterbury electric car, Part II. The vehicle design philosophy". Proceedings of Transportation and Traffic Engineering Group, N.Z.I.E., Vol.4, issue 4 (Tr), pp 453-66.
- HARMAN, R. T. C. and BYERS, D. J. (1980). "An AC induction motor electric vehicle". Proceedings of Electric Vehicle Exposition EVE-80, Flinders University, South Australia, pp.469-88.
- HARPER, D. A., (1975). (Editor), Handbook of Plastics and Elastomers. McGraw-Hill Book Company, 1975.
- HARTLEY, JOHN., (1976). Engine Design Series - Timing Drives. I. Mech. E. Automotive Engineer, Vol.1, Number 5, June/July 1976.
- HARTLEY, JOHN, (1977). BMW 7 Series, Automotive Engineer, Oct/Nov. 1977.
- HARTSOCK, J. A., (1966). Experiments on Shear and Buckling in Foam. Filled Pannels. Journal of Cellular Plastics, November 1966.
- HARTSOCK, J. A., (1967). Experiments on the Creep of Rigid Urethane Foam in Shear. Journal of Cellular Plastics, February 1967.
- HEDGES, J. L., NORVILLE, C. C., and GURDOGAN, O., (1970). Stress Analysis of an Automobile Chassis Frame from the Application of Finite Element Techniques to the Analysis of an Automobile Structure, I. Mech. E. Proceedings - Automobile Division, Proc. 1970-71, Vol.184, 44/71.
- HESSEL, J. J., LAMMERS, S. J., (1971). Solution of Automotive Structural Problems Using the Finite Element Method and Computer Graphics SAE 710243.

- HORVATH, JACK K., (1975). Structural and System Models SAE 750135.
- JANEWAY, R. N., (1948). Vehicle Vibration Limits to Fit the Passenger. Society of Automotive Engineers Inc., (1948).
- JARRELL, C. M., (1977). Composites Reinforced with Kevlar 49 Aramid. Society of Plastics Engineers, Regional Technical Conference Connecticut, U.S.A., 1977.
- MIL-HDBK-17A. Plastics for Aerospace Vehicles, Part 1. Reinforced Plastics, Military Handbook Department of Defence, U.S.A. January 1971.
- OLEESKY, S. S., and MOHR, J. G., (1964). Handbook of Reinforced Plastics of the Society of Plastics Industries Incorporated. Reinhold Publishing Corporation, New York, 1964.
- PACEJKA, HANS B., (1973). Simplified Analysis of Steady-state Turning Behaviour of Motor Vehicles, Parts 1, 2 and 3. Vehicle System Dynamics 2(1973).
- PARKYN, B., Designing with Composites. Institution of Mechanical Engineers.
- PARKYN, B., (1970), (Editor). Glass Reinforced Plastics. Iliffe Books London, Butterworth & Co. Ltd, 1970.
- PETERSON, W., (1971). Application of Finite Element Method to Predict Static Responses of Automobile Body Structure. SAE 710263.
- PEVSNER, J. M., (1957). Equalizing Types of Suspension. Automobile Engineer, January 1957.
- RADAJ, D., ZUNMER, A., GEISSLER, H., (1970). Finite Element Analysis, An Automobile Engineer's Tool. SAE 70338.
- RADT, HUGO, S. and PACEJKA, Hans, B. (1963). Analysis of the Steady-state Turning Behaviour of an Automobile. Symposium of Control of Vehicles. Institution of Mechanical Engineers, 1963.
- SAYIGH, A. A. M., (1966). Sandwich Beams and Panels Under Bending and Buckling Loads. University of London, Ph.D. Thesis 24986, 1966.
- SETRIGHT, L. J. K., (1972). Automobile Tyres. Chapman and Hall, 1972.

- SHACKET, S. R. (1979). The Complete Book of Electric Vehicles. Quality Books, 1979.
- SHARMAN, P. W., (1976). Saving Weight on Trailer Frames, I. Mech. E. Automotive Engineer, Vol.1, Number 5, June/July 1976.
- S.A.E. (1947). Manual on Design and Manufacture of Torsion Bar Springs by Society of Automotive Engineers, Incorporated, August 1947.
- SORSCHKE, J. H., ENKE, K., BAUER, K., (1974). Some Aspects of Suspension and Steering Design for Modern Compact Cars. SAE Paper 741039.
- STEEDS, W., (1958). Roll Axes. Automobile Engineer, February 1958.
- VANDENDUNGEN, E., (1976). Electric Town Car. Bachelor of Engineering Project Report 21a. University of Canterbury 1976.
- WHITE, R. G. S., (1967). A Rating Scheme for Aerodynamic Drag on Automobiles, MIRA Report 1967/9.

APPENDIX 2.4.1INTERCONNECTED SUSPENSION PROGRAMDATA INPUT AND ANSWER CODE HANDBOOKData Input:

All data input is stored in a single array "Data List" labelled DL. The input units are SI. The last data card must be blank (i.e. the ninth data card is blank).

Answers:

All calculation results or answers are stored in a single array labelled "ANS".



First Data Card      Format 8I5

Control Card

Columns	5	10	15	20	25	30	35	40
	ITF	ITR	IAL	ITA	IVG	LBA	ITA	
DL	(1)	(2)	(3)	(4)	(5)	(6)	(7)	(8)

ITF - Front torsion bar      0 - no data/calculations.  
                                  1 - circular torsion bar.  
                                  2 - rectangular torsion bar.

ITR - Rear torsion bar      0 - no data/calculations.  
                                  1 - circular torsion bar.  
                                  2 - rectangular torsion bar.

IAL - Arm length data      0 - no data/calculations.  
                                  1 - calculate.

IAD - Initial arm data      0 - no data/calculations.  
                                  1 - calculate.

IVG - Vehicle geometry      0 - no data/calculations  
                                  1 - calculate.

LBA - Load/brake/accel-  
                                  eration      0 - no data/calculations  
                                  1 - calculate.

ITA - Auxiliary t'bar      0 - no data/calculations.  
                                  1 - circular torsion bar.  
                                  2 - rectangular torsion bar.

DL (8)      for future use.

Second Data Card

Format 8F 10.4

Front Torsion Bar

ITF = DL(1)

ITF = 0

Blank card.

ITF = 1

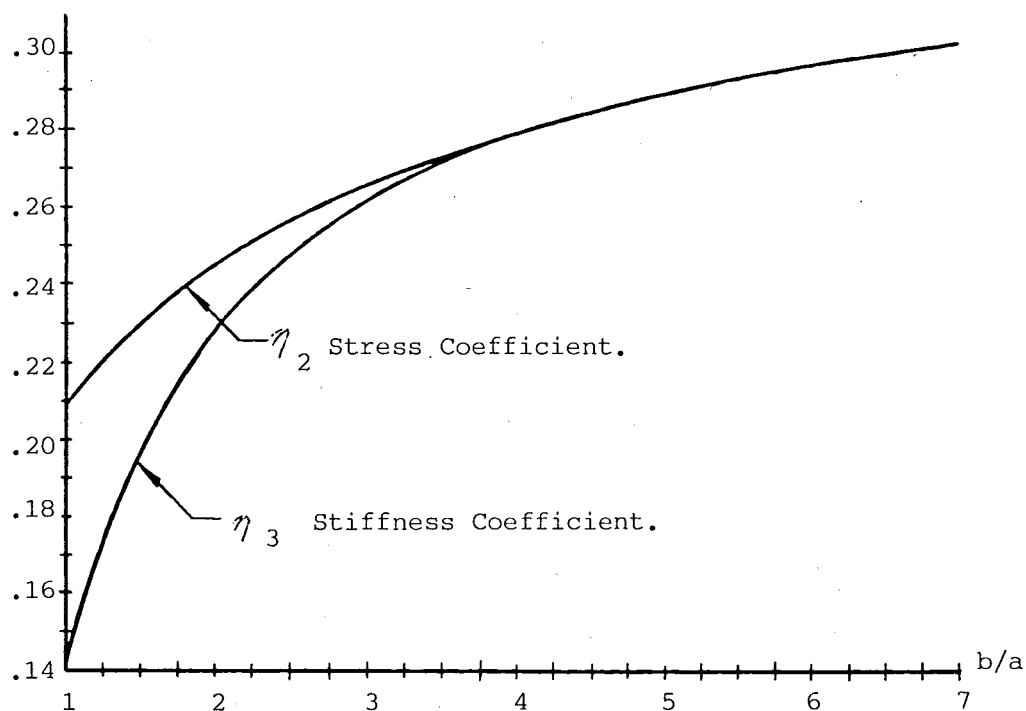
Circular torsion bar.

Columns	10	20	30	40	50	60	70	80
	G	L	DIAM					
DL	(9)	(10)	(11)	(12)	(13)	(14)	(15)	(16)

ITF = 2

Columns	10	20	30	40	50	60	70	80
	G	L	a	b	$\eta_2$	$\eta_3$		
DL	(9)	(10)	(11)	(12)	(13)	(14)	(15)	(16)

$G$  = Shear modulus  $N/m^2$   
 $L$  = Length of torsion bar m  
 $DIAM$  = Diameter of circular section m  
 $a$  = 'Short' side of rectangular section m  
 $b$  = 'Long' side of rectangular section m  
 $\eta_2$  = Saint Venant's stress coefficient.  
 $\eta_3$  = Saint Venant's stiffness coefficient.



Saint Venant's Coefficients for Rectangular Bar in Torsion.

Third Data Card

Format 8 F 10.4

Rear Torsion Bar      ITR = DL(2)

ITR = 0      Blank card.

ITR = 1      Circular Torsion Bar.

Columns	10	20	30	40	50	60	70	80
	G	L	DIAM					
DL	(17)	(18)	(19)	(20)	(21)	(22)	(23)	(24)

ITR = 2      Rectangular Torsion Bar.

Columns	10	20	30	40	50	60	70	80
	G	L	a	b	$\eta_2$	$\eta_3$		
DL	(17)	(18)	(19)	(20)	(21)	(22)	(23)	(24)

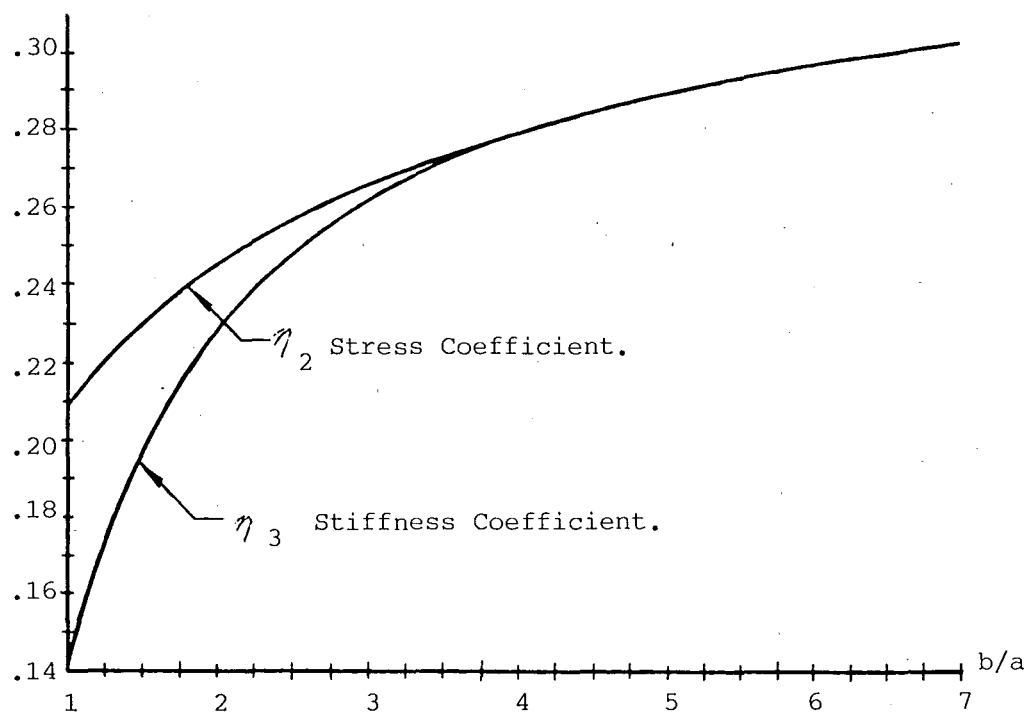
G = Shear Modulus       $\text{N/m}^2$ 

L = Length of torsion bar      m

DIAM = Diameter of circular section      m

a = 'Short' side of rectangular section      m

b = 'Long' side of rectangular section      m

 $\eta_2$  = Saint Venant's Stress Coefficient. $\eta_3$  = Saint Venant's Stiffness Coefficient

Saint Venant's Coefficients for Rectangular Bar in Torsion.

Fourth Data Card

Format 8 F 10.4

Arm Length Data

IAL = DL(3)

IAL = 0

Blank card.

IAL = 1

Actual length of arms.

Columns	10	20	30	40	50	60	70	80
	AL1	AL2	AL3	AL4	AL5	AL6	L3	
DL	(25)	(26)	(27)	(28)	(29)	(30)	(31)	(32)

AL1 = arm length 1 = Front wheel to tbar CL

AL2 = arm length 2 = Rear wheel to tbar CL.

AL3 = arm length 3 = Front tbar CL to cable joint.

AL4 = arm length 4 = Rear tbar CL to cable joint.

AL5 = arm length 5 = Front to rear tbar centre distance.

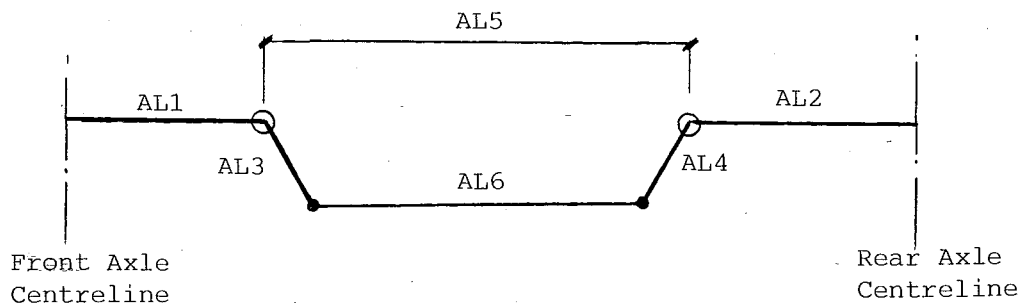
AL6 = arm length 6 = cable length.

L3 = Effective length of front pitch arm.

Note (1) As program is currently written, L3 must be specified and AL3, AL4 and AL6 are calculated, i.e. L3 is specified and AL3, AL4 and AL6 are inputted as zero.

(2) All lengths in metres.

(3) "t bar CL "means" torsion bar centreline".



Fifth Data Card

Format 8F 10.4

Initial Angle Data

IAD = DL(4)

IAD = 0

Blank card.

IAD = 1

Initial angles.

Columns	10	20	30	40	50	60	70	80
	A1	A2	A3	A4	A5	A6		
DL	(33)	(34)	(35)	(36)	(37)	(38)	(39)	(40)

A1 = Angle of front arm (AL1) from longitudinal axis. Clockwise positive.

A2 = Angle of rear arm (AL2) from longitudinal axis. Clockwise positive.

A3 = Acute angle of arm (AL3) from longitudinal axis.

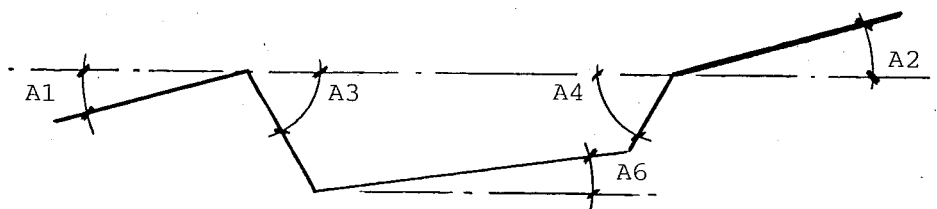
A4 = Acute angle of arm (AL4) from longitudinal axis.

A5 = 0 (Torsion bars same height).

A6 = Angle of cable from longitudinal axis.

Note (1) As program is currently written specify A3 and A4 and program calculates A6.

(2) All angles in radians.



Sixth Data Card

Format 8F 10.4

Vehicle Geometry

IVG = DL:(5)

IVG = 0

Blank card.

IVG = 1

Vehicle geometry

Columns	10	20	30	40	50	60	70	80
	WB	A	B	H	M	K		
DL	(41)	(42)	(43)	(44)	(45)	(46)	(47)	(48)

WB = Wheelbase. metres.

A = Distance of C of G from front axle as a ratio of the wheelbase  
( $0 < A < 1$ ).

B = Distance of C of G from rear axle as a ratio of the wheelbase  
( $0 < B < 1$ ).

H = Height of the C of G as a ratio of the wheelbase.

M = Vehicle mass in kg.

K = Radius of gyration as a ratio of the wheelbase.

Note:  $A + B = 1$  by definition. If  $A + B \neq 1$  the program will abort.

Seventh Data Card

Format 8F 10.4

Load - Brake - Acceleration

LBA = DL(6)

LBA = 0

Blank card.

LBA = 1

Load-Brake-Acceleration data.

Columns	10	20	30	40	50	60	70	80
	DFL	MFL	DRL	MRL	DB	MB	DA	MA
DL	(49)	(50)	(51)	(52)	(53)	(54)	(55)	(56)

DFL = Delta front load, kg.

MFL = Maximum front load, kg. (i.e. apply a variable additional static load at the front up to MFL in steps of DFL).

DRL = Delta rear load, kg.

MRL = Maximum rear load, kg. (i.e. apply a variable additional static load at the rear up to a MRL in steps of DRL).

DB = Delta braking acceleration, g's.

MB = Maximum braking acceleration, g's. (i.e. apply variable braking loads up to MB in steps of DB).

DA = Delta acceleration force, g's.

MA = Maximum acceleration force, g's. (i.e. apply variable acceleration loads up to MA in steps of DA).

Note The purpose of applying these additional loads is to examine the pitch variation due to the application of various load inputs.

Eighth Data Card

Format 8F 10.4

Auxiliary Torsion Bar

ITA = DL(7)

ITA = 0

Blank card.

ITA = 1

Circular torsion bar.

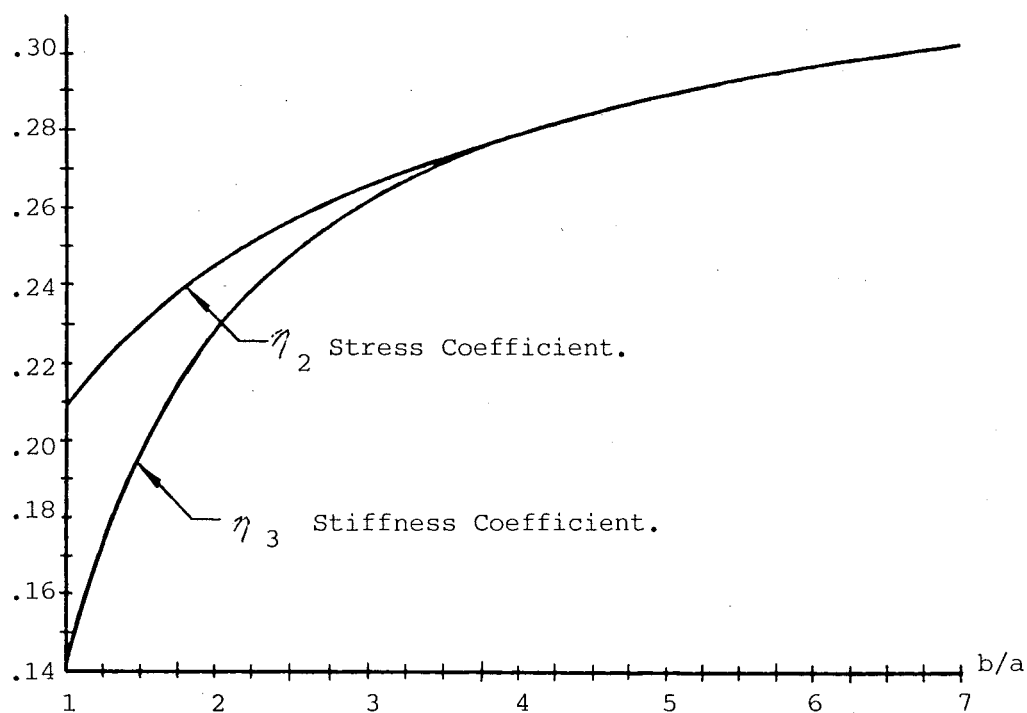
Columns	10	20	30	40	50	60	70	80
	G	L	DIAM					
DL	(57)	(58)	(59)	(60)	(61)	(62)	(63)	(64)

ITA = 2

Rectangular torsion bar.

Columns	10	20	30	40	50	60	70	80
	G	L	a	b	$\eta_2$	$\eta_3$		
DL	(57)	(58)	(59)	(60)	(61)	(62)	(63)	(64)

- G = Shear Modulus.  $\text{N/m}^2$   
 L = Length of torsion bar, m.  
 DIAM = Diameter of circular section, m.  
 a = 'Short' side of rectangular section, m.  
 b = 'Long' side of rectangular section.  
 $\eta_2$  = Saint Venant's Stress Coefficient.  
 $\eta_3$  = Saint Venant's Stiffness Coefficient.



Saint Venant's Coefficients for Rectangular Bar in Torsion.



CALCULATED RESULTS

(Array ANS. abbreviation for answers).

ANS(1) = Front torsion bar springrate, kNm/radian. =  $C_1$

ANS(2) = Front torsion bar stressrate, MPa/radian.

ANS(3) =  $C_2$  = Rear torsion bar springrate, kN m/radian.

ANS(4) = Rear torsion bar stressrate, MPa/radian.

ANS(5) =  $C_3$  = Auxiliary torsion bar springrate, kN m/radian.

ANS(6) = Auxiliary torsion bar stressrate, MPa/radian.

ANS(7) = Initial ratio of length =  $\frac{B}{A} \frac{AL1 \cos A1}{AL2 \cos A2} = \frac{l_3}{l_4}$

ANS(8) = Cable angle A6, radians.

ANS(9) = Angle of front pitch arm A3, radians.

ANS(10) = Angle of rear pitch arm A4, radians.

ANS(11) = Front locked pitch angle on front bump. Unequal pitch arms.  
(i.e. angle of front pitch arm corresponding to the condition  
in ANS(12)), radians.

ANS(12) = Rear locked pitch angle on front bump. Unequal pitch arms.  
(i.e. angle at which the rear pitch arm and the cable are in  
a straight line), radians.

ANS(13) = Front locked pitch angle on rear bump. Unequal pitch arms.  
(i.e. angle at which the front pitch arm and the cable are in  
a straight line), radians.

ANS(14) = Rear locked pitch angle on rear bump. Unequal pitch arms.  
(i.e. angle of rear pitch arm corresponding to the condition  
in ANS(13)), radians.

ANS(15) = Angle  $A_1$ , radians.

ANS(16) = Angle  $A_2$ , radians.

ANS(17) = Angle  $\theta_1$ , positive for front bump, radians.

ANS(18) = Angle  $\theta_2$ , positive for rear bump, radians.

ANS(19) = Angle  $\theta_3$ , positive for front bump, radians.

ANS(20) = Angle  $\theta_4$ , positive for rear bump, radians.

ANS(21) = Effective length  $\ell_1 = AL_1 \cdot \cos A_1$ , m.

ANS(22) = Effective length  $\ell_2 = AL_2 \cdot \cos A_2$ , m.

ANS(23) = Effective length  $\ell_3 = AL_3 \cdot \sin (A_3 - A_6)$ , m.

ANS(24) = Effective length  $\ell_4 = AL_4 \cdot \sin (A_4 + A_6)$ , m.

ANS(25) = Ratio of effective lengths  $RL_{34} = \ell_3 / \ell_4$ .

ANS(26) = Ratio of angles  $RA_{34} = \theta_3 / \theta_4$ .

ANS(27) = 
$$RATIO = \frac{\ell_3}{\ell_4} \cdot \frac{\theta_4}{\theta_3} = \frac{RL_{34}}{RA_{34}}$$

ANS(28) = Cable Tension  $T$ , kN.

ANS(29) = Front wheel displacement  $f_1$ , m. bump positive (up).

ANS(30) = Rear wheel displacement  $f_2$ , m. bump positive (up).

ANS(31) = Front wheel reaction  $P_1$ , kN.

ANS(32) = Rear wheel reaction  $P_2$ , kN.

ANS(33) = Springrate  $C_{11}$  (wheelrate), kN/m.

ANS(34) = Springrate  $C_{22}$  (wheelrate), kN/m.

ANS(35) = Springrate  $C_{12}$  (wheelrate), kN/m.  
 ANS(36) = Springrate  $C_{21}$  (wheelrate), kN/m.  
 ANS(37) = Partial bounce frequency  $\omega_z$  = PFB, Hz.  
 ANS(38) = Partial pitch frequency  $\omega_\alpha$  = PFP, Hz.  
 ANS(39) = Coupling coefficient  $\eta_{C1}$  = CC1.  
 ANS(40) = Coupling coefficient  $\eta_{C2}$  = CC2.  
 ANS(41) = Pitch frequency  $\Omega_1$  = PF, Hz.  
 ANS(42) = Bounce frequency  $\Omega_2$  = BF, Hz.  
 ANS(43) =  $\omega_z^2$  = PFB\*\*2, (radian/sec)<sup>2</sup>.  
 ANS(44) =  $\omega_\alpha^2$  = PFP\*\*2, (radian/sec)<sup>2</sup>.  
 ANS(45) =  $\Omega_1^2$  = PF\*\*2, (radian/sec)<sup>2</sup>.  
 ANS(46) =  $\Omega_2^2$  = BF\*\*2, (radian/sec)<sup>2</sup>.  
 ANS(47) = Angle  $\theta_2$  at zero wheel loading, radians.  
 ANS(48) = Angle  $\theta_2$  at zero wheel loading, radians.  
 ANS(49) =  $f_{02}$  = static front wheel deflection, m.  
 ANS(50) =  $f_{02}$  = static rear wheel deflection, m.  
 ANS(51) =  $G_1$  = static front wheel loading, kN.  
 ANS(52) =  $G_2$  = static rear wheel loading, kN.  
 ANS(53) = 2\*CC1 = Total front springrate, kN/m.  
 ANS(54) = 2\*CC2 = Total rear springrate, kN/m

ANS(55) =  $2 \cdot C_{12}$  = Total interconnected springrate, front due to rear,  
kN/m.

ANS(56) =  $2 \cdot C_{21}$  = Total interconnected springrate, rear due to front,  
kN/m.

ANS(57) =  $P_1/G_1$  = Dynamic/Static wheel load.

ANS(58) =  $P_2/G_2$  = Dynamic/Static wheel load.

ANS(59) =  $\theta_1$  = Windup angle for torsion bar  $C_1$ , radians.

ANS(60) =  $\theta_2$  = Windup angle for torsion bar  $C_2$ , radians.

ANS(61) =  $S_1$  = Stress for torsion bar  $C_1$ , MPa.

ANS(62) =  $S_2$  = Stress for torsion bar  $C_2$ , MPa.

ANS(63) =  $S_3$  = Stress for torsion bar  $C_3$ , MPa.

## APPENDIX 2.4.2

### INTERCONNECTED SUSPENSION ANALYSIS, INTERSUSP.

Purpose. To calculate suspension characteristics of the cable inter-connected torsion bar suspension as designed and built for the Electric Town Car.

Input\* Vehicle spring and physical properties plus initial lever arm length and angles.

Output\* Individual torsion bar properties, pitch arm and cable lengths and static wheel deflections.

For different permutations of front and rear bumps, the following are printed:

F1	-	front wheel displacement.
F2	-	rear wheel displacement.
P1	-	front wheel reaction force.
P2	-	rear wheel reaction force.
THT 1	-	angular displacement of A1.
THT 2	-	angular displacement of A2.
THT 3	-	angular displacement of A3.
THT 4	-	angular displacement of A4.
P1/G1	-	ratio dynamic/static force (front).

\* ref "Interconnected Suspension Program, Data Input and Answer Code Handbook".

P2/G2	=	ratio dynamic/static force (rear).
RATIO	=	$l_3/l_4 \cdot \theta_4/\theta_3 = \frac{RL34}{RA34}$
T	=	cable tension, kN.
ITS	=	number of iterations requires within program.

The following wheelrates,

C11	=	front springrate due to front displacement.
C22	=	rear springrate due to rear displacement.
C12	=	front springrate due to rear displacement.
C21	=	rear springrate due to front displacement.

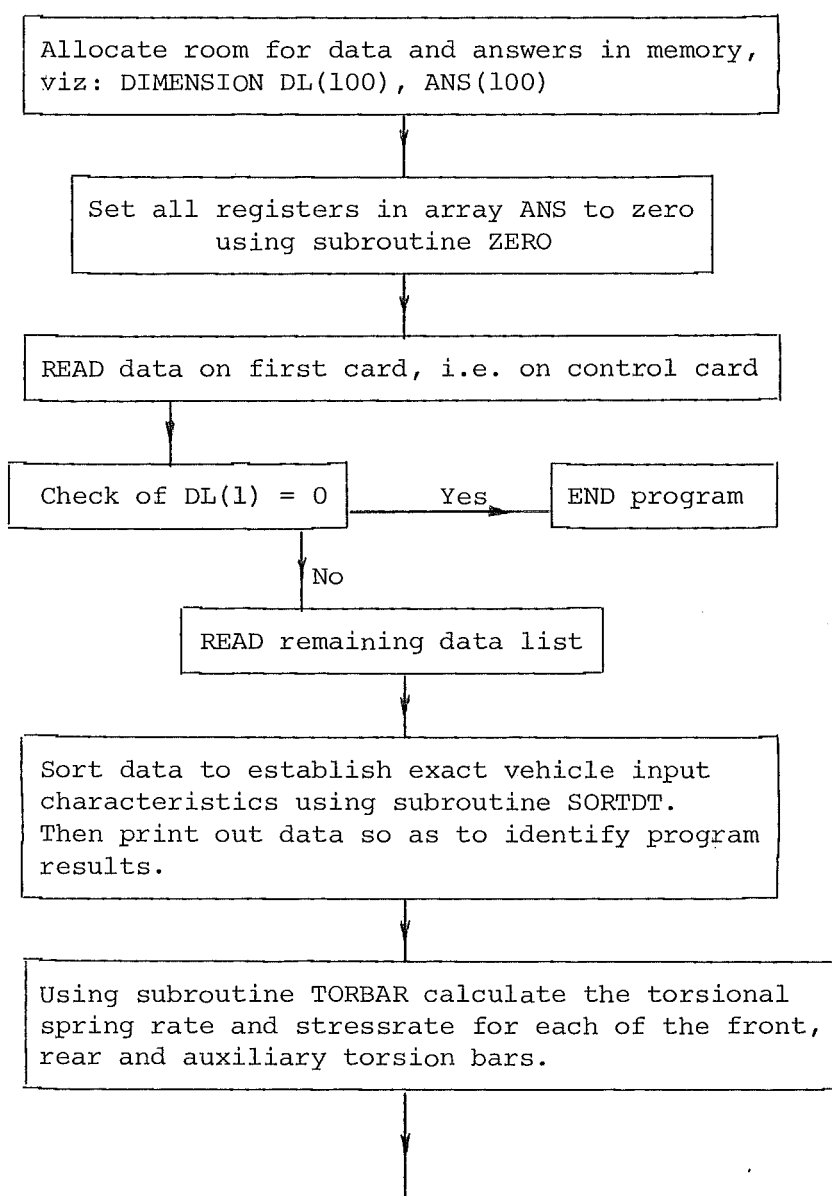
The following frequencies,

pitch frequency,  
 bounce frequency,  
 partial frequency - pitch and bounce,  
 coupling coefficients.

The following torsion bar properties,

PHI 1 = windup angle of torsion bar 1,  
 PHI 2 = windup angle of torsion bar 2,  
 S1 = stress in torsion bar 1,  
 S2 = stress in torsion bar 2,  
 S3 = stress in auxiliary torsion bar.

#### FLOWCHART



Calculate effective length of rear pitch arm, then the actual length of the front and rear pitch arms, the cable length and the initial cable angle. Further, calculate the angles for both front and rear arms, when they become locked, i.e. when either arm and the cable are in a straight line, for both front and rear bumps using subroutine ARMLTH.

Using subroutine STDEFL with  $F1 = F2 = 0$  calculate  $P1$ ,  $P2$ ,  $THT\ 1$ ,  $THT\ 2$ ,  $THT\ 3$ ,  $THT\ 4$ ,  $P/G_1$ ,  $P/G_2$ ,  $RATIO$  and  $T$ . In the static condition  $F1 \neq F2 = THT\ 1 = THT\ 2 = THT\ 3 = THT\ 4 = 0$  and  $P1/G1 = P2/G2 = 1.0$ . With  $P/G = 1.0$  then  $P1$  and  $P2$  as calculated are in fact  $G1$  and  $G2$ , i.e. the static wheel loading.

Further, in the condition where  $P1$  and  $P2 = 0$ , recalculate the angles  $THT\ 1$  and  $THT\ 2$  which correspond to the initial front and rear torsion bar wind up angles. Calculate also the static deflection front and rear.

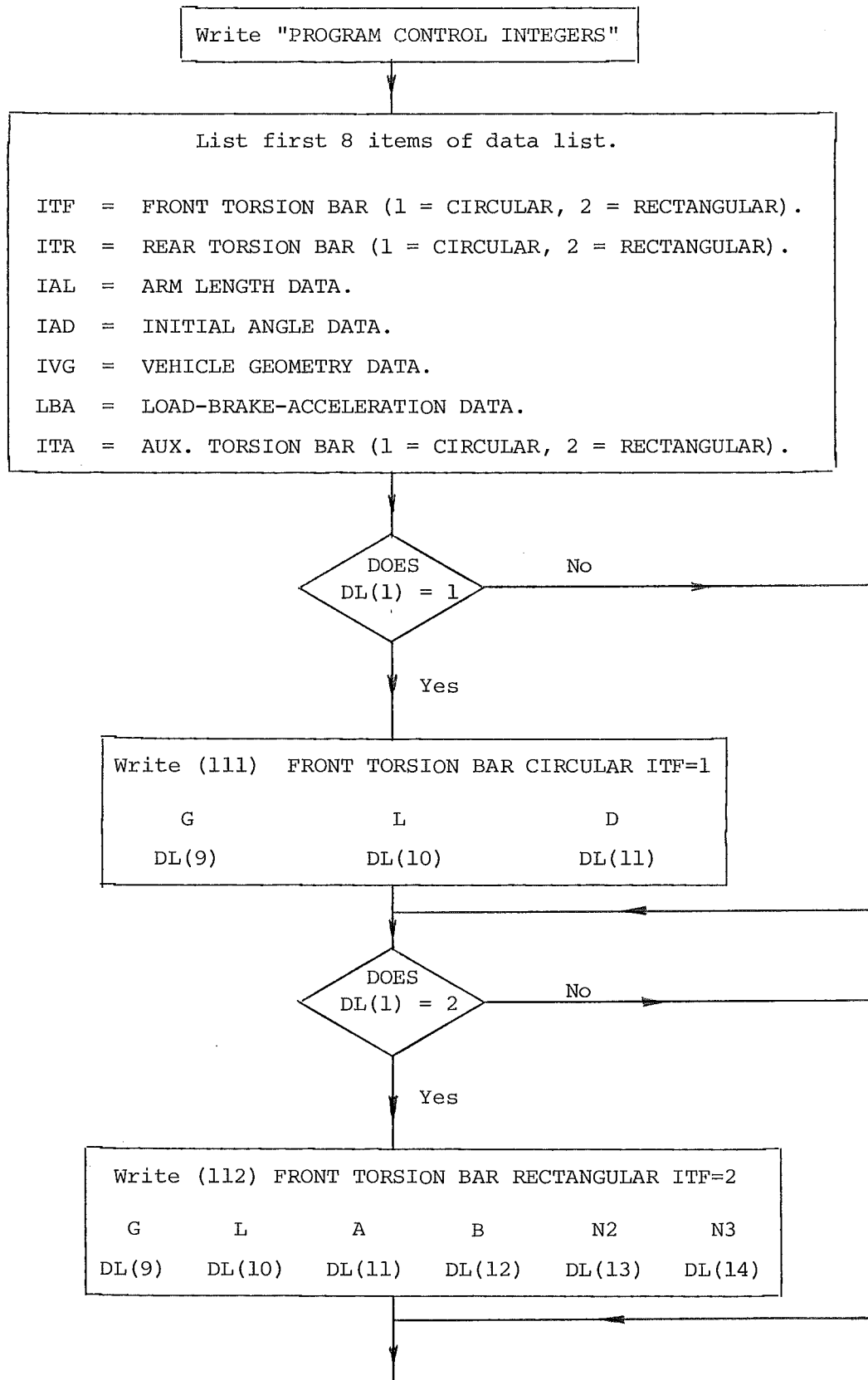
Using subroutine BUMP calculate suspension characteristics for different permutations of bounce and rebound, i.e. different values of  $F1$  and  $F2$  both positive and negative.

For each permutation print  
 $F1$ ,  $F2$ ,  $P1$ ,  $P2$ ,  $THT1$ ,  $THT2$ ,  $THT3$ ,  $THT4$ ,  $P/G1$ ,  
 $P/G2$ ,  $RATIO$ ,  $ITS$ ,  $C11$ ,  $C22$ ,  $C12$ ,  $C21$ ,  $PF$ ,  $BF$ ,  
 $PPF$ ,  $CC1$ ,  $CC2$ ,  $PHI1$ ,  $PHI2$ ,  $S1$ ,  $S2$  and  $S3$ .

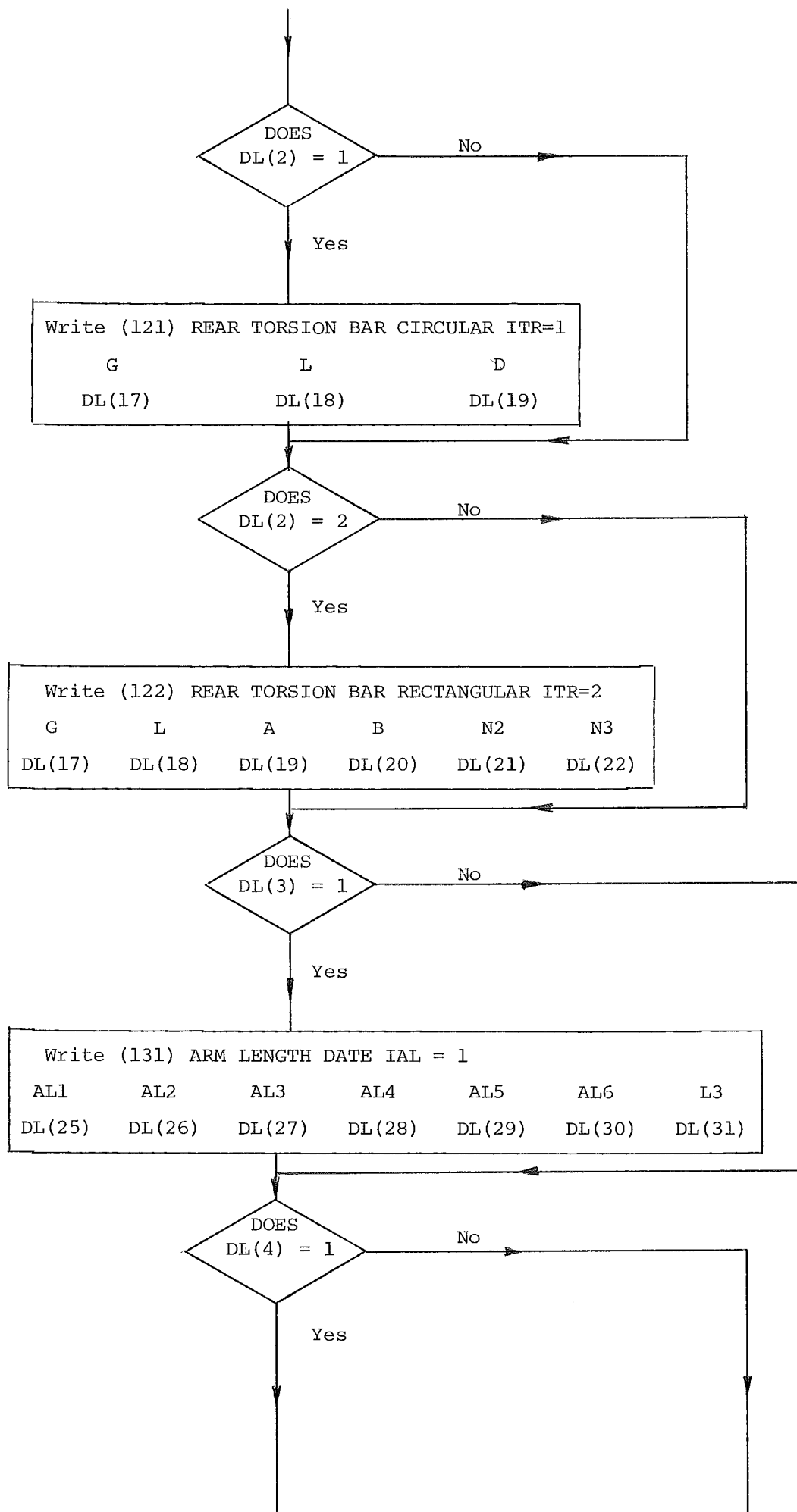
END PROGRAM

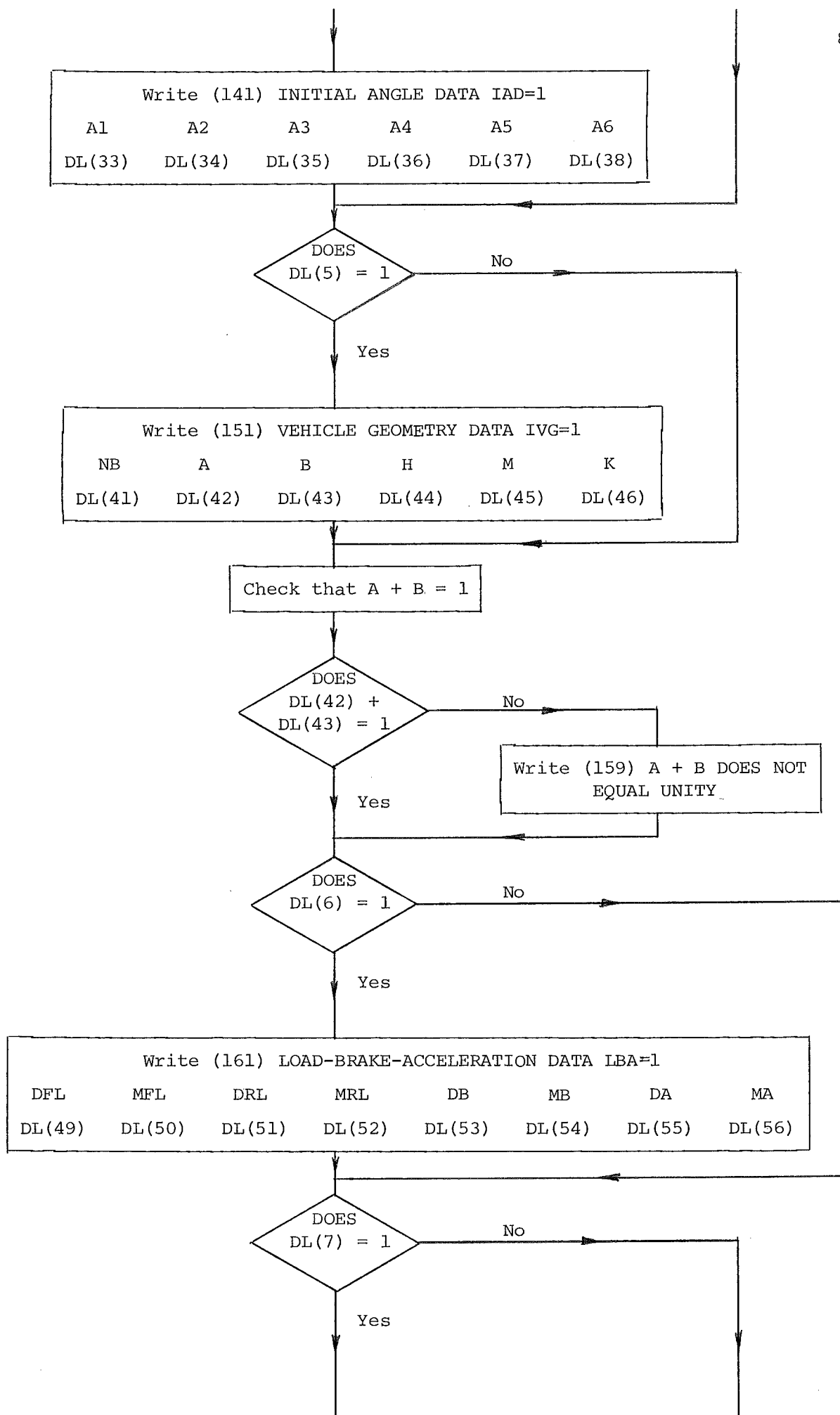
SUBROUTINE SORTDT (DL)

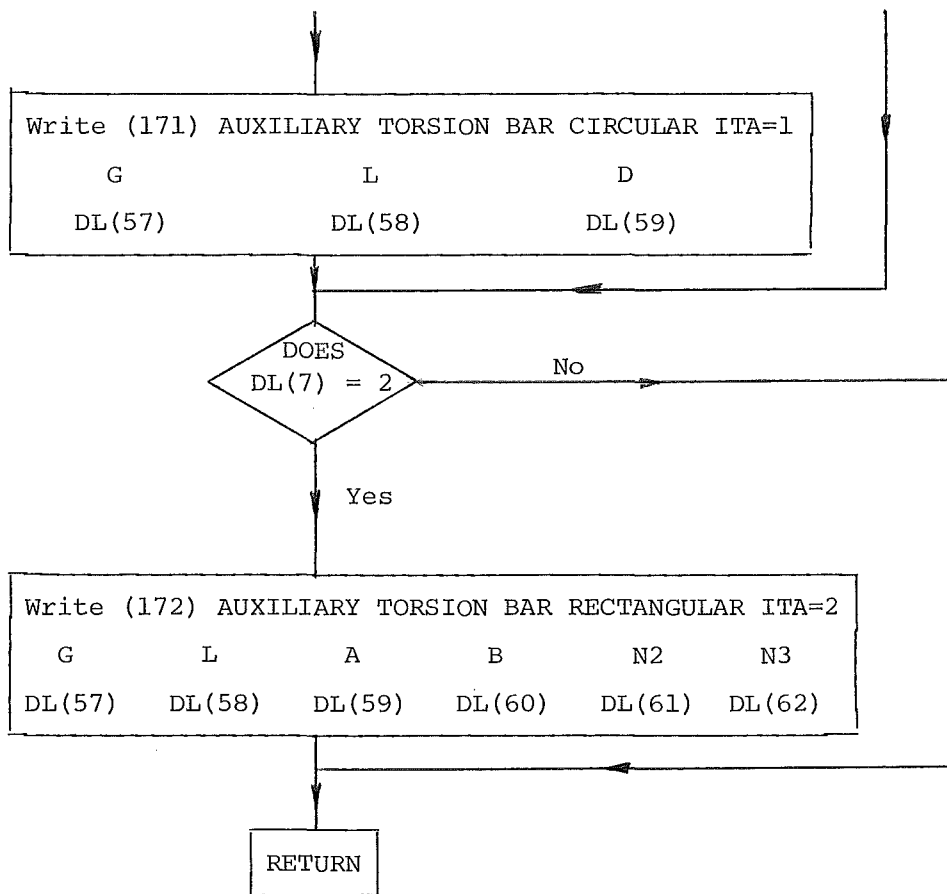
Purpose: To sort and write data.

FLOWCHART









# SUBROUTINE TORBAR (DL, ANS)

Purpose. To calculate the torsional springrate in kNm/radian and the stressrate in MPa/radian of the front, rear and auxiliary torsion bars as either circular or rectangular torsion bars.

Input. The relevant data has been read into the "data list" array. By calling the "data list" into the subroutine, no further input is required.

The numeric value of DL(1), DL(2) and DL(7) determine whether the front, rear and auxiliary torsion bars respectively are circular or rectangular.

Output. Having used DL(1), DL(2) and DL(7) as control integers, the appropriate torsional springrate and stressrates are calculated.

	<u>Torsional Rate</u>	<u>Stressrate</u>
Front	ANS (1)	ANS (2)
Rear	ANS (3)	ANS (4)
Auxiliary	ANS (5)	ANS (6)

## Discussion

Using the "Manual on Design and Manufacture of Torsion Bar Springs" by Society of Automobile Engineers August 1947.

For a circular torsion bar

$$\text{Windup angle } \phi = \frac{32 T L}{\pi d^4 G} \quad \text{radians}$$

$$\text{Torsional rate } T' = \frac{T}{\phi} = \frac{\pi d^4 G}{32 L} \quad \text{Nm/radian}$$

$$\text{Stress } S = \frac{16 T}{\pi d^3} = \frac{\phi d G}{2 L} \quad \text{Pa}$$

$$\text{Stress rate } S/\phi = \frac{d G}{2 L} \quad \text{Pa/radian}$$

For a rectangular torsion bar

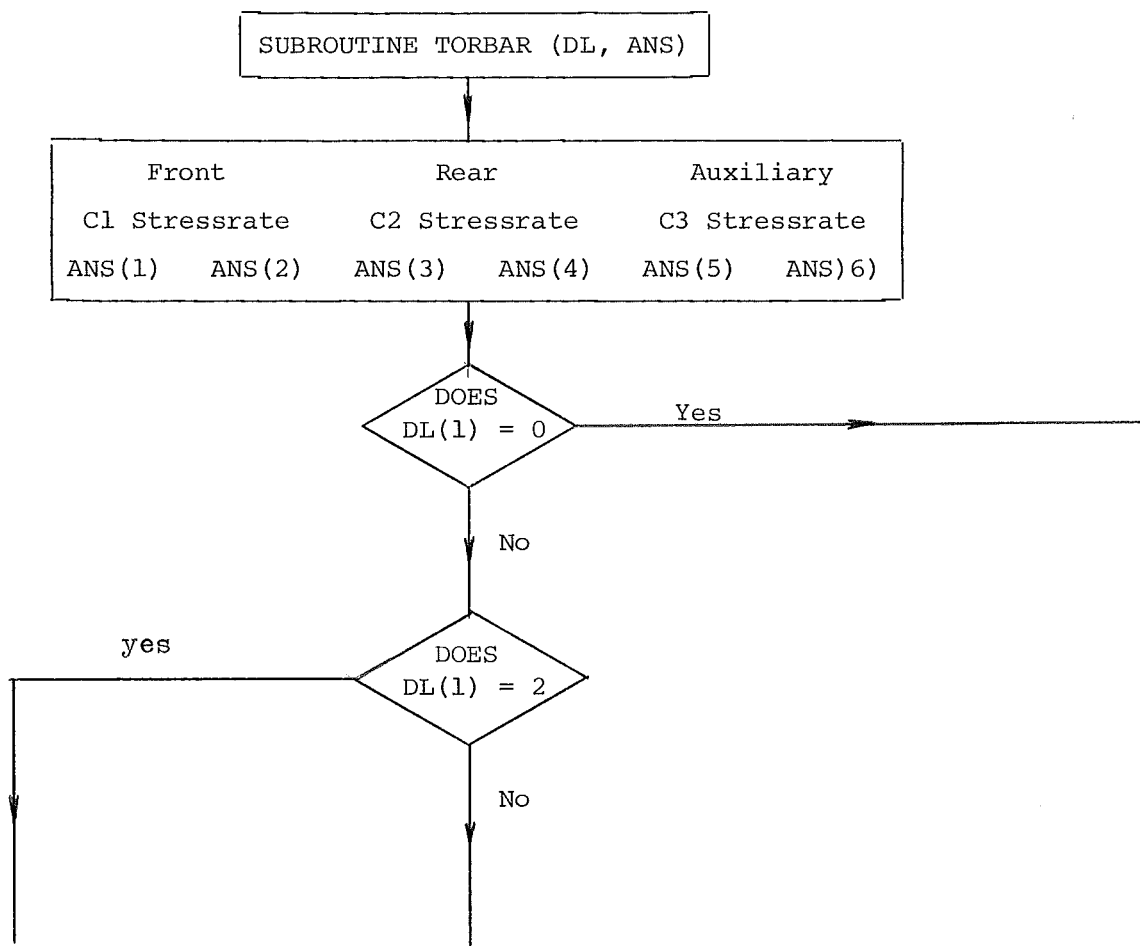
$$\text{Windup angle } \phi = \frac{T L}{\eta_3 a^3 b G} \quad \text{radians}$$

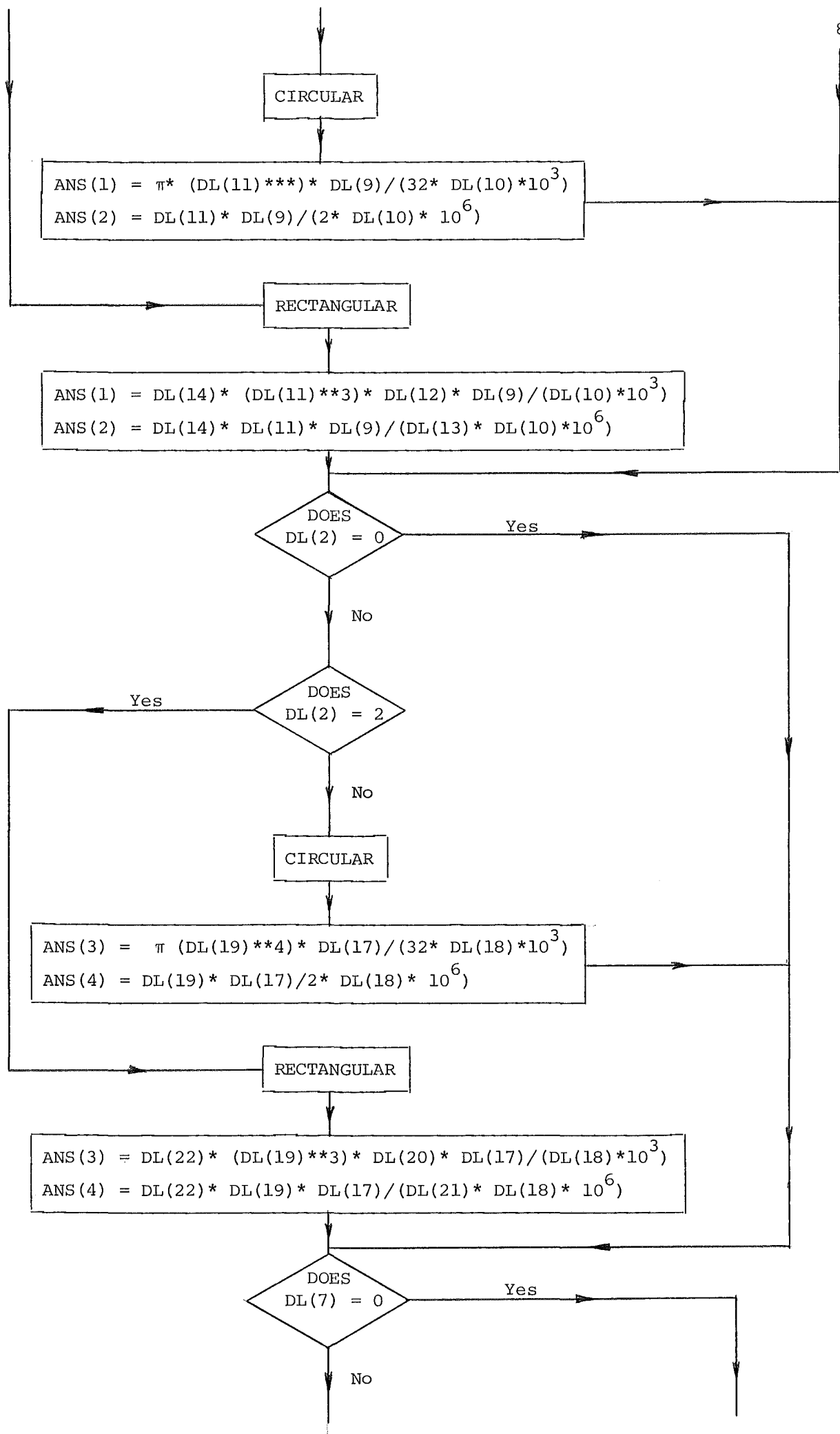
$$\begin{aligned} \text{Torsional rate } T' &= \frac{T}{\phi} = \frac{\eta_3 a^3 b G}{L} && \text{Nm/rad.} \\ \text{Stress } S &= \frac{T}{\eta_2 a^2 b} = \frac{\eta_3 \phi a G}{\eta_2 L} && \text{Pa} \\ \text{Stress rate } \frac{S}{\phi} &= \frac{\eta_3 a G}{\eta_2 L} && \text{Pa/radian} \end{aligned}$$

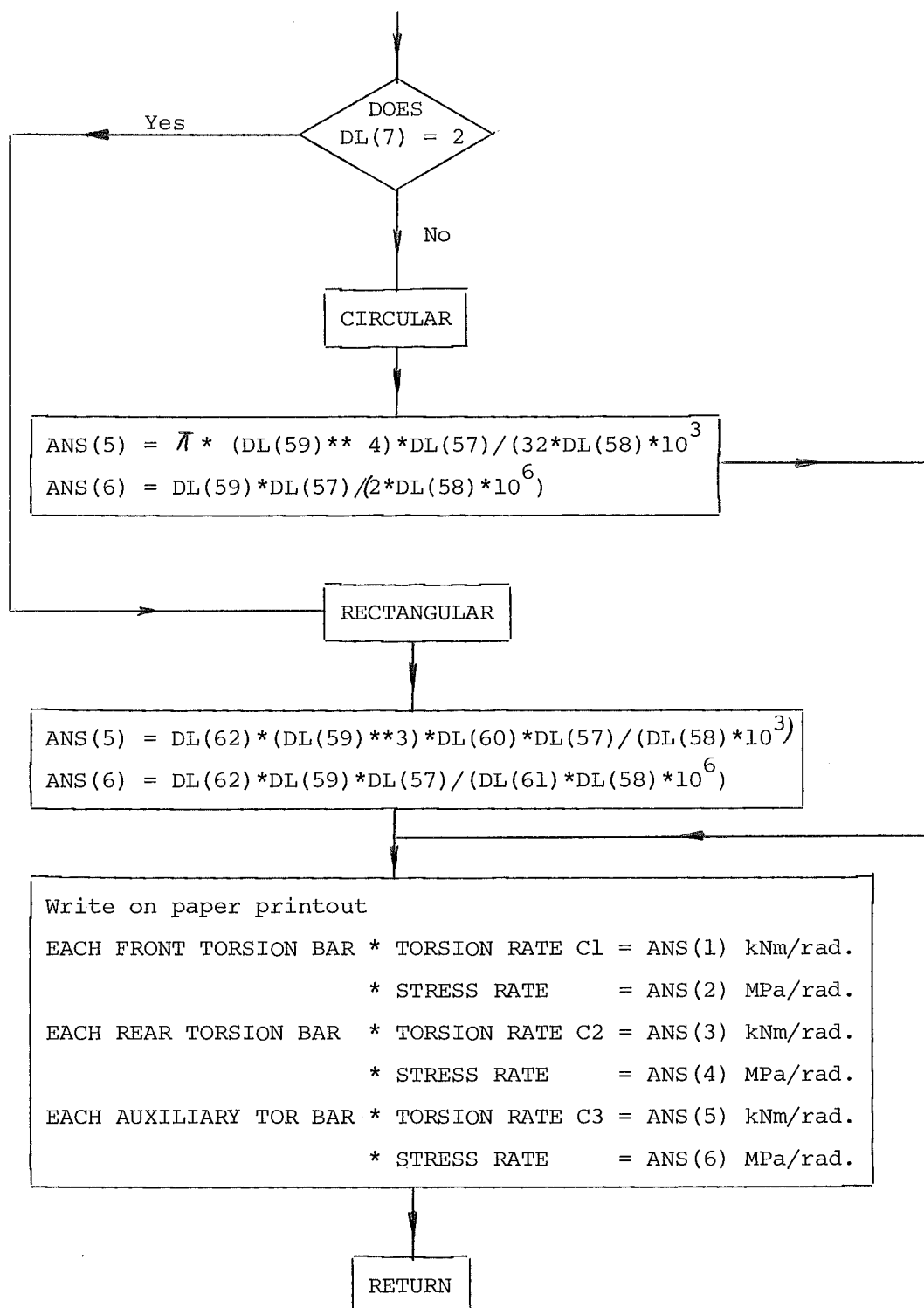
where

T	= Torque applied at bar	Nm
T'	= Torsion spring rate of bar	Nm/radian
L	= Active length of bar	m
d	= Diameter of round bar	m
a	= Short side of rectangular bar	m
b	= Long side of rectangular bar	m
$\eta_2$	= Saint Venant's stress coefficient	
$\eta_3$	= Saint Venant's stiffness coefficient	
$\phi$	= Angle of windup	
S	= Shear stress	
G	= Shear modulus.	

#### FLOWCHART



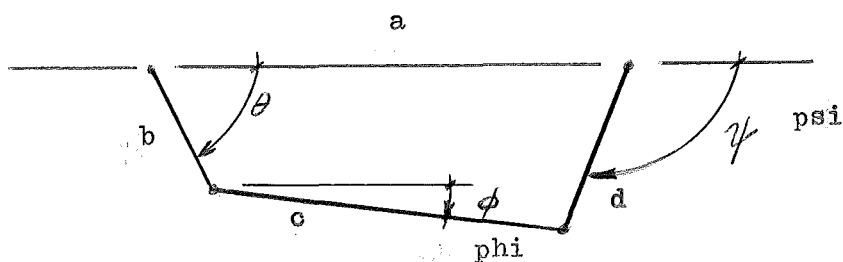




SUBROUTINE FBLANG (K,D,A)

Purpose. To find the two angles of a four bar linkage system, given one angle and the four linkage lengths.

The four lengths are the cable length, the front and rear pitch arms and the pitch arm pivot centres. The input angle is that of the front pitch arm.



Machine Design  
June 9 1977 p 94.

$$\phi = \pm \cos^{-1} \left\{ \frac{(a^2 + b^2 - 2ab \cos \theta) + c^2 - d^2}{2c \sqrt{a^2 + b^2 - 2ab \cos \theta}} \right\} - \tan^{-1} \left( \frac{b \sin \theta}{a - b \cos \theta} \right)$$

$$\psi = 180 \pm \cos^{-1} \left\{ \frac{(a^2 + b^2 - 2ab \cos \theta) + d^2 - c^2}{2d \sqrt{a^2 + b^2 - 2ab \cos \theta}} \right\} - \tan^{-1} \left( \frac{b \sin \theta}{a - b \cos \theta} \right)$$

FBLANG means Four Bar Linkage Angles.

Input. K - control integer

DL - data list array

ANS - answer array.

subroutine uses ANS(9) DL(27) (28) (29) (30)

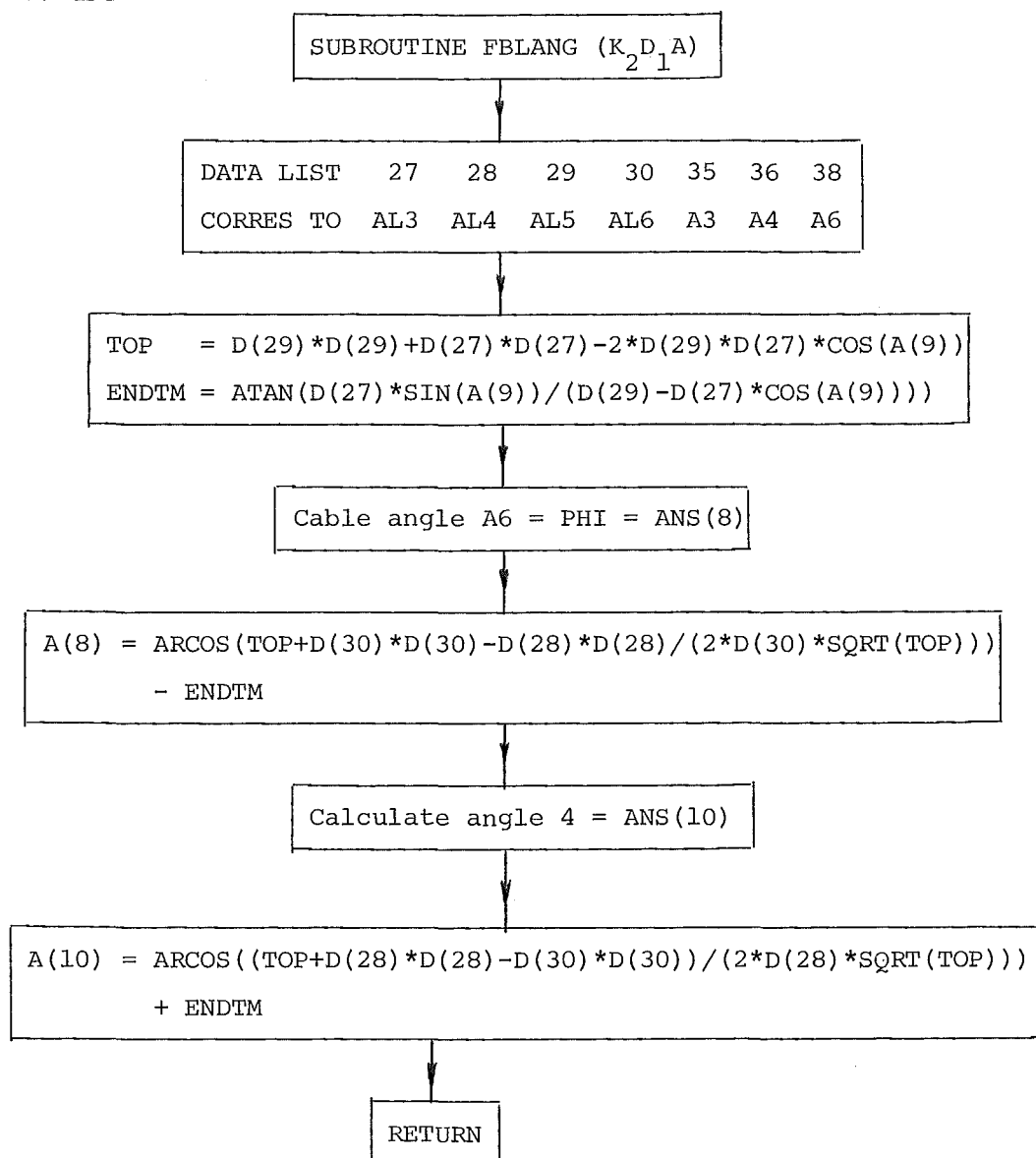
which are A3 AL3 AL4 AL5 AL6

Note:- Within this subroutine the arrays data list DL and answers ANS are referred to as arrays D and A respectively.

Output. ANS(8) the cable angle A6.

ANS(10) the angle of the rear pitch arm A4.



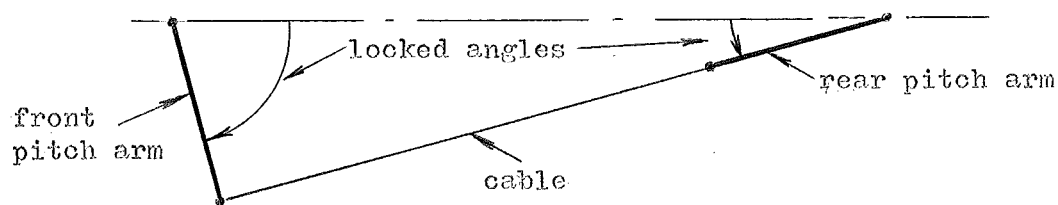
FLOWCHART

# SUBROUTINE ARMLTH (DL,ANS)

Purpose. To calculate the actual length of the front and rear pitch arms and the length of the connecting cable to enable further calculations in the bounce/rebound configuration to be made.

The initial cable angle is also calculated as is the locked pitch angles. These locked angles are calculated maximum angles that the pitch angles can attain during a bump or rebound condition and are used as a check further in the program.

The pitch arms are deemed to be locked when the front or rear arm and the cable are in a straight line.



Locked Pitch Angles - front bump.

Input. DL - data list array

ANS - answer array.

subroutine uses DL 25 26 27 28 29 30 31 33 34 35 36 38  
 which correspond to AL1 AL2 AL3 AL4 AL5 AL6 L3 A1 A2 A3 A4 A6  
 42 43  
 A B

Output. ANS (7) = RL34 = initial ratio  $l_3/l_4$ .

ANS(11) = Front locked pitch angle front bump.

ANS(12) = Rear locked pitch angle front bump.

ANS(13) = Front locked pitch angle, rear bump.

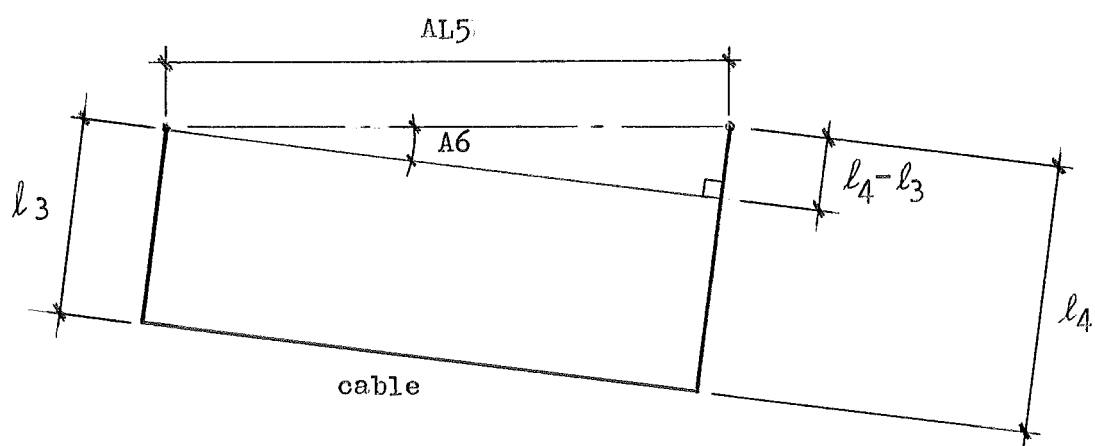
ANS(14) = Rear locked pitch angle, rear bump.

ANS(23) = Effective length  $l_3$ .

ANS(24) = Effective length  $l_4$ .

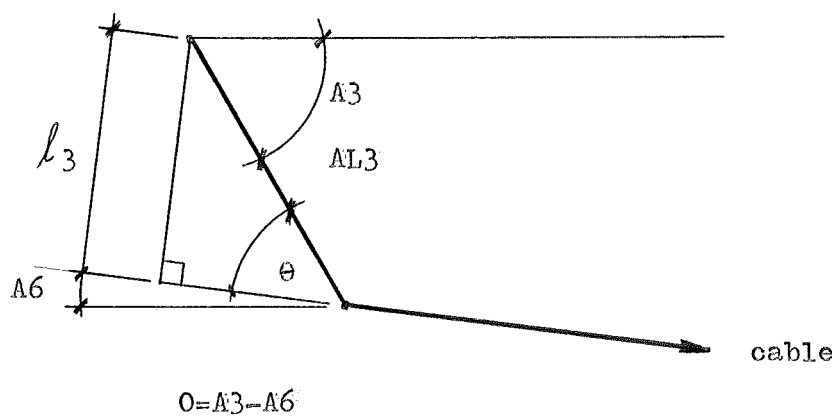


$$\text{Cable angle } A6 = DL(38) = \sin^{-1} \left( \frac{l_4 - l_3}{AL5} \right)$$



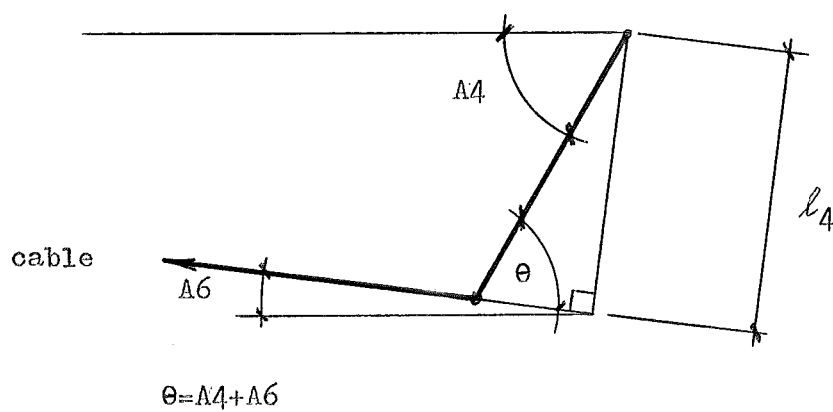
Actual front pitch arm length

$$AL3 = DL(27) = l_3 / \sin(A3 - A6)$$



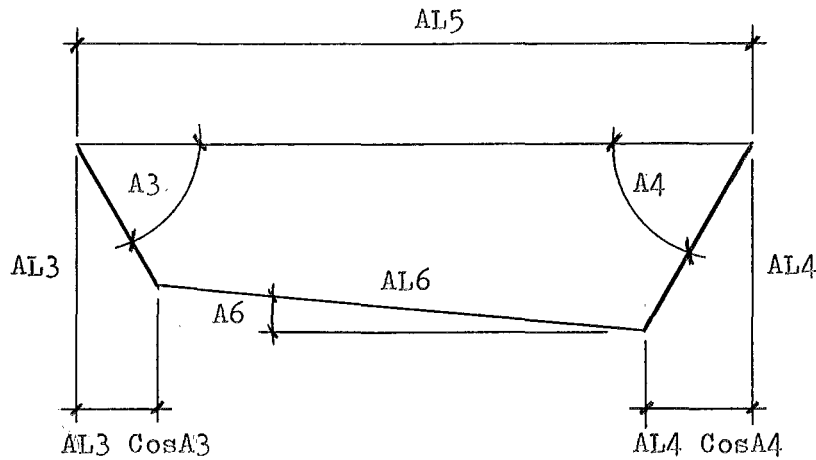
Actual rear pitch arm length

$$AL4 = DL(28) = l_4 / \sin(A4 + A6)$$

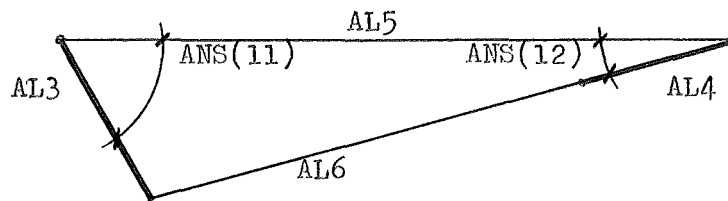


Actual cable length

$$DL(30) = AL6 = \frac{(AL5 - AL3 \cos(A3) - AL4 \cos(A4))}{\cos(A6)}$$



Calculate  $S = \frac{1}{2}$  the perimeter of the triangle shown below.



Front Bump Locked Pitch Angles.

Front locked angle = ANS(11)

$$ANS(11) = 2 \operatorname{ARSIN} \left( \sqrt{\frac{(S - AL3)(S - AL5)}{AL3 \cdot AL5}} \right)$$

Corresponding locked rear angle.

$$ANS(12) = 2 \operatorname{ARCOS} \left( \sqrt{\frac{S(S - AL3)}{AL5(AL6 + AL4)}} \right)$$

Similarly for rear bump locked pitch arms.

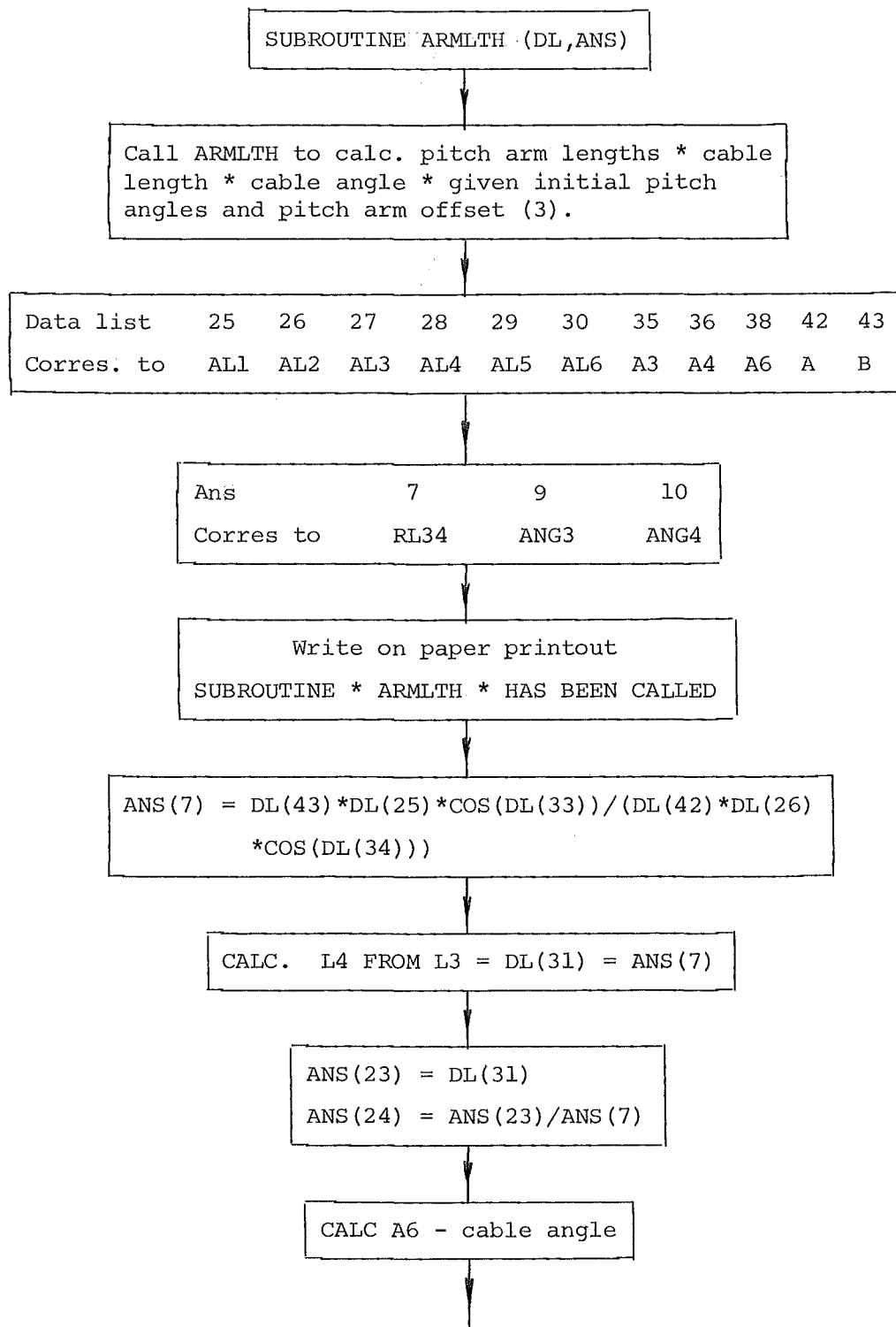
Front locked angle

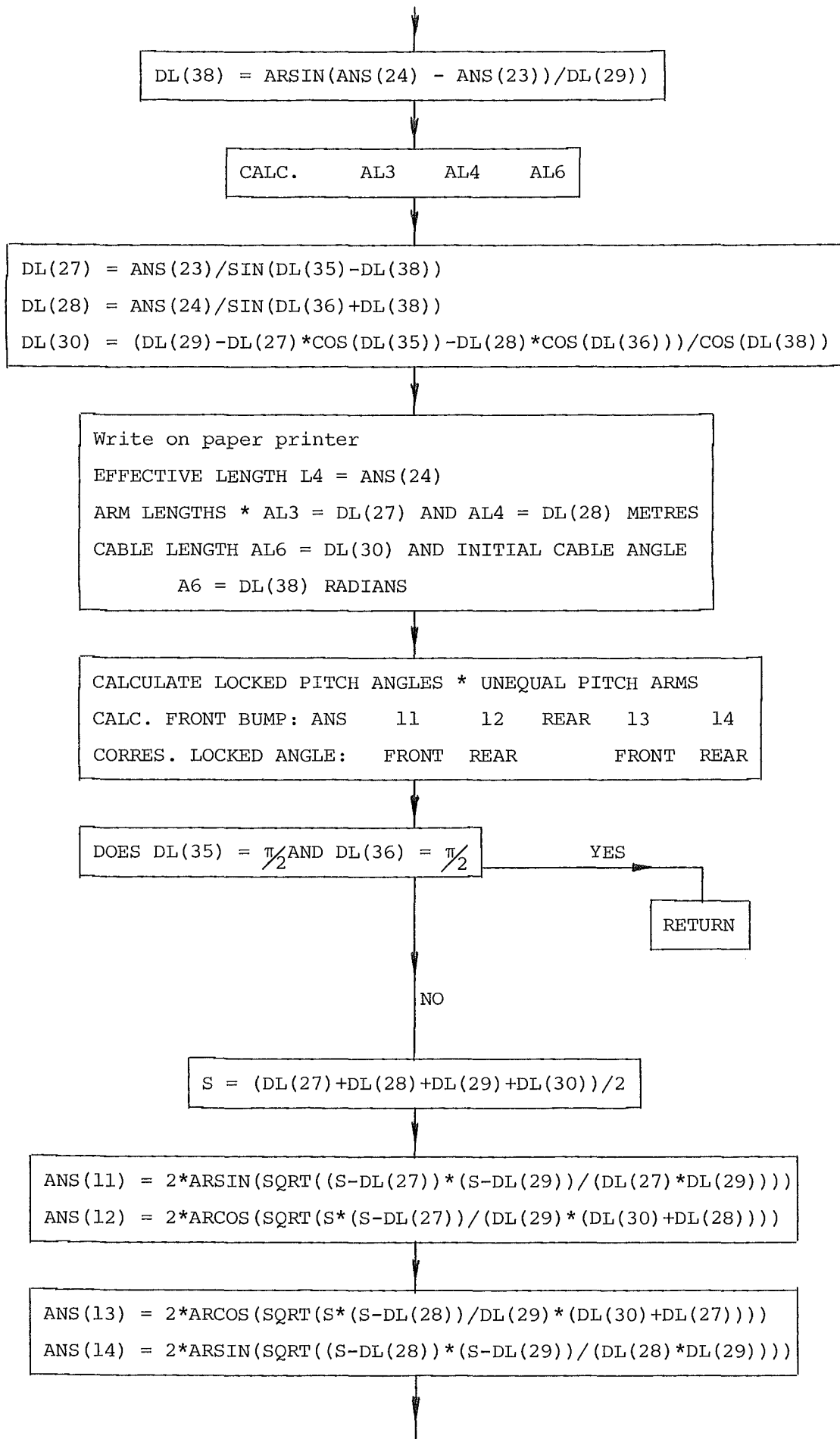
$$\text{ANS}(13) = 2.\text{ARCOS} \left( \sqrt{\frac{S(S-\text{AL4})}{\text{AL5}(\text{AL6}+\text{AL3})}} \right)$$

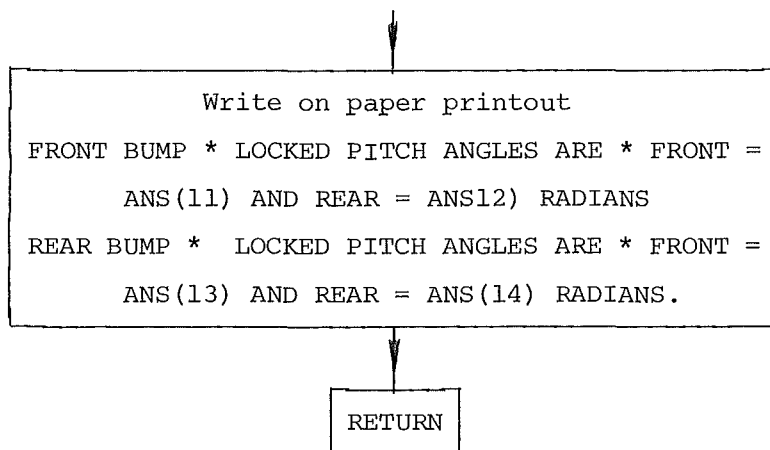
Corresponding rear locked angle

$$\text{ANS}(14) = 2.\text{ARSIN} \left( \sqrt{\frac{(S-\text{AL4})(S-\text{AL5})}{\text{AL4}.\text{AL5}}} \right)$$

# FLOWCHART









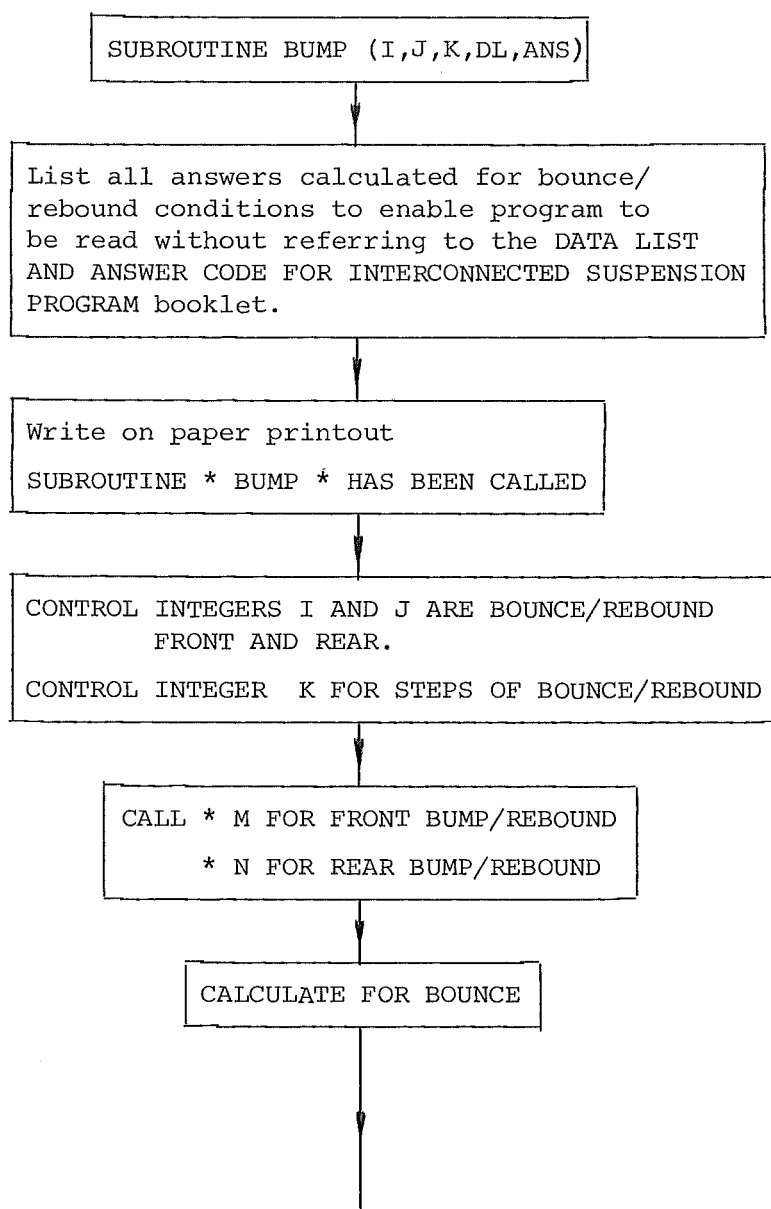
SUBROUTINE BUMP (I,J,K,DL,ANS)

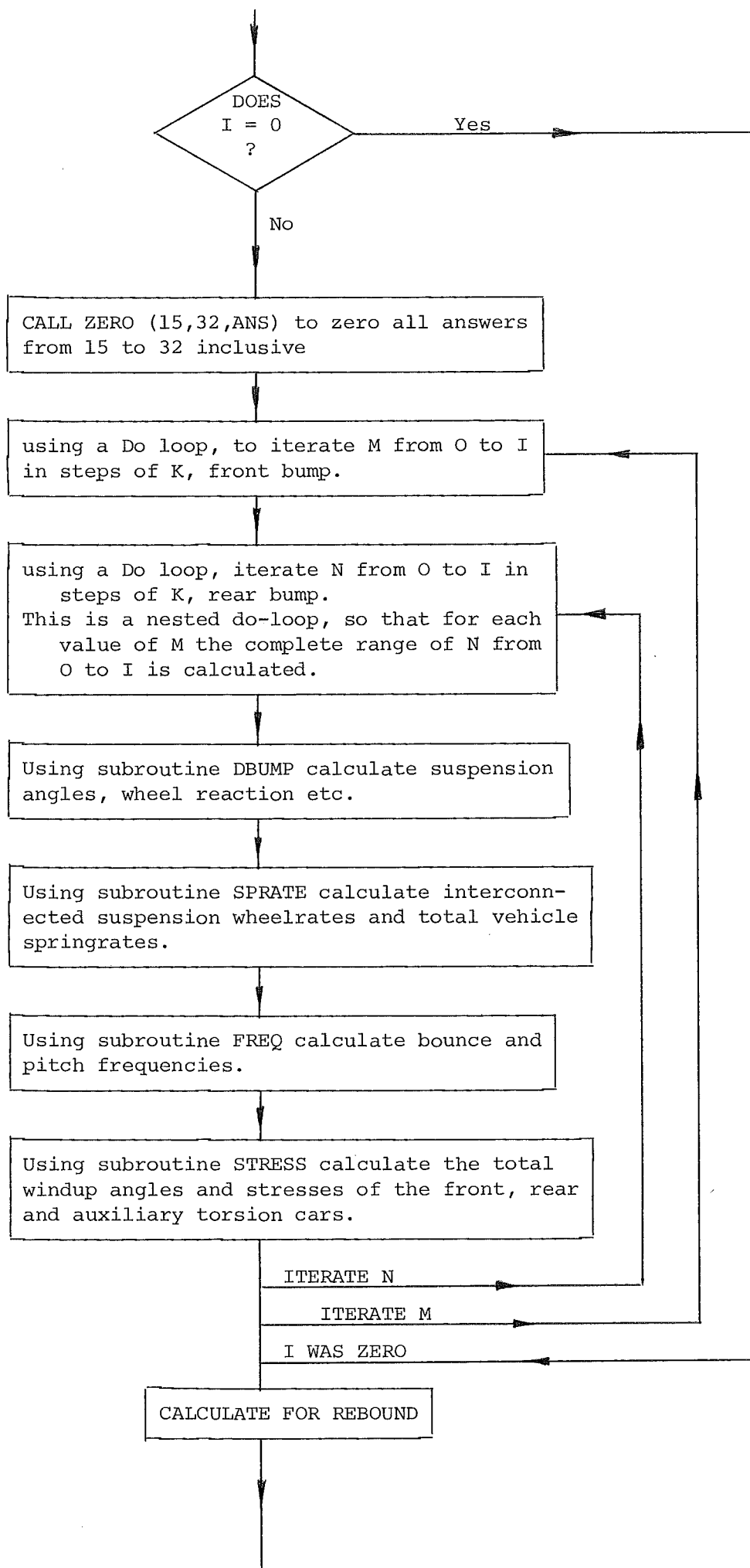
Purpose. Once subroutine BUMP has been called in the main program, this subroutine calls the necessary subroutines to calculate, for all the required bounce/rebound permutations, the wheel reactions, springrates, frequencies and torsion bar stresses.

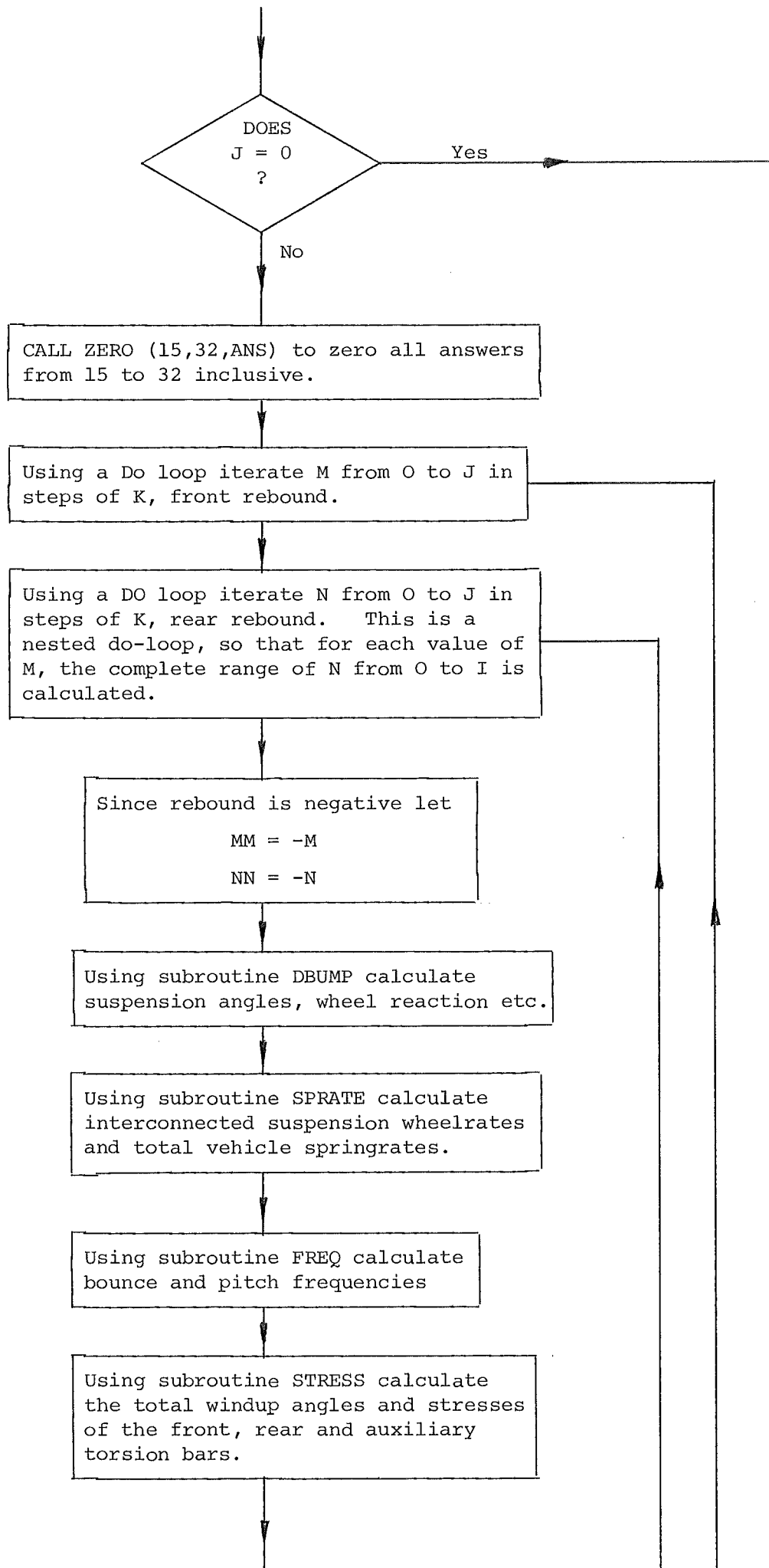
Input.

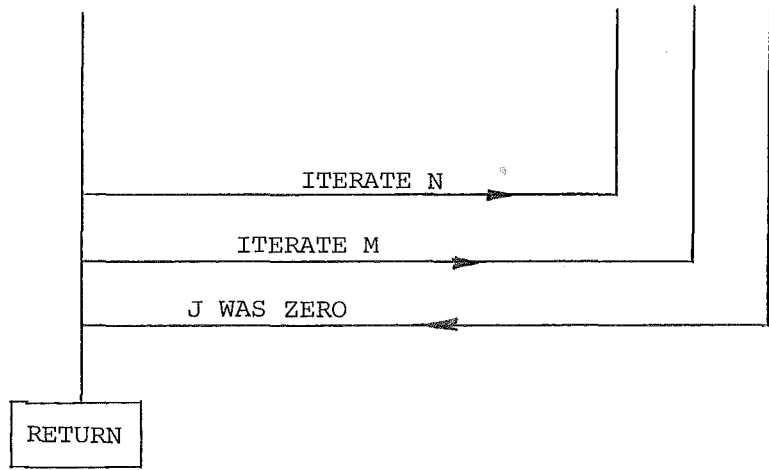
- I = Maximum bounce mm.
- J = Maximum rebound mm.
- K = Steps for I/J iteration mm.
- DL = Data List Array.
- ANS = Answers Array.

Output. All information that is required for each bounce/rebound condition, calculated in subroutines DBUMP, SPRATE, FREQ and STRESS.

FLOWCHART







SUBROUTINE DBUMP (M, N, DL, ANS)

Purpose. To calculate all the mechanical detail for any front and rear (M and N) bump and rebound (+ve and -ve, M and N) condition to enable the frequencies and torsion bar stresses to be subsequently calculated.

Input. M = front bump or rebound bump +ve, rebound -ve  
dimensions in mm.  
N = rear bump or rebound bump +ve, rebound -ve  
dimensions in mm.  
DL = Data list array.  
ANS = Answer array.

Subroutine uses

DL(25) = AL1 = Arm length 1, front wheel to torsion bar.  
DL(26) = AL2 = Arm length 2, rear wheel to torsion bar.  
DL(27) = AL3 = Arm length 3, front pitch arm length.  
DL(28) = AL4 = Arm length 4, rear pitch arm length.  
DL(33) = A1 = Initial angle of front arm 1.  
DL(34) = A2 = Initial angle of rear arm 2.  
DL(35) = A3 = Initial angle of pitch arm 3.  
DL(36) = A4 = Initial angle of pitch arm 4.  
DL(42) = A = Distance front axle to C of G as ratio of wheelbase.  
DL(43) = B = Distance rear axle to C of G as ratio of wheelbase.  
DL(45) = M = Vehicle mass kg.  
ANS(1) = C<sub>1</sub> = Front torsion bar springrate.  
ANS(3) = C<sub>2</sub> = Rear torsion bar springrate.  
ANS(5) = C<sub>3</sub> = Auxiliary torsion bar springrate.  
ANS(8) = A<sub>6</sub> = Cable angle.  
ANS(9) = A<sub>3</sub> = Front pitch arm angle.  
ANS(10) = A<sub>4</sub> = Rear pitch arm angle.  
ANS(51) = G<sub>1</sub> = Static front wheel loading.  
ANS(52) = G<sub>2</sub> = Static rear wheel loading.

Output.

Subroutine calculates the following,

ANS(15) = A<sub>1</sub> = Instantaneous angle of arm 1.  
ANS(16) = A<sub>2</sub> = Instantaneous angle of arm 2.  
ANS(21) = ℓ<sub>1</sub> = Effective length of arm 1.  
ANS(22) = ℓ<sub>2</sub> = Effective length of arm 2.

ANS(23) =  $\ell_3$  = Effective length of arm 3.  
 ANS(24) =  $\ell_4$  = Effective length of arm 4.  
 ANS(25) = RL34 = Ratio lengths  $\ell_3/\ell_4$ .  
 ANS(26) = RA34 = Ratio angles  $\theta_3/\theta_4$ .

Subroutine calculates and prints the following,

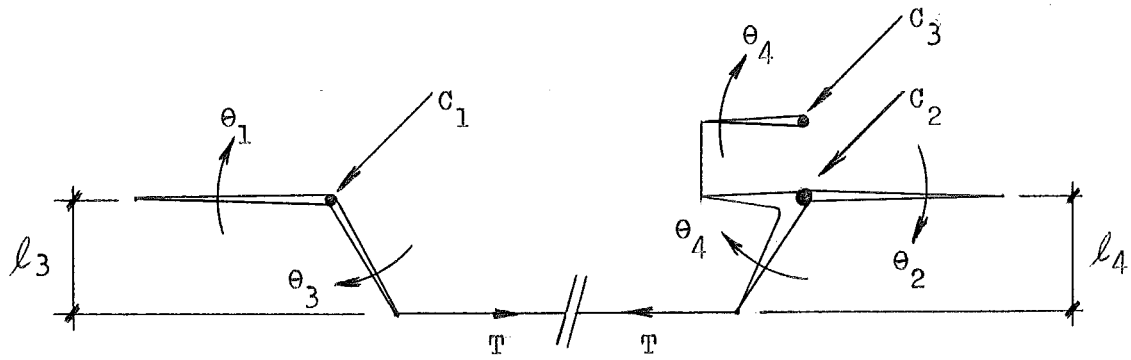
ANS(17) =  $\theta_1$  = Angle deviation from static for arm 1.  
 ANS(18) =  $\theta_2$  = Angle deviation from static for arm 2.  
 ANS(19) =  $\theta_3$  = Angle deviation from static for arm 3.  
 ANS(20) =  $\theta_4$  = Angle deviation from static for arm 4.  
 ANS(27) = RATIO = RL34/RA34 =  $\ell_3/\ell_4 \cdot \theta_4/\theta_3$ .  
 ANS(28) = T = Cable tension.  
 ANS(29) =  $F_1$  = Front wheel displacement.  
 ANS(30) =  $F_2$  = Rear wheel displacement.  
 ANS(31) =  $P_1$  = Front wheel load reaction.  
 ANS(32) =  $P_2$  = Rear wheel load reaction.

#### Description.

This subroutine does the background work for the Interconnected Suspension Program, it calculates the position of all the arms, then, from these, the instantaneous front and rear wheel loadings as well as the cable tension (used for cable size selection and chassis loading) for each and every permutation of bounce and rebound, front and rear within the limits specified in the main program.

The subroutine from the wheel displacements inputted, first calculates the angular displacement of the front and rear suspension arms, which is the rotation of the outboard and of the torsion bars, namely  $\theta_1$  and  $\theta_2$ .

The inboard end of the torsion bars, connected to the pitch arms which are in turn connected to each other via the cable, must come to an equilibrium position. This equilibrium is dependent on the lengths and angles of the pitch arms and the cable and on the rotational springrate of the front, rear and auxiliary torsion bars.



$\theta_1$  is the positive for front bounce.

$\theta_2$  is negative for rear bounce.

$C_1, C_2, C_3$  are torsional springrate for front, rear and auxiliary torsion bars respectively.

$l_3, l_4$  are effective arm lengths.

Front torsion bar, cable tension  $T$  is

$$T = \frac{C_1(\theta_1 - \theta_3)}{l_3}$$

Rear torsion bar, cable tension  $T$  is

$$T = \frac{-[C_2(\theta_2 - \theta_4) + C_3(0 - \theta_4)]}{l_4}$$

$$T = \frac{-C_2\theta_2 + (C_2 + C_3)\theta_4}{l_4}$$

Equating the two expressions of  $T$ , to find  $\theta_3$

$$\theta_3 = \theta_1 + \frac{l_3/l_4(C_2\theta_2 - (C_2 + C_3)\theta_4)}{C_1}$$

However,  $l_3, l_4$  and  $\theta_4$  are all dependent on  $\theta_3$ , either directly or indirectly, so that  $\theta_3$  (and hence  $\theta_4$  etc.) must be found by iteration.

Using the notation  $\theta$  for  $\theta_3$  so that  $\theta_n$  is the  $n$ th iteration toward finding  $\theta$ .

$\theta_n$  strictly means  $(\theta_3)_n$

Given  $\theta_n$ , we can calculate from equilibrium considerations, as above, what  $\theta_n$  should be, that is, have  $\theta_n$  can calculate  $f(\theta_n)$  such that they should be equal.

Define  $F(\theta_n) = f(\theta_n) - \theta_n = 0$  and the Newton-Raphson Method of Successive Approximations can be used,

$$\theta_{n+1} = \theta_n - \frac{F(\theta_n)}{F'(\theta_n)}$$

If  $F(\theta_n) = f(\theta_n) - \theta_n$  then  $F'(\theta_n) = f'(\theta_n) - 1$ , and  $f'(\theta_n)$  can be approximated as,

$$f'(\theta_n) \approx \frac{f(\theta_n) - f(\theta_{n-1})}{\theta_n - \theta_{n-1}}$$

and making an assumption that

$$f(\theta_{n-1}) = \theta_n$$

though not strictly correct, it does not slow convergence appreciably, so that

$$f'(\theta_n) = \frac{f(\theta_n) - \theta_n}{\theta_n - \theta_{n-1}}$$

$$\text{then } \theta_{n+1} = \theta_n + \frac{f(\theta_n) - \theta_n}{1 - f'(\theta_n)}$$

or

$$\text{THTNP1} = \theta + \frac{\text{FTHT} - \theta}{1 - S}$$

$$\text{where } S = \frac{\text{FTHT} - \theta}{\theta - \text{THTNMI}}$$

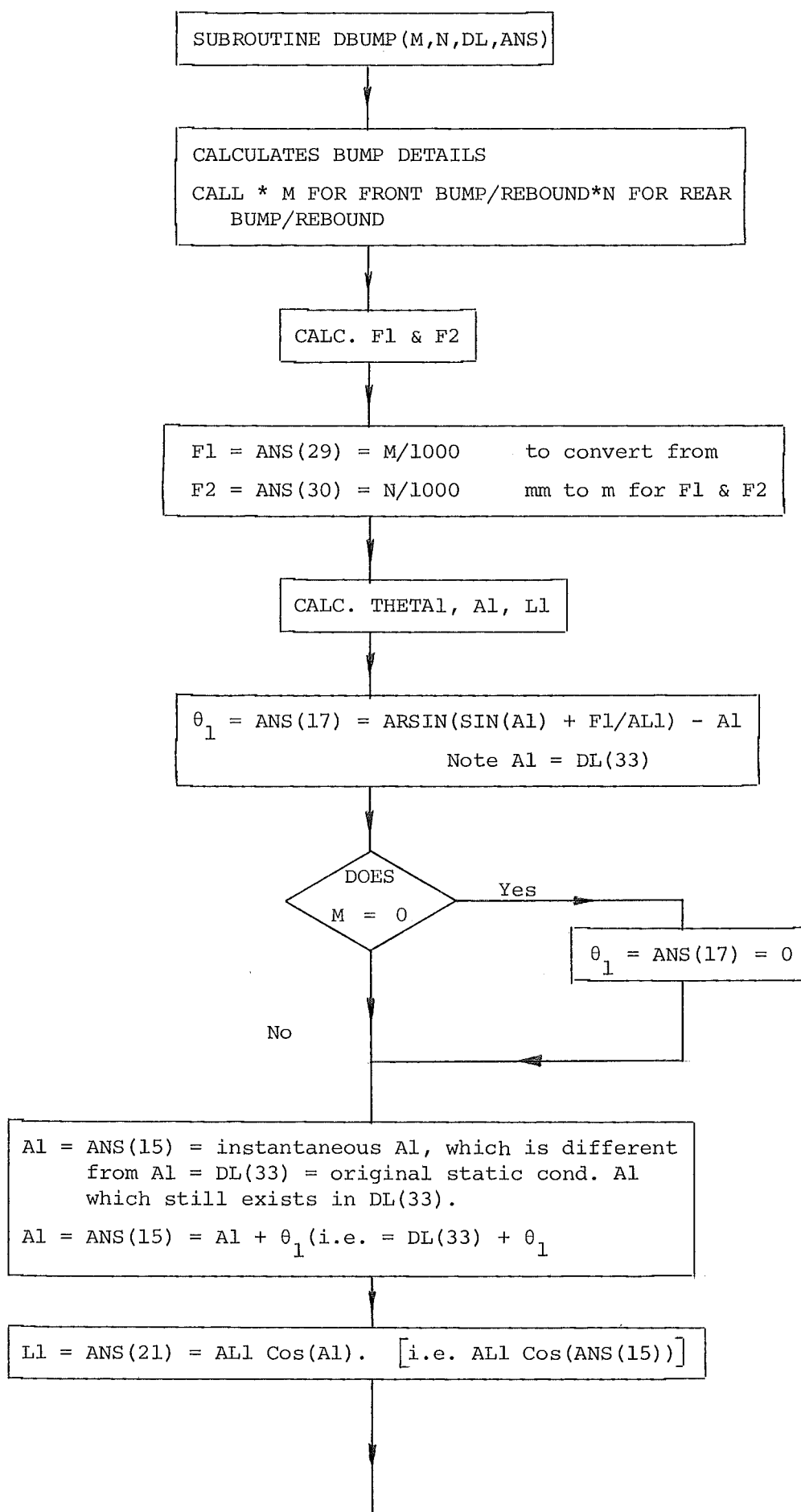
Iterations are stopped when  $f(\theta_n) = \theta_n$ , i.e. when

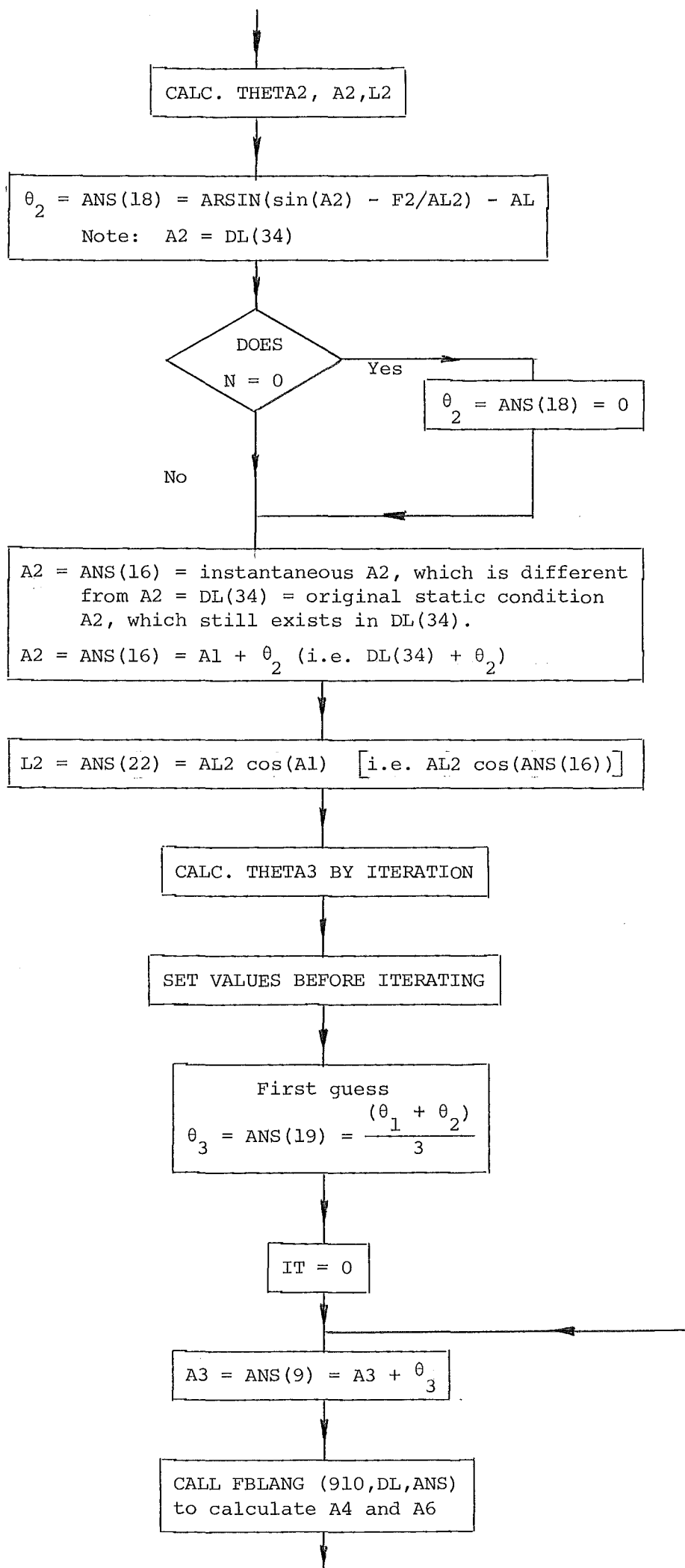
$$\text{ABS}(f(\theta_n) - \theta_n) < 10^{-8}$$

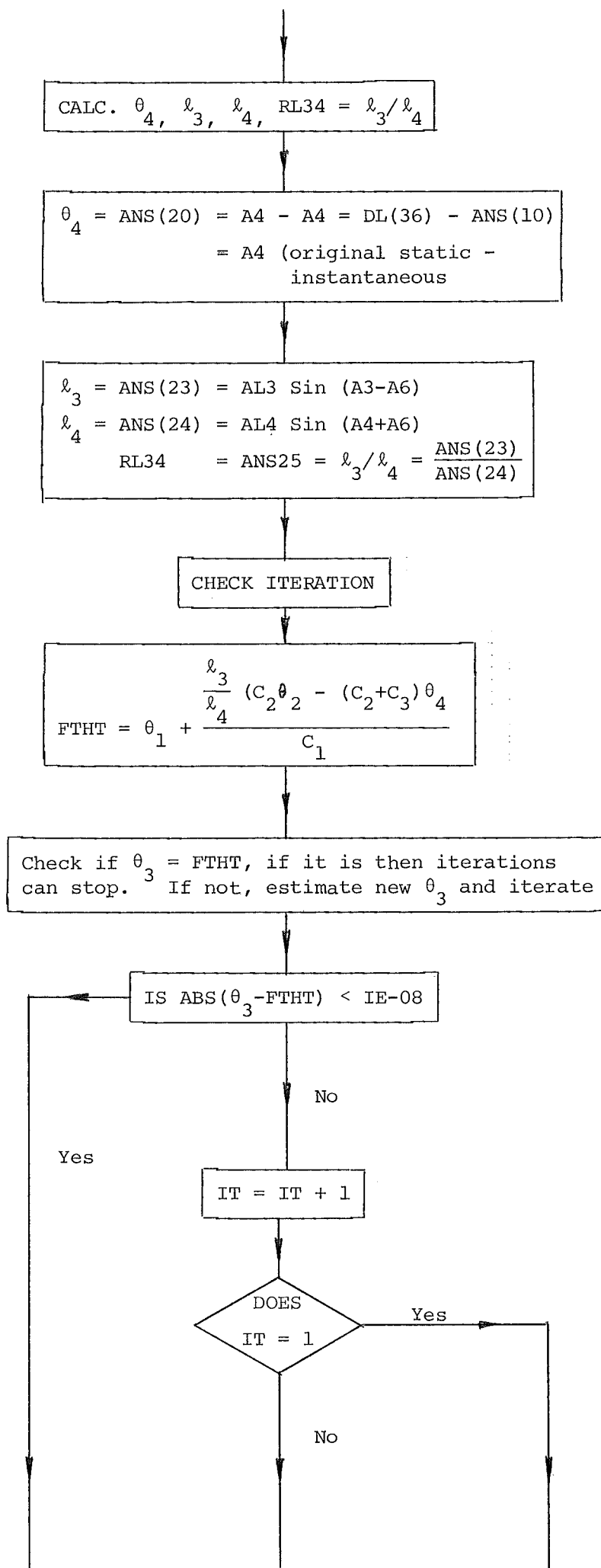
The subroutine counts and prints out the number of iterations ITS for each bump/rebound permutation specified.

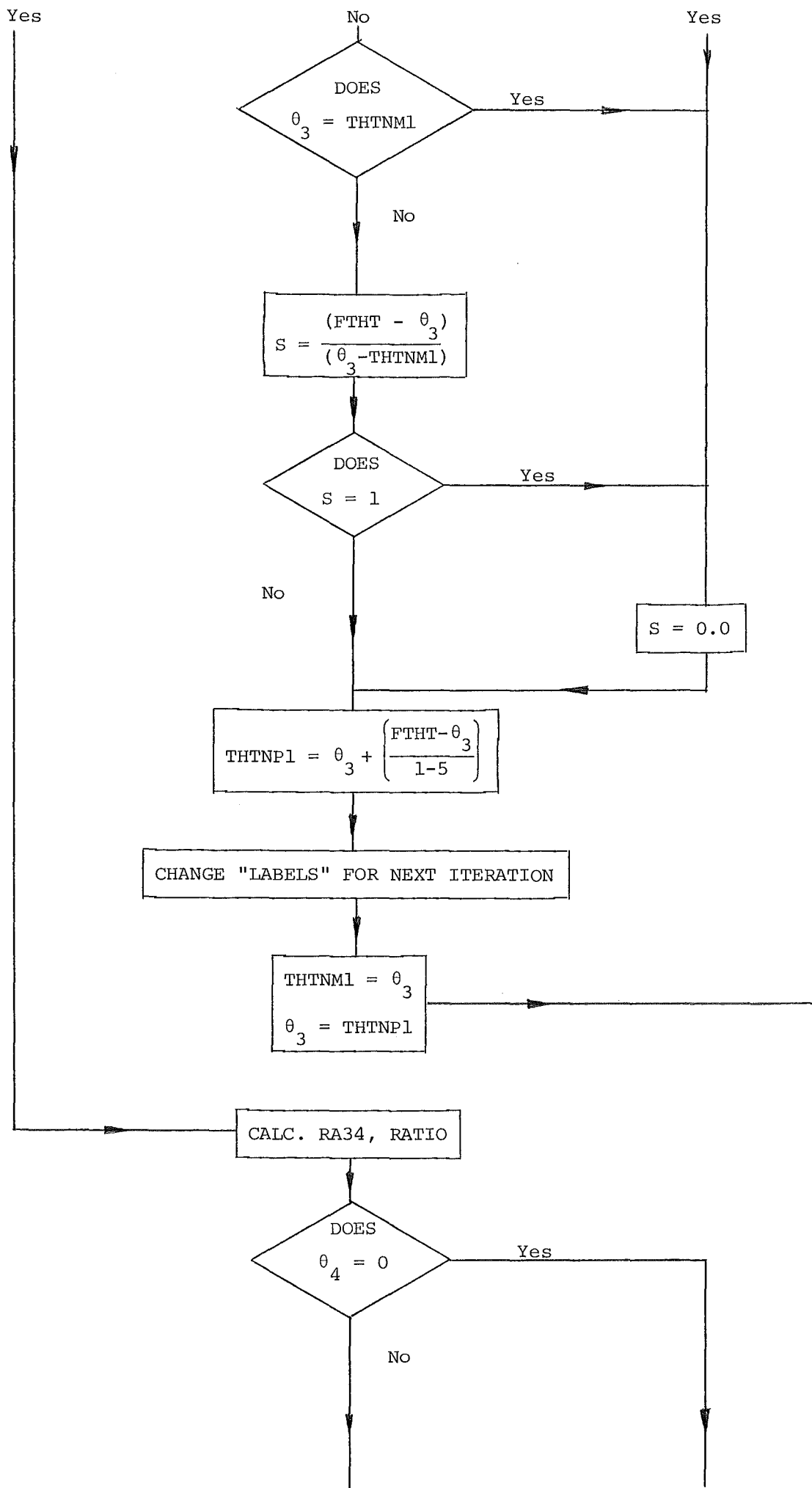


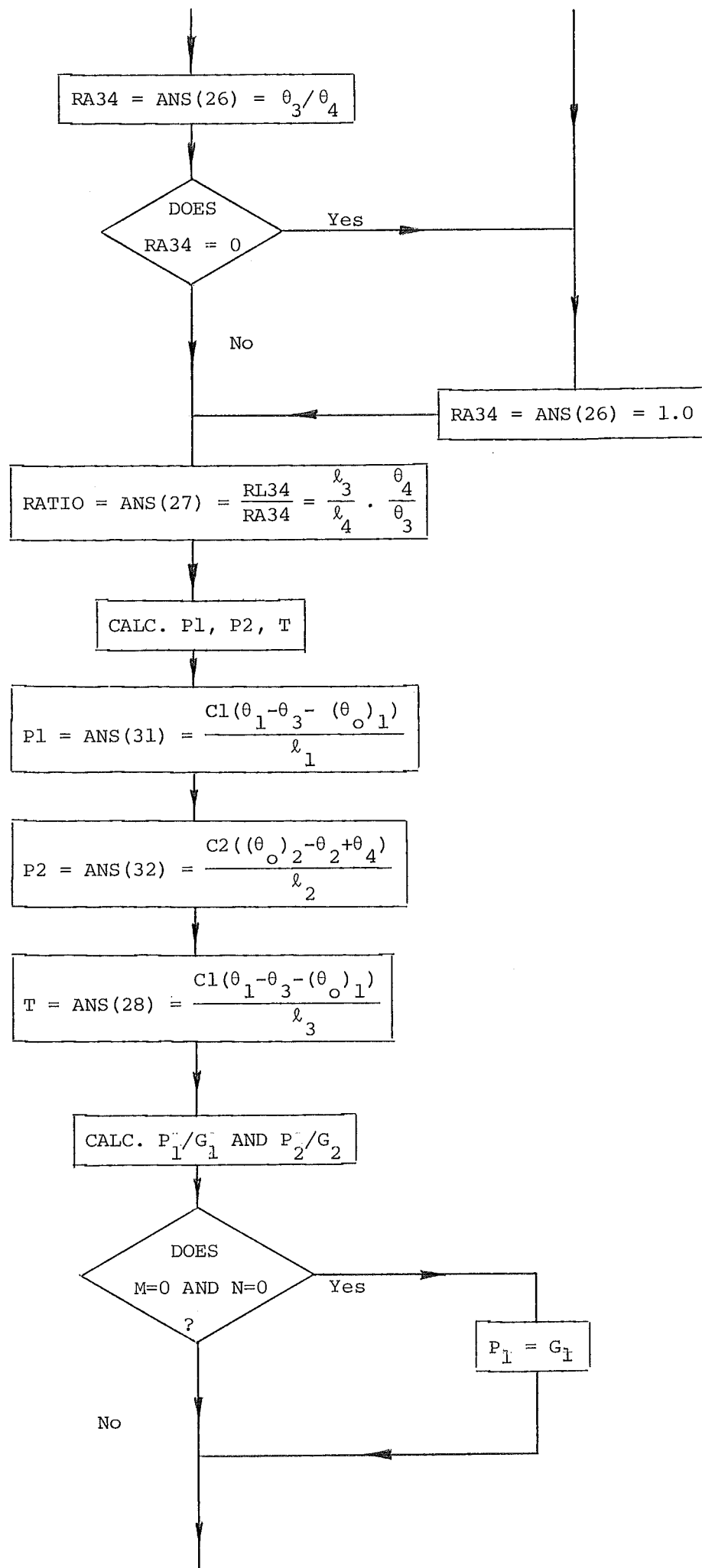
## FLOWCHART

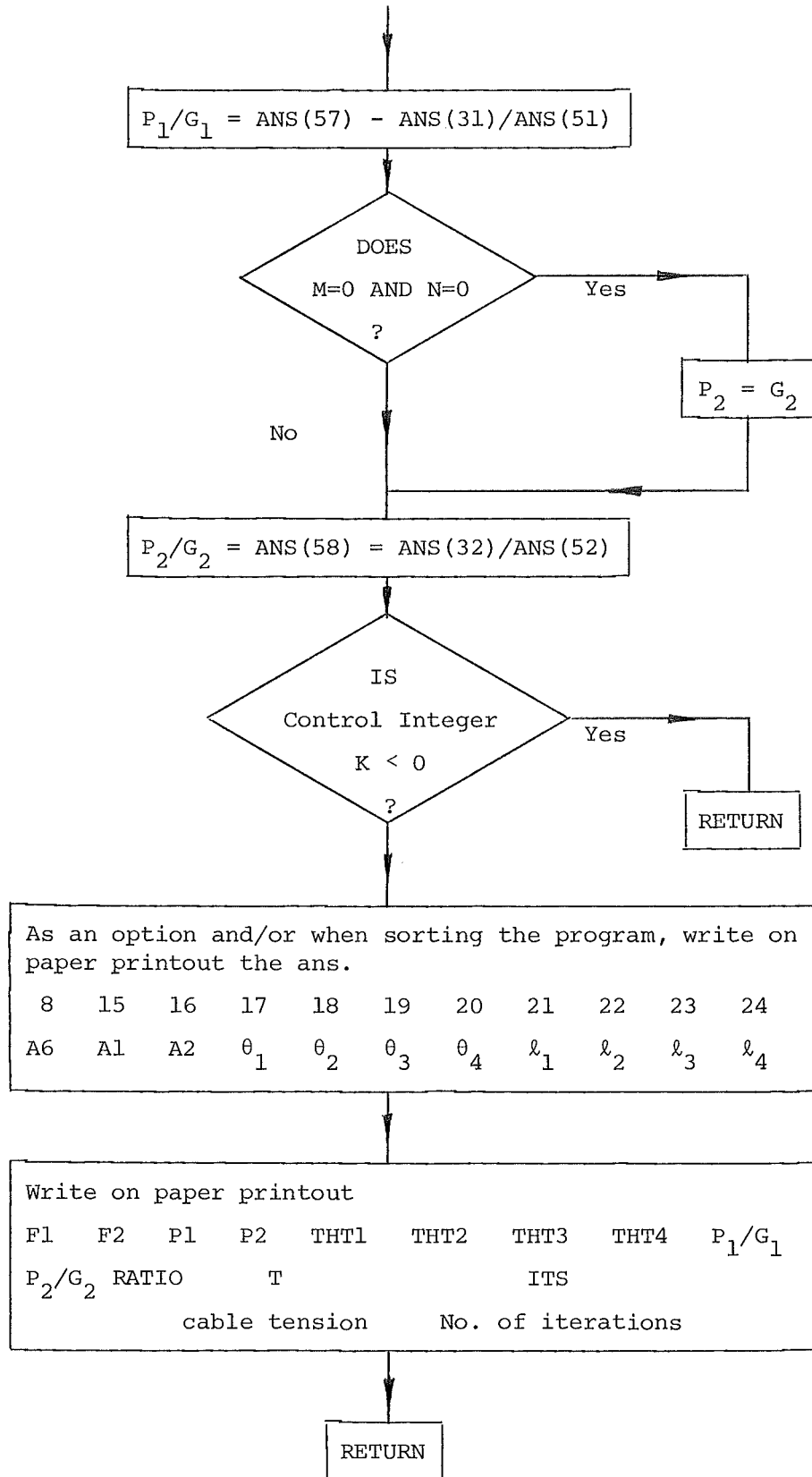












# SUBROUTINE SPRATE (K, DL, ANS)

Purpose. To calculate the interconnected springrates, both wheelrates and total vehicle rates.

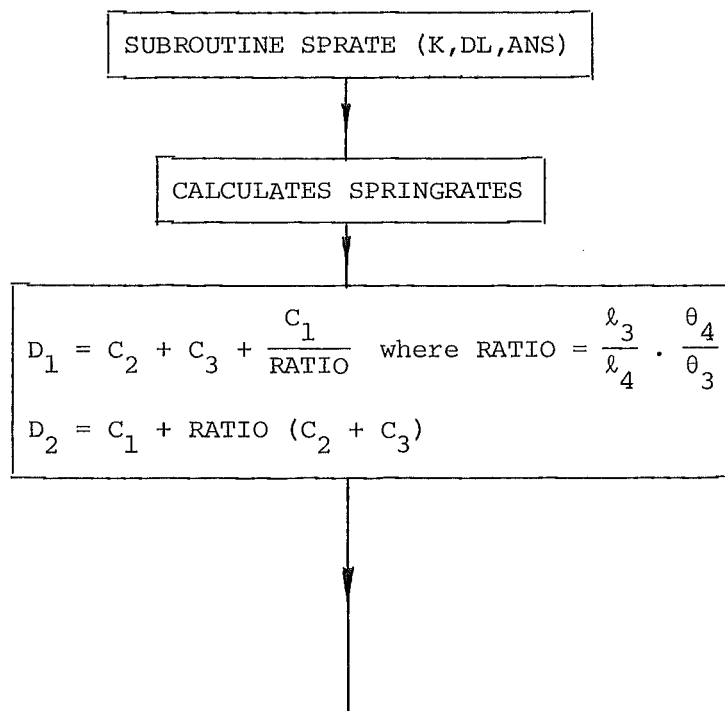
Input. Subroutine uses:

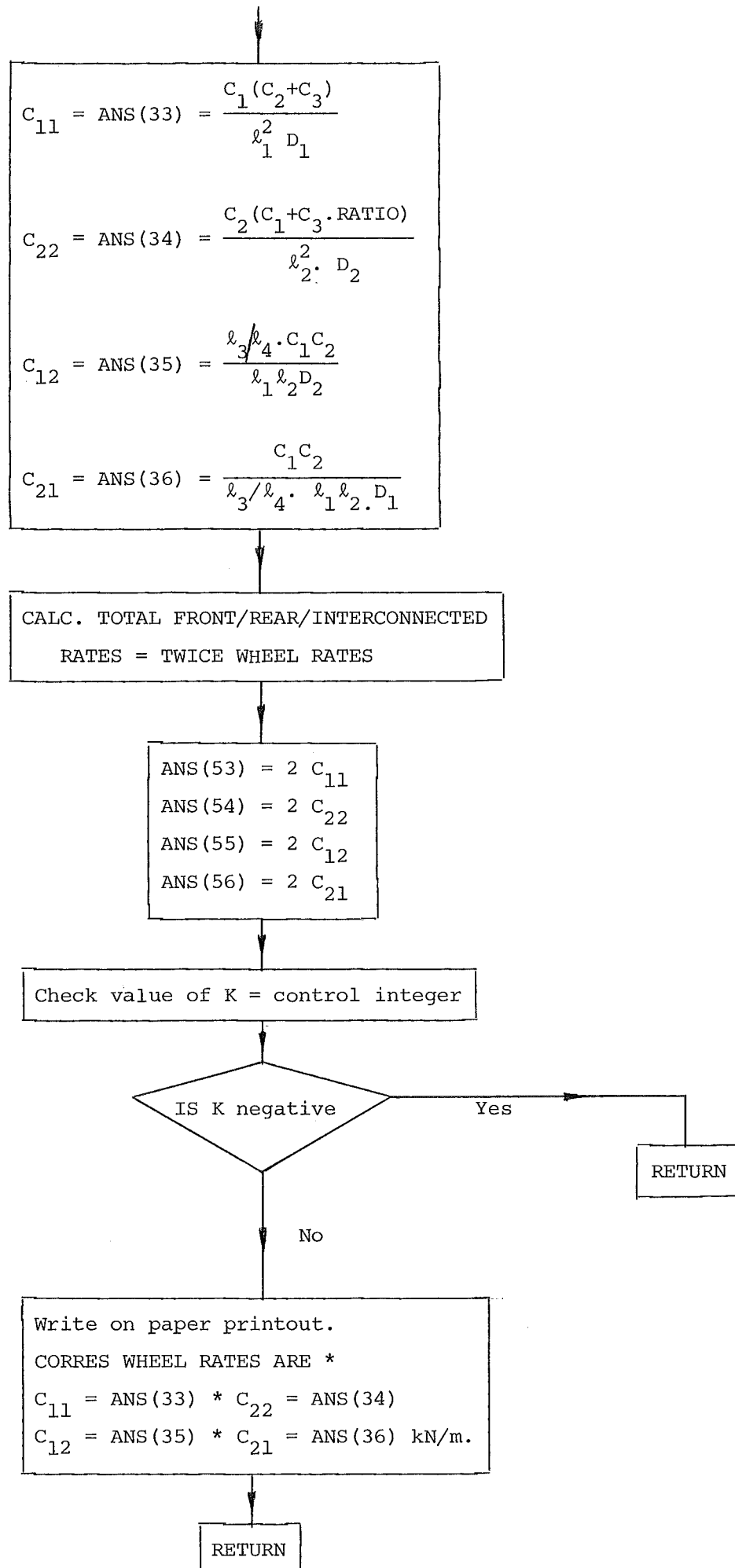
ANS(1) =  $C_1$  = Front torsion bar springrate.  
 ANS(3) =  $C_2$  = Rear torsion bar springrate.  
 ANS(5) =  $C_3$  = Auxiliary torsion bar springrate.  
 ANS(21) = Effective length  $l_1$ .  
 ANS(22) = Effective length  $l_2$ .  
 ANS(25) = Ratio of effective lengths  $l_3/l_4$ .  
 ANS(27) =  $RATIO = l_3 \theta_4 / l_4 \theta_3$ .

Output. Subroutine calculates the following:

ANS(33) =  $C_{11}$  = front wheelrate.  
 ANS(34) =  $C_{22}$  = rear wheelrate.  
 ANS(35) =  $C_{12}$  = front wheelrate due to rear.  
 ANS(36) =  $C_{21}$  = rear wheelrate due to front.  
 ANS(53) =  $2 C_{11}$  = car springrate front.  
 ANS(54) =  $2 C_{22}$  = car springrate rear.  
 ANS(55) =  $2 C_{12}$  = car springrate front/rear.  
 ANS(56) =  $2 C_{21}$  = car springrate rear/front.

## FLOWCHART







SUBROUTINE FREQ (DL, ANS)

Purpose. To calculate the bounce and pitch frequencies of the car, these frequencies being largely responsible for the comfort of the car. The partial frequencies of bounce and pitch and the coupling coefficients are also calculated.

Input. The springrates and vehicle geometry are required.

$$\text{ANS}(53) = 2 \times C_{11}$$

$$\text{ANS}(54) = 2 \times C_{22}$$

$$\text{ANS}(55) = 2 \times C_{12}$$

$$\text{ANS}(56) = 2 \times C_{21}$$

where  $C_{11}$ ,  $C_{22}$ ,  $C_{12}$  and  $C_{21}$  are individual wheelrates

$$\text{DL}(41) = \text{WB} = L$$

$$\text{DL}(42) = A$$

$$\text{DL}(43) = B$$

$$\text{DL}(45) = M$$

$$\text{DL}(46) = K$$

Output.

$$\text{ANS}(41) = \text{PF} = \text{pitch frequency.}$$

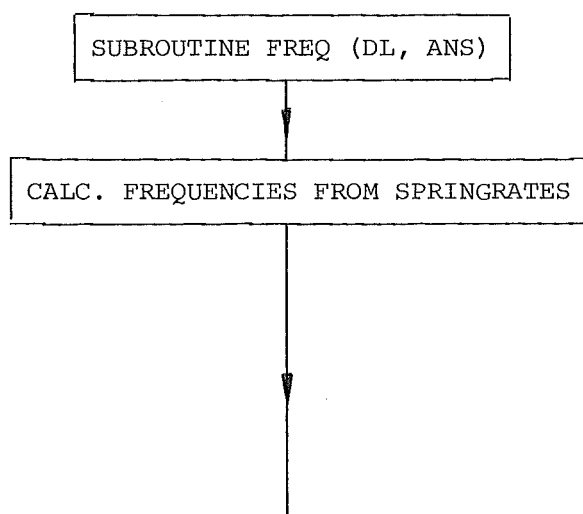
$$\text{ANS}(42) = \text{BF} = \text{bounce frequency.}$$

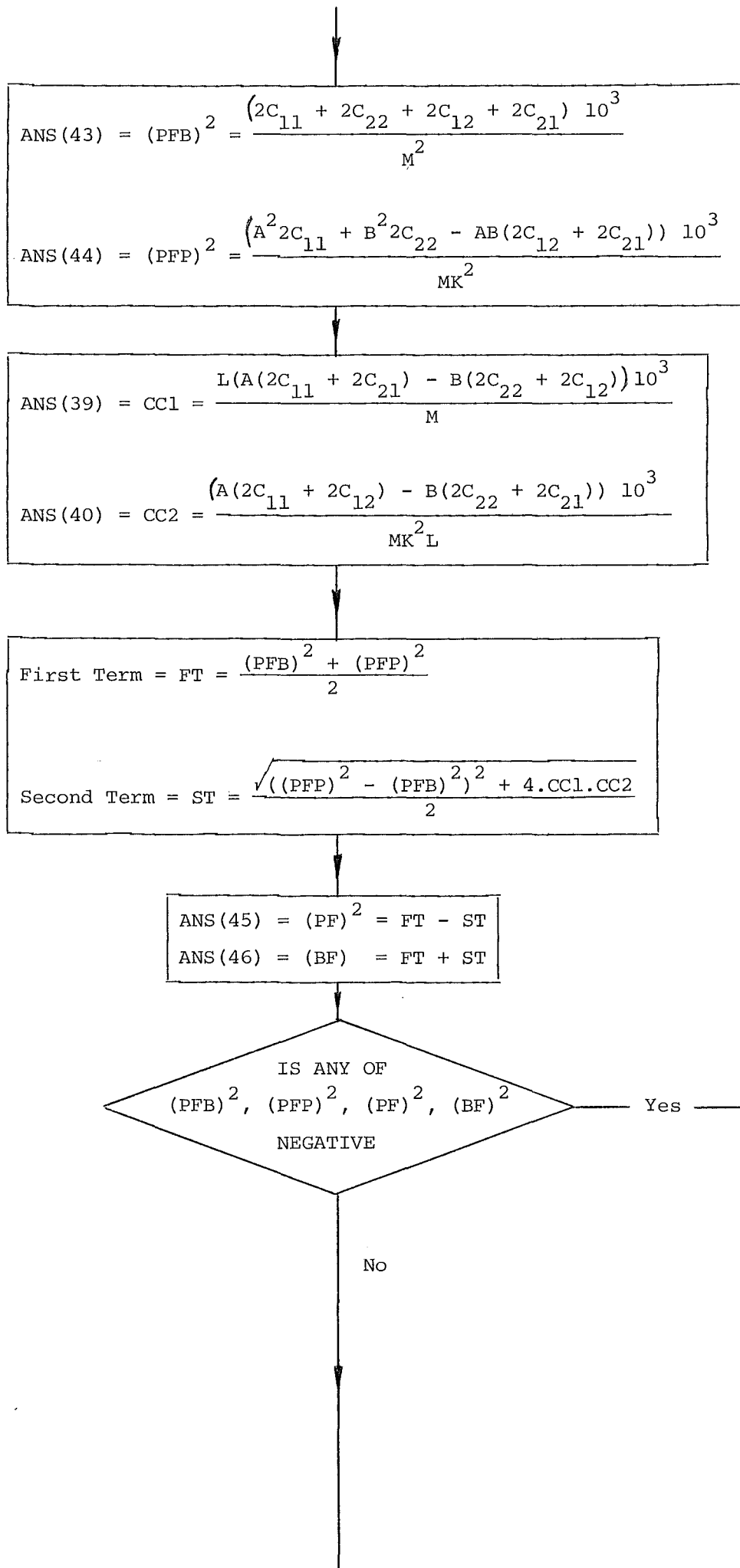
$$\text{ANS}(37) = \text{PFB} = \text{partial bounce frequency.}$$

$$\text{ANS}(38) = \text{PFP} = \text{partial pitch frequency.}$$

$$\text{ANS}(39) = \text{CC1} = \text{coupling coefficient 1.}$$

$$\text{ANS}(40) = \text{CC2} = \text{coupling coefficient 2.}$$

FLOWCHART



$$\text{ANS}(37) = \text{PFB} = \frac{\sqrt{(\text{PFB})^2}}{2\pi}$$

$$\text{ANS}(38) = \text{PFP} = \frac{\sqrt{(\text{PFP})^2}}{2\pi}$$

$$\text{ANS}(41) = \text{PF} = \frac{\sqrt{(\text{PF})^2}}{2\pi}$$

$$\text{ANS}(42) = \text{BF} = \frac{\sqrt{(\text{BF})^2}}{2\pi}$$

Write on paper printout.

CORRES FREQ'S ARE \* PITCH ANS(41) \* BOUNCE ANS(42) Hz  
\* PFB ANS(37) \* PFP ANS(38) Hz.

C. COEFFS ANS(39), ANS(40).

RETURN

Write on paper printout.

FREQS \* C.COEFFS ANS(39), ANS(40)

PFB\*\*2 ANS(43) PFP\*\*2 ANS(44)

PF\*\*2 ANS(45) BF\*\*2 ANS(46)

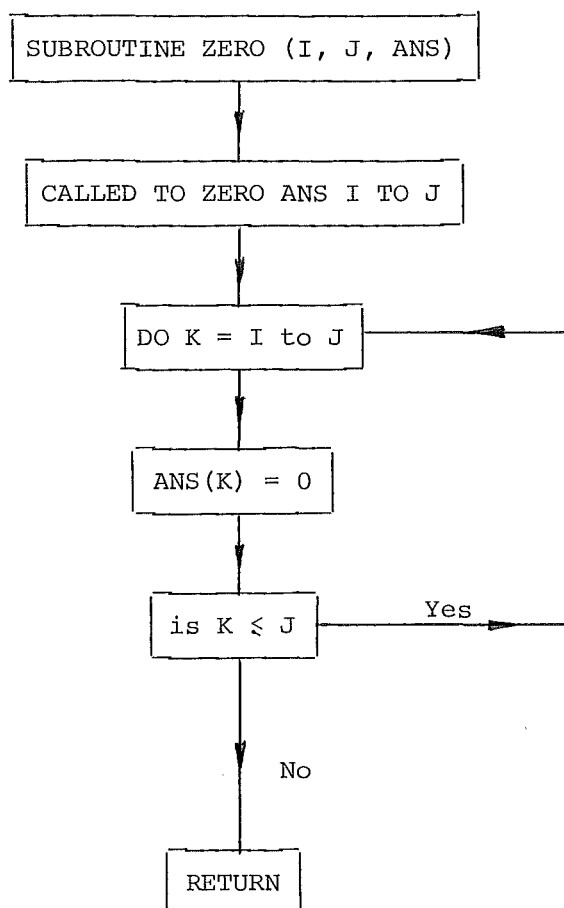
RETURN

SUBROUTINE ZERO (I, J, ANS)

Purpose. To set to zero those elements in the ANS array from I to J inclusive.

Input. I = lowest ANS(I) to be set to zero.  
J = highest ANS(j) to be set to zero.  
ANS = Answer array.

Output. ANS(I), ANS(I+1) .... ANS(J) = 0.

FLOWCHART

SUBROUTINE STDEFL (K, DL, ANS)

Purpose. To calculate the angle of twist of the front and rear torsion bars when the vehicle is in its static condition, for subsequent total twist and stress calculations.

From the initial angle of twist is calculated the static front and rear wheel deflection and the static wheel loadings.

Input. K = control integer.  
DL = Data list array.  
ANS = Answers array.

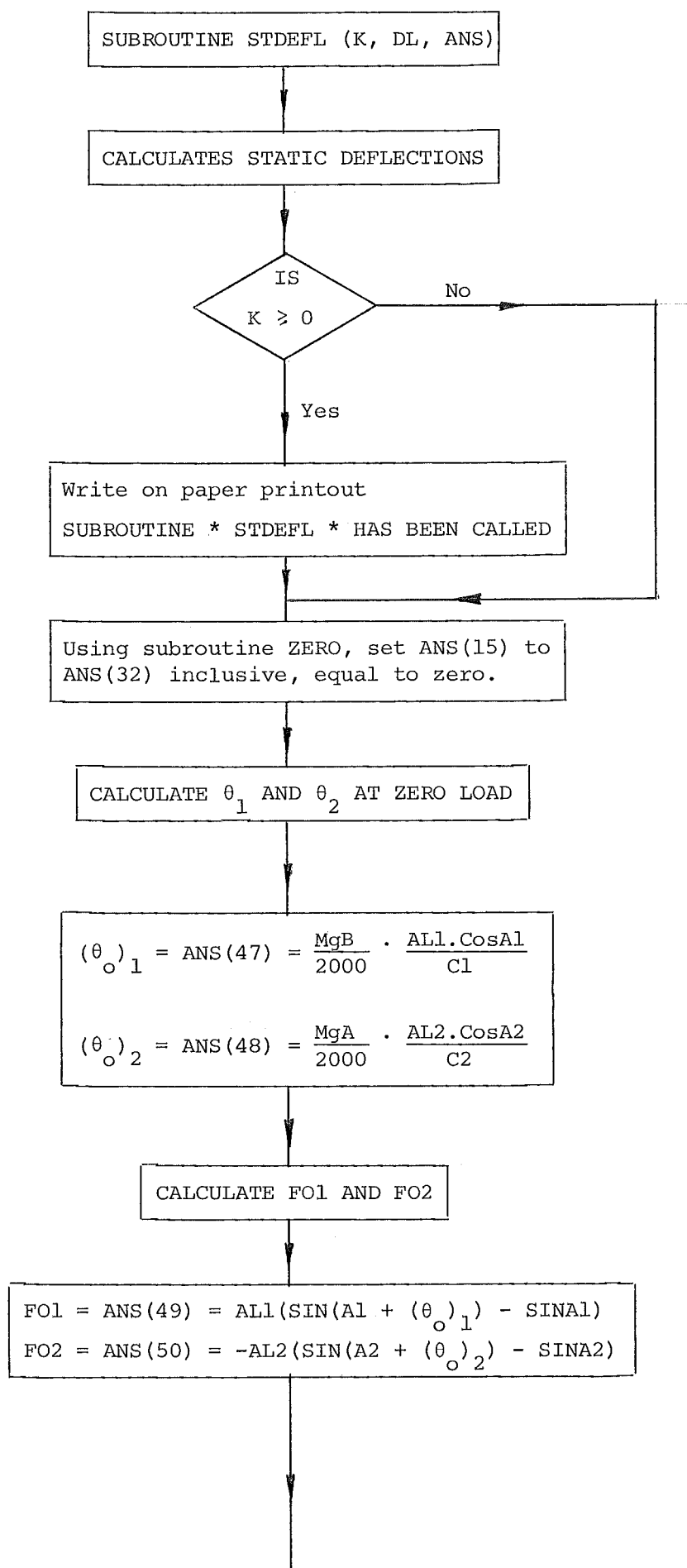
This subroutine uses,

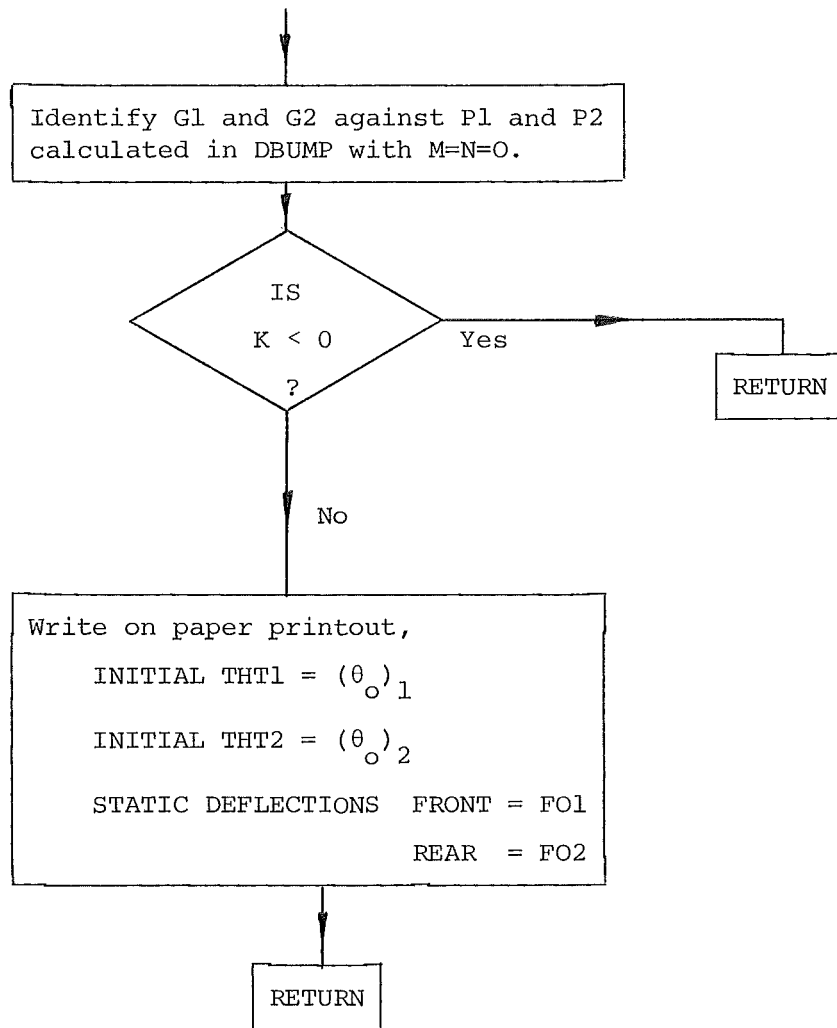
subroutine ZERO and DBUMP  
DL(25) = AL1 = Front wheel to torsion bar, arm length.  
DL(26) = AL2 = Rear wheel to torsion bar arm length.  
DL(33) = A1 = Static angle of arm AL1.  
DL(34) = A2 = Static angle of arm AL2.  
DL(42) = A = A x WB is distance of C of G from front.  
DL(43) = B = B x WB is distance of C of G from rear.  
DL(45) = M = Vehicle mass.  
ANS(1) = C<sub>1</sub> = Front torsion bar springrate.  
ANS(3) = C<sub>2</sub> = Rear torsion bar springrate.  
ANS(31) = P<sub>1</sub> = Front wheel reaction.  
ANS(32) = P<sub>2</sub> = Rear wheel reaction.

Output. Subroutine calculates.

ANS(47) = ( $\theta_o$ )<sub>1</sub> = angle  $\theta_1$  at zero wheel loading.  
ANS(48) = ( $\theta_o$ )<sub>2</sub> = angle  $\theta_2$  at zero wheel loading.  
ANS(49) = F<sub>01</sub> = static front wheel deflection.  
ANS(50) = F<sub>02</sub> = static rear wheel deflection.  
ANS(51) = G<sub>1</sub> = static front wheel loading.  
ANS(52) = G<sub>2</sub> = static rear wheel loading.

## FLOWCHART





# SUBROUTINE STRESS (K, D, A)

Purpose. To calculate the total windup angles and stresses of the front, rear and auxiliary torsionbars for design purposes.

Input. K = control integer.  
D = Data List Array.  
A = Answers Array.

Subroutine uses:

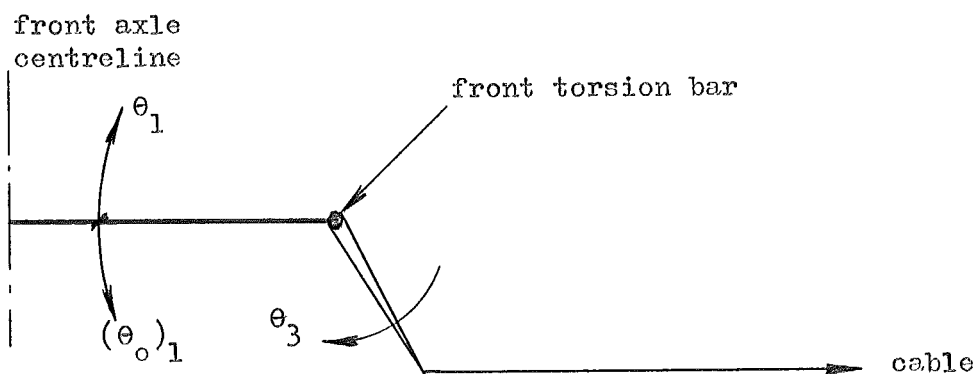
A(17) =  $\theta_1$  = front arm angular displacement, bump +ve.  
A(19) =  $\theta_3$  = front pitch arm angular displacement.  
A(47) =  $(\theta_o)_1 = \theta_1$  at zero wheel loading (-ve).  
A(18) =  $\theta_2$  = rear arm angular displacement, bump +ve.  
A(20) =  $\theta_4$  = rear pitch arm angular displacement.  
A(48) =  $(\theta_o)_2 = \theta_2$  at zero wheel loading (+ve).  
A(2) = Front torsion bar stressrate.  
A(4) = Rear torsion bar stressrate.  
A(6) = Auxiliary torsion bar stressrate.

Output. A = Answer Array.

A(59) =  $\phi_1$  = windup angle for torsion bar  $C_1$  (front).  
A(60) =  $\phi_2$  = windup angle for torsion bar  $C_2$  (rear).  
A(61) =  $S_1$  = stress for torsion bar  $C_1$  (front).  
A(62) =  $S_2$  = stress for torsion bar  $C_2$  (rear).  
A(63) =  $S_3$  = stress for torsion bar  $C_3$  (auxiliary).

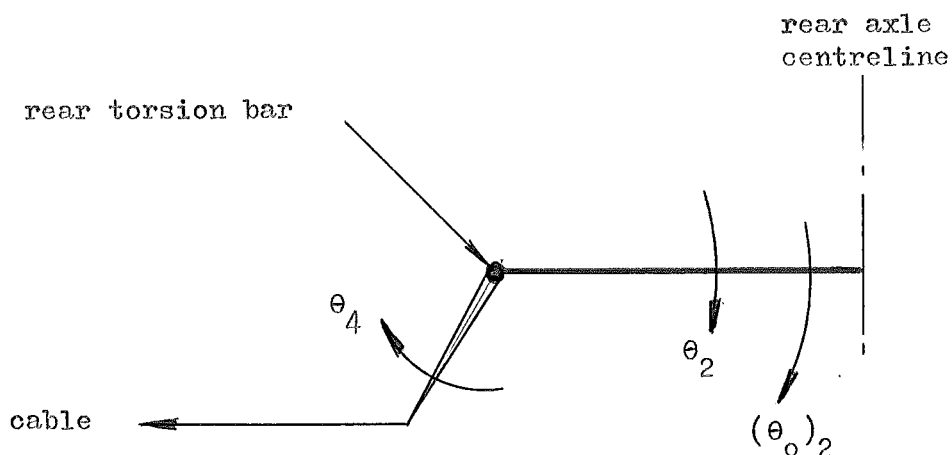
## Description

A(59) =  $\phi_1 = \theta_1 - \theta_3 - (\theta_o)_1$ ;  $(\theta_o)_1$  is negative.





$$A(60) = \phi_2 = \theta_2 - \theta_4 - (\theta_o)_2 ; (\theta_o)_2 \text{ is positive.}$$



$\theta_1, \theta_3$  are positive for front wheel bump.

$\theta_2, \theta_4$  are negative for rear wheel bump.

$(\theta_o)_1, (\theta_o)_2$  correspond to zero wheel or torsion bar load, so that at static conditions when  $\theta_1 = \theta_2 = 0$ ,  $\theta_1 = -(\theta_o)_1$ , is positive and  $\theta_2 = -(\theta_o)_2$  is negative.

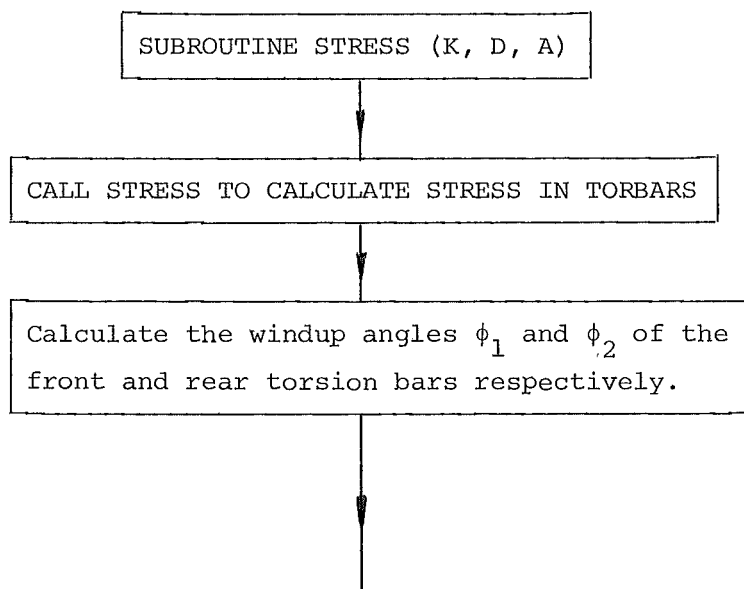
$$A(61) = S_1 = (\text{stresrate})_1 \cdot \theta_1$$

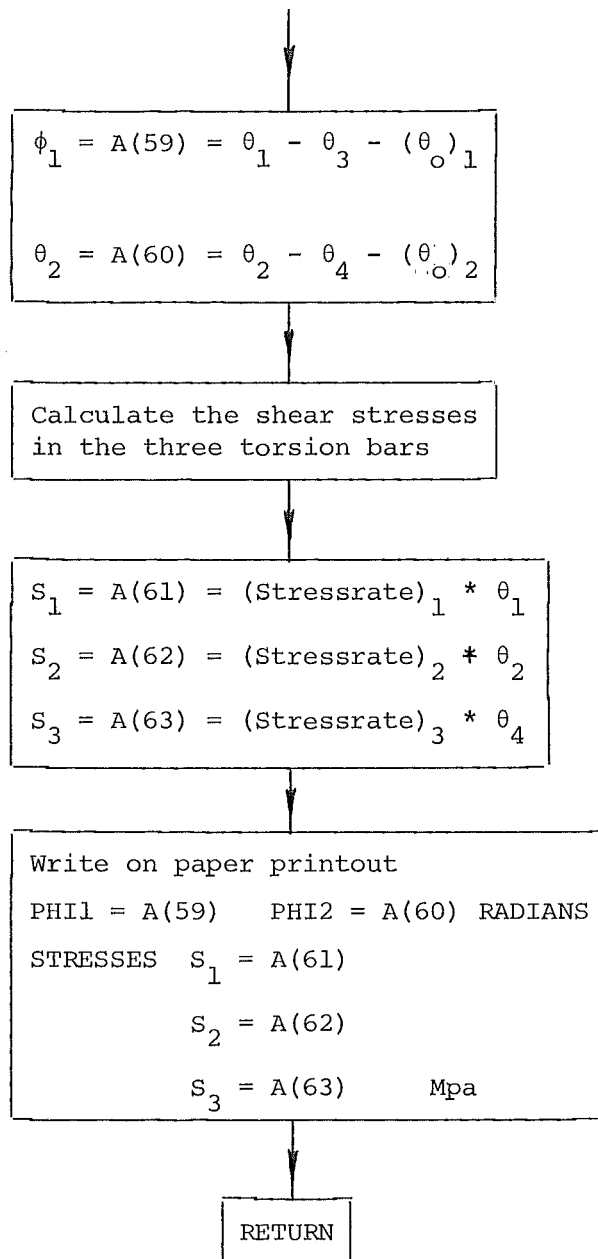
$$A(62) = S_2 = (\text{stressrate})_2 \cdot \theta_2$$

$$A(63) = S_3 = (\text{stressrate})_3 \cdot \theta_4$$

For calculating  $S_3$ , the angle of twist is  $\theta_4$ , that is, it is equal to that of the rear pitch arm. The auxiliary torsion bar is connected linearly to the rear pitch arm.

#### FLOWCHART





# I N T E R S U S P = = = = =

C DATA MUST BE FOLLOWED WITH A BLANK CARD

C DIMENSION DL(100),ANS(100)

1 CALL ZERO(1,50,ANS)  
READ(5,2)(DL(I),I=1,8)

002:0010:1 IS THE LOCATION FOR EXCEPTIONAL ACTION ON THE I/O STATE  
IF(DL(1).EQ.0)GO TO 99

READ(5,2)(DL(I),I=9,64)  
002:0021:1 IS THE LOCATION FOR EXCEPTIONAL ACTION ON THE I/O STATE

CALL SORTDT(DL)  
CALL TORBAR(DL,ANS)  
CALL ARMLTH(DL,ANS)  
CALL STDEFL(0,DL,ANS)  
CALL BUMP(100,100,50,DL,ANS)

99 CONTINUE  
END

C TO SUBROUTINE SORTDT(DL)  
SORT AND WRITE DATA  
DIMENSION DL(1)  
WRITE(6,200)

200 FORMAT(//,'PROGRAM CONTROL INTEGERS')  
WRITE(6,100)(DL(I),I=1,8)  
100 FORMAT(//,'IF =',I5,' FRONT TORSION BAR (1=CIRCULAR,2=RECTANGUL  
'AR)',/,I5,' ITR =',I5,' REAR TORSION BAR (1=CIRCULAR,2=RECTANGULAR)'  
'IAL =',I5,' ARM LENGTH DATA',  
'IAD =',I5,' INITIAL ANGLE DATA',  
'IVG =',I5,' VEHICLE GEOMETRY DATA',  
'LBA =',I5,30H ' LOAD-BRAKE-ACCELERATION DATA',  
'ITA =',I5,44H ' AUX TORSION BAR (1=CIRCULAR,2=RECTANGULAR),  
'(I5)'  
IF (DL(1).EQ.1)WRITE(6,111)DL(1),(DL(I),I=9,16)  
111 FORMAT(//,'FRONT TORSION BAR \* \* CIRCULAR \* \* IF =',I5,  
T/,6X,'G',9X,'L',9X,'D',/,1X,E10.5,7F10.4)  
IF (DL(1).EQ.2)WRITE(6,112)DL(1),(DL(I),I=9,16)  
112 FORMAT(//,'FRONT TORSION BAR \* \* RECTANGULAR \* \* IF =',I5,  
T/,6X,'G',9X,'L',9X,'A',9X,'B',8X,'N2',8X,'N3',/,1X,E10.5,7F10.4)  
IF (DL(2).EQ.1)WRITE(6,121)DL(2),(DL(I),I=17,24)  
121 FORMAT(//,'REAR TORSION BAR \* \* CIRCULAR \* \* ITR =',I5,  
T/,6X,'G',9X,'L',9X,'D',/,1X,E10.5,7F10.4)  
IF (DL(2).EQ.2)WRITE(6,122)DL(2),(DL(I),I=17,24)  
122 FORMAT(//,'REAR TORSION BAR \* \* RECTANGULAR \* \* ITR =',I5,  
T/,6X,'G',9X,'L',9X,'A',9X,'B',8X,'N2',8X,'N3',/,1X,E10.5,7F10.4)  
IF (DL(3).EQ.1)WRITE(6,131)DL(3),(DL(I),I=25,32)  
131 FORMAT(//,'ARM LENGTH DATA \* \* IAL =',I5,  
T/,4X,'AL1',7X,'AL2',7X,'AL3',7X,'AL4',7X,'AL5',7X,'AL6',8X,'L3',  
T/,8F10.4)  
IF (DL(4).EQ.1)WRITE(6,141)DL(4),(DL(I),I=33,40)  
141 FORMAT(//,'INITIAL ANGLE DATA \* \* IAD =',I5,  
T/,5X,'A1',8X,'A2',8X,'A3',8X,'A4',8X,'A5',8X,'A6',/,8F10.4)  
IF (DL(5).EQ.1)WRITE(6,151)DL(5),(DL(I),I=41,48)  
151 FORMAT(//,'VEHICLE GEOMETRY DATA \* \* IVG =',I5,  
T/,5X,'WB',9X,'A',9X,'B',9X,'H',9X,'M',9X,'K',/,8F10.4)  
IF(DL(42)+DL(43).NE.1.0)WRITE(6,159)  
159 FORMAT(3//,33H ' \* A+B DOES NOT EQUAL UNITY \* \*)  
IF(DL(6).EQ.1)WRITE(6,161)DL(6),(DL(I),I=49,56)  
161 FORMAT(//,36H ' LOAD-BRAKE-ACCELERATION DATA \* \* LBA =',I5,  
T/,4X,3HDFL,7X,3HMF,7X,3HMURL,7X,3HMRL,8X,2HDB,8X,2HMP,8X,2HDA,  
T8X,2HMA,/,8F10.4)  
IF (DL(7).EQ.1)WRITE(6,171)DL(7),(DL(I),I=57,64)  
171 FORMAT(//,46H ' AUXILIARY TORSION BAR \* \* CIRCULAR \* \* ITA =',I5,  
T/,6X,'G',9X,'L',9X,'D',/,1X,E10.5,7F10.4)  
IF (DL(7).EQ.2)WRITE(6,172)DL(7),(DL(I),I=57,64)  
172 FORMAT(//,46H ' AUXILIARY TORSION BAR \* \* RECTANGULAR \* \* ITA =',I5,  
T/,6X,'G',9X,'L',9X,'A',9X,'B',8X,'N2',8X,'N3',/,1X,E10.5,7F10.4)  
RETURN  
END

```

SUBROUTINE TORBAR(DL,ANS)
C TO CALCULATE * * TORSIONAL RATE * * STRESS RATE * *
  DIMENSION DL(1),ANS(1)
C
C * FRONT TORATE C1 STRESSRATE * * REAR TORATE C2 STRESS RATE *
C   ANS(1) ANS(2) ANS(3) ANS(4)
C
  IF (DL(1).EQ.0) GO TO 2
  IF (DL(1).EQ.2) GO TO 1
C CIRCULAR
  ANS(1)=3.1415926536*(DL(11)**4)*DL(9)/(32*DL(10)*1.E+03)
  ANS(2)=DL(11)*DL(9)/(2*DL(10)*1.E+06)
  GO TO 2
1 CONTINUE
C RECTANGULAR
  ANS(1)=DL(14)*DL(11)*DL(11)*DL(11)*DL(12)*DL(9)/(DL(10)*1.E+03)
  ANS(2)=DL(14)*DL(11)*DL(9)/(DL(13)*DL(10)*1.E+06)
2 CONTINUE
  IF (DL(2).EQ.0) GO TO 4
  IF (DL(2).EQ.2) GO TO 3
C CIRCULAR
  ANS(3)=3.1415926536*(DL(19)**4)*DL(17)/(32*DL(18)*1.E+03)
  ANS(4)=DL(19)*DL(17)/(2*DL(18)*1.E+06)
  GO TO 4
3 CONTINUE
C RECTANGULAR
  ANS(3)=DL(22)*DL(19)*DL(19)*DL(19)*DL(20)*DL(17)/(DL(18)*1.E+03)
  ANS(4)=DL(22)*DL(19)*DL(17)/(DL(21)*DL(18)*1.E+06)
4 CONTINUE
  IF (DL(7).EQ.0) GO TO 6
  IF (DL(7).EQ.2) GO TO 5
C CIRCULAR
  ANS(5)=3.1415926536*(DL(59)**4)*DL(57)/(32*DL(58)*1.E+03)
  ANS(6)=DL(59)*DL(57)/(2*DL(58)*1.E+06)
  GO TO 6
5 CONTINUE
C RECTANGULAR
  ANS(5)=DL(62)*DL(59)*DL(59)*DL(59)*DL(60)*DL(57)/(DL(58)*1.E+03)
  ANS(6)=DL(62)*DL(59)*DL(57)/(DL(61)*DL(58)*1.E+06)
6 CONTINUE
  WRITE(6,100) (ANS(I),I=1,6)
100 FORMAT(7,' EACH FRONT TORSION BAR * TORSION RATE C1 =',F10.3,
  T', KNM/RAD',/,23X,' * STRESSRATE =',F10.3,' MPA/RAD',
  T//,' EACH REAR TORSION BAR * TORSION RATE C2 =',F10.3,' KNM/RAD',
  T//,23X,' * STRESS RATE =',F10.3,' MPA/RAD',
  T//,' EACH AUXILIARY TOR BAR * TORSION RATE C3 =',F10.3,' KNM/RAD',
  T//,23X,' * STRESSRATE =',F10.3,' MPA/RAD')
99 CONTINUE
  RETURN
  END

```

```

SUBROUTINE FRLANG(K,D,A)
C SUBROUTINE TO FIND THE FOUR-BAR-LINKAGE ANGLES GIVEN ONE ANGLE AND THE
C K IS A CONTROL INTEGER
  DIMENSION D(1),A(1)
C DATA LIST 27 28 29 30 35 36 38
CORRES TO AL3 A4 AL5 AL6 A3 A4 A6
  TOP=D(29)*D(29)+D(27)*D(27)-2*D(29)*D(27)*COS(A(9))
  ENDTM=ATAN(D(27)*SIN(A(9))/(D(29)-D(27)*COS(A(9))))
CABLE ANGLE A6 = PHI = ANS(8)
  A(8)=ARCOS((TOP+D(30)*D(30)-D(28)*D(28))/(2*D(30)*SQRT(TOP)))
  T=ENDTM
CALC ANGLE4 = A(10)
  A(10)=ARCOS((TOP+D(28)*D(28)-D(30)*D(30))/(2*D(28)*SQRT(TOP)))
  T=ENDTM
99 RETURN
  END

```

```

SUBROUTINE ARMLTH(DL,ANS)
CALL ARMLTH TO CALC PITCH ARM LENGTHS * CABLE LENGTH * CABLE ANGLE *
GIVEN INITIAL PITCH ANGLES AND PITCH ARM OFFSET(3)
C DATA LIST 25 26 27 28 29 30 35 36 38 42 43
CORRES TO AL1 AL2 AL3 AL4 AL5 AL6 A3 A4 A6 A A B
C ANS 7 9 10
CORRES RL34 ANG3 ANG4
DIMENSION DL(1),ANS(1)
WRITE(6,104)
104 FORMAT(/,38H SUBROUTINE * ARMLTH * HAS BEEN CALLED)
ANS(7)=DL(43)*DL(25)*COS(DL(33))/(DL(42)*DL(26)*COS(DL(34)))
CALC L4 FROM L3=DL(31)+ANS(23)
ANS(23)=DL(31)
ANS(24)=ANS(23)/ANS(7)
CALC A6
DL(38)=ARCSIN((ANS(24)-ANS(23))/DL(29))
CALC AL3 AL4 AL6
DL(27)=ANS(23)/SIN(DL(35)-DL(38))
DL(28)=ANS(24)/SIN(DL(36)+DL(38))
DL(30)=(DL(29)-DL(27)*COS(DL(35))-DL(28)*COS(DL(36)))/COS(DL(38))
WRITE(6,100)ANS(24),DL(27),DL(28),DL(30),DL(38)
100 FORMAT(/,22H EFFECTIVE LENGTH L4 =,F10.4,/,
T20H ARM LENGTHS * AL3 =,F10.4,11H AND AL4 =,F10.4,7H METRES,/,
T19H CABLE LENGTH AL6 =,F10.4,29H AND INITIAL CABLE ANGLE A6 =,
TF10.4,8H RADIANS)
CALCULATE LOCKED PITCH ANGLES * UNEQUAL PITCH ARMS
CALC FRONT BUMP 11 12 * REAR BUMP 13 14
CORRES LOCKED ANGLE FRONT REAR FRONT REAR
IF(DL(35).EQ.1.5708.AND.DL(36).EQ.1.5708)RETURN
IF(DL(35).EQ.3.1415926536/2..AND.DL(36).EQ.3.1415926536/2.) RETURN
S=(DL(27)+DL(28)+DL(29)+DL(30))/2
ANS(11)=2*ARCSIN(SQRT((S-DL(27))*(S-DL(29))/(DL(27)*DL(29))))
ANS(12)=2*ARCCOS(SQRT(S*(S-DL(27))/(DL(29)*(DL(30)+DL(28)))))
ANS(13)=2*ARCCOS(SQRT(S*(S-DL(28))/(DL(29)*(DL(30)+DL(27)))))
ANS(14)=2*ARCSIN(SQRT((S-DL(28))*(S-DL(29))/(DL(28)*DL(29))))
WRITE(6,105)ANS(1),I=11,14)
105 FORMAT(/,47H FRONT BUMP * LOCKED PITCH ANGLES ARE * FRONT =,
TF10.4,11H AND REAR =,F10.4,8H RADIANS,/,46H REAR BUMP * LOCKED PIT
TCH ANGLES ARE * FRONT =,F10.4,11H AND REAR =,F10.4,8H RADIANS)
RETURN
END

```

```

SUBROUTINE BUMP(I,J,K,DL,ANS)
CALC BUMP CONFIGURATION, REACTIONS, SPRINGRATES, FREQUENCIES
DIMENSION DL(1),ANS(1)
CODE ANSWERS 8 9 10 15 16 17 18 19 20 41 22 23
CORRES TO A6 A3 A4 A1 A2 THT1 THT2 THT3 THT4 L1 L2 L3
C
CODE ANSWERS 24 25 26 27 28 29 30 31 32 33 34 35
CORRES TO L4 RL34 RA34 RATIO T F1 F2 P1 P2 C11 C22 C12
C
CODE ANSWERS 36 37 38 39 40 41 42 47 48 49 50
CORRES TO C21 PFB PFP CC1 CC2 PF BF ITH1 ITH2 F01 F02
C
CODE ANSWERS 51 52 53 54 55 56 57 58
CORRES TO G1 G2 2C11 2C22 2C12 2C21 P/G1 P/G2
C

```

```

WRITE(6,103)
103 FORMAT(/,36H SUBROUTINE * BUMP * HAS BEEN CALLED)
CONTROL INTEGERS I AND J ARE BOUNCE/REBOUND FRONT AND REAR
CONTROL INTEGER K FOR STEPS OF BOUNCE/REBOUND
CALL * M FOR FRONT BUMP/REBOUND * N FOR REAR BUMP/REBOUND
CALCULATE FOR BOUNCE AND REBOUND
IF(I.EQ.0)GO TO 1
CALL ZERO(15,32,ANS)
DO 1 M=-J,I,K
DO 1 N=-J,I,K
CALL DBUMP(M,N,DL,ANS)
CALL SPRATE(K,DL,ANS)
CALL FREQ(DL,ANS)
CALL STRESS(I,DL,ANS)
1 CONTINUE
RETURN
END

```

```

SUBROUTINE DRUMP(M,N,DL,ANS)
CALCULATES BUMP DETAILS
CALL * M FOR FRONT BUMP/REBOUND * N FOR REAR BUMP/REBOUND
DIMENSION DL(1),ANS(1)
CALC F1 AND F2
  ANS(29)=M/1000.
  ANS(30)=N/1000.
CALC THETA1, A1, L1
  ANS(17)=ARCSIN(SIN(DL(33))+ANS(29)/DL(25))-DL(33)
  IF(M.EQ.0)ANS(17)=0.0
  ANS(15)=DL(33)+ANS(17)
  ANS(21)=DL(25)*COS(ANS(15))
CALC THETA2, A2, L2
  ANS(18)=ARCSIN(SIN(DL(34))-ANS(30)/DL(26))-DL(34)
  IF(N.EQ.0)ANS(18)=0.0
  ANS(16)=DL(34)+ANS(18)
  ANS(22)=DL(26)*COS(ANS(16))
CALC THETA3 BY ITERATION
C SET VALUES BEFORE ITERATING
  ANS(19)=(ANS(17)+ANS(18))/3.0
  IT=0
1 CONTINUE
  ANS(9)=DL(35)+ANS(19)
  CALL FBLANG(910,DL,ANS)
CALC THETA4, L3, L4, RL34
  ANS(20)=DL(36)-ANS(10)
  ANS(23)=DL(27)*SIN(ANS(9)-ANS(8))
  ANS(24)=DL(28)*SIN(ANS(10)+ANS(8))
  ANS(25)=ANS(23)/ANS(24)
CHECK ITERATION
  FTHT=ANS(17)+ANS(25)*(ANS(3)*ANS(18)-(ANS(3)+ANS(5))*ANS(20))/
  TANS(1)
  IF(ABS(ANS(19)-FTHT).LT.1E-08)GO TO 2
  IT=IT+1
  IF(IT.EQ.1)GO TO 5
  IF(ANS(19).EQ.THTNM1)GO TO 5
  S=(FTHT-ANS(19))/(ANS(19)-THTNM1)
  IF(S.EQ.1.0)GO TO 5
  GO TO 5
5 S=0.0
6 CONTINUE
  THTNPI=ANS(19)+(FTHT-ANS(19))/(1.0-S)
CHANGE FOR NEW ITERATIONS
  THTNM1=ANS(19)
  ANS(19)=THTNPI
  GO TO 1
2 CONTINUE
CALC RA34,RATIO
  IF(ANS(20))3.7,3
7 ANS(26)=1.0
  GO TO 4
3 CONTINUE
  ANS(26)=ANS(19)/ANS(20)
  IF(ANS(26).EQ.0.0)ANS(26)=1.0
4 CONTINUE
  ANS(27)=ANS(25)/ANS(26)
CALC P1,P2,T
  ANS(31)=ANS(1)*(ANS(17)-ANS(19)-ANS(47))/ANS(21)
  ANS(32)=ANS(3)*(ANS(48)-ANS(18)+ANS(20))/ANS(22)
  ANS(28)=ANS(1)*(ANS(17)-ANS(19)-ANS(47))/ANS(23)
CALC P1/G1 AND P2/G2
  IF(M.EQ.0.AND.N.EQ.0)ANS(51)=ANS(31)
  ANS(57)=ANS(31)/ANS(51)
  IF(M.EQ.0.AND.N.EQ.0)ANS(52)=ANS(32)
  ANS(58)=ANS(32)/ANS(52)
  IF(K.LT.0)RETURN
C WRITE(6,100)8,(I,I=15,24),ANS(8),(ANS(I),I=15,24)
100 FORMAT(11I10,/,11F10.4)
  WRITE(6,101)(ANS(I),I=29,32),(ANS(I),I=17,20),
  TANS(57),ANS(58),ANS(27),ANS(28),IT
101 FORMAT(/,2H *,6X,2HF1,8X,2HF2,8X,2HP1,8X,2HP2,6X,4HTHT1,6X,4HTHT2
  T,6X,4HTHT3,6X,4HTHT4,6X,4HP/G1,6X,4HP/G2,5X,5HRATIO,9X,1HT,7X,3HT
  TS,/,12F10.4,110)
  RETURN
END

```

```

SUBROUTINE SPRATE(K,DL,ANS)
CALCULATES SPRINGRATES
DIMENSION DL(1),ANS(1)
D1=ANS(3)+ANS(5)+ANS(1)/ANS(27)
D2=ANS(1)+ANS(27)*(ANS(3)+ANS(5))
C11  ANS(33)=ANS(1)*(ANS(3)+ANS(5))/(ANS(21)*ANS(21)*D1)
C22  ANS(34)=ANS(3)*(ANS(1)+ANS(5)*ANS(27))/(ANS(22)*ANS(22)*D2)
C12  ANS(35)=ANS(25)*ANS(1)*ANS(3)/(ANS(21)*ANS(22)*D2)
C21  ANS(36)=ANS(1)*ANS(3)/(ANS(25)*ANS(21)*ANS(22)*D1)
CALC TOTAL FRONT/REAR/INTERCONNECTED RATES = TWICE WHEEL RATES
DO 1 I=33,36
1  ANS(I+20)=ANS(I)*2.
  IF(K.LT.0)RETURN
  WRITE(6,100)ANS(I),I=33,36)
100 FORMAT(29H CORRES WHEEL RATES ARE * C11,F10.4,6H * C22,F10.4,6H *
  T C12,F10.4,6H * C21,F10.4,5H KN/M)
  RETURN
END

```

```

SUBROUTINE FREQ(DL,ANS)
CALC FREQUENCIES FROM SPRINGRATES
DIMENSION DL(1),ANS(1)
CALC ANS 37 38 39 40 41 42 43 44 45 46
CORRES TO PFB PFP CC1 CC2 PF BF PFB**2 PFP**2 PF**2 BF**2
C
CALC ANS 53 54 55 56
CORRES TO 2C11 2C22 2C12 2C21
C
ANS(43)=(ANS(53)+ANS(54)+ANS(55)+ANS(56))*1E3/DL(45)
ANS(44)=(DL(42)*DL(42)*ANS(53)+DL(43)*DL(43)*ANS(54)-DL(42)*DL(43)
T*(ANS(55)+ANS(56)))*1E3/(DL(45)*DL(46)*DL(46))
ANS(39)=DL(41)*(DL(42)*(ANS(53)+ANS(56))-DL(43)*(ANS(54)+ANS(55)))
T*1E3/DL(45)
ANS(40)=(DL(42)*(ANS(53)+ANS(55))-DL(43)*(ANS(54)+ANS(56)))*1E3/(D
TL(45)*DL(46)*DL(46)*DL(41))
FT=0.5*(ANS(43)+ANS(44))
ST=0.5*SQRT((ANS(44)-ANS(43))*(ANS(44)-ANS(43))+4.*ANS(39)*ANS(40)
T)
ANS(45)=(FT-ST)
ANS(46)=(FT+ST)
DO 2 I=43,46
  IF(ANS(I).LT.0.0)GO TO 1
2 CONTINUE
ANS(37)=SQRT(ANS(43))/(2.*3.1415926536)
ANS(38)=SQRT(ANS(44))/(2.*3.1415926536)
ANS(41)=SQRT(ANS(45))/(2.*3.1415926536)
ANS(42)=SQRT(ANS(46))/(2.*3.1415926536)
WRITE(6,100)ANS(41),ANS(42),ANS(I),I=37,40)
100 FORMAT(25H CORRES FREQS ARE * PITCH,F10.4,9H * BOUNCE,F10.4,3H HZ
T,5X,6H PFB =,F10.4,6H PFP =,F10.4,3H HZ,5X,11H C COEFFS =,2F10.4)
  RETURN
1 CONTINUE
WRITE(6,101)ANS(39),ANS(40),ANS(I),I=43,46)
101 FORMAT(18H FREQS * C COEFFS ,2F10.4,10H * PFB**2 ,F10.4,10H * PFP
T**2 ,F10.4,9H * PF**2 ,F10.4,9H * BF**2 ,F10.4,8H SEC**-2)
  RETURN
END

```

```

SUBROUTINE ZERO(I,J,ANS)
CALLED TO ZERO ANS I TO J
DIMENSION ANS(1)
DO 1 K=I,J
  ANS(K)=0.0
1 CONTINUE
RETURN
END

```

```

SUBROUTINE STDEFL(K,DL,ANS)
CALL STDEFL TO CALCULATE STATIC DEFLECTIONS
DIMENSION DL(1),ANS(1)
IF(K.GE.0)WRITE(6,100)
100 FORMAT(/,38H SUBROUTINE * STDEFL * HAS BEEN CALLED)
CALL ZERO(15.32,ANS)
CALC THT1 AND THT2 AT ZERO LOAD
ANS(47)=-DL(45)*9.80665*DL(43)*DL(25)*COS(DL(33))/(2000*ANS(1))
ANS(48)=-DL(46)*9.80665*DL(42)*DL(26)*COS(DL(34))/(2000*ANS(3))
CALC F01 AND F02
ANS(49)=-DL(25)*(SIN(DL(33)+ANS(47))-SIN(DL(33)))
ANS(50)=-DL(26)*(SIN(DL(34)+ANS(48))-SIN(DL(34)))
CALL DBUMP(0.0,DL,ANS)
CALC G1 AND G2
ANS(51)=ANS(31)
ANS(52)=ANS(32)
IF(K.LT.0)RETURN
WRITE(6,101) (ANS(I),I=47,50)
101 FORMAT(16H INITIAL THT1 = ,F10.4,18H * INITIAL THT2 = ,F10.4,
T/,29H STATIC DEFLECTIONS * FRONT = ,F10.4,9H * REAR = ,F10.4,2H M)
RETURN
END

```

```

SUBROUTINE STRESS(K,D,A)
CALL STRESS TO CALC STRESS IN TORBARS
CALC WINDUP ANGLES PHI1 AND PHI2
DIMENSION A(1),D(1)
A(59)=A(17)-A(19)-A(47)
A(60)=A(18)-A(20)-A(48)
CALC STRESS S1, S2 AND S3
A(61)=A(2)*A(59)
A(62)=A(4)*A(60)
A(63)=A(6)*A(20)
WRITE(6,100) (A(I),I=59,63)
100 FORMAT(' COORDS ANGLES * PHI1 = ',F10.4,' * PHI2 = ',
F10.4,' RAD AND STRESS * S1 = ',F10.4,' * S2 = ',F10.4,
T' * S3 = ',F10.4,' MPA')
RETURN
END

```



## APPENDIX 3.2

### WISHBONE ANALYSIS PROGRAM, WISHANAL

Purpose. To calculate suspension geometry for a standard four-bar-linkage type wishbone suspension, under static, bounce and rebound conditions.

Input. Seven sets of x,y coordinates that describe the suspension are inputted. The y-axis is the vertical centreline and the x-axis is the groundline. The limits of bounce and rebound are also inputted.

Output. The lengths of the upper and lower suspension arms are printed.

The lengths of various arms and linkages L12, L13, L24, L34, L35, L36 and L37, where for example L12 means the length from the point  $(x_1, y_1)$  to the point  $(x_2, y_2)$ , are printed.

Various angles of linkage to the x-axis are printed, i.e. AX12, AX13, AX24, AX34, AX35, AX36 and AX37, for the static condition.

Angles A435, A436 and A437 are also outputted, where for example A435 means the angle at point P3 subtended by the line from P4 and P5 in the triangle made up of points P4, P3 and P5.

The kingpin angle is calculated and printed.

Then for each bounce or rebound condition the following output is provided.

- K       = The deviation in x-coordinate of the upper-outboard balljoint (P3) from its static condition. Bounce is positive, rebound negative.
  
- Y7       = The y-coordinate of the lowest point of the tyre (i.e. tyre/road contact point).
  
- RY       = Instantaneous roll, centre height relative to the chassis of the car (i.e. relative to the axes system which assumes that the wheel moves relative to 0,0).
  
- RY-Y7   = Roll centre height relative to the tyre (the y-coordinate of which is Y7).

CAMBER = The camber angle of the tyre, that is, the angle the wheel centreline makes to vertical. Negative camber is the top of the tyre leaning towards the centre of the vehicle. CAMBER assumes no body roll.

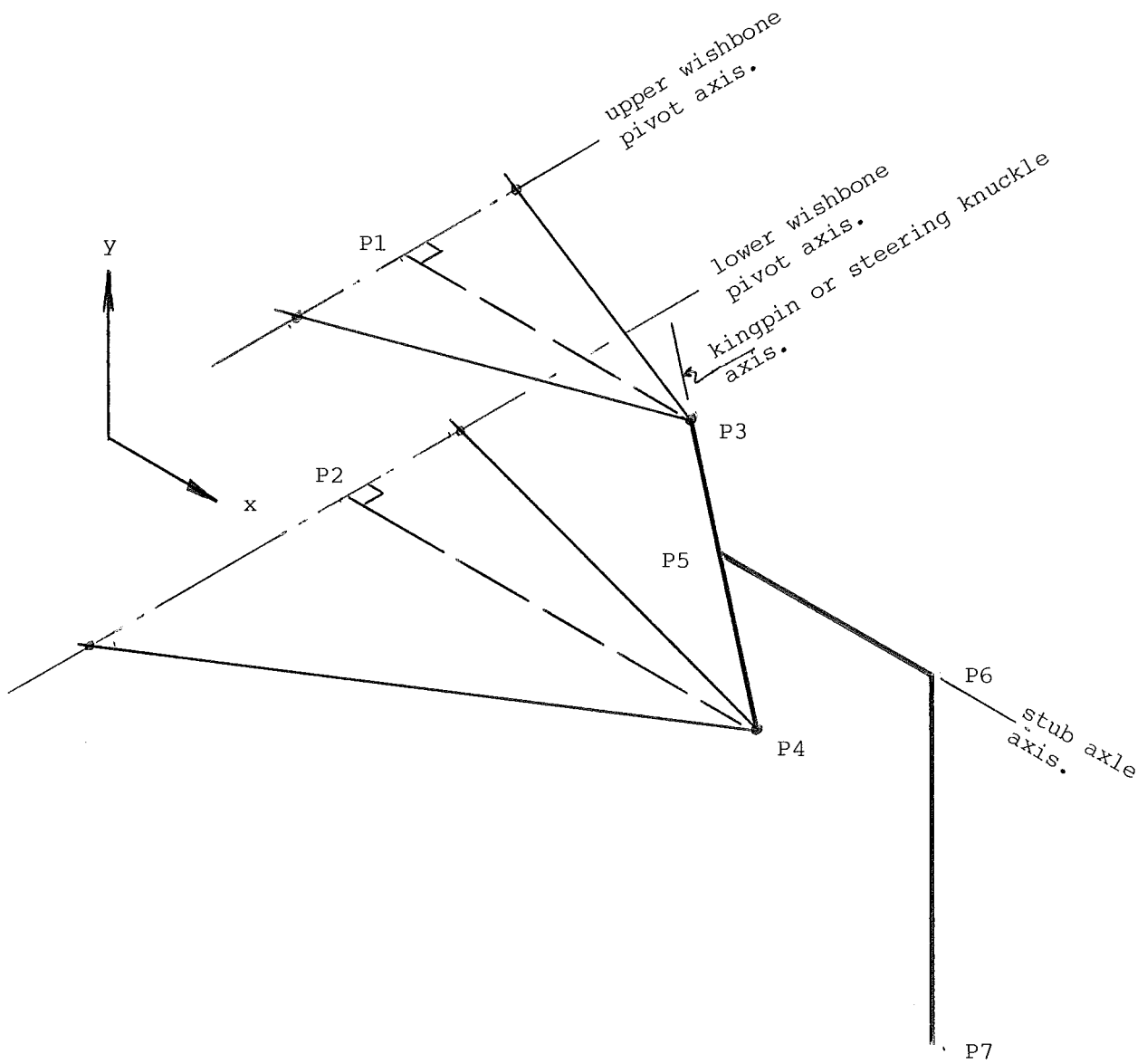
SCRUB = The lateral (sideways) displacement of the bottom of the tyre (road interface) from its static position. Scrub is positive outwards.

SARM = The instantaneous swingarm length. That is, the length of the line (perpendicular to the wheel centreline) from the instantaneous swingarm centre (where the top and bottom suspension arms geometrically intersect) to the wheel centreline.

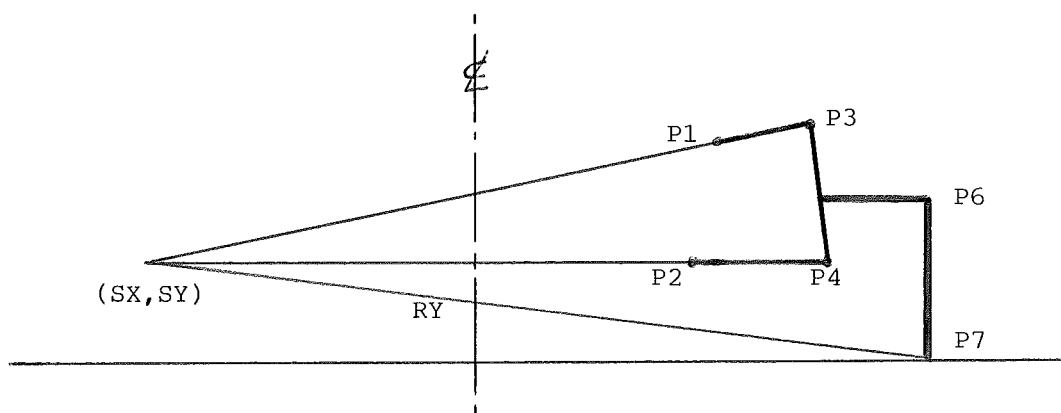
RATIO =  $\frac{\text{SARM}}{\text{TRACK}} = \frac{\text{swingarm length}}{\text{distance between front wheels}}$

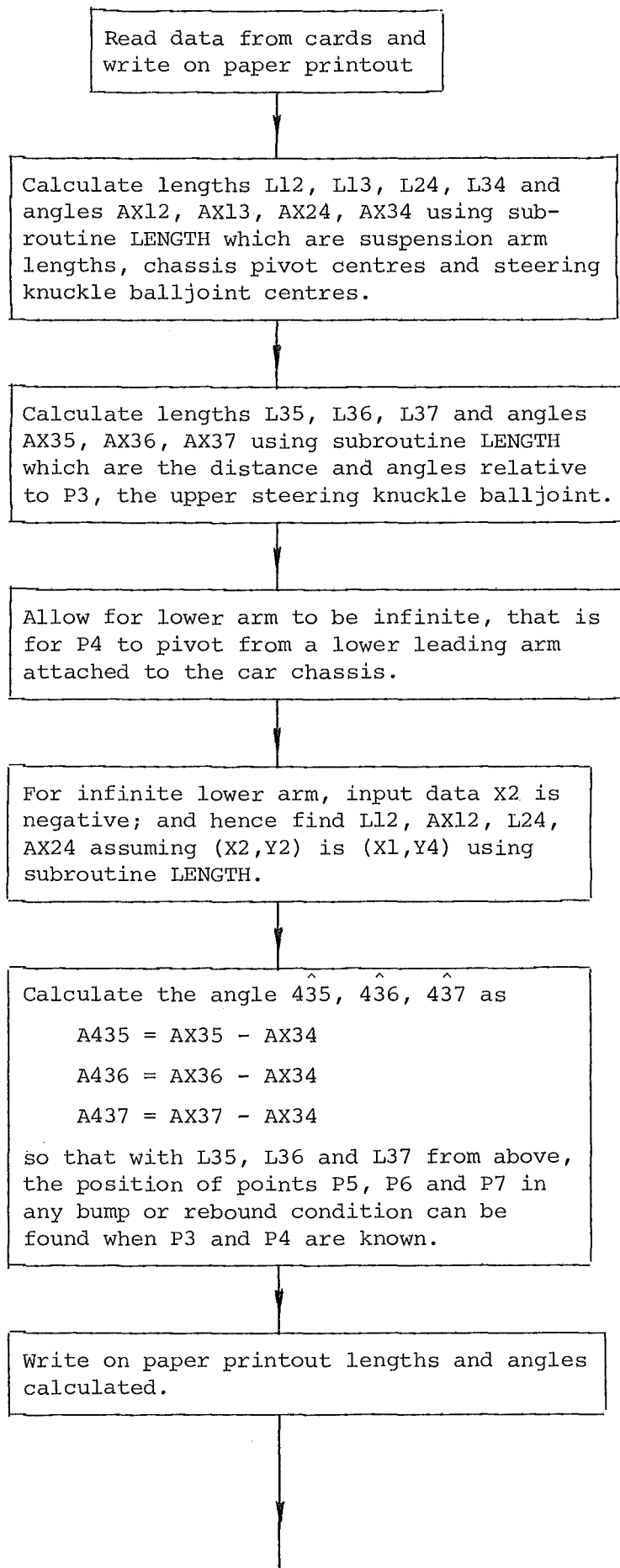
### Terminology

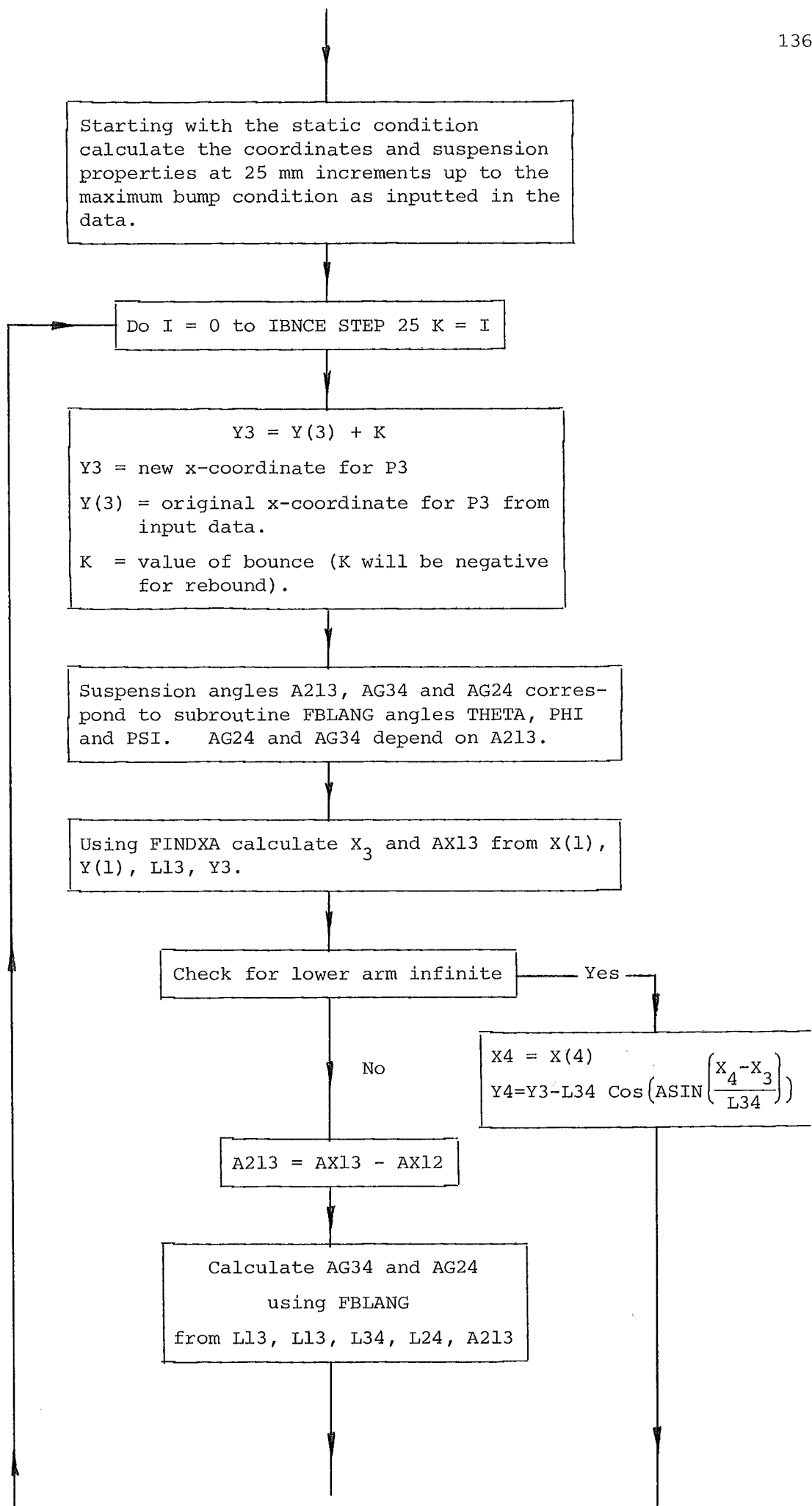
- P1 - coordinates  $(x_1, y_1)$  is the top pivot affixed to the chassis.
- P2 - coordinates  $(x_2, y_2)$  is the bottom pivot affixed to the chassis.  
P1 and P2 can be actual pivot points or the intersection of the pivot axes with the vertical plane through the front axle centreline.
- P3 - coordinates  $(x_3, y_3)$  is the top pivot or balljoint of the kingpin axis.
- P4 - coordinates  $(x_4, y_4)$  is the bottom pivot or balljoint of the kingpin axis.
- P5 - coordinates  $(x_5, y_5)$  is the intersection of the stub axle with the kingpin axis. (Note  $x_5, y_5$  need not be defined for the program to run).
- P6 - coordinates  $(x_6, y_6)$  is the intersection of the stub axle with the wheel centreline.
- P7 - coordinate  $(x_7, y_7)$  is the intersection of the wheel centreline with the groundline. i.e. the theoretical centre of the tyre contact patch. In static conditions  $y_7 = 0$  and the front track =  $2x_7$ .

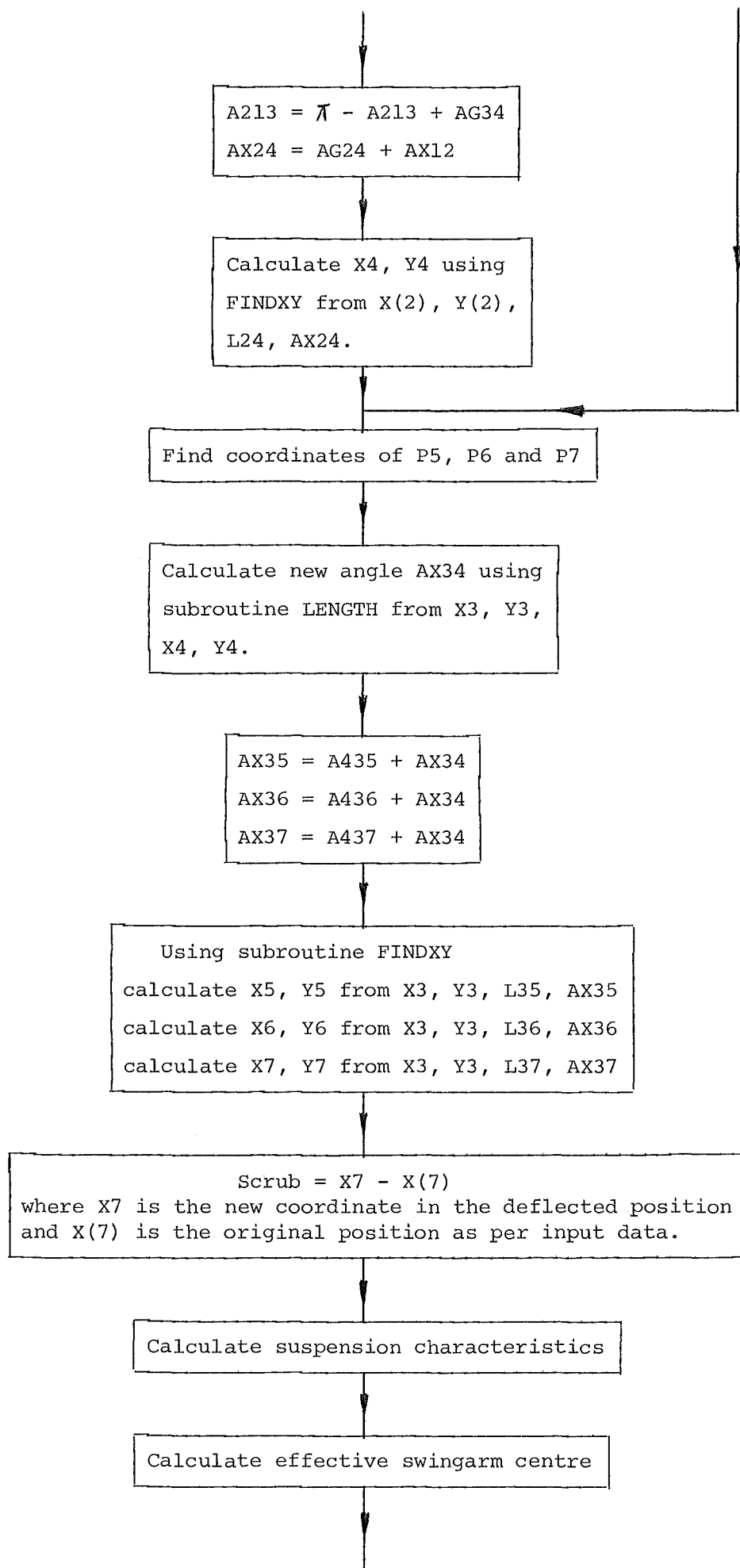


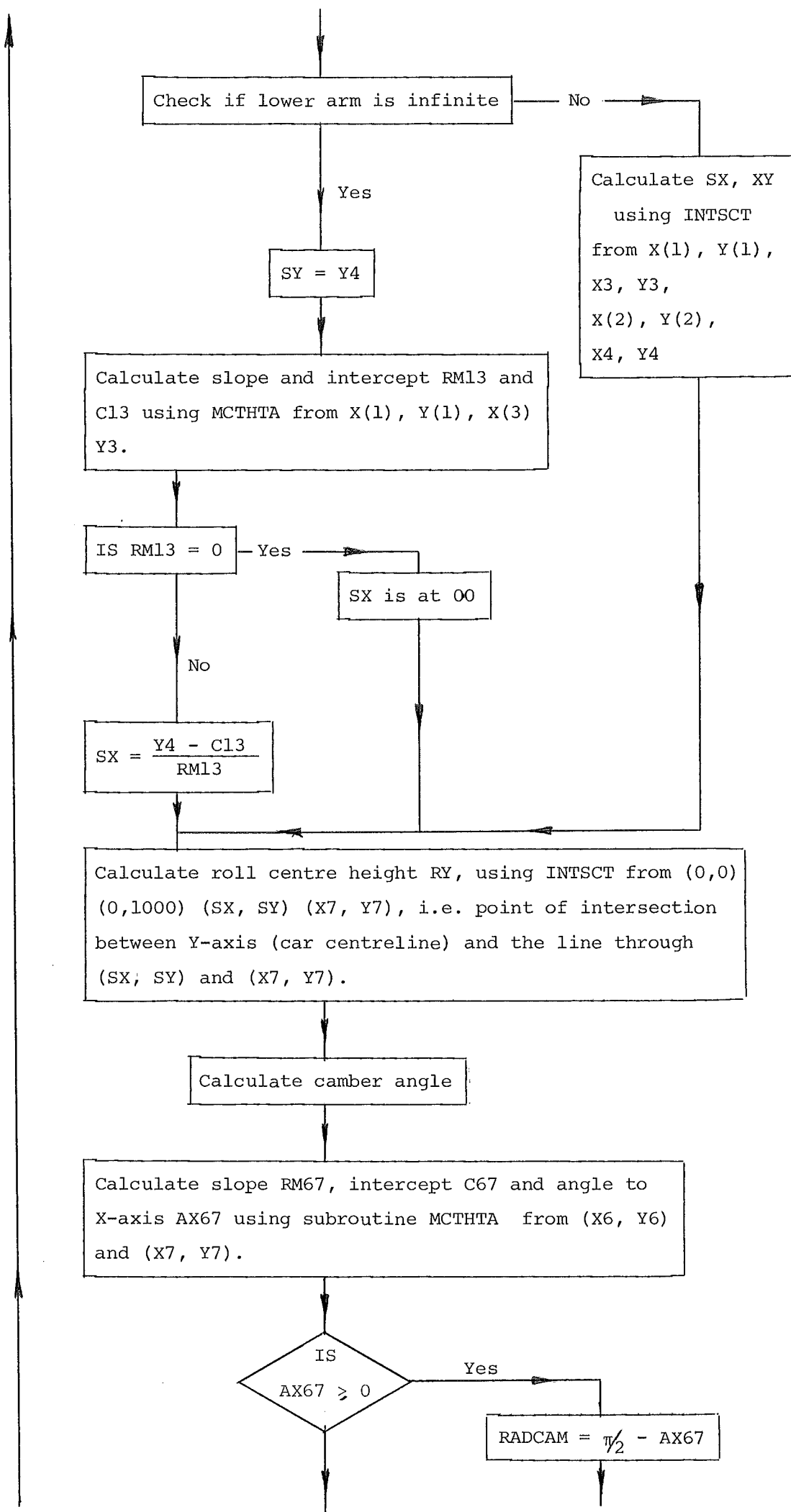
Wishbone Suspension Layout.

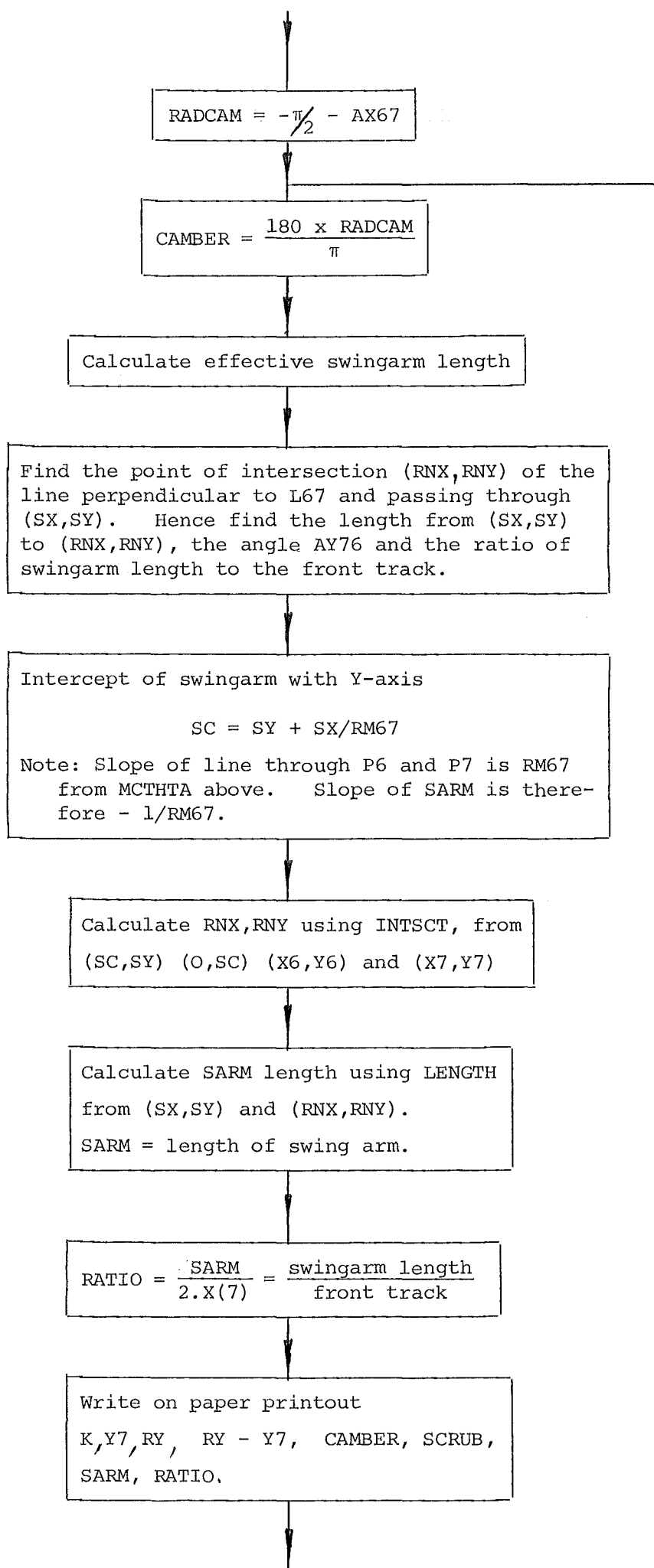
Cross-Section in  $xy$ -plane showing swingarm centre and roll centre.

FLOWCHART

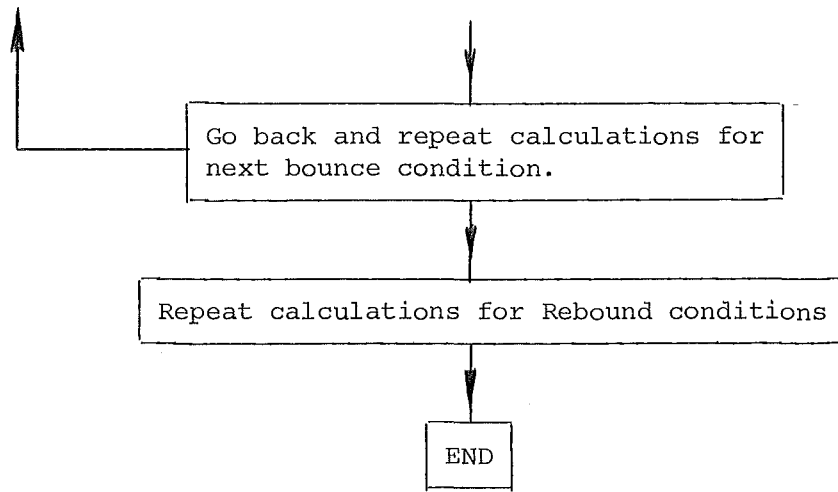










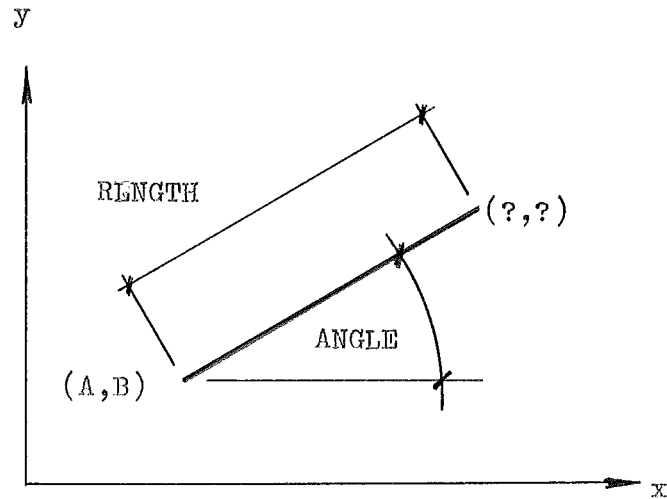
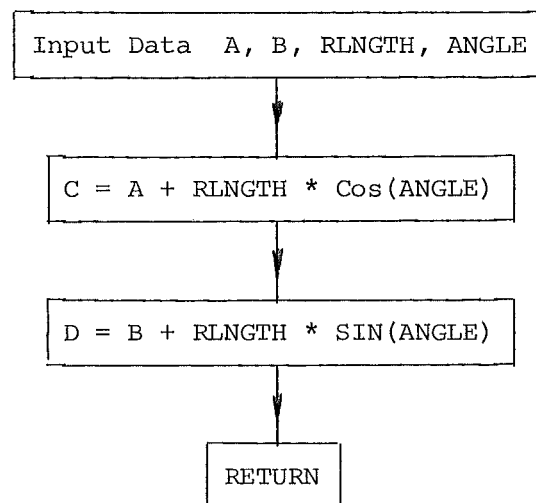


SUBROUTINE FINDXY

Purpose. To find the coordinates of a point given the length and angle of a line from another known point.

Input. Coordinates of known point (A,B) length RLNGTH and angle ANGLE.

Output. Coordinates (C,D)

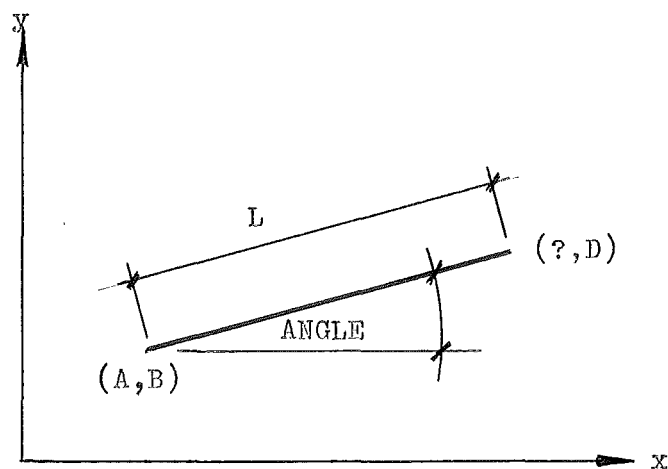
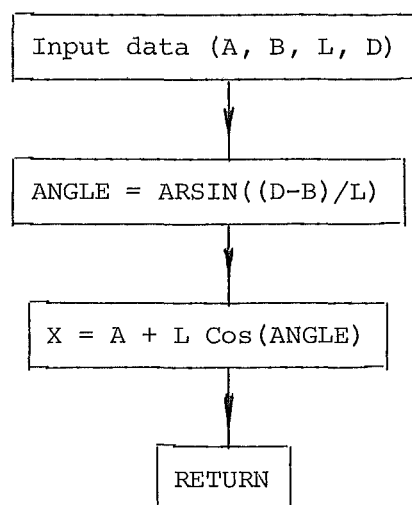
FLOWCHART

SUBROUTINE FINDXA

Purpose. To find the x-coordinate of a point, given the y-coordinate, and the length of the line from another known point. Also to find the angle to the x-axis of the said line.

Input. The y-coordinate D, the length of the line L and the coordinates of the known point (A,B).

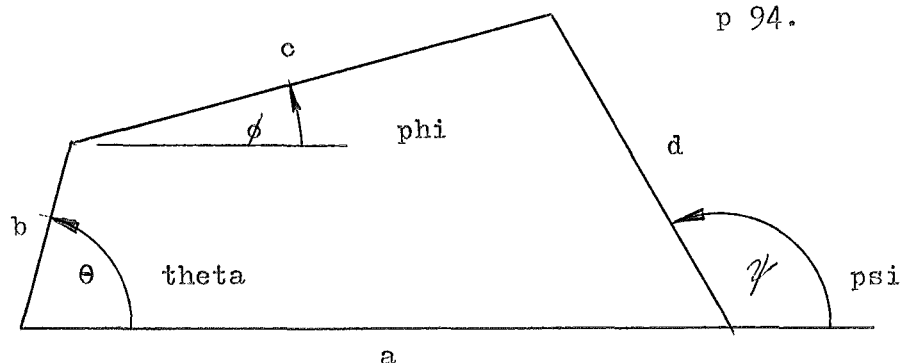
Output. The x-coordinate, x and angle THETA.

FLOWCHART

SUBROUTINE FBLANG

Purpose. To find the output angles for a Four-Bar-Linkage.

Machine Design  
June 9, 1977  
p 94.



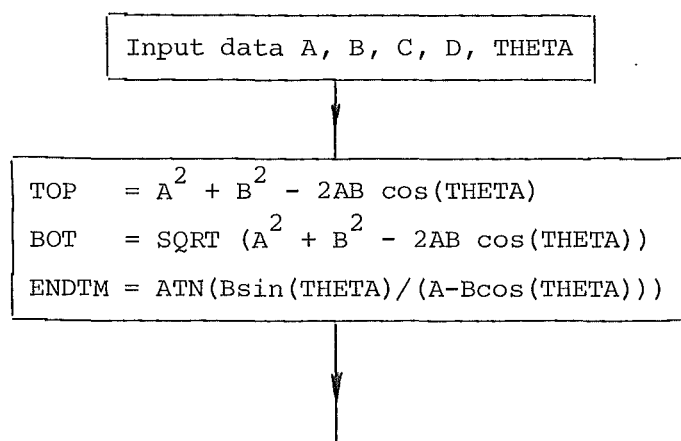
$$\phi = \pm \cos^{-1} \left\{ \frac{(a^2 + b^2 - 2ab \cos \theta) + c^2 - d^2}{2c \sqrt{a^2 + b^2 - 2ab \cos \theta}} \right\} - \tan^{-1} \left\{ \frac{b \sin \theta}{a - b \cos \theta} \right\}$$

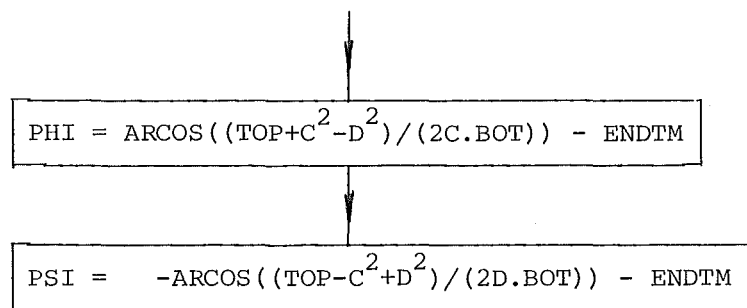
$$\psi = 180^\circ \pm \cos^{-1} \left\{ \frac{(a^2 + b^2 - 2ab \cos \theta) + d^2 - c^2}{2d \sqrt{a^2 + b^2 - 2ab \cos \theta}} \right\} - \tan^{-1} \left\{ \frac{b \sin \theta}{a - b \cos \theta} \right\}$$

FBLANG means Four Bar Linkage Angles.

Input. Four lengths A, B, C, D and input angle  $\theta$  (THETA).

Output. Angles  $\phi$  (PHI) and  $\psi$  (PSI).

FLOWCHART



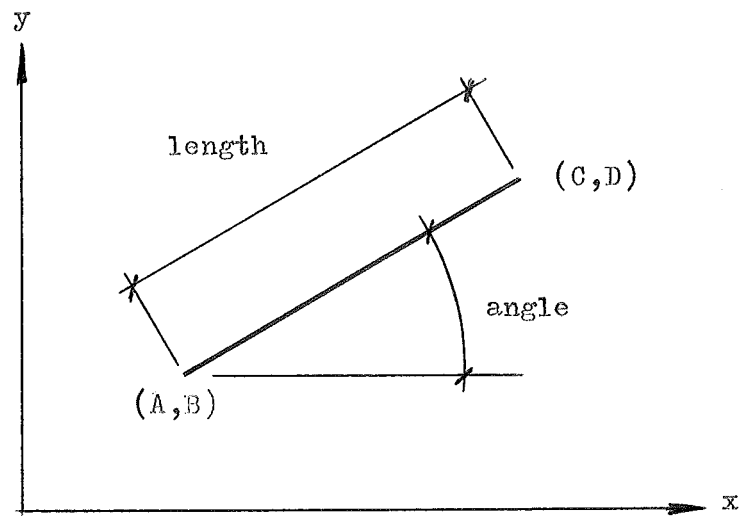
SUBROUTINE LENGTH

Purpose. To find the length of the line between two points and the angle that line makes with the x-axis.

Input. Two pairs of coordinates (A,B) and (C,D).

Output. The length and angle.

Discussion.



$$\text{angle} = \text{ATAN} \left( \frac{D-B}{C-A} \right)$$

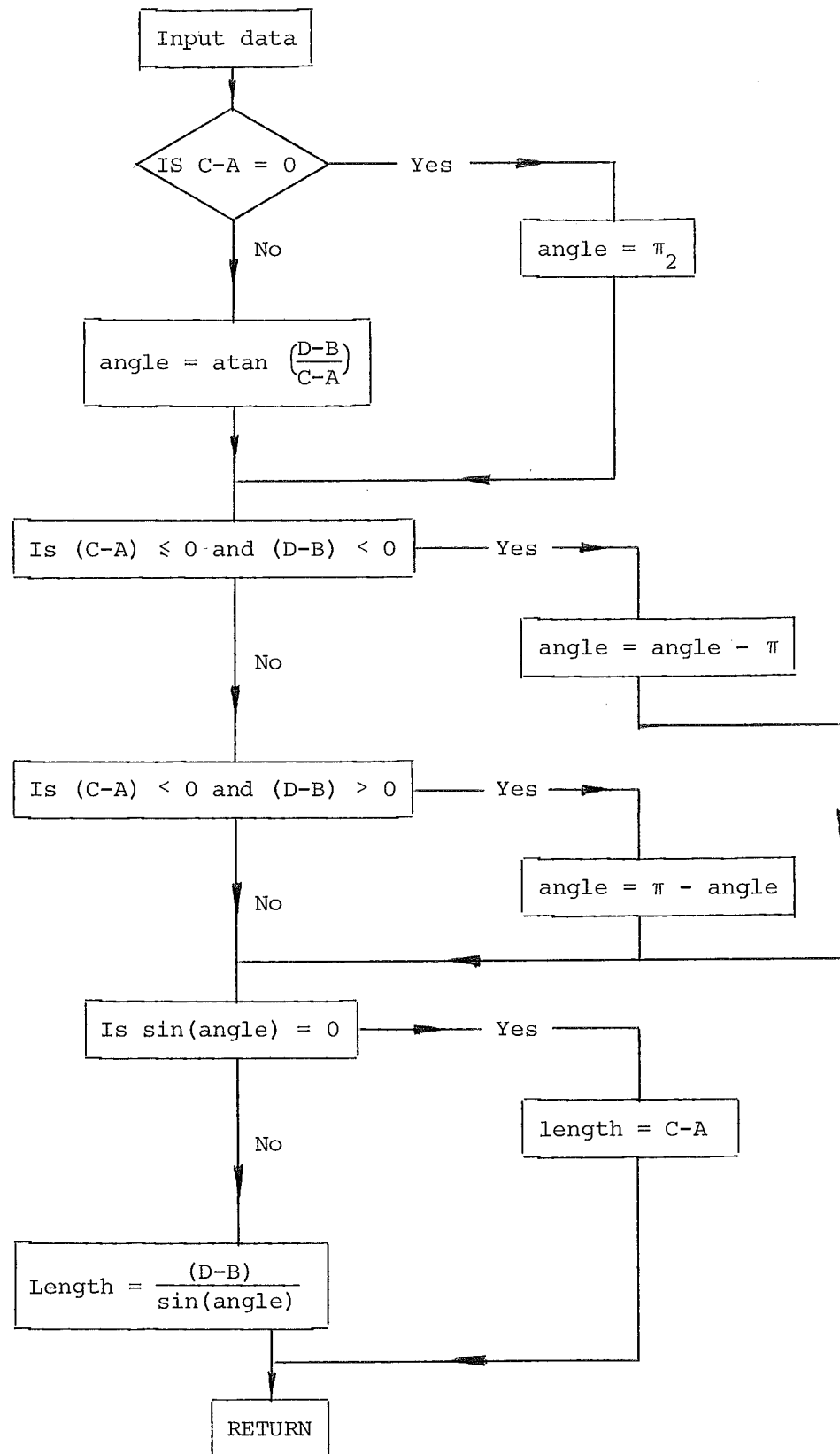
must check for  $0 < \text{angle} < 360$ .

1. If  $(D-B) > 0 + (C-A) > 0$  then  $0 < \text{angle} < 90$ .
2. If  $(D-B) > 0 + (C-A) < 0$  then  $270 < \text{angle} < 360$ , or  $-90 < \text{angle} < 0$
3. If  $(D-B) < 0 + (C-A) > 0$  then  $90 < \text{angle} < 180$ .
4. If  $(D-B) < 0 + (C-A) < 0$  then  $180 < \text{angle} < 270$ .

Given the angle, then

$$\text{Length} = \frac{(D-B)}{\sin(\text{angle})}$$

except that if  $\sin(\text{angle}) = 0$  then  $\text{length} = (C-A)$ .

FLOWCHART

SUBROUTINE MCTHTA

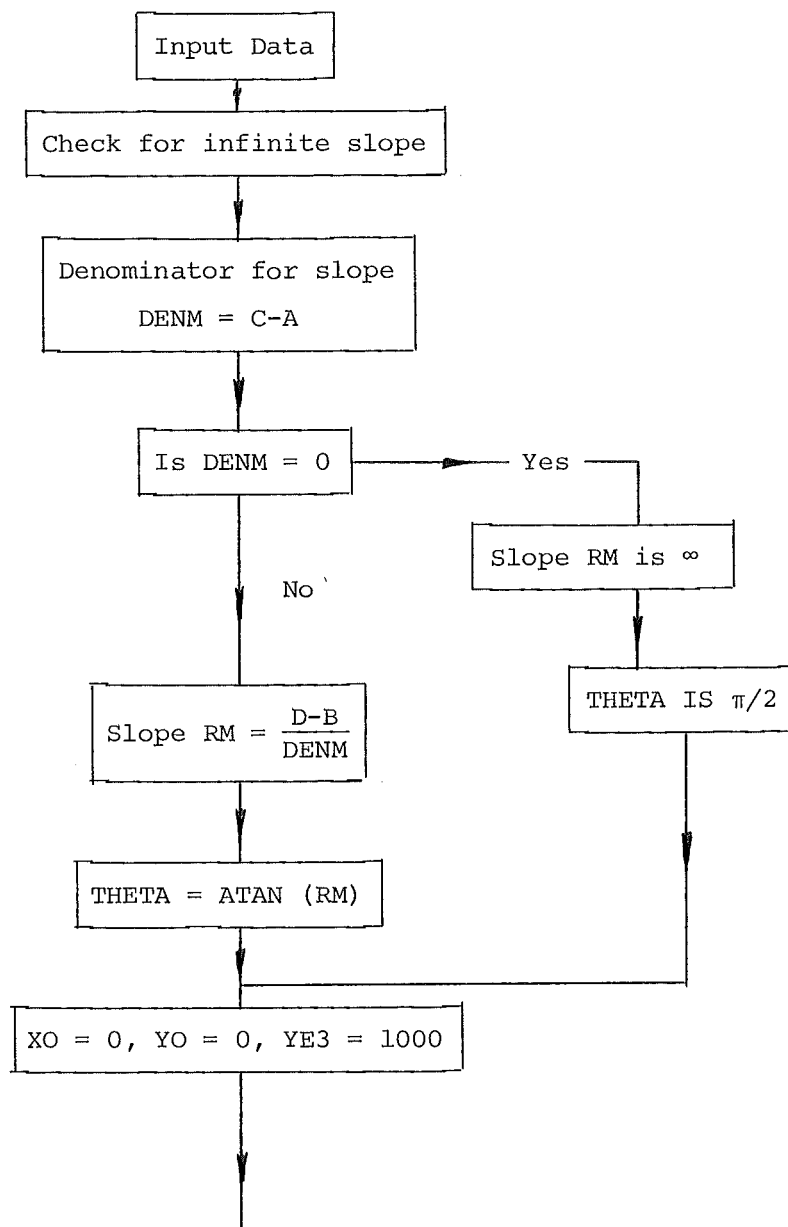
Purpose. To find the slope and intercept of a line  $y = Mx + C$  defined by two points. From the slope find also the angle to the x-axis.

Input. Two pairs of coordinates (A,B) (C,D).

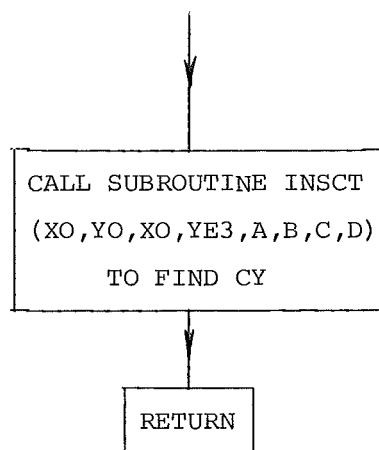
Output. Slope RM, intercept DY and angle THETA.

Discussion.

From coordinates (A,B) and (C,D) find the line  $y = Mx + C$ . The slope  $RM = \frac{D-B}{C-A}$ , so that the angle  $THETA = ATAN (RM)$  and the y-intercept is found using subroutine INTSCT.

FLOWCHART





SUBROUTINE INTSCT

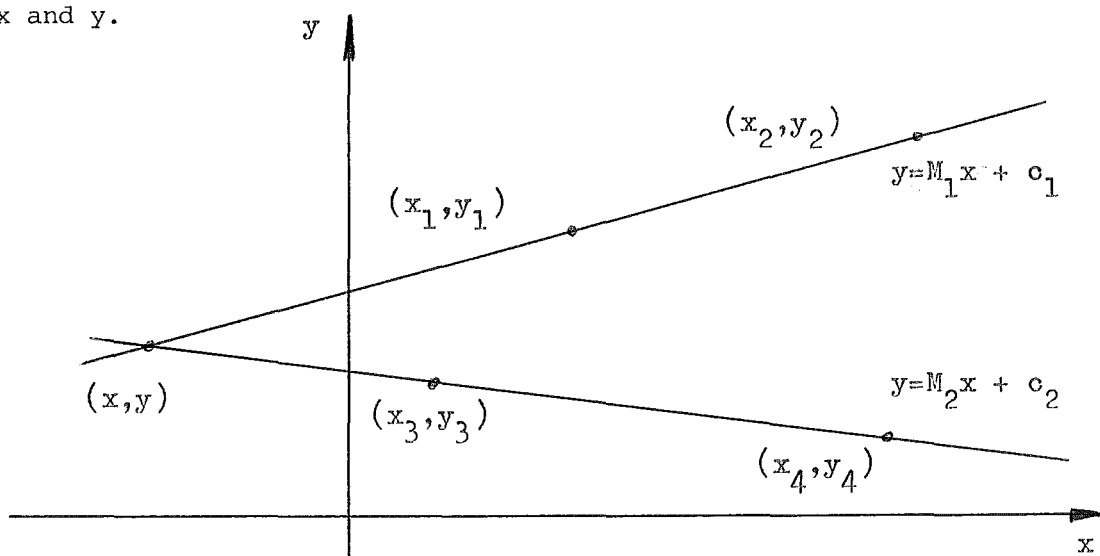
Purpose. To find the point of intersection  $(x,y)$  of two lines. Each line is defined by two pair of points.

Input. Four pairs of coordinates  $(x_1,y_1)$   $(x_2,y_2)$  and  $(x_3,y_3)$   $(x_4,y_4)$ .

Output. One point of intersection  $(x,y)$ .

Discussion.

Define the two lines in the form of  $y = mx + c$  and solve for  $x$  and  $y$ .



$$M_1 = \frac{y_2 - y_1}{x_2 - x_1}$$

$$M_2 = \frac{y_4 - y_3}{x_4 - x_3}$$

$$C_1 = \frac{x_2 y_1 - x_1 y_2}{x_2 - x_1}$$

$$C_2 = \frac{x_4 y_3 - x_3 y_4}{x_4 - x_3}$$

$$x = \frac{C_2 - C_1}{M_1 - M_2} = \frac{(x_2 - x_1)(x_4 y_3 - x_3 y_4) - (x_4 - x_3)(x_2 y_1 - x_1 y_2)}{(x_4 - x_3)(y_2 - y_1) - (x_2 - x_1)(y_4 - y_3)}$$

or as in program

$$x = \frac{(x_3 - x_4)(y_1 x_2 - x_1 y_2) - (x_1 - x_2)(y_3 x_4 - x_3 y_4)}{(y_1 - y_2)(x_3 - x_4) - (y_3 - y_4)(x_1 - x_2)}$$

From  $\frac{y_2 - y}{x_2 - x} = \frac{y_1 - y}{x_1 - x}$

$$y = \frac{y_1(x - x_2) - y_2(x - x_1)}{(x_1 - x_2)}$$

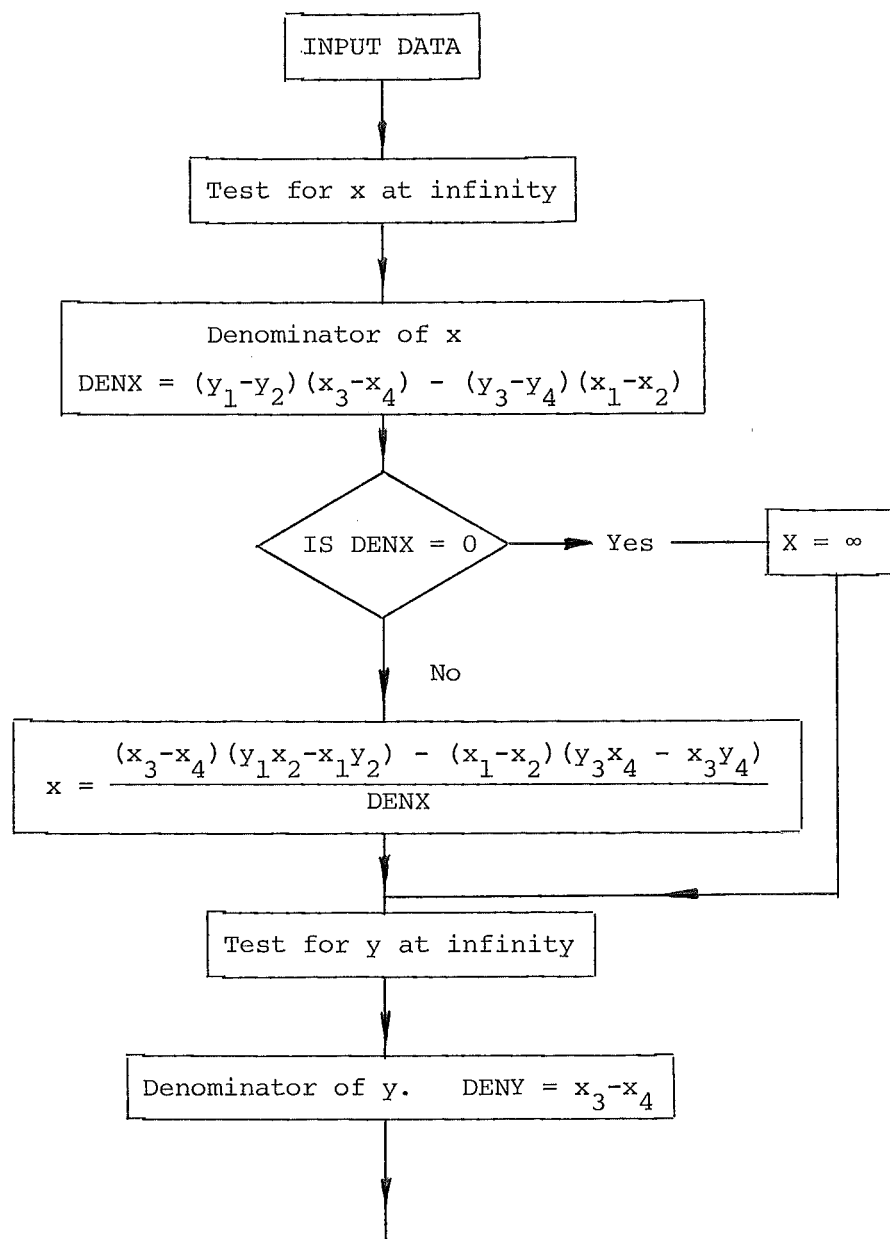
similarly

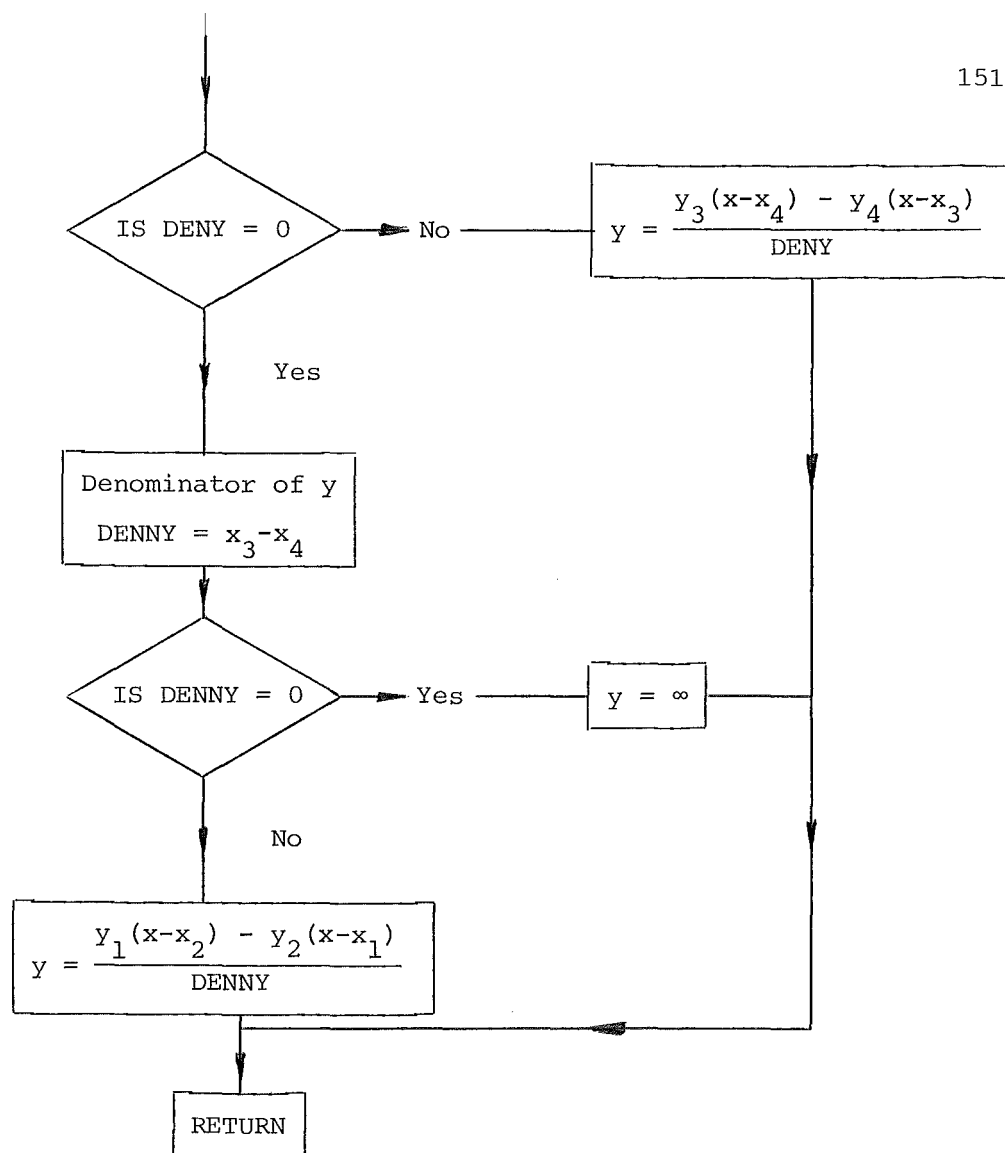
$$y = \frac{y_3(x - x_4) - y_4(x - x_3)}{(x_3 - x_4)}$$

If  $(y_1 - y_2)(x_3 - x_4) - (y_3 - y_4)(x_1 - x_2) = 0$  then  $x$  is at infinity.

If  $(x_3 - x_4) = 0$  then check if  $(x_1 - x_2) = 0$  if both then  $y$  is at infinity.

#### FLOWCHART





C PRELIMINARY ANALYSIS OF WISHBONE SUSPENSION GEOMETRY  
C

```

C      DIMENSION X(7),Y(7)
C      DATA READ IN ON ONE CARD SEPERATED BY COMMAS
C      PLUS ANOTHER CARD FOR BOUNCE,REBOUND
C      MUST HAVE CARD WITH 14 COMMAS AFTER DATA AND BEFORE END JOB
C      FOR LOWER ARM INFINITE # SPECIFY X2 AS NEGATIVE
C
1  CONTINUE
   READ(5,2)(X(I),Y(I),I=1,7)

   002:0012:1 IS THE LOCATION FOR EXCEPTIONAL ACTION ON THE I/O STATE
   IF(X(1).EQ.0.0) GO TO 99
   READ(5,2)IBNCE,IREBND
   002:001E:1 IS THE LOCATION FOR EXCEPTIONAL ACTION ON THE I/O STATE
   WRITE (6,101)

   WRITE (6,103)
   WRITE (6,102)(I,X(I),Y(I),I=1,7)
   WRITE(6,100)
   WRITE(6,107)IBNCE,IREBND
C  L13 IS THE UPPER WISHBONE LENGTH, L24 IS THE LOWEE WISHBONE LENGTH
C  A , B , C , D ARE LENGTHS IN A FOUR BAR LINKAGE CORRES TO LENGTHS
C  L12,L13,L34,L24 FOR THE SUSPENSION
C
NOTE ALL ANGLES IN RADIANS; EXCEPT CAMBER AND AKPIN
C
L12,L13,L34,L24 REMAIN CONSTANT THROUGHOUT
ANGLE AX12 REMAINS CONSTANT THROUGHOUT
CALL LENGTH(X(1),Y(1),X(2),Y(2),L12,AX12)
CALL LENGTH(X(1),Y(1),X(3),Y(3),L13,AX13)
CALL LENGTH(X(2),Y(2),X(4),Y(4),L24,AX24)
CALL LENGTH(X(3),Y(3),X(4),Y(4),L34,AX34)
C  TO WRITE(6,106)L13,L24
C  CALC A435 ETC AND L35 ETC
CALL LENGTH(X(3),Y(3),X(5),Y(5),L35,AX35)
CALL LENGTH(X(3),Y(3),X(6),Y(6),L36,AX36)
CALL LENGTH(X(3),Y(3),X(7),Y(7),L37,AX37)
WRITE(6,300)
WRITE(6,210)L12,L13,L24,L34,L35,L36,L37
WRITE(6,301)
WRITE(6,210)AX12,AX13,AX24,AX34,AX35,AX36,AX37
C  ALLOW FOR INFINITE LOWER ARM
IF (X(2))7,8,8
7  CONTINUE
CALL LENGTH(X(1),Y(1),X(4),Y(4),L12,AX12)
CALL LENGTH(X(1),Y(4),X(4),Y(4),L24,AX24)
WRITE(6,307)L12,L24,AX12,AX24
8  CONTINUE
A435=AX35-AX34
A436=AX36-AX34
A437=AX37-AX34
WRITE(6,303)
WRITE(6,211)A435,A436,A437
C  CALCULATE AKPIN = KINGPIN ANGLE
CALL LENGTH(X(6),Y(6),X(7),Y(7),L67,AX67)
AKPIN=180.0*(AX34-AX67)/3.1415926536
WRITE(6,213)AKPIN
WRITE(6,212)
C  ABOVE THIS POINT , VALUES ARE CONSTANT

```



## C CALC SUSP CHARACTERISTICS

C CALC EFFECTIVE SARM CENTRE = S

IF (X(2))12,13,13

12 CONTINUE

CALL MCTHTA(X(1),Y(1),X3,Y3,RM13,C13,ANG13)

SY=Y4

IF(RM13)15,16,15

16 SX=1.E40

GO TO 14

15 CONTINUE

SX=(Y4-C13)/RM13

GO TO 14

13 CONTINUE

CALL INTSCT(X(1),Y(1),X3,Y3,X(2),Y(2),X4,Y4,SX,SY)

14 CONTINUE

C CALC ROLL CENTRE POSITION = R ROLL CENTRE HEIGHT = RY

X0=0.0

Y0=0.0

YE3=1000.0

CALL INTSCT(X0,Y0,X0,YE3,SX,SY,X7,Y7,RX,RY)

C CALC CAMBER ANGLE

C RM67 IS THE SLOPE THRU P6 AND P7

CALL MCTHTA(X6,Y6,X7,Y7,RM67,C67,AX67)

IF(AX67.GE.0.0)RADCAM=1.5707963268-AX67

IF(AX67.LT.0.0)RADCAM=-1.5707963268-AX67

CAMBER=180.0#RADCAM/3.1415926536

C CALC EFFECTIVE SARM LENGTH = SARM

C REQD TO FIND LGTH OF LINE THRU P6 AND P7 AND PASSING THRU S

SC=SY+SX/RM67

CALL INTSCT(SX,SY,X0,SC,X6,Y6,X7,Y7,RNX,RNY)

CALL LENGTH(SX,SY,RNX,RNY,SARM,NGLARM)

RATIO=SARM/(2\*X(7))

RYDASH=RY-Y7

WRITE(6,105)K,Y7,RY,RYDASH,CAMBER,SCRUB,SARM,RATIO

21 CONTINUE

20 CONTINUE

IF(IREBND.EQ.0)GO TO 1

N=IREBND

IF(IBNCL.EQ.0.AND.K.EQ.0) K=1

IF (K) 1,1,5

99 CONTINUE

100 FORMAT(//,' TO CALCULATE FOR BOUNCE AND REBOUND')

101 FORMAT(//,' PRELIMINARY ANALYSIS OF WISHBONE SUSPENSION GEOMETRY

T')

102 FORMAT(5X,I5,5X,F9.1,5X,F9.1)

103 FORMAT(013X,' X-COORD',7X,' Y-COORD')

104 FORMAT(7,5X,'K',6X,'Y7',8X,'RY',7X,'RY-Y7',4X,'CAMBER',4X,'SCRUB'

T,6X,'SARM',5X,'RATIO')

105 FORMAT(' #',I4,7F10.3)

106 FORMAT(7,' LENGTH OF UPPER ARM IS ',F8.3,/'

T/, ' LENGTH OF LOWER ARM IS ' F8.3)

107 FORMAT(20X,I5,10X,I5)

200 FORMAT(7,2F15.4)

201 FORMAT(7,3F15.4)

202 FORMAT(7,F15.3)

203 FORMAT(7,E15.4)

204 FORMAT(7,6F15.6)

210 FORMAT(10X,8F10.3)

211 FORMAT(10X,3F10.3)

212 FORMAT(7,' SCRUB IS POSITIVE OUTWARDS')

213 FORMAT(7,' KINGPIN ANGLE = ',F10.3)

214 FORMAT(10X,10F10.3)

300 FORMAT(7,' LENGTHS',8X,'L12',7X,'L13',7X,'L24',7X,'L34',7X,'L35',

T7X,'L36',7X,'L37')

301 FORMAT(7,' ANGLES',8X,'AX12',6X,'AX13',6X,'AX24',6X,'AX34',6X,

T'AX35',6X,'AX36',6X,'AX37')

303 FORMAT(7,' ANGLES',9X,'A435',7X,'A436',7X,'A437')

304 FORMAT(7,' ANGLES',9X,'A213',7X,'AG34',7X,'AG24')

305 FORMAT(7,' NEW COORDS',3X,'X3',8X,'Y3',8X,'X4',8X,'Y4',8X,'X5',

T8X,'Y5',8X,'X6',8X,'Y6',8X,'X7',8X,'Y7')

306 FORMAT(7,' ANGLES',7X,'A213',6X,'AX13',6X,'AG24')

307 FORMAT(7,' LOWER ARM IS OF INFINITE LENGTH',/,

T' NEW CALC LENGTHS \* L12 =',F10.3,' L24 =',F10.3,

T/,18X,' AX12 =',F10.3,' AX24 =',F10.3)

308 FORMAT(' SARM CENTRE',2F15.3,' ROLL CENTRE',2F10.3)

1000 FORMAT(7F10.3,4,7F10.3)

1001 FORMAT(215)

END

```

SUBROUTINE INTSCT(X1,Y1,X2,Y2,X3,Y3,X4,Y4,X,Y)
C (X,Y) IS THE POINT OF INTERSECTION OF TWO LINES
C TEST FOR X AT INFINITY
DENX=((Y1-Y2)*(X3-X4)-(Y3-Y4)*(X1-X2))
IF (DENX) 2,1,2
1 X=1E40
GO TO 5
2 CONTINUE
X=((X3-X4)*(Y1*Y2-X1*Y2)-(X1-X2)*(Y3*Y4-X3*Y4))/
TDENX
5 CONTINUE
C TEST THAT Y IS NOT AT INFINITY
DENY=(X3-X4)
IF (DENY.EQ.0.0) GO TO 3
Y=(Y3*(X-X4)-Y4*(X-X3))/DENY
GO TO 6
3 CONTINUE
DENNY=(X1-X2)
IF (DENNY.EQ.0.0) GO TO 4
Y=(Y1*(X-X2)-Y2*(X-X1))/DENNY
GO TO 6
4 Y=1E40
6 CONTINUE
RETURN
END

```

```

SUBROUTINE MCTHTA(A,B,C,D,RM,CY,THETA)
C M, C, THETA ARE SLOPE, INTERCEPT, THETA RESP.
C A,B,C,D ARE THE COORDS OF THE TWO POINTS
DENM=(C-A)
IF (DENM) 2,1,2
1 CONTINUE
RM=1E40
THETA=1.5707963268
GO TO 3
2 RM=(D-B)/DENM
THETA=ATAN(RM)
3 CONTINUE
X0=0.0
Y0=0.0
YE3=1000.0
CALL INTSCT(X0,Y0,X0,YE3,A,B,C,D,CX,CY)
RETURN
END

```

```

SUBROUTINE LENGTH(A,B,C,D,RLNGTH,ANGLE)
C LENGTH FINDS LENGTH, ANGLE GIVEN TWO POINTS
C A,B,C,D ARE THE COORDS OF THE TWO POINTS
IF ((C-A).EQ.0.0) GO TO 1
ANGLE=ATAN((D-B)/(C-A))
GO TO 2
1 ANGLE=1.5707963268
2 CONTINUE
IF ((C-A).LE.0.0.AND.(D-B).LT.0.0) GO TO 3
IF ((C-A).LT.0.0.AND.(D-B).GT.0.0) GO TO 4
GO TO 9
3 ANGLE=ANGLE-3.1415926536
GO TO 9
4 ANGLE=3.1415926536-ANGLE
9 CONTINUE
IF (SIN(ANGLE)) 5,6,5
5 CONTINUE
RLNGTH=(D-B)/SIN(ANGLE)
GO TO 99
6 RLNGTH=C-A
99 CONTINUE
RETURN
END

```



```

SUBROUTINE FBLANG(A,B,C,D,THETA,PHI,PSI)
C FBLANG MEANS FOUR BAR LINKAGE ANGLES
C A,B,C,D ARE THE LENGTHS OF THE LINKAGES
TOP=A*A+B*B-2*A*B*COS(THETA)
BOT=SQRT(A*A+B*B-2*A*B*COS(THETA))
ENDTM=ATAN((B*SIN(THETA))/(A-B*COS(THETA)))
PHI=ARCCOS((TOP+C*C-D*D)/(2*C*BOT))-ENDTM
PSI=3.1415926536-ARCCOS((TOP-C*C+D*D)/(2*D*BOT))-ENDTM
RETURN
END

```

```

SUBROUTINE FINDXA(A,B,L,D,X,ANGLE)
C FINDXA CALCS X-COORD AND ANGLE GIVEN A POINT, LENGTH AND Y-COORD
C NOTE: POINTS FOUND ARE IN QUADRANTS ONE AND FOUR ONLY
ANGLE=ARSIN((D-B)/L)
X=A+(L*COS(ANGLE))
RETURN
END

```

```

SUBROUTINE FINDXY(A,B,RLNGTH,ANGLE,C,D)
C FINDXY CALCS COORDS GIVEN A POINT, LENGTH AND ANGLE
C A,B,C,D ARE THE COORDS OF THE TWO POINTS
C=A+RLNGTH*COS(ANGLE)
D=B+RLNGTH*SIN(ANGLE)
RETURN
END

```

# PRELIMINARY ANALYSIS OF WISHBONE SUSPENSION GEOMETRY

	X-COORD	Y-COORD
1	330.0	419.0
2	262.0	219.0
3	522.0	414.0
4	555.0	207.0
5	0.0	0.0
6	632.0	280.0
7	637.0	0.0

TO CALCULATE FOR BOUNCE AND REBOUND  
100 100

LENGTH OF UPPER ARM IS 192.065

LENGTH OF LOWER ARM IS 293.246

LENGTHS	L12	L13	L24	L34	L35	L36	L37
	211.244	192.065	293.246	209.614	666.243	173.367	429.675

ANGLES	AX12	AX13	AX24	AX34	AX35	AX36	AX37
	-1.899	-0.026	-0.041	-1.413	-2.474	-0.883	-1.300

ANGLES	A435	A436	A437
	-1.058	0.529	0.113

KINGPIN ANGLE = 8.035

SCRUB IS POSITIVE OUTWARDS

	K	Y7	RY	RY-Y7	CAMBER	SCRUB	SARM	RATIO
*	0	0.000	35.418	35.418	-1.023	0.000	13887.968	10.901
*	25	25.521	34.152	8.631	-1.280	0.880	3598.710	2.825
*	50	51.705	34.223	-17.483	-1.851	0.691	2067.577	1.623
*	75	78.701	37.487	-41.413	-2.771	-0.571	1413.204	1.109
*	100	106.821	45.553	-61.268	-4.121	-2.866	1031.493	0.810
*	0	0.000	35.418	35.418	-1.023	0.000	13887.968	10.901
*	-25	-24.890	36.360	61.250	-1.078	-1.896	6399.862	5.023
*	-50	-49.068	34.557	84.625	-1.481	-4.674	2458.269	1.773
*	-75	-72.290	25.026	97.315	-2.321	-8.043	1159.415	0.910
*	-100	-93.974	-6.404	87.570	-3.786	-11.351	616.642	0.484

APPENDIX 4.1.

CORRESPONDENCE BETWEEN THE  
UNIVERSITY OF CANTERBURY  
AND  
UNIROYAL LIMITED.

P.O. Box 2261  
 Christchurch  
 NEW ZEALAND  
 5 - 7 - 77

Sales Engineering Department  
 (Powergrip HTD)  
 Uniroyal Limited  
 82 Horseferry Road  
 London SW1P 2AH  
 ENGLAND

Dear Sir

At the University of Canterbury we are very interested in your company's Powergrip HTD Belts. I am currently carrying out postgraduate work on the design of a prototype electric town car, to replace the interim vehicle currently running at the University. This project has come about from the development of a variable speed AC Motor-drive system, patented by Mr D.J.Byers of our electrical department.

The existing vehicle - using motors rated at 2.2 kW - has two Synchro  $\frac{1}{2}$ " pitch belts obtained locally. The first, a  $1\frac{1}{2}$ " belt, ratio 2.4 and the second a 2" belt, ratio 1.85, for each of the two driven wheels.

The <sup>to</sup> prototype vehicle will, with one belt require a ratio of 6.0 or 5.54 (because of the different tyre diameter being used) for which the Synchro  $\frac{1}{2}$ " pitch belt will be unsuitable, especially with tooth jumping under regenerative braking.

The larger of the two motors that can be used is rated at 4.1 kW at 1500 rpm. However the AC System provides a constant torque of 26 Nm up to 3000 rpm, whereupon the torque drops until the maximum speed of 4500 rpm is reached. The power therefore is 8.2 kW at 3000 rpm. A dropout torque of 2 to 2.5 times the rated torque is available if required. However, the belt will not be subjected to this dropout torque continuously, but only during maximum acceleration, hill climbing etc..

Would an 8 mm pitch 50 mm wide belt with a ratio of 6.0 and pulleys 24/144 at a centre distance of 257.1 mm and belt length of 1280 mm be satisfactory? Is there a pitch size available between 8 mm and 14 mm? Using a borrowed 1974 Powergrip HTD handbook and amendment, and accounting for the additional 0.4 speedup factor (regenerative braking) it appears that an 8 mm pitch 50 mm wide belt may just suffice. If this is the case, could it be run at 4500 rpm on occasions? (1000 rpm corresponds to 19.5 kph; 3000 rpm to 58 kph - speed limit is 50 kph and 4500 rpm to 88 kph - open road speed limit is 80 kph) Could we expect any trouble with the belt jumping teeth under regenerative braking?

The belt life is not very critical. It would be reasonable, (depending on the belt cost) for a production model, to replace the belts when the tyres are replaced.

The larger pulley of cast iron is unacceptable, as it is unsprung weight on the rear wheel. I understand that filled nylon is the latest development in pulley material, and this would be acceptable. Is your company in a position to make special pulleys ?

We would greatly appreciate any information and aid your company is able to give us on this project (which may lead to production). Looking forward to your reply and to doing business with your company in the future.

Yours faithfully

Edgar Vandendungen



RTC/SMP

**UNIROYAL LIMITED**

62 Horseferry Road  
London  
SW1P 2AH  
Telephone: 01-222 5611  
Telex: 22814

161

Registered in Edinburgh  
Registration Number 1771  
Registered Office: Newbridge, Midlothian, Scotland.

19 July 1977

cc. Mr. A.S. Forgas,  
PowerGrip Industries

Edgar Vandendungen, Esq.,  
Mechanical Engineering,  
P.O. Box 2261,  
Christchurch,  
New Zealand.

Dear Mr. Vandendungen,

Thank you very much for your letter of July 5 giving details and enclosing photographs of the proto-type electric town car on which you are working.

This is extremely interesting and we will be only too happy to assist you in this project. We have sent a copy of your letter to our Product Engineering Department for study and we hope to have their comments on this in the course of the next few days.

I will therefore, be writing to you again as soon as these comments come to hand.

In the meantime, we would advise that our distributor in South East Asia is:

PowerGrip Industries,  
37-39 Lexton Road,  
Box Hill,  
Victoria 3128,  
Australia,

to whom we are sending a copy of your letter as we believe that it will probably be easier and cheaper for you to obtain your pulleys directly from them.

However, we will be able to let you have further information concerning our recommendations for pulleys when we answer your letter in detail.

Assuring you of our best attention at all times.

Yours faithfully,  
UNIROYAL LIMITED

R. T. Chalk  
European Marketing Manager



RTC/SMP

UNIROYAL LIMITED

62 Horseferry Road  
London  
SW1P 2AH  
Telephone: 01-222 5611  
Telex: 22814

162

Registered in Edinburgh  
Registration Number 1771  
Registered Office: Newbridge, Midlothian, Scotland.

27 July 1977

cc. Mr. A.S. Forgas

Mr. E. Vandendungen,  
Mechanical Engineering,  
P.O. Box 2261,  
Christchurch,  
New Zealand.

Dear Mr. Vandendungen,

Further to my letter of July 19 I have now received a reply from our Product Engineering Department concerning the proposed application of our PowerGrip HTD drives to your proto-type electric town car. Details are as follows:

1. Drive specification

Driver pulley	24-8M-50F
Driven pulley	144-8M-50
Max power	4.1 Kw at 1500 rpm
Rated torque	26 nm
Max torque	$26 \times 2.5 = 65$ nm
Max rpm	4,500

2. The 50 mm wide drive which we have recommended will be running well within its limits **providing** the torque during regenerative braking is not more than approximately 80 nm.
3. We note that the driven pulley is unsprung mass on the rear wheel. The drive will have to be arranged so that the suspension movement does not affect belt tension or alignment of the pulleys, i.e. suspension centre of rotation will have to coincide with driving pulley centre.
4. The drive must be guarded against stones, etc. from the road.
5. It is highly unlikely that the driven pulley could be injection moulded in any sort of plastic to the required tolerances although it could be machined from nylon if a big enough piece could be obtained or a fabric filled phenolic, particularly if this were graphite loaded could also be used. Alternatively, an aluminium alloy pulley hard anodised would probably be the easiest and most suitable material for the driven pulley with mild steel being used for the drive pulley.

Cont. /...

Mr. E. Vandendungen  
27 July 1977  
(2)

163

6. If it is possible to consider a two stage drive reduction, this would give a more compact drive using 26 and 64 groove pulleys on both primary and secondary drives. A 50 mm wide belt would be used on the primary drive and an 85 mm wide belt would be needed for the secondary drive. The maximum pulley OD of 161.6 mm would then be a more reasonable size for moulding.

We hope that these comments will be of assistance to you and we will be most interested to learn of future developments with this electric vehicle. However, if there is any further information we can give you on this matter, please do not hesitate to contact us.

Yours sincerely,



R. T. Chalk



Edgar Vandendungen  
P.O. Box 2261  
Christchurch  
NEW ZEALAND  
21 Sept. 77

Mr R.T. Chalk  
Uniroyal Limited  
62 Horseferry Road  
London SW1P 2AH  
ENGLAND

Dear Mr Chalk

Thank you very much for your letters dated 19 and 27 July. We found the information very helpful and the offer of assistance most gratifying. We intend to use your companies belts for the electric town car and have altered the design width of the chassis and bodywork to suit the narrower 50 mm belts.

The driven pulley, as you point out, is in fact unsprung mass on the rear wheels, as is the motor and driver pulley, thus ensuring a fixed pulley-centre distance. However the effective unsprung mass of the motor is approximately 40% of the actual mass, and when calculated, the unsprung mass is approximately 70% that of a Ford Escort live axle, for instance.

Of some concern is the amount of flex of the rear suspension arm that can be tolerated, ie: how much angular misalignment between one pulley and the other can be tolerated before the belt will start running off. Do you have any figures on this ?

Taking your advice, we now have a local company that is prepared to hard anodize our aluminium driven pulleys. Would it be possible, when the time comes, for us to machine the driven pulleys in Christchurch to your specifications, or would it be advisable for your distributor in Australia to do the required machining.

A two stage drive reduction was considered at one time, but was rejected on the grounds that it required an extra belt and two pulleys, plus the extra layshaft and bearing on each end, as well

as taking up extra space. The motor located near the pivot on the swingarm, appears the best compromise.

Thank you once again for your assistance. We look forward to hearing from you, and working with your company in the future.

Yours faithfully

Edgar Vandendungen.



Registered in Edinburgh  
Registration Number 1771  
Registered Office: Newbridge, Midlothian, Scotland.

## UNIROYAL LIMITED

62 Horseferry Road  
London  
SW1P 2AH  
Telephone: 01-222 5611  
Telex: 22814

c.c. Mr. A.S. Forgas,  
PowerGrip Industries

166

Mr. Edgar Vandendungen,  
Mechanical Engineering,  
P.O. Box 2261,  
Christchurch,  
NEW ZEALAND.

Our Ref: RTC/MYB

20 October 1977

Dear Mr. Vandendungen,

Thank you for your letter of 21 September 1977, raising points concerning potential angular misalignment on the proposed PowerGrip HTD Drive, which you are considering for your electric car.

I have raised this matter with our Product Engineering Department, and their comments are as follows:-

"My misgivings about mounting the driven pulley as unsprung weight on the back axle were due mainly to the possibility of drastic variations in belt tension. This could be due either to the centres of rotation of the axle and driving pulley not coinciding, or to compliance in the suspension bushes permitting longitudinal movement of the axle. The compliance of the belt will almost certainly be lower than that of rubber bushes, which would result in the belt acting as a sort of radius arm.

The effect of angular misalignment is to elongate the outside edges of the belt with respect to the centre by an amount equal to:

$$\sqrt{\left(W \sin \frac{\theta}{2}\right)^2 + C^2} - C$$

where W = Belt Width  
 $\theta$  = Misalignment  
C = Belt Span between Pulleys

This is not too serious if C is reasonably large and W reasonably small.

These comments notwithstanding, unorthodox things often work, but it is better to be aware of possible difficulties".

cont .....

- 2 -

I hope that these comments will be of help to you. However, I should be most interested to learn of your developments, and if there is any further information you may require at any time, please do not hesitate to let me know.

Yours sincerely,



R. T. Chalk,  
European Marketing Manager,  
Power Transmission Division.

May 10, 1978

Power Grip Industries,  
37-39 Lexton Rd.,  
Box Hill,  
Victoria 3128,  
AUSTRALIA.

Dear Sirs,

University of Canterbury, Electric Vehicle Project

I am writing to follow up some correspondence between Mr. R.T. Chalk of Uniroyal Ltd., London and a student whom I supervise, Mr. E. Vandendungen. Mr. Chalk gave me your address and said he would send you a copy of the correspondence. I confirmed our continuing interest to Paykel Bros. Ltd., Christchurch on October 28, 1977, in response to a query from you as I understand it.

The design of our Mk.II vehicle is well under way, and we are now in a position to order belts and pulleys for it. There will be only one car at first but there is the possibility of a very small production run of evaluation vehicles to the same design. Each car will have two belt drives as follows:

Belts - Uniroyal Powergrip HTD, pitch 8 mm  
width 50 mm  
length 1280 mm

Drive N pulleys - 144-8M-50, hard anodized aluminium  
Drive R pulleys - 26-8M-50F or 28-8M-50F, iron or steel

While the belts and driver pulleys are standard, we are interested in means of obtaining suitable lightweight driven pulleys to mount beside the rear wheels. The form required will be a simple toothed ring with a central internal attachment flange, as sketched below. Three are required, to include a spare in case of trouble.

Would you please advise on the following:

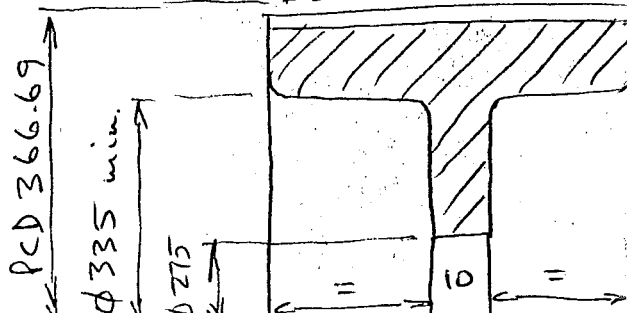
1. Price and availability for the belts and the optional driver pulleys as listed above.
2. Price and delivery date for three rings as sketched for the driven pulleys, fully machined and anodised.
3. The possibility of your supplying a tooth profile cutter and machining instructions so we may arrange our own driven pulleys.

Looking forward to your reply.

Yours sincerely,

R.T.C. Harman  
Senior Lecturer in Mechanical Engineering

c.c. Mr. T.J. Whall, Paykel Bros. Ltd., P.O. Box 382, Christchurch





# POWERGRIP INDUSTRIES (AUSTRALIA) PTY. LTD.

POWER TRANSMISSION & CONVEYOR BELT MANUFACTURERS  
IMPORTERS & EXPORTERS

169

RS/BF

37-39 LEXTON ROAD, BOX HILL, VIC., 3128, AUSTRALIA.

P.O. BOX 223, BOX HILL, 3128. Phone: 89 0344 (7 lines). Telex: AA33610

Distributors of

Uniroyal, Powergrip Timing Belt, U.S.A.

Telegrams & Cables: "POWERBELT," MELBOURNE.

IN N.S.W.: Powergrip (N.S.W.) Pty. Ltd., 51 Crystal Street, Petersham, 2049.

IN QLD.: Powergrip Industries (Qld.) Pty. Ltd., 237 Montague Road, West End, Queensland, 4101.

Distributors: South Australia, Western Australia, Tasmania.

University of Canterbury,  
Department of Mechanical Engineering,  
CHRISTCHURCH. 1.  
NEW ZEALAND.

8th June, 1978.

For Attention: Mr. R.T.C. Harman,  
Senior Lecturer in Mechanical Engineering.

Dear Sir,

We are writing to apologize for delays in our quotation for the supply of Uniroyal Powergrip HTD Drives. The problem at this end has been finding a suitable supplier for the hard anodized aluminium from which the driven pulleys are to be machined. We assure you, however, as soon as we are able to obtain a price for this material our quotation for the drives will be forwarded to our New Zealand Agents, Paykel Bros. Ltd. who in turn will be in touch with you.

Yours faithfully,  
POWERGRIP INDUSTRIES (AUST.) PTY.LTD.

R. SMITH,  
PURCHASING OFFICER.

c.c. Mr. T.J. Whall,  
Paykel Bros. Ltd.,  
P.O. Box 382,  
CHRISTCHURCH. N.Z.

June 14, 1978

Powergrip Industries (Australia) Pty.Ltd.,  
P.O. Box 223,  
Box Hill,  
Victoria 3128,  
AUSTRALIA.

Attention: Mr. R. Smith, Purchasing Officer

Dear Mr. Smith,

Many thanks for your letter of 8th. June. I am replying quickly because your letter implies that the material of the pulleys would be hard anodized before machining. In fact, they need to be machined in an as cast state, and then anodized to harden the wearing surfaces of the teeth. My apologies if I have misunderstood you on this point.

I am not sure which particular aluminium alloy is required for this process, but it is used and hard anodized here for the manufacture of tyre moulds. If necessary, we could have much of the manufacture completed locally.

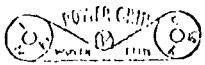
We are hoping to have this material to hand in early August. The pulley sizes required are still as requested but the belts will change to the next longer size, becoming 1360 mm long.

Hoping that this gives you adequate time to obtain and make the required parts.

Yours faithfully,

R.T.C. Harman  
Senior Lecturer in Mechanical Engineering

c.c. Mr. T.J. Whall,  
Paykel Bros. Ltd.,  
P.O. Box 382,  
CHRISTCHURCH



# POWERGRIP INDUSTRIES

25% duty.

171

RD/BF

POWER TRANSMISSION & CONVEYOR BELT MANUFACTURERS  
IMPORTERS & EXPORTERS

37-39 LEXTON ROAD, BOX HILL, VIC., 3128, AUSTRALIA

P.O. BOX 223, BOX HILL, 3128, AUSTRALIA. Phone: 89 0344 (7 lines)

Telegrams & Cables: "POWERBELT", MELBOURNE, AUSTRALIA.

LCF 1.3.2

Paykel Bros. Ltd.,  
P.O. Box 5046,  
AUCKLAND. NEW ZEALAND.

17th July, 1978.

Attention: Mr. B. Mitchell, Manager, Transmission Division.

Quotation No. 1993/Mr. R.T.C. Harman, Dept. Mech. Eng.  
University of Canterbury, Christchurch. N.Z.

Dear Barry,

Enclosed is a letter received from Mr. R.T.C. Harman of the Department of Mechanical Engineering, University of Canterbury, Christchurch. Further to this letter we have much pleasure in quoting the following.

Item 1. 3 - 144-8M-50 Aluminium Hard, Anodized HTD Pulleys,

NZ @ \$645.97 NET Each.

Item 2. 3 - 28-8M-50F Steel HTD Pulleys,

\* \$480.48  
@ \$63.48 NET Each.

Item 3. 1280-8M-50 HTD Timing Belts,

\* \$47.61  
NZ @ \$42.42 NET Each. NIC

Item 4. 3 - 1440-8M-50 HTD Timing Belts,

\* \$47.02 NET Each. NIC

## ALTERNATIVE TO ITEM 1.

3 - 144-8M-50 HTD Pulley, Steel Fabrication

Lightweight, @ \$527.18 NET Each.

Delivery of HTD Pulleys - 8 weeks.

HTD Timing Belts - 20 weeks Sea Freight.

Air Freight.

Letter dated June 14th refers to a belt size of 1360mm long, but our next standard size is 1440mm.

As HTD is a patented product we cannot supply HTD Cutters - Uniroyal will prosecute anyone trying to duplicate the cutting of HTD Timing Pulleys.

Looking forward to an early reply,

Yours sincerely,

*B. Dale*

S. J. M. M. M.

POWERGRIP INDUSTRIES (AUST.) PTY. LTD.

R. DALE, SALES MANAGER.

\* LESS 25% DUTY

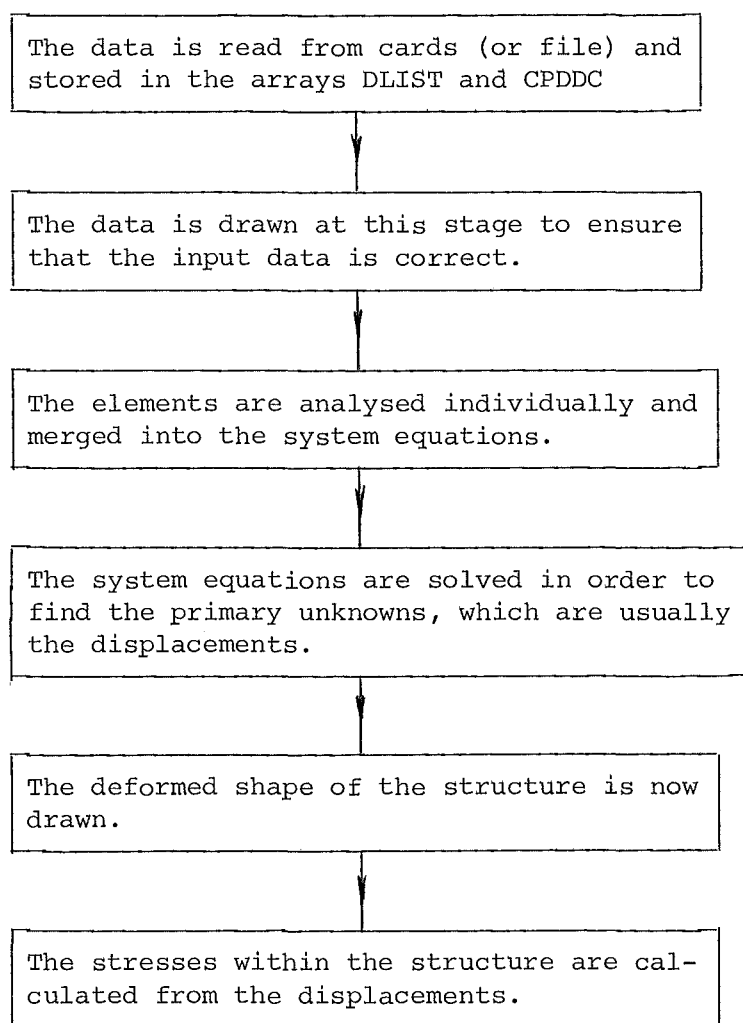
BELTS DUTY NOT APPLICABLE

less machinery tax?



APPENDIX 4.2

FINITE ELEMENT ANALYSIS USING PAFEC 75 ON  
A B6700 COMPUTER. APPLICABLE TO THE REAR  
SUSPENSION ARM OF AN ELECTRIC TOWN CAR

FLOWCHART

Discussion. The finite element program PAFEC, which stands for Program for Automatic Finite Element Calculations, is run in 10 separate steps called phases. Each step has a different function to perform which is summarised below.

Phase 1	Data input and expansion.
Phase 2	Mesh generation using Pafblocks.
Phase 3	Draw finite element mesh.
Phase 4	Allocates degrees of freedom to nodes.
Phase 5	Draw degrees of freedom.
Phase 6	Generates element stiffnesses.
Phase 7	Merging and solution routines.
Phase 8	Displaced shape or temperature contour plots.
Phase 9	Calculates element stresses.
Phase 10	Stress vector or contour plots.

Data for PAFEC is divided into separate blocks called Modules (ref. PAFEC 75 EASIDATA MANUAL DEC. 1977). The type of calculation to be performed (e.g. static or dynamic analysis) and the number and type of Phases to be run may be specified in the CONTROL MODULE which is one module of the data file.

The program as set up uses the control module and phases one, three, four, six, seven, eight and nine. This is reflected in the flow chart above. The drawings from phases three and eight are included in Chapter 4. Phase one interprets and lists the input data. The output from phase four is a list of all 408 degrees of freedom for the 68 nodes, plus the addresses and tags for each degree of freedom. The output from phase six is a list of the group number, element type, property number and material number for the 83 elements.

The output from phase seven tabulates the reactions at the constrained nodes, the trailing arm pivots, for each of the three load cases analysed. It also tabulates, separately for each load case, the coordinates for each node and the displacement of each of the degrees-of-freedom, that is, the x, y and z displacements and the rotations about the x, y and z local axes. The output from phase nine lists all the stresses for each element and/or each node of each element for each load case. For the 3-node triangular elements, the maximum stress, the minimum stress and the angle between them for each of the positive surface, the neutral surface and the negative surface for each of the load cases is listed, while for the four node elements this is done at each node of each element for each load case. For beam elements, the axial force and shear force in both directions and the torsional moment and bending moment in both directions is listed for all load cases.

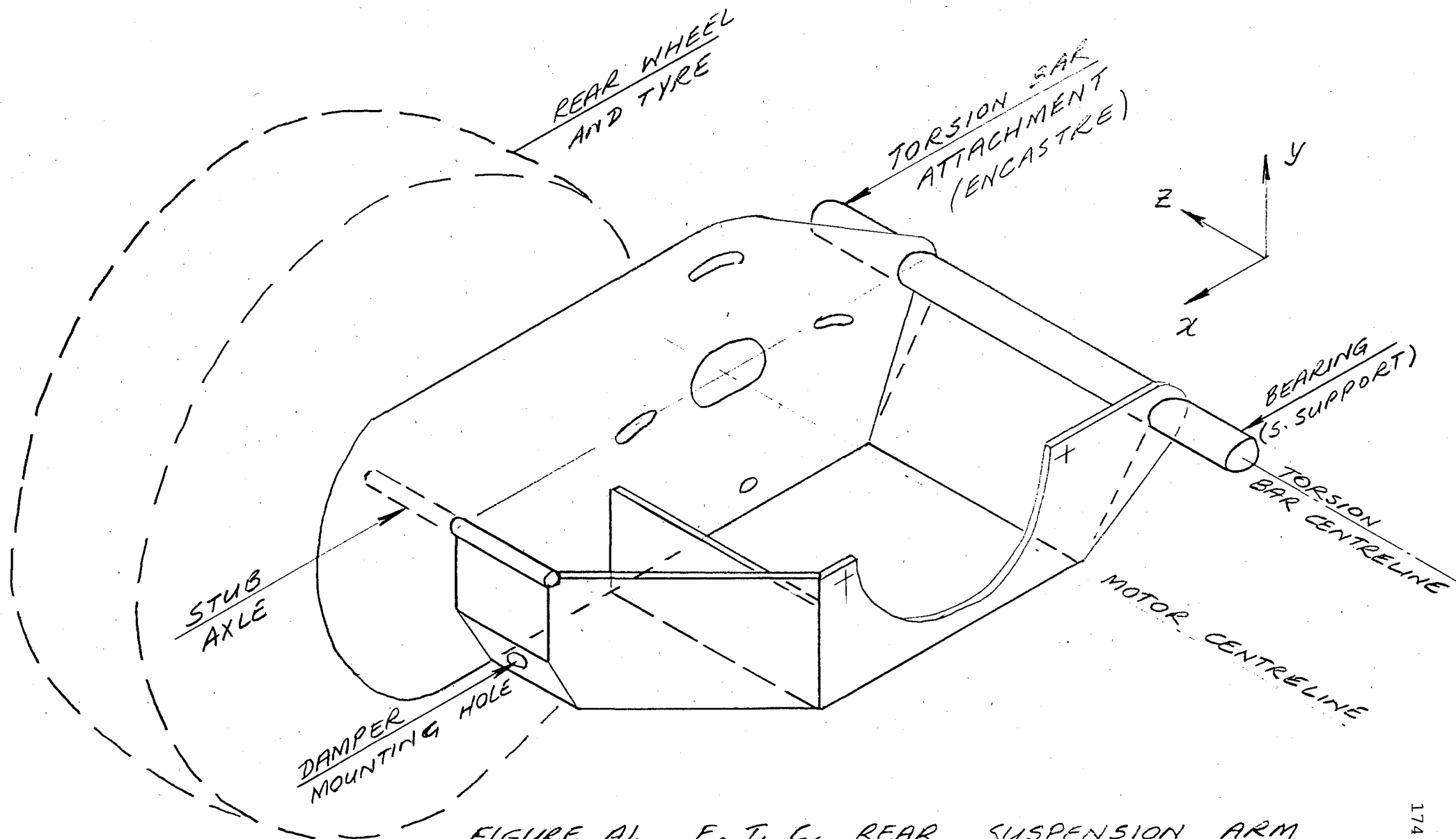
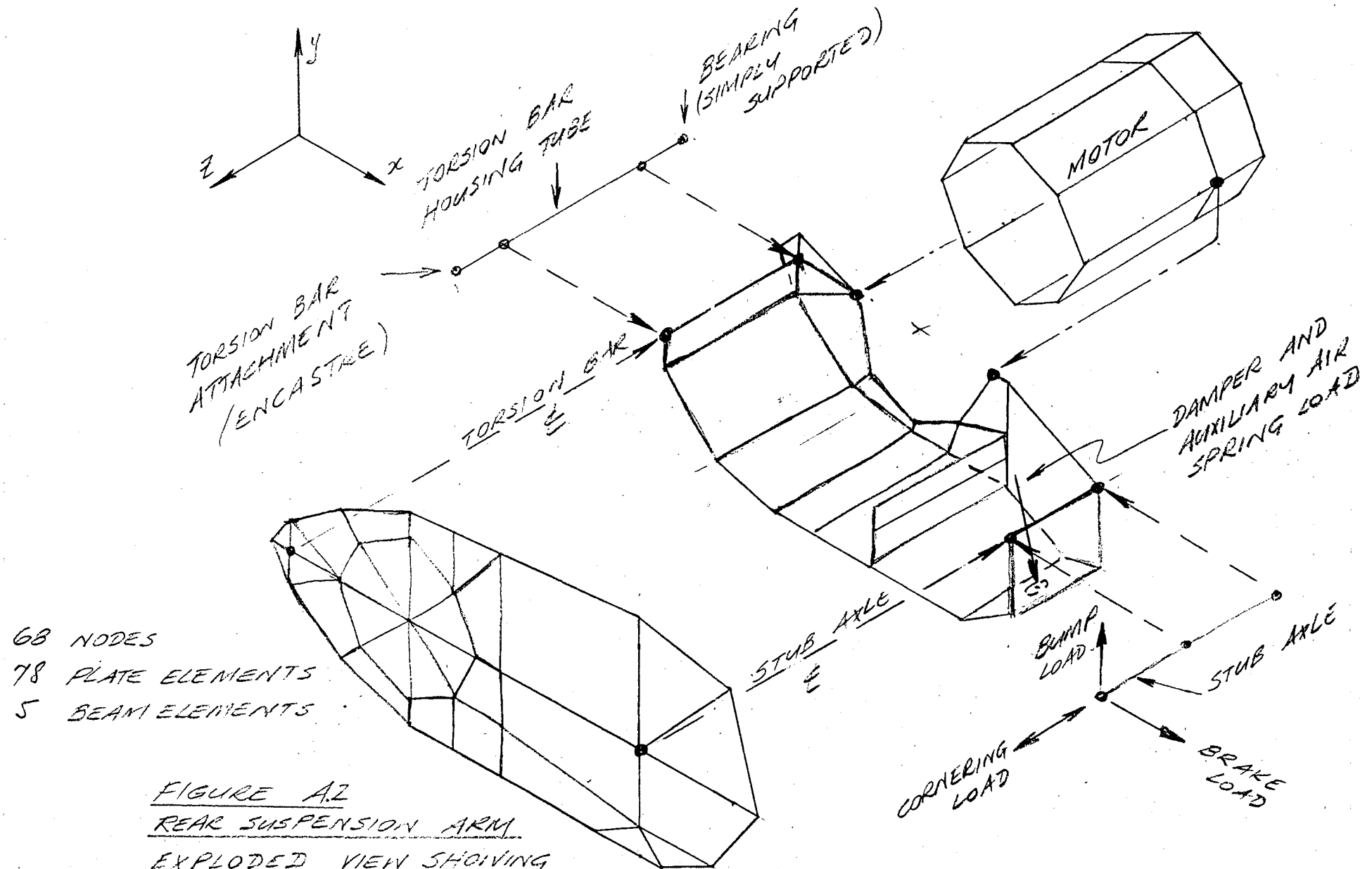


FIGURE A1. E. T. C. REAR SUSPENSION ARM



68 NODES  
78 PLATE ELEMENTS  
5 BEAM ELEMENTS

FIGURE A.2  
REAR SUSPENSION ARM  
EXPLODED VIEW SHOWING  
FINITE ELEMENTS.

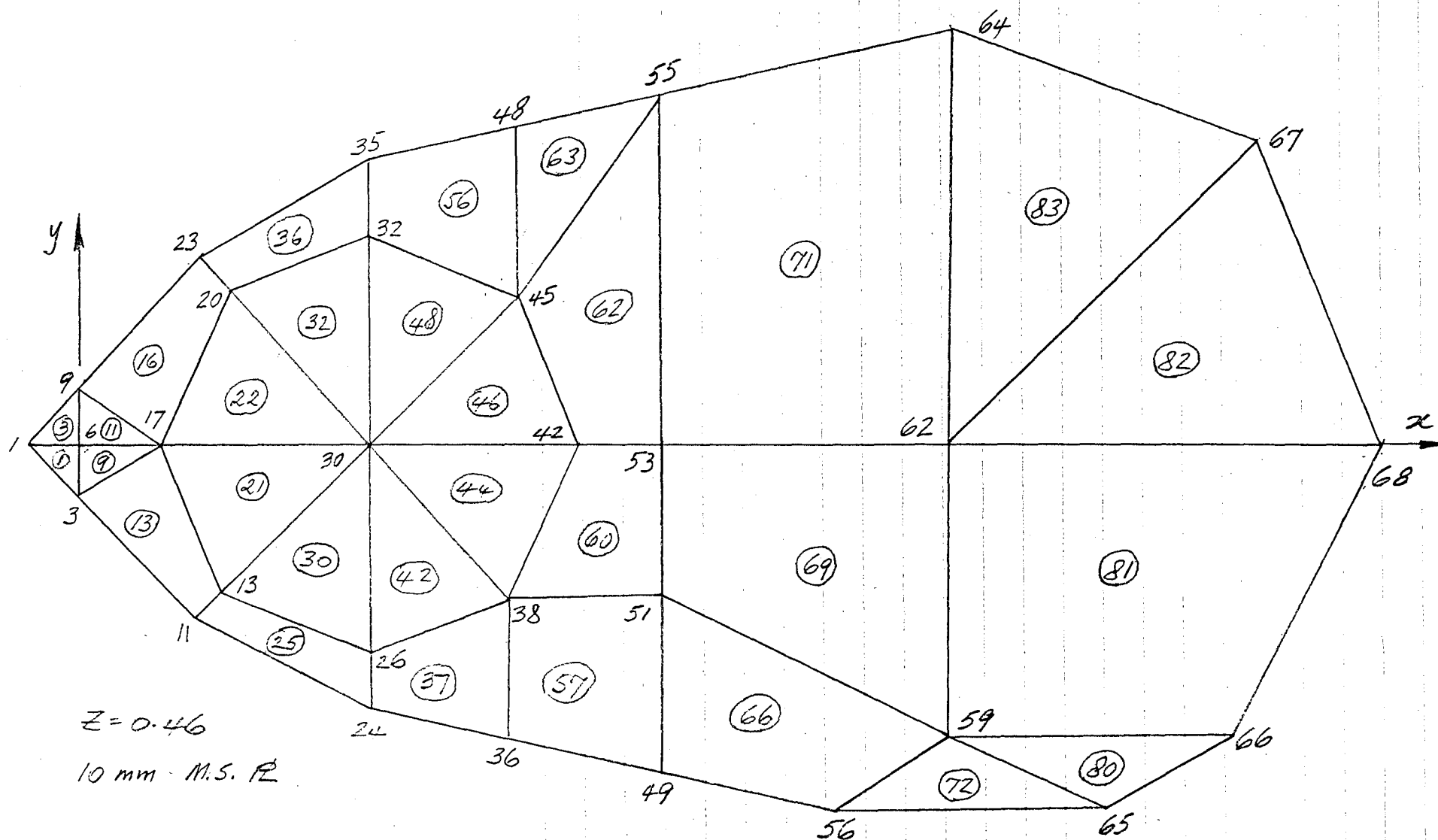


FIGURE A.3. FINITE ELEMENT NODES AND ELEMENTS FOR OUTER SIDE PLATE.

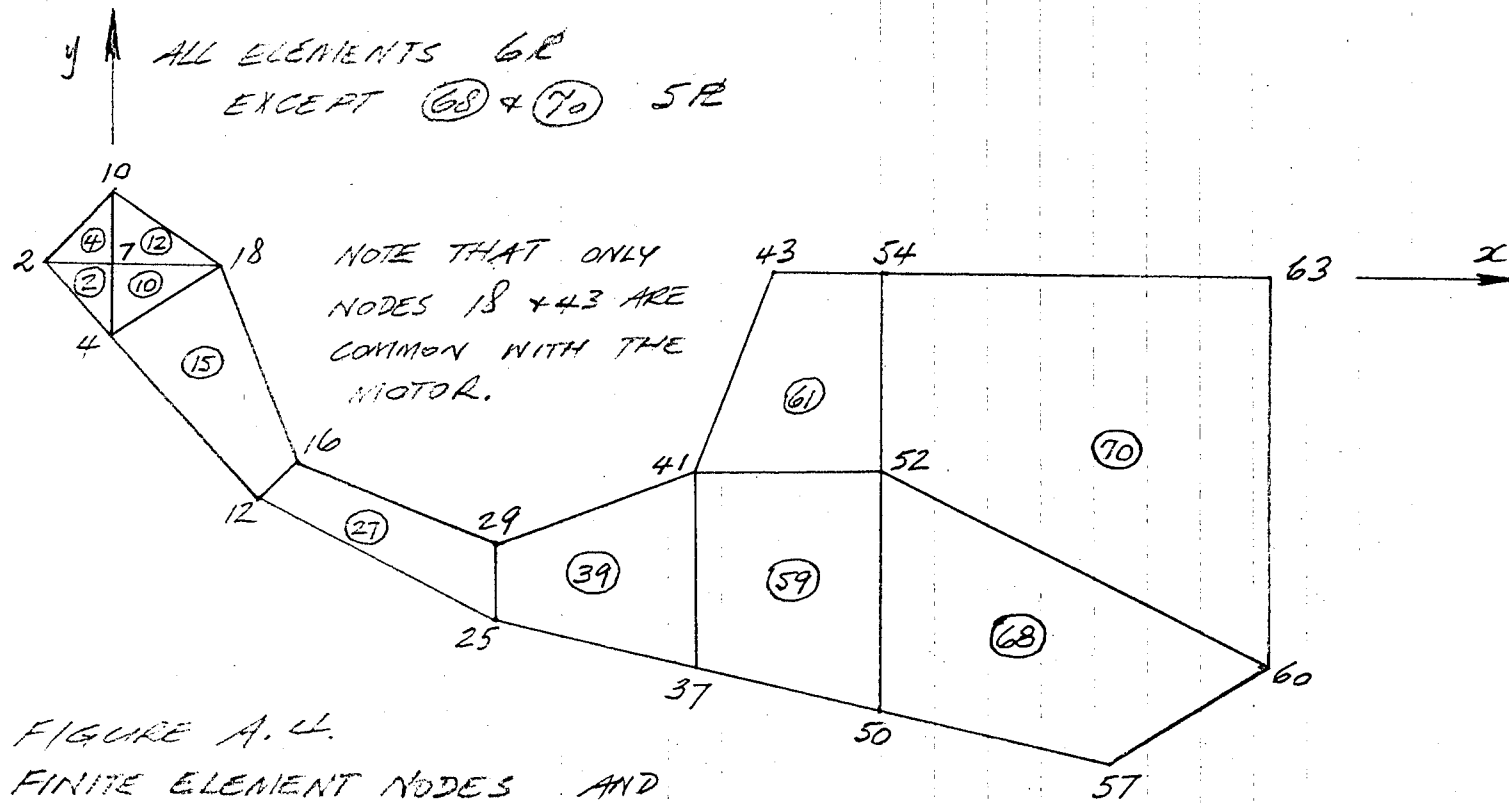


FIGURE A.4.  
FINITE ELEMENT NODES AND  
ELEMENTS FOR INNER SIDE PLATE

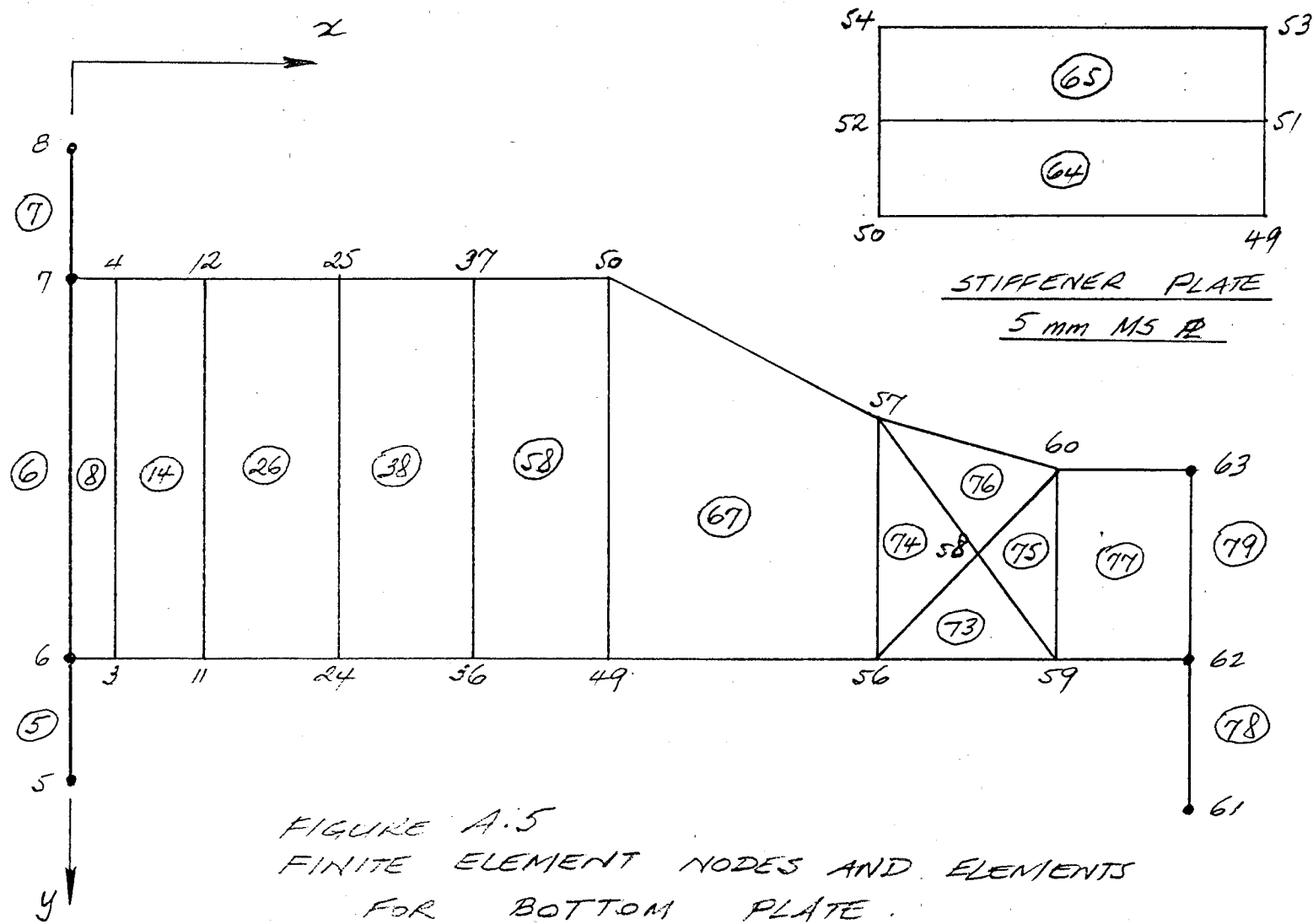


FIGURE A.5  
FINITE ELEMENT NODES AND ELEMENTS  
FOR BOTTOM PLATE.  
6 mm MS PL.

NOTE THAT ONLY  
NODES 18 AND 43  
ARE COMMON WITH  
INNER SIDE PLATE.

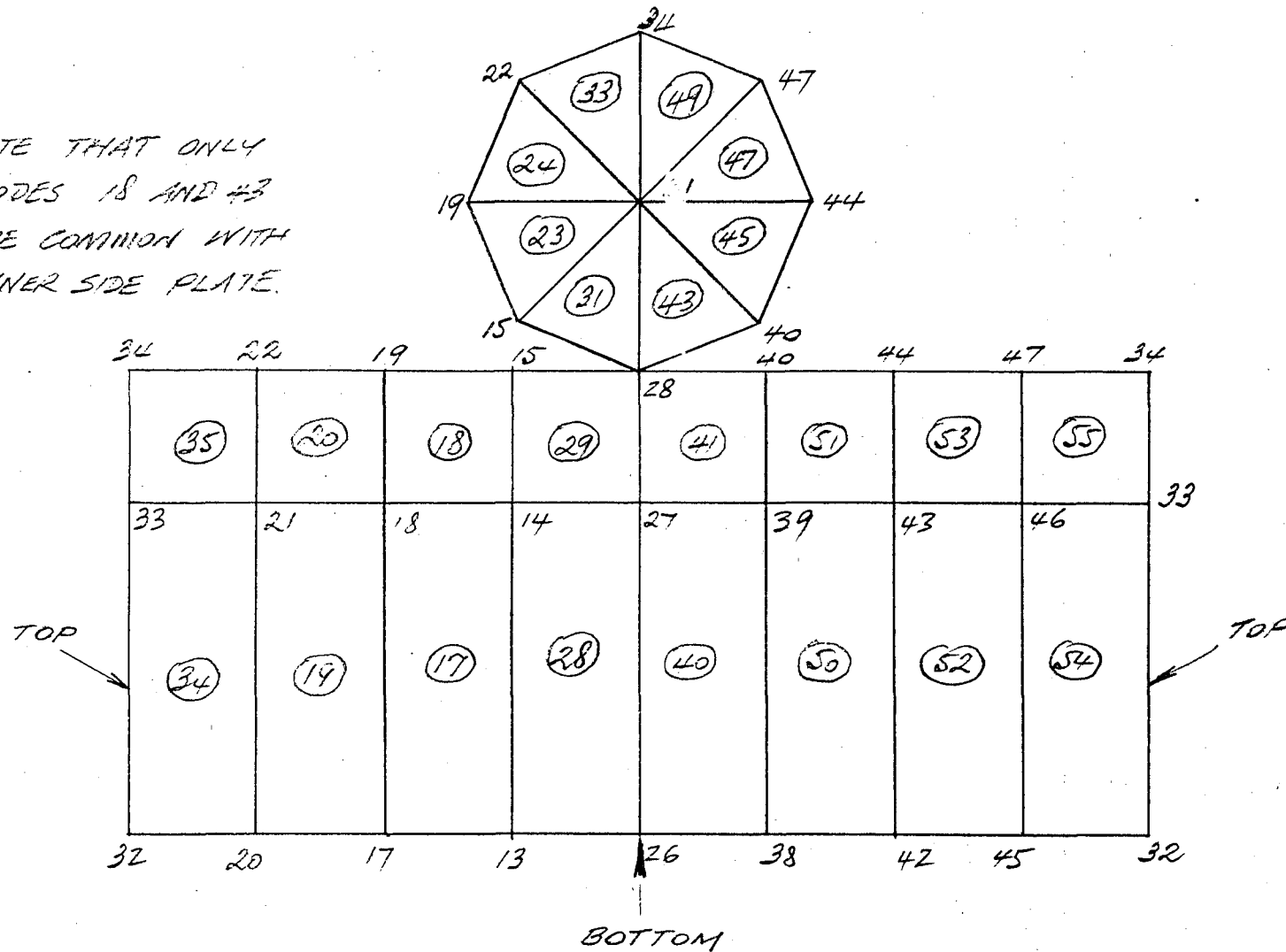


FIGURE A.6  
FINITE ELEMENT NODE AND ELEMENTS  
FOR MOTOR (SHOWN DEVELOPED)




### Data Preparation

Figure A.1 illustrates the rear suspension arm, with the motor omitted for clarity. Drawings 7937/1 and 7956 in Appendix 6.1 provide the detail dimensions. Figure A.2 illustrates the rear suspension arm in exploded view, showing the finite elements, while Figures A.3 to A.6 inclusive illustrate the mode numbers and element numbers, prepared in accordance with the appropriate PAFEC 75 Manuals. The list of FINITE ELEMENT DATA is based on Figures A.3 to A.6 with element types, properties and topologies and other data in accordance with the appropriate PAFEC 75 Manuals.

### FINITE ELEMENT DATA

Node numbers not punched, assumed consecutive.



TITLE*ETC*REAR*SUSPENSION*STRESS*ANALYSIS NODES			
	x	y	z
1	-.02	0	.46
2	-.02	0	.22
3	0	-.02	.46
4	0	-.02	.22
5	0	0	.54
6	0	0	.46
7	0	0	.22
8	0	0	.075
9	0	.02	.46
10	0	.02	.22
11	.067	-.092	.46
12	.067	-.092	.22
13	.082	-.078	.46
14	.082	-.078	.22
15	.082	-.078	.145
16	.078	-.082	.22
17	.05	0	.46
18	.05	0	.22
19	.05	0	.145
20	.082	.078	.46
21	.082	.078	.22
22	.082	.078	.145
23	.067	.092	.46

## TITLE\*ETC\*REAR\*SUSPENSION\*STRESS\*ANALYSIS NODES

24	.16	-.13	.46
25	.16	-.13	.22
26	.16	-.11	.46
27	.16	-.11	.22
28	.16	-.11	.145
29	.16	-.115	.22
30	.16	0	.46
31	.16	0	.145
32	.16	.11	.46
33	.16	.11	.22
34	.16	.11	.145
35	.16	.13	.46
36	.238	-.145	.46
37	.238	-.145	.22
38	.238	-.078	.46
39	.238	-.078	.22
40	.238	-.078	.145
41	.242	-.082	.22
42	.270	0	.46
43	.270	0	.22
44	.270	0	.145
45	.238	.078	.46
46	.238	.078	.22
47	.238	.078	.145
48	.238	.145	.46
49	.33	-.168	.46
50	.33	-.168	.22
51	.33	-.08	.46
52	.33	-.08	.22
53	.33	0	.46
54	.33	0	.22
55	.33	.160	.46
56	.45	-.195	.46
57	.45	-.195	.315
58	.48	-.175	.4
59	.51	-.155	.46
60	.51	-.155	.36
61	.51	0	.62

## TITLE\*ETC\*REAR\*SUSPENSION\*STRESS\*ANALYSIS NODES

62	.51	0	.46
63	.51	0	.36
64	.51	.195	.46
65	.57	-.195	.46
66	.628	-.138	.46
67	.648	.138	.46
68	.705	0	.46

## ELEMENTS

PROP = 1

ELEMENT. TYPE = 41320

NUMBER	TOPOLOGY
1	1, 3, 6
3	1, 6, 9
9	3, 17, 6
11	6, 17, 9
21	13, 30, 17
22	17, 30, 20
30	13, 26, 30
32	20, 30, 32
42	26, 38, 30
44	38, 42, 30
46	30, 42, 45
48	30, 45, 48
63	45, 55, 48
72	56, 65, 59
80	65, 66, 59
82	62, 68, 67
83	62, 67, 64

ELEMENT. TYPE = 44200

NUMBER.	TOPOLOGY
13	3, 11, 17, 13
16	17, 20, 9, 23
25	11, 24, 13, 26
36	20, 32, 23, 35
37	24, 36, 26, 38
56	32, 45, 35, 48
57	36, 49, 38, 51
60	38, 51, 42, 53
62	42, 53, 45, 55
66	49, 56, 51, 59
69	51, 59, 53, 62
71	53, 62, 55, 64
81	59, 66, 62, 68

ELEMENT. TYPE = 41320

PROP = 2

NUMBER	TOPOLOGY
73	56, 59, 58
74	56, 58, 57
75	58, 59, 60
76	58, 60, 57

ELEMENT. TYPE = 41320

PROP = 3

NUMBER	TOPOLOGY
2	2, 4, 7
4	2, 7, 10
10	4, 18, 7
12	7, 18, 10

ELEMENT. TYPE = 41320

PROP = 4

NUMBER	TOPOLOGY
23	15, 31, 19
24	19, 31, 22
31	15, 28, 31
33	22, 31, 34
43	28, 40, 31
45	31, 40, 44
47	31, 44, 47
49	31, 47, 34

ELEMENT. TYPE = 44200

PROP = 2

NUMBER	TOPOLOGY
25	24, 25, 11, 12
38	36, 37, 24, 25
58	49, 50, 36, 37
64	51, 52, 49, 50
65	53, 54, 51, 52
67	56, 57, 49, 50
68	50, 57, 52, 60
70	52, 60, 54, 63
77	62, 63, 59, 60

ELEMENT. TYPE = 44200

PROP = 4

NUMBER	TOPOLOGY
17	13, 14, 17, 18
18	14, 15, 18, 19
19	17, 18, 20, 21
20	18, 19, 21, 22
28	26, 27, 13, 14
29	27, 28, 14, 15
34	20, 21, 32, 33
35	21, 22, 33, 34

NUMBER	TOPOLOGY
40	38, 39, 26, 27
41	39, 40, 27, 28
50	42, 43, 38, 39
51	43, 44, 39, 40
52	45, 46, 42, 43
53	46, 47, 43, 44
54	32, 33, 45, 46
55	33, 34, 46, 47

ELEMENT. TYPE = 44200

PROP = 3

NUMBER	TOPOLOGY
8	3, 4, 6, 7
14	11, 12, 3, 4
15	4, 12, 18, 16
27	12, 25, 16, 29
39	25, 37, 29, 41
59	37, 50, 41, 52
61	41, 52, 43, 54

ELEMENT. TYPE = 34000

NUMBER,	PROP,	TOPOLOGY
5	3	5, 6
6	3	6, 7
7	3	6, 8
78	4	61, 62
79	3	62, 63

PLATES.AND.SHELLS

PLATE.NUMBER,	MATE.NUMBER,	THICK
1	1	.01
2	1	.005
3	1	.006
4	1	.002

## BEAMS

SECT.NUMB,MATE.NUMB,IYY,IZZ,AXIS.NUMB,TORS.CONST.AREA

3, 1, 1.701E-7, 1.701E-7, 3, 3.402E-7, 7.278E-4

4, 1, 3.976E-8, 3.976E-8, 3, 7.958E-8, 7.069 E-4.

## LOADS

CASE.OF.LOAD, NODE. NUMB, DIRECTN. OF LOAD, VALUE.OF.LOAD.

1	61	2	2658
2	61	2	14752
2	58	1	10385
2	58	2	-10385
3	61	1	6557
3	61	2	9835
3	61	3	-6557
3	58	1	5468
3	58	2	-5468

## ENCASTRE

LIST.OF.NODES

5

## SIMPLE.SUPPORTS

LIST.OF.NODES

8

## STRESS.ELEMENT

START, FINISH

1	16
21,	22
25,	27
30,	30
32,	32
36,	39
42,	42
44,	44

46,      46  
 58,      48  
 56,      83

END.OF.DATA

### Load Cases

Load case 1 is the static 1 g loading configuration, assuming a vehicle mass of 1151 kg (2 persons) with  $a/L = 0.471$ , so that individual rear wheel loading is 2658 N acting at node 61 vertically upward, that is, in the y-direction (direction 2).

Load case 2 is a 4.5 g bump with 4 persons assuming 1281 kg and  $a/L = 0.522$ . The load taken by the torsion bar is nominally  $P/G_2 = 1.643$  from the interconnected suspension analysis.

Rear torsion bar load = 1.643 x static	=	4367
Bump stop/damper/auxiliary spring	=	10385
Total 4.5 g wheel load	=	14752 N

so that;

	N	Direction
Node 61	14752	2
Node 58	-10385	2
	10385	1

Load case 3 is a 3 g bump, a 2 g corner and 2 g braking for 4 persons, all combined.

Bump 3 g.

Rear torsion bar load	4367
Bump stop/damper/auxiliary spring	5468
Total 3 g wheel load	9835 N

Corner/Braking 2 g = 6557 N, so that

	N	Direction	
Node 61	6557	1	brake
	9835	2	bump
	-6557	3	corner
Node 58	5468	1	
	-5468	2	



Node 61 is the end of the stub axle, and node 58 is the damper/auxiliary spring mounting hole, see Figures A1 and A5.

#### Suspense Arm Twist

With reference to the displacements/rotations printout from phase seven, the angular misalignment between the motor shaft and the end of the stub axle in rear elevation, is the difference in angle PHIX, for nodes 61 (Figure A.5) and 30 (Figure A.3).

Consider load case 2, the 4.5 g bump condition with 4 persons. The angles, dividing by 100 as per printout, are

$$\begin{array}{ll} \text{Node 61,} & \text{PHIX} = -0.032593 \\ \text{Node 30,} & \text{PHIX} = -(-0.002825) \\ & \hline & -0.029768 \text{ radians} \end{array}$$

The angular misalignment or twist is 1.7 degrees.

#### Remove Metal to Save Unsprung Weight

That section of the suspension arm comprising nodes 48, 55, 64, 67, 68, 66 and 65 Figure A.3 was originally provided to offer protection for aluminium belt pulley and provide a basis for a belt guard. Chain is now being used and the same level of protection is not necessary, it is therefore proposed to cut off part of the arm.

The suspected understressed elements, Figure A.3. are 63, 71, 83, 82, 81 and 80. The triangular elements 63, 83, 82 and 80 are stressed per element whereas the 4-noded elements are stressed per node, the relevant nodes are 55, 64, 68 and 66. Two printout pages from phase nine are included, from these and other relevant pages the following stresses  $\text{MN/m}^2$  are read.

Triangular Element	L o a d    C a s e		
	1	2	3
63	+11, -15	+54, -74	+40, -55
83	+ 9, -10	+53, -55	+30, -30
82	+ 2, - 3	+13, -17	+ 5, - 9
80	+ 2, - 6	+41, -33	+16, - 8

4-Node Element	Node	L o a d    C a s e		
		1	2	3
71	55	+ 8, -12	+42, -61	+19, -26
71	64	+ 7, -13	+45, -67	+17, -40
81	68	+ 5, - 5	+25, -27	+10, -14
81	66	+10, -13	+64, -83	+41, -43

In the static condition, load case 1, the stresses are insignificant, and even at 4.5 g bump, load case 2, which is an extreme condition, the maximum stress is only 83 MPa compression. Material can be removed without any detrimental effect.

SCALED COORDINATES  
DIVIDE BY 10.000

SCALED DISPLACEMENTS/ROTATIONS FOR LOAD CASE 1  
\* INDICATES A CONSTRAINT HAS BEEN APPLIED

DIVIDE BY 100.00  
NODES 1- 68

COORDINATES			NODE NO.	DISPLACEMENTS			ROTATIONS		
X	Y	Z		UX	UY	UZ	PHIX	PHIY	PHIZ
-0.2000	0.0000	4.6000	1	-0.0003	-0.0297	0.0004	0.0033	0.0421	0.0000
-0.2000	0.0000	2.2000	2	0.0001	-0.0276	0.0002	-0.0219	0.0125	0.0000
0.0000	-0.0200	4.6000	3	0.0288	0.0005	0.0002	0.0014	0.0413	1.9391
0.0000	-0.0200	2.2000	4	0.0243	-0.0025	0.0004	-0.0069	0.0430	1.4184
0.0000	0.0000	5.4000	5	*	*	*	*	*	*
0.0000	0.0000	4.6000	6	-0.0003	0.0005	-0.0001	0.0020	0.0079	0.3458
0.0000	0.0000	2.2000	7	0.0001	-0.0023	0.0001	0.0005	-0.0011	0.7850
0.0000	0.0000	0.7500	8	*	*	*	-0.0236	0.0011	0.7850
0.0000	0.0000	4.6000	9	-0.0315	0.0006	-0.0000	-0.0027	0.0719	0.0000
0.0000	-0.0200	2.2000	10	-0.0262	-0.0022	0.0002	0.0001	0.0005	0.0000
0.6700	-0.0200	4.6000	11	0.1406	0.1043	0.0003	-0.0047	0.0431	1.4285
0.6700	-0.0200	2.2000	12	0.1236	0.0890	0.0005	-0.1100	0.0695	1.3956
0.8200	-0.0730	4.6000	13	0.1189	0.1274	-0.0011	-0.0078	0.0270	1.5422
0.8200	-0.0730	2.2000	14	0.1067	0.1092	-0.0016	-0.0205	0.0441	1.4738
0.8200	-0.0730	1.4500	15	0.1058	0.1087	-0.0023	-0.0034	0.0219	1.5265
0.7800	-0.8200	2.2000	16	0.1091	0.1053	-0.0013	-0.0090	0.0632	0.0000
0.5000	0.0000	4.6000	17	0.0012	0.0777	-0.0045	-0.0044	0.0925	1.5416
0.5000	0.0000	2.2000	18	-0.0016	0.0644	-0.0043	-0.0036	0.1354	1.5396
0.5000	0.0000	1.4500	19	-0.0140	0.0598	-0.0032	-0.0021	0.1115	1.5386
0.8200	0.0730	4.6000	20	-0.1216	0.1272	-0.0096	-0.0035	0.0565	1.5504
0.8200	0.0730	2.2000	21	-0.1338	0.1180	-0.0107	-0.0059	0.0403	1.6147
0.8200	0.0730	1.4500	22	-0.1344	0.1095	-0.0115	-0.0044	0.0166	1.5547
0.6700	0.9200	4.6000	23	-0.1434	0.1041	-0.0092	-0.0010	0.0780	0.0000
1.6000	0.3000	4.6000	24	-0.1493	0.2481	-0.0033	0.0129	0.0584	1.5727
1.6000	0.3000	2.2000	25	-0.1817	0.2300	-0.0034	-0.0752	0.0709	1.5640
1.6000	0.3000	1.4500	26	-0.1685	0.2481	-0.0032	-0.0007	0.0490	1.5500
1.6000	0.3000	1.4500	27	-0.1581	0.2345	-0.0030	-0.0002	0.0302	1.5689
1.6000	0.3000	1.4500	28	-0.1549	0.2289	-0.0028	-0.0090	0.0436	1.5481
1.6000	0.3000	2.2000	29	-0.1587	0.2301	-0.0046	-0.0797	0.0655	0.0000
1.6000	0.3000	4.6000	30	-0.0013	0.2477	-0.0077	-0.0032	0.0115	0.0000
1.6000	0.3000	1.4500	31	-0.0145	0.2291	-0.0099	-0.0077	0.0503	0.0000
1.6000	0.3000	1.4500	32	-0.1712	0.2477	-0.0156	-0.0026	0.0426	1.5375
1.6000	0.3000	2.2000	33	-0.1811	0.2333	-0.0158	-0.0035	0.0122	1.5493
1.6000	0.3000	1.4500	34	-0.1839	0.2293	-0.0157	-0.0039	0.0415	1.5274
1.6000	0.3000	4.6000	35	-0.2020	0.2477	-0.0172	-0.0039	0.0527	0.0000
2.3800	0.3000	4.6000	36	-0.2221	0.3685	-0.0077	-0.0102	0.0607	1.5350
2.3800	0.3000	2.2000	37	-0.2051	0.3055	-0.0078	-0.0057	0.0678	1.5302
2.3800	0.3000	1.4500	38	-0.1194	0.3886	-0.0063	-0.0165	0.0904	1.5383
2.3800	0.3000	2.2000	39	-0.1101	0.3510	-0.0085	-0.0034	0.0151	1.5432
2.3800	0.3000	1.4500	40	-0.1055	0.3489	-0.0088	-0.0023	0.0516	1.5380
2.4200	0.0000	2.2000	41	-0.1081	0.3565	-0.0107	-0.0225	0.0809	0.0000
2.7000	0.0000	4.6000	42	-0.0010	0.4170	-0.0151	-0.0019	0.1414	1.5444
2.7000	0.0000	2.2000	43	-0.0149	0.4025	-0.0142	0.0131	0.1918	1.5556
2.7000	0.0000	1.4500	44	-0.0148	0.3983	-0.0137	-0.0006	-0.0149	1.5426
2.3800	0.0000	4.6000	45	-0.1219	0.3678	-0.0175	-0.1019	0.1009	1.5461
2.3800	0.0000	2.2000	46	-0.1314	0.3545	-0.0174	-0.0781	0.0050	1.5243
2.3800	0.0000	1.4500	47	-0.1347	0.3493	-0.0175	-0.0010	0.0434	1.5376
2.3800	0.0000	4.6000	48	-0.2254	0.3679	-0.0243	-0.0032	0.1137	0.0000
2.3800	0.0000	2.2000	49	-0.2575	0.5107	-0.0124	-0.0077	0.0716	1.5308
2.3800	0.0000	1.4500	50	-0.2400	0.4905	-0.0124	-0.0080	0.0711	1.5216
2.3800	0.0000	4.6000	51	-0.1210	0.5109	-0.0198	-0.0061	0.1405	1.5411
2.3800	0.0000	2.2000	52	-0.1069	0.4904	-0.0199	-0.0081	0.1113	1.5053
2.3800	0.0000	1.4500	53	-0.0021	0.5097	-0.0263	-0.0097	0.2037	1.5597
2.3800	0.0000	4.6000	54	-0.0127	0.4911	-0.0267	-0.0086	0.1723	1.4704
2.3800	0.0000	2.2000	55	-0.2487	0.5102	-0.0411	-0.0090	0.2068	0.0000
2.3800	0.0000	1.4500	56	-0.2969	0.6958	-0.0187	-0.1227	0.0714	1.5395
2.3800	0.0000	4.6000	57	-0.2878	0.6803	-0.0187	-0.0063	0.0768	1.4837
2.3800	0.0000	2.2000	58	-0.2642	0.7343	-0.0232	-0.0045	-0.0000	1.5046
2.3800	0.0000	1.4500	59	-0.2373	0.7683	-0.0276	-0.1234	0.0641	1.5523
2.3800	0.0000	4.6000	60	-0.2319	0.7735	-0.0278	-0.1457	0.0704	1.4747
2.3800	0.0000	2.2000	61	-0.0112	0.8623	-0.0506	-0.5031	0.0578	1.4742
2.3800	0.0000	1.4500	62	-0.0019	0.7884	-0.0506	-0.1086	0.0578	1.4742
2.3800	0.0000	4.6000	63	-0.0050	0.7730	-0.0505	-0.1378	0.0751	1.4735
2.3800	0.0000	2.2000	64	-0.3030	0.7883	-0.0757	-0.1314	0.1436	0.0000
2.3800	0.0000	1.4500	65	-0.2990	0.8809	-0.0250	-0.1107	0.0092	0.0000
2.3800	0.0000	4.6000	66	-0.2110	0.9705	-0.0314	-0.1106	0.0051	0.0000
2.3800	0.0000	2.2000	67	-0.0014	1.0014	-0.0748	-0.1306	0.0406	0.0000
2.3800	0.0000	1.4500	68	-0.0020	1.0893	-0.0511	-0.1642	0.0096	0.0000

SCALED COORDINATES DIVIDE BY 10.000			SCALED DISPLACEMENTS/ROTATIONS FOR LOAD CASE 2 * INDICATES A CONSTRAINT HAS BEEN APPLIED						DIVIDE BY 100.00 NODES 1- 68		
COORDINATES			NODE NO.	DISPLACEMENTS			ROTATIONS				
X	Y	Z		UX	UY	UZ	PHIX	PHIY	PHIZ		
0.2000	0.0000	4.6000	1	0.0023	-0.0983	0.0003	-0.0401	0.1075	0.0000		
0.2000	0.0000	2.2000	2	0.0102	-0.1032	0.0012	-0.0863	0.0633	0.0000		
0.0000	-0.2000	4.6000	3	0.0967	-0.0008	0.0019	-0.0332	0.1000	6.2875		
0.0000	0.2000	2.2000	4	0.0875	-0.0231	0.0025	-0.1095	0.1666	4.5284		
0.0000	0.0000	5.4000	5	*	*	*	*	*	*		
0.0000	0.0000	4.6000	6	0.0023	-0.0008	-0.0002	-0.0505	-0.0322	1.1148		
0.0000	0.0000	2.2000	7	0.0101	-0.0225	0.0004	0.0331	0.0282	2.3243		
0.0000	0.0000	0.7500	8	*	*	*	0.0331	0.0900	0.0000		
0.0000	0.2000	4.6000	9	-0.0985	-0.0005	-0.0013	-0.2134	0.0218	0.0000		
0.0000	0.0000	2.2000	10	-0.0738	-0.0221	0.0009	-0.0229	0.0459	0.0000		
0.6700	0.2000	4.6000	11	0.4580	0.3352	0.0077	-0.2686	0.1291	4.6175		
0.6700	0.2000	2.2000	12	0.4058	0.2695	0.0063	-0.4438	0.2253	4.4872		
0.8200	0.7300	4.6000	13	0.3864	0.4098	0.0026	-0.2829	0.0475	4.9891		
0.8200	0.7300	2.2000	14	0.3551	0.3348	0.0013	-0.1929	0.1370	4.7369		
0.8200	0.7300	1.4500	15	0.3526	0.3249	-0.0007	-0.2035	0.0562	4.9070		
0.7800	0.8200	2.2000	16	0.3591	0.3219	0.0017	-0.4082	0.2060	0.0000		
0.5000	0.0000	4.6000	17	-0.0002	0.2491	0.0149	-0.0210	0.3237	4.9860		
0.5000	0.0000	2.2000	18	0.0048	0.1902	0.0153	-0.0950	0.4510	4.9788		
0.5000	0.0000	1.4500	19	-0.0327	0.1679	0.0118	-0.0213	0.3235	4.9530		
0.8200	0.7300	4.6000	20	-0.3896	0.4094	0.0374	-0.0201	0.1557	5.0138		
0.8200	0.7300	2.2000	21	-0.4220	0.3628	0.0416	-0.3332	0.0721	5.0261		
0.8200	0.7300	1.4500	22	-0.4202	0.3276	0.0446	-0.3726	0.0111	5.0044		
0.6700	0.9200	4.6000	23	-0.4598	0.3344	0.0376	-0.4584	0.2471	0.0000		
1.6000	1.1300	4.6000	24	0.6484	0.8002	0.0003	-0.0042	0.1721	5.0921		
1.6000	1.1300	2.2000	25	0.5932	0.7241	0.0006	-0.0330	0.2048	5.0264		
1.6000	1.1300	1.4500	26	0.5489	0.8001	0.0001	-0.0602	0.1315	5.0131		
1.6000	1.1300	2.2000	27	0.5196	0.7363	0.0015	-0.0227	0.0847	5.0447		
1.6000	1.1300	1.4500	28	0.5106	0.7114	0.0020	-0.0312	0.1107	4.9820		
1.6000	1.1500	2.2000	29	0.5192	0.7244	0.0057	-0.0330	0.1901	0.0000		
1.6000	0.0000	4.6000	30	0.0003	0.7990	0.0202	-0.0285	0.0287	0.0000		
1.6000	0.0000	1.4500	31	0.0343	0.7120	0.0306	-0.0270	0.1434	0.0000		
1.6000	1.1000	4.6000	32	-0.5497	0.7987	0.0580	-0.4042	0.1139	4.9676		
1.6000	1.1000	2.2000	33	-0.5739	0.7324	0.0589	-0.2797	0.0483	4.9729		
1.6000	1.1000	1.4500	34	-0.5794	0.7126	0.0586	-0.2035	0.1026	4.9951		
1.6000	1.1300	4.6000	35	-0.6494	0.7987	0.0660	-0.4497	0.1683	0.0000		
1.6000	1.1450	4.6000	36	-0.7226	1.1896	0.0126	-0.0057	0.1719	4.9458		
1.6000	1.1450	2.2000	37	-0.6674	1.1082	0.0131	-0.0053	0.2415	4.8343		
1.6000	1.1450	1.4500	38	-0.3902	1.1900	0.0164	-0.0070	0.3125	4.9717		
1.6000	1.1780	4.6000	39	-0.3655	1.1110	0.0173	-0.0083	0.0230	4.9066		
1.6000	1.1780	2.2000	40	-0.3518	1.0472	0.0184	-0.0236	0.1394	4.9344		
1.6000	1.1780	1.4500	41	-0.3590	1.1275	0.0277	-0.1186	0.3060	0.0000		
1.6000	0.0000	4.6000	42	0.0009	1.3464	0.0441	-0.0278	0.5521	4.9994		
1.6000	0.0000	2.2000	43	0.0319	1.2744	0.0419	-0.0405	0.7946	5.0461		
1.6000	0.0000	1.4500	44	0.0349	1.2558	0.0409	-0.0209	0.0506	4.9705		
1.6000	0.7800	4.6000	45	-0.3903	1.1873	0.0610	-0.0532	0.4065	5.0037		
1.6000	0.7800	2.2000	46	-0.4160	1.1169	0.0588	-0.0304	0.0508	4.9454		
1.6000	0.7800	1.4500	47	-0.4212	1.0981	0.0585	-0.0207	0.0819	4.9530		
1.6000	1.1450	4.6000	48	-0.7251	1.1876	0.0953	-0.4706	0.4937	0.0000		
1.6000	1.1450	4.6000	49	-0.8372	1.6497	0.0257	-0.4442	0.2739	5.0951		
1.6000	1.1450	2.2000	50	-0.7784	1.5533	0.0256	-0.4246	0.2097	4.9376		
1.6000	1.1450	1.4500	51	-0.3957	1.5004	0.0613	-0.3370	0.6421	4.9905		
1.6000	0.0000	2.2000	52	-0.3552	1.5527	0.0611	-0.4484	0.3114	4.6837		
1.6000	0.0000	4.6000	53	-0.0028	1.6472	0.0926	-0.3358	0.3396	5.0923		
1.6000	0.0000	2.2000	54	-0.0245	1.5551	0.0934	-0.3303	0.7426	4.6879		
1.6000	1.1000	4.6000	55	-0.8007	1.6481	0.1723	-0.4401	0.9621	0.0000		
1.6000	1.1000	4.6000	56	-0.9713	2.2485	0.0432	-1.0273	0.0021	4.2453		
1.6000	1.1750	3.1500	57	-0.9315	2.1683	0.0434	-0.4606	1.0492	4.6513		
1.6000	1.1750	4.6000	58	-0.8826	2.3233	0.0624	-0.6035	0.0000	4.9464		
1.6000	1.1750	4.6000	59	-0.7720	2.5478	0.0814	-0.7503	0.1210	6.0092		
1.6000	1.1750	3.6000	60	-0.7578	2.4703	0.0823	-0.0209	0.4622	5.1558		
1.6000	0.0000	6.2000	61	-0.0823	2.4949	0.2002	-0.2593	0.5016	4.0249		
1.6000	0.0000	4.6000	62	-0.0021	2.5487	0.2002	-0.0987	0.5016	4.0249		
1.6000	0.0000	3.6000	63	-0.0549	2.4685	0.2001	-0.7107	0.6017	4.0199		
1.6000	0.9750	4.6000	64	-0.9766	2.5480	0.3298	-0.6818	0.6228	0.0000		
1.6000	0.9750	4.6000	65	-0.9719	2.3476	0.5527	-0.6545	0.0784	0.0000		
1.6000	1.1380	4.6000	66	-0.6870	3.1377	0.0750	-0.5341	0.1810	0.0000		
1.6000	1.1380	4.6000	67	-0.6915	3.2378	0.3026	-0.8227	0.0413	0.0000		
1.6000	0.0000	4.6000	68	-0.0023	3.5223	0.1679	-0.8679	0.1123	0.0000		

SCALED COORDINATES DIVIDE BY 10.000			SCALED DISPLACEMENTS/ROTATIONS FOR LOAD CASE 3 * INDICATES A CONSTRAINT HAS BEEN APPLIED			DIVIDE BY 100.00 NODES 1- 68			
COORDINATES			NODE NO.	DISPLACEMENTS			ROTATIONS		
X	Y	Z		UX	UY	UZ	PHIX	PHIY	PHIZ
0.2000	0.0000	4.6000	1	-0.0010	-0.0782	0.0028	-0.0001	0.2774	0.0000
0.2000	0.0000	2.2000	2	-0.0027	-0.0706	-0.0001	-0.0081	0.0313	0.0000
0.0000	0.2000	4.6000	3	0.0751	0.0000	0.0010	0.0072	0.2860	5.0866
0.0000	0.2000	2.2000	4	0.0262	-0.0143	0.0016	-0.0299	0.2238	3.1110
0.0000	0.0000	5.4000	5	*	*	*	*	*	*
0.0000	0.0000	4.6000	6	-0.0010	-0.0000	-0.0005	-0.0246	0.0838	0.8504
0.0000	0.0000	2.2000	7	-0.0277	-0.0138	0.0002	0.0200	-0.0424	1.8781
0.0000	0.0000	0.7500	8	*	*	*	0.1131	-0.0265	1.8781
0.0000	0.2000	4.6000	9	-0.0812	0.0002	-0.0006	-0.1553	0.4234	0.0000
0.0000	0.0000	2.2000	10	-0.0134	-0.0134	0.0011	-0.0291	-0.0404	0.0000
0.6700	0.9200	4.6000	11	0.3653	0.2689	0.0068	-0.4300	0.3284	3.6853
0.6700	0.9200	2.2000	12	0.2547	0.1956	0.0065	-0.3407	0.4751	3.3510
0.8200	0.7400	4.6000	13	0.3092	0.3285	0.0150	-0.3243	0.2547	3.9095
0.8200	0.7400	2.2000	14	0.2151	0.2417	0.0170	-0.4278	0.4131	3.5325
0.8200	0.7400	1.4500	15	0.1987	0.380	0.0204	-0.4734	0.2595	3.2770
0.7800	0.8200	2.2000	16	0.2199	0.357	0.0166	-0.4758	0.4327	0.0000
0.5000	0.0000	4.6000	17	0.0022	0.2000	0.0276	-0.2133	0.6029	3.9837
0.5000	0.0000	2.2000	18	0.0332	0.1378	0.0263	-0.0505	0.8463	3.9870
0.5000	0.0000	1.4500	19	0.1076	0.1142	0.0206	-0.1108	0.7109	3.9493
0.8200	0.7400	4.6000	20	0.3132	0.3282	0.0564	-0.1040	0.4229	4.0131
0.8200	0.7400	2.2000	21	0.4063	0.2873	0.0625	-0.4467	0.3195	4.3316
0.8200	0.7400	1.4500	22	0.4173	0.2425	0.0670	-0.4495	0.1977	4.0232
0.6700	0.9200	4.6000	23	0.3693	0.2683	0.0520	-0.1748	0.5295	0.0000
1.0000	-1.3000	4.6000	24	0.5175	0.4408	0.0367	0.0032	0.4214	4.0766
1.0000	-1.3000	2.2000	25	0.4008	0.5512	0.0372	-0.3844	0.4731	4.0507
1.0000	-1.1000	4.6000	26	0.4378	0.6408	0.0361	-0.4008	0.3752	4.0012
1.0000	-1.1000	2.2000	27	0.3510	0.5736	0.0349	-0.2924	0.3173	4.0026
1.0000	-1.1000	1.4500	28	0.3241	0.5464	0.0340	-0.3407	0.3561	3.9888
1.0000	-1.1300	2.2000	29	0.3416	0.5519	0.0431	-0.4127	0.4521	0.0000
1.0000	0.0000	4.6000	30	0.0017	0.6398	0.0569	-0.3239	0.2071	0.0000
1.0000	0.0000	1.4500	31	0.1102	0.5475	0.0693	-0.2552	0.3872	0.0000
1.0000	1.1300	4.6000	32	0.4410	0.6395	0.0973	-0.3718	0.3666	3.9883
1.0000	1.1000	2.2000	33	0.5219	0.5678	0.0986	-0.3182	0.1738	3.6850
1.0000	1.1300	1.4500	34	0.5448	0.5487	0.0979	-0.2618	0.3408	3.8752
1.0000	1.3000	4.6000	35	0.5208	0.6395	0.1051	-0.4145	0.4045	0.0000
1.3800	1.4500	4.6000	36	0.5771	0.9524	0.0687	-0.0444	0.4353	3.9839
1.3800	1.4500	2.2000	37	0.4609	0.8042	0.0692	-0.2970	0.4878	3.9492
1.3800	0.7400	4.6000	38	0.3110	0.9525	0.0716	-0.1010	0.5742	3.9777
1.3800	0.7400	2.2000	39	0.2321	0.8624	0.0730	-0.1558	0.2299	3.9866
1.3800	0.7400	1.4500	40	0.1970	0.8536	0.0752	-0.2434	0.4087	3.9423
1.2000	0.8200	2.2000	41	0.2102	0.8601	0.0853	-0.1198	0.5381	0.0000
1.2000	0.8200	4.6000	42	0.0005	1.0777	0.1104	-0.3182	0.8222	4.0010
1.2000	0.0000	2.2000	43	0.1049	1.0002	0.1056	-0.0920	1.0057	4.0044
1.2000	0.0000	1.4500	44	0.1117	0.9808	0.1030	-0.2967	0.8053	3.9658
1.3800	0.7400	4.6000	45	0.3135	0.9504	0.1180	-0.4022	0.6036	4.0038
1.3800	0.7400	2.2000	46	0.3931	0.8817	0.1169	-0.3939	0.1484	3.8803
1.3800	0.7400	1.4500	47	0.4192	0.8560	0.1176	-0.2468	0.3481	3.9158
1.3800	1.4500	4.6000	48	0.5813	0.9506	0.1482	-0.4180	0.6220	0.0000
1.3800	1.4500	4.6000	49	0.6691	1.3206	0.1050	-0.4222	0.5123	0.0571
1.3800	1.4500	2.2000	50	0.5504	1.2251	0.1051	-0.4218	0.4783	3.9672
1.3800	0.0000	4.6000	51	0.3157	1.3211	0.1399	-0.3915	0.7975	3.9946
1.3800	0.0000	2.2000	52	0.2072	1.2247	0.1404	-0.4429	0.5966	3.8214
1.3800	0.0000	4.6000	53	0.0032	1.3184	0.1704	-0.3180	1.0020	4.0060
1.3800	0.0000	2.2000	54	0.0999	1.2264	0.1727	-0.4175	0.9430	3.7639
1.3800	1.6000	4.6000	55	0.6417	1.3191	0.2300	-0.3704	0.9721	0.0000
1.3800	1.4500	4.6000	56	0.7766	1.8001	0.1534	-0.7456	0.3514	3.6053
1.3800	1.4500	3.1500	57	0.7025	1.7309	0.1535	-0.0247	0.9163	3.7977
1.3800	1.4500	4.6000	58	0.8810	1.8687	0.1783	-0.4840	0.0000	3.9659
1.3800	1.4500	4.6000	59	0.6172	2.0397	0.2031	-0.3926	0.4221	4.5269
1.3800	1.4500	3.6000	60	0.5734	1.9793	0.2036	-0.2489	0.6039	4.2037
1.3800	0.0000	6.2000	61	0.1390	2.3207	0.2970	-2.2581	1.2184	3.2505
1.3800	0.0000	4.6000	62	0.0020	2.0402	0.2963	-0.7452	0.2084	3.2505
1.3800	0.0000	3.6000	63	0.0104	1.9784	0.2958	-0.5555	0.0216	3.5031
1.3800	1.4500	4.6000	64	0.0395	2.0395	0.4043	-0.5558	0.7676	0.0000
1.3800	1.4500	4.6000	65	0.7771	2.795	0.2027	-0.5606	0.3591	0.0000
1.3800	1.3300	4.6000	66	0.5493	2.116	0.2530	-0.5461	0.3335	0.0000
1.3800	1.3300	4.6000	67	0.5542	2.118	0.4409	-0.6347	0.4683	0.0000
1.3800	0.0000	4.6000	68	0.0023	2.195	0.3662	-0.6735	0.3823	0.0000

32	1	-.813E+05	-.731E+07	-72.4	-.206E+07	-.357E+07	-34.7	.161E+07	-.548E+07	5.4
32	2	.597E+07	-.225E+08	-74.8	-.685E+07	-.103E+08	-18.7	.701E+07	-.247E+08	9.4
32	3	.543E+07	-.257E+08	-81.6	-.303E+07	-.844E+07	-21.5	.194E+08	-.108E+08	10.7
42	1	.158E+08	.500E+07	-17.7	.740E+07	-.409E+07	-9.3	.651E+06	-.153E+08	-3.2
42	2	.650E+08	.247E+08	-22.6	.209E+08	-.161E+08	-11.5	.163E+07	-.333E+08	-3.0
42	3	.696E+08	.364E+08	-29.8	.256E+08	-.117E+08	-15.1	.132E+08	-.601E+08	-6.8
44	1	.153E+08	-.143E+08	-77.7	-.325E+06	-.246E+08	-79.0	.159E+08	-.331E+08	-30.4
44	2	.714E+08	-.306E+08	-77.4	.233E+07	-.758E+08	-79.1	.667E+08	-.113E+09	-81.8
44	3	.842E+08	-.111E+08	-77.2	.921E+07	-.614E+08	-79.2	.255E+08	-.112E+09	-83.2
46	1	.275E+08	.903E+07	-28.2	.143E+08	-.293E+08	-40.1	.256E+07	-.104E+08	-31.7
46	2	.110E+09	.500E+08	-22.6	.474E+08	-.994E+07	-38.1	.762E+07	-.778E+08	-51.2
46	3	.107E+09	.414E+08	-18.2	.424E+08	-.475E+07	-34.7	.988E+07	-.611E+08	-55.8
48	1	.542E+07	.277E+07	-85.1	-.383E+05	.731E+07	80.6	.530E+07	-.176E+08	77.7
48	2	.315E+08	.253E+08	-42.8	.262E+06	.236E+08	62.9	.276E+08	-.767E+08	79.3
48	3	.301E+08	.172E+08	-37.9	.456E+06	.157E+09	67.6	.214E+08	-.511E+08	77.9
63	1	.105E+08	.119E+07	-22.7	.247E+07	-.349E+07	-30.1	.162E+07	-.134E+08	-46.0
63	2	.540E+08	.391E+07	-24.7	.872E+07	-.137E+08	-31.8	.568E+07	-.736E+08	-49.5

SUBROUTINE R91320 TRIANGULAR HYBRID ELEMENT STRESSING ROUTINE  
 SIGMA1 IS THE MAXIMUM VALUE OF STRESS IN THE PLANE, SIGMA2 IS THE MINIMUM IN THE PLANE  
 THE ANGLE IS THAT OF SIGMA1 MEASURED +IVE TO THE ELEMENT Y-AXIS FROM THE ELEMENT X-AXIS  
 ELEM. LOAD \*\*\* POSITIVE \*\*\* SURFACE \*\*\* NEUTRAL \*\*\* SURFACE \*\*\* NEGATIVE \*\*\* SURFACE \*\*\*  
 NUMB. CASE SIGMA 1 SIGMA 2 ANGLE SIGMA 1 SIGMA 2 ANGLE SIGMA 1 SIGMA 2 ANGLE

63	1	.395E+08	-.413E+07	-31.7	.792E+07	-.101E+08	-30.0	.648E+07	-.333E+08	-44.2
72	1	.279E+07	-.357E+07	-78.1	.208E+07	-.318E+07	-8.5	.765E+07	-.347E+07	-7.2
72	2	.327E+06	-.477E+08	-26.6	.768E+07	-.112E+08	-8.4	.431E+08	-.462E+07	-40.2
72	3	.396E+07	-.267E+08	-18.6	.631E+07	-.743E+07	-8.8	.237E+08	-.143E+07	-43.2
73	1	.173E+07	-.784E+06	-31.9	.455E+07	-.345E+06	-27.2	.390E+07	-.223E+07	-31.1
73	2	.203E+08	-.167E+09	-82.5	.162E+08	-.110E+07	-41.4	.181E+09	-.411E+08	-0.2
73	3	.144E+08	-.854E+08	-82.7	.954E+07	-.129E+07	-36.4	.976E+08	-.239E+08	-0.8
74	1	.707E+06	-.566E+07	-1.0	.150E+07	-.603E+07	-28.8	.615E+06	-.839E+07	-45.4
74	2	.855E+08	-.129E+09	-73.7	.129E+07	-.120E+08	-51.5	.112E+09	-.811E+08	-2.2
74	3	.464E+08	-.674E+06	-72.2	.188E+05	.706E+07	-38.7	.600E+08	-.415E+08	-4.3
75	1	.360E+07	-.589E+07	-50.3	.213E+07	-.531E+07	-28.3	.316E+07	-.744E+07	-8.7
75	2	.849E+06	-.125E+09	-53.3	.148E+07	-.185E+08	-21.4	.132E+09	-.71CE+08	-3.1
75	3	.428E+08	-.679E+08	-53.7	.932E+07	-.106E+08	-25.9	.706E+08	-.176E+08	-16.5
76	1	.377E+06	-.127E+08	-20.3	.115E+06	-.130E+08	-33.1	.102E+07	-.14CE+08	-43.7
76	2	.101E+09	-.155E+09	-45.1	.385E+07	-.375E+08	-39.1	.111E+09	-.76CE+08	-29.4
76	3	.529E+06	-.155E+08	-39.6	.30CE+07	-.288E+08	-35.0	.596E+08	-.36CE+08	-28.4
80	1	.925E+06	-.534E+07	-55.9	.192E+07	-.163E+06	-35.3	.682E+07	-.415E+07	-16.6
80	2	.410E+07	-.327E+08	-72.0	.692E+07	-.121E+07	-32.0	.407E+08	-.414E+07	-9.0
80	3	.355E+07	-.750E+07	-71.9	.519E+07	-.158E+07	-18.6	.163E+08	-.116E+07	-5.0
82	1	.222E+07	-.108E+07	-20.7	.368E+06	-.669E+06	-61.3	.830E+06	-.335E+07	-76.9
82	2	.129E+08	-.688E+07	-12.8	.167E+07	-.330E+07	-64.9	.509E+07	-.174E+08	-78.9
82	3	.468E+07	-.123E+07	-34.1	.254E+07	-.354E+07	-65.7	.156E+07	-.948E+07	-73.6
83	1	.349E+06	-.102E+08	-2.2	.444E+06	-.189E+07	-48.2	.940E+07	-.169E+07	-79.8
83	2	.506E+06	-.553E+08	-0.3	.189E+07	-.696E+07	-50.3	.532E+08	-.756E+07	-81.4
83	3	.316E+07	-.298E+08	-4.0	.254E+07	-.643E+07	-54.8	.301E+08	-.465E+07	-78.9

THIN FACET SHELL STRESSES/MOMENTS ELEMENT TYPE=44200, 4 NODES ANGLES OF MOS1  
 POSITIVE VALUE  
 TO X AXES  
 ELEMENT GLOBAL

ELEM NO	LOAD CASE	NODE NO	PRINCIPAL-BEND-MOMENTS MOST.PLUS MOST.MINUS	PRINCIPAL-STRESSES MOST.PLUS MOST.MINUS	THICKNESS POSITION	TO X AXES ELEMENT GLOBAL
6	1	3	-138. -598.	.993E+08 .219E+08 .125E+07 .264E+07 .240E+08 .100E+09	TUP MIDDLE BOTUM	10.4 1090.0 -81.0 1090.0 60.3 1090.0 11.9 1090.0
6	1	6	.718E+04 .216E+04	-.361E+09 -.120E+10 .192E+07 .271E+07 .120E+10 .359E+09	TUP MIDDLE BOTUM	-89.6 1090.0 0.5 1090.0 55.5 1090.0 -89.8 1090.0
8	1	4	46.1 -149.	.341E+08 .355E+07 .180E+08 .248E+07 .220E+08 .188E+08	TUP MIDDLE BOTUM	-62.2 1090.0 76.2 1090.0 52.2 1090.0 -89.4 1090.0
8	1	7	.267E+04 798.	-.129E+09 -.428E+09 .184E+08 .267E+07 .463E+09 .137E+09	TUP MIDDLE BOTUM	-1.4 1090.0 77.3 1090.0 89.6 1090.0
8	2	3	-422. -.197E+04	.321E+09 .669E+08 .406E+07 .138E+08 .731E+08 .334E+09	TUP MIDDLE BOTUM	11.9 1090.0 -80.1 1090.0 51.1 1090.0 13.6 1090.0
8	2	6	.233E+05 .701E+04			-89.7 1090.0

					.147E+08	-.546E+08	MIDDLE	38.6	1090.0
					.220E+08	-.662E+08	BCITUM	39.1	1090.0
77	2	60	189.	-384.				12.4	1090.0
					.668E+08	-.289E+08	TUP	-80.0	1090.0
					.171E+08	-.240E+08	MIDDLE	18.2	1090.0
					.622E+08	-.116E+09	BCITUM	13.8	1090.0
77	3	62	-126.	-170.				-20.8	1090.0
					.528E+08	-.139E+08	TUP	61.1	1090.0
					.122E+08	-.168E+08	MIDDLE	58.1	1090.0
					-.281E+08	-.475E+08	BCITUM	52.1	1090.0
77	3	59	-109.	-207.				18.2	1090.0
					.603E+08	-.427E+08	TUP	-72.7	1090.0
					.165E+08	-.107E+08	MIDDLE	21.1	1090.0
					-.977E+07	-.389E+08	BCITUM	18.8	1090.0
77	3	63	20.2	-30.8				41.1	1090.0
					-.176E+07	-.265E+08	TUP	45.2	1090.0
					.306E+07	-.338E+08	MIDDLE	43.9	1090.0
					.790E+07	-.412E+08	BCITUM	43.2	1090.0
77	3	60	103.	-197.				13.7	1090.0
					.361E+08	-.127E+08	TUP	-79.0	1090.0
					.123E+08	-.114E+08	MIDDLE	19.4	1090.0
					.367E+08	-.584E+08	BCITUM	15.1	1090.0
81	1	59	323.	-68.7				24.4	32.6
					.548E+07	-.181E+08	TUP	-68.3	-60.1
					.242E+07	-.186E+08	MIDDLE	69.5	77.7
					.207E+08	-.287E+07	BCITUM	27.1	35.3
81	1	62	-161.	-313.				47.9	56.1
					.200E+08	-.109E+08	TUP	-48.9	-40.7
					.233E+07	-.185E+06	MIDDLE	89.2	-82.6
					-.816E+07	-.176E+08	BCITUM	54.3	62.5
81	1	66	-104.	-194.				33.2	41.4
					.102E+08	-.603E+07	TUP	-56.1	-47.9
					-.191E+06	-.140E+07	MIDDLE	30.8	39.0
					-.642E+07	-.130E+08	BCITUM	32.6	41.0
81	1	68	83.7	-32.9				-23.7	-15.5
					.228E+07	-.516E+07	TUP	69.9	78.1
					.587E+06	-.416E+06	MIDDLE	-80.3	-72.1
					.494E+07	-.172E+07	BCITUM	-27.6	-19.4
81	2	59	.198E+04	-43.1				31.1	39.3
					.847E+07	-.109E+09	TUP	-61.7	-53.5
					.140E+08	-.161E+07	MIDDLE	65.6	73.8
					.129E+09	.274E+07	BCITUM	33.7	41.9
81	2	62	-.110E+04	-.184E+04				41.3	49.5
					.118E+09	.719E+08	TUP	-55.9	-47.7
					.129E+08	-.124E+07	MIDDLE	88.0	-83.8
					-.584E+08	-.104E+09	BCITUM	48.8	57.0
81	2	66	-545.	-.123E+04				26.3	34.5
					.644E+08	.317E+08	TUP	-62.9	-54.7
					-.922E+06	-.923E+07	MIDDLE	23.3	31.5
					-.336E+08	-.828E+08	BCITUM	25.8	34.0
81	2	68	430.	-170.				-26.1	-17.9
					.106E+08	-.267E+08	TUP	67.5	75.7
					.215E+07	-.280E+07	MIDDLE	-76.9	-68.7
					.253E+08	-.101E+08	BCITUM	-29.9	-21.7
81	3	59	790.	62.4				35.6	43.8
					-.154E+07	-.394E+08	TUP	-58.2	-50.1
					.913E+07	.112E+07	MIDDLE	55.3	63.5
					.558E+08	.564E+07	BCITUM	38.5	46.7
81	3	62	-630.	-958.				28.4	36.6
					.608E+08	.399E+08	TUP	-72.7	-64.5
					.664E+07	-.126E+07	MIDDLE	72.1	80.3
					-.342E+08	-.558E+08	BCITUM	39.2	47.4
81	3	66	-320.	-699.				20.5	28.7
					.405E+08	.213E+08	TUP	-70.2	-62.0
					.206E+07	-.149E+07	MIDDLE	23.9	32.1
					-.172E+08	-.434E+08	BCITUM	20.4	29.1
81	3	68	196.	-24.9				-23.3	-15.1
					.316E+07	-.140E+08	TUP	69.7	77.9
					.182E+07	-.242E+07	MIDDLE	79.2	87.4

APPENDIX 6.1

ENGINEERING WORKSHOP DRAWINGS

FOR THE MANUFACTURE OF

AN ELECTRIC TOWN CAR

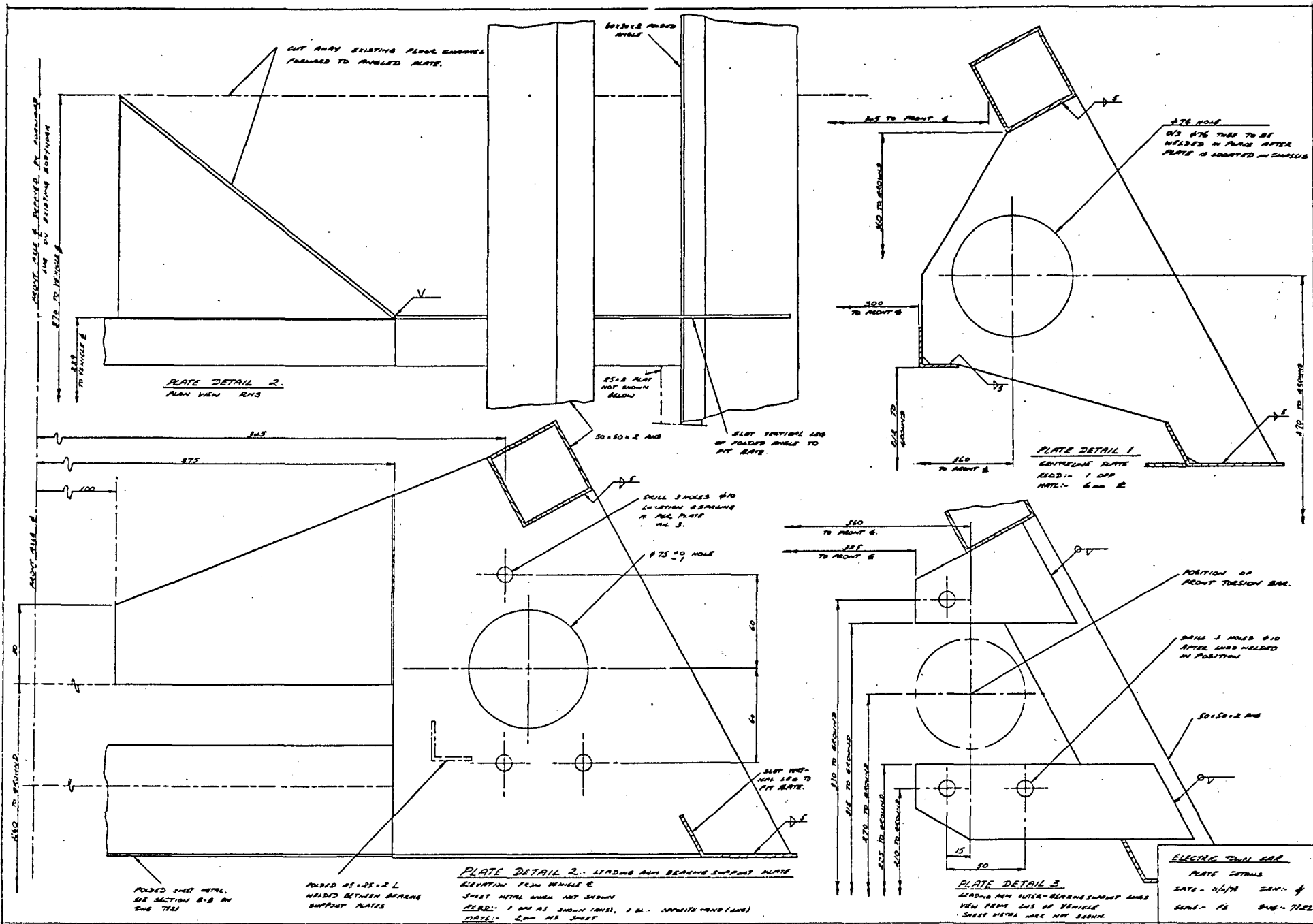


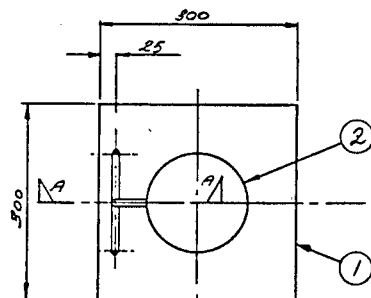
ALL DIMENSIONS IN MM

NOTE - THIS DRAWING TO  
BE READ IN CONJUN. TO  
WITH DRAWING 7822

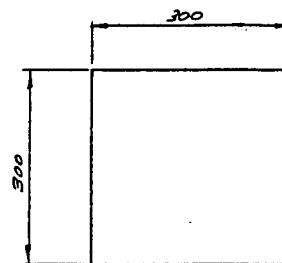
ELECTRIC TUNING GEAR  
DETAIL OF SUB. METAL  
FROM PATENT

DATE - 6/1/78 D.V. - A  
SCALE - 1:10:12 SW. - 3/4  
0.5

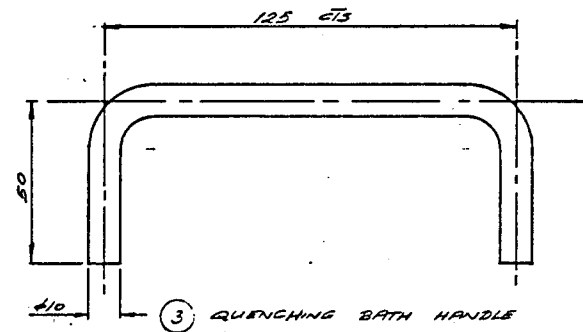




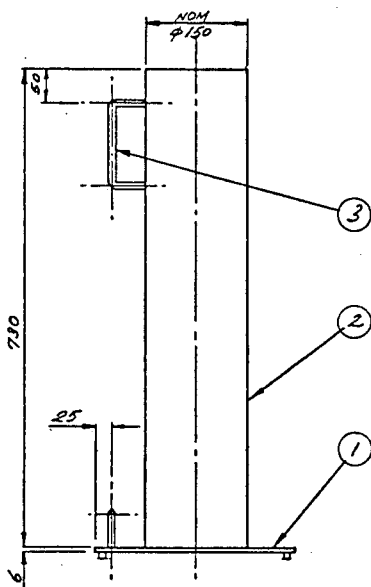
GENERAL ARRANGEMENT  
PLAN VIEW



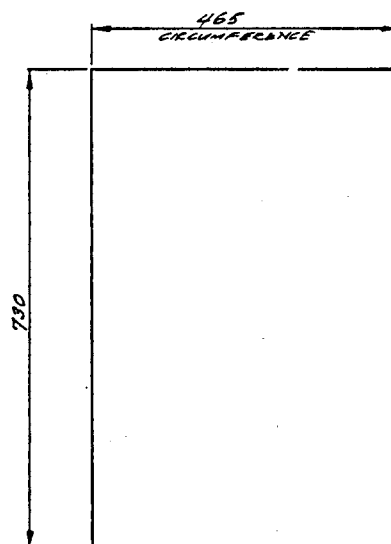
① BASE PLATE  
REQD:- 1 OFF  
MTRL:- 6 mm PL



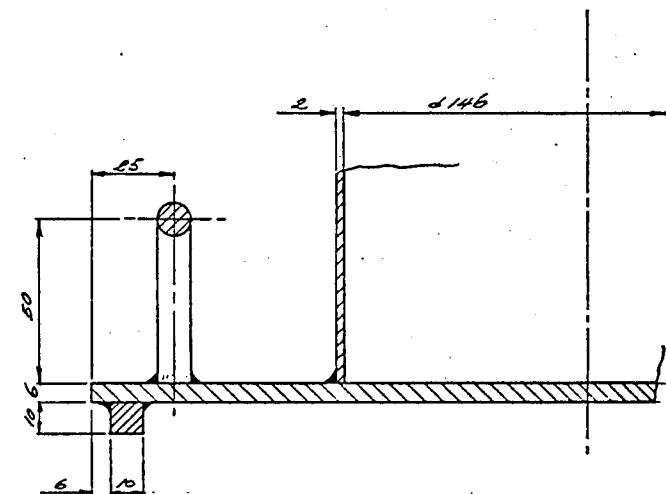
③ QUENCHING BATH HANDLE  
REQD:- 2 OFF  
MTRL:-  $\phi$  10 MS BLACK.



GENERAL ARRANGEMENT  
ELEVATION.



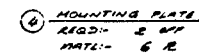
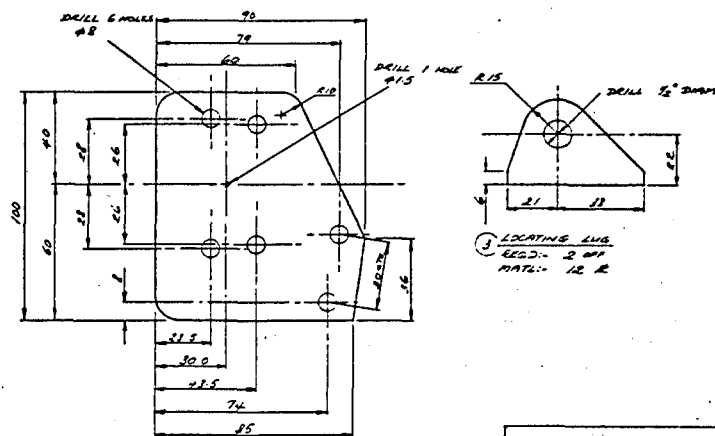
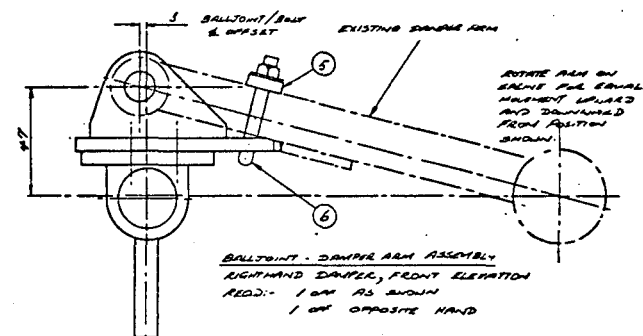
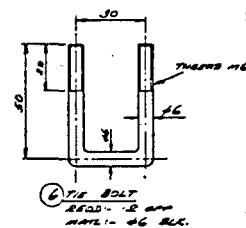
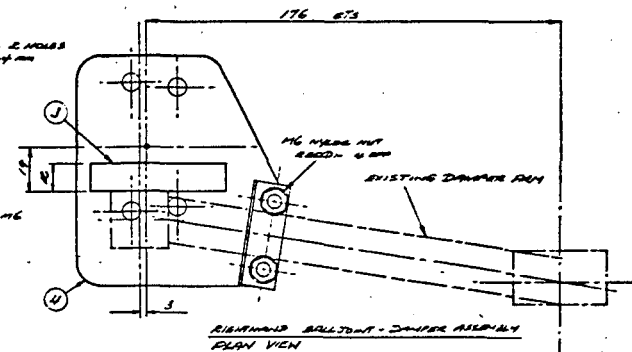
② CYLINDER DEVELOPMENT.  
REQD:- 1 OFF  
MTRL:- 2 mm MS SHEET.



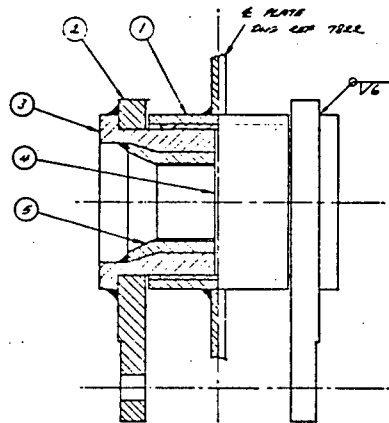
SECTION DETAIL A-A.

ELECTRIC TOWN CAR  
TORSION BAR QUENCHING  
BATH.  
DATE:- 26/1/78 DWG:- 4  
SCALE:- NTS XLG:- 782

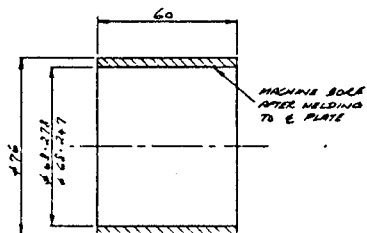




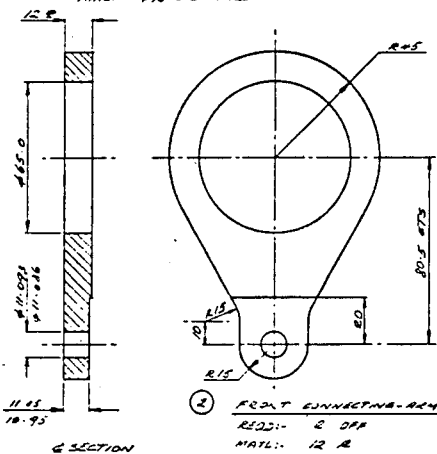
ELECTRIC TOWN CAR  
FRONT SUSPENSION  
BELLJOINT MOUNTING  
DETAILS  
DATE:- 6/6/78 DRAW:-  
SCALE:- F.S. DCS:- 7827



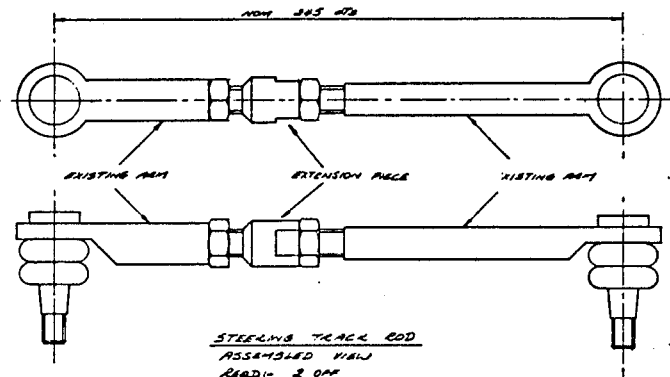
GENERAL ARRANGEMENT  
FRONT PITCH AXIS BEARING ASSEMBLY



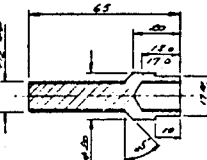
1 BEARING HOUSING  
REQD: 2 OFF (FRONT & REAR)  
MTRL: 47% STEEL TUBE



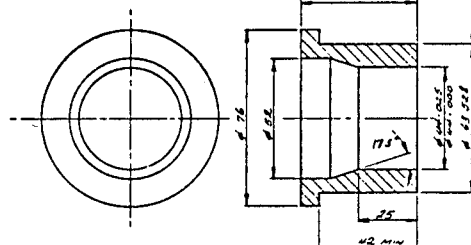
2 FRONT CONNECTING ARM  
REQD: 2 OFF  
MTRL: 12 R



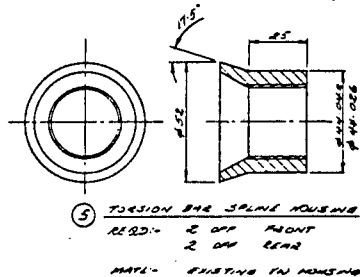
STEERING TRACK ROD  
ASSEMBLED VIEW  
REQD: 2 OFF



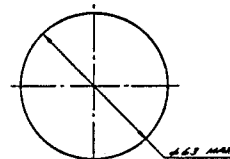
3 EXTENSION PIECE  
REQD: 2 OFF  
MTRL: 420 ROUN



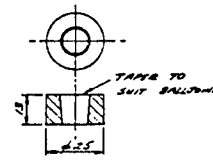
4 CONNECTING ARM SPINDLE  
REQD: 2 OFF FRONT  
2 OFF REAR  
MTRL: 47% ROUN



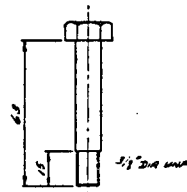
5 TORSION BAR SPLINE HOUSING  
REQD: 2 OFF FRONT  
2 OFF REAR  
MTRL: EXISTING IN HOUSING



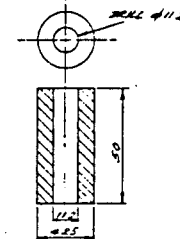
6 SEPARATING DISC  
REQD: 1 OFF FRONT  
1 OFF REAR  
MTRL: 1/2" POLYETHYLENE



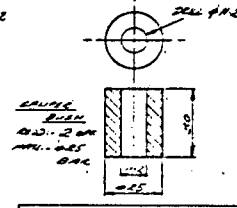
7 BALL JOINT BUSH  
REQD: 2 OFF  
MTRL: 425 BAC



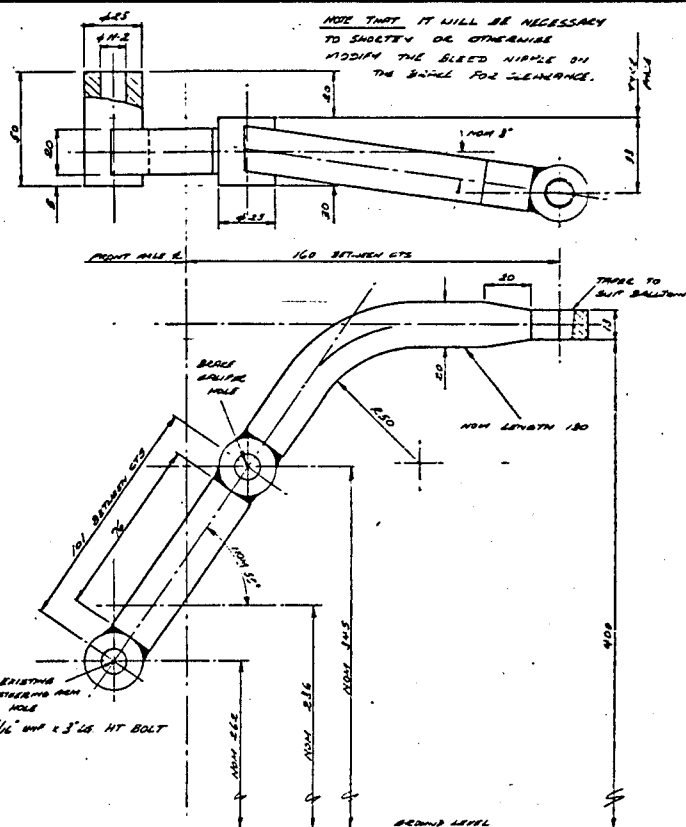
8 CALIPER BOLT  
REQD: 2 OFF  
MTRL: 1/2" DIA MHP  
HIGH TENSILE BOLT  
3" LONG  
(4 BOLTS REQD TOTAL)



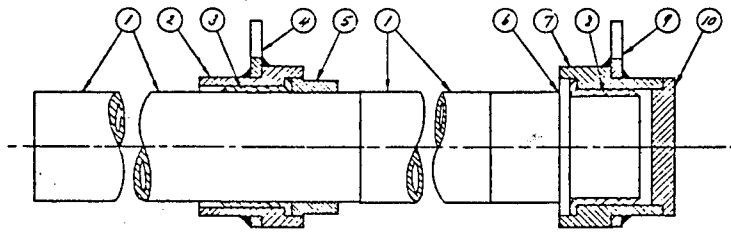
9 STEERING ARM BUSH  
REQD: 2 OFF  
MTRL: 425 BAC



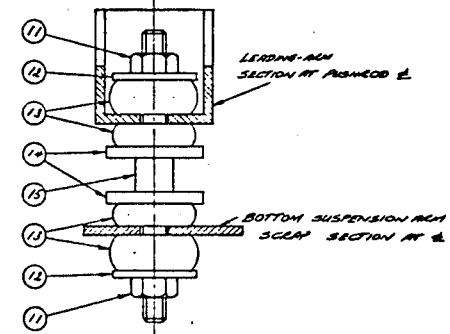
10 ELECTRIC TOW BAR  
STEERING AND SUSPENSION  
AND DETAILS  
DWN: 210/71 2IN - 4  
SCAL - 15 DWS - 7112



11 STEERING ARM  
REQD: 1 OFF AS SHOWN (ENS)  
1 OFF OPPOSITE ARM (ENS)  
MTRL: 20x20 MS BLC  
NOTE: FABRICATE ARM IN POSITION  
ON SUSPENSION UPRIGHT.

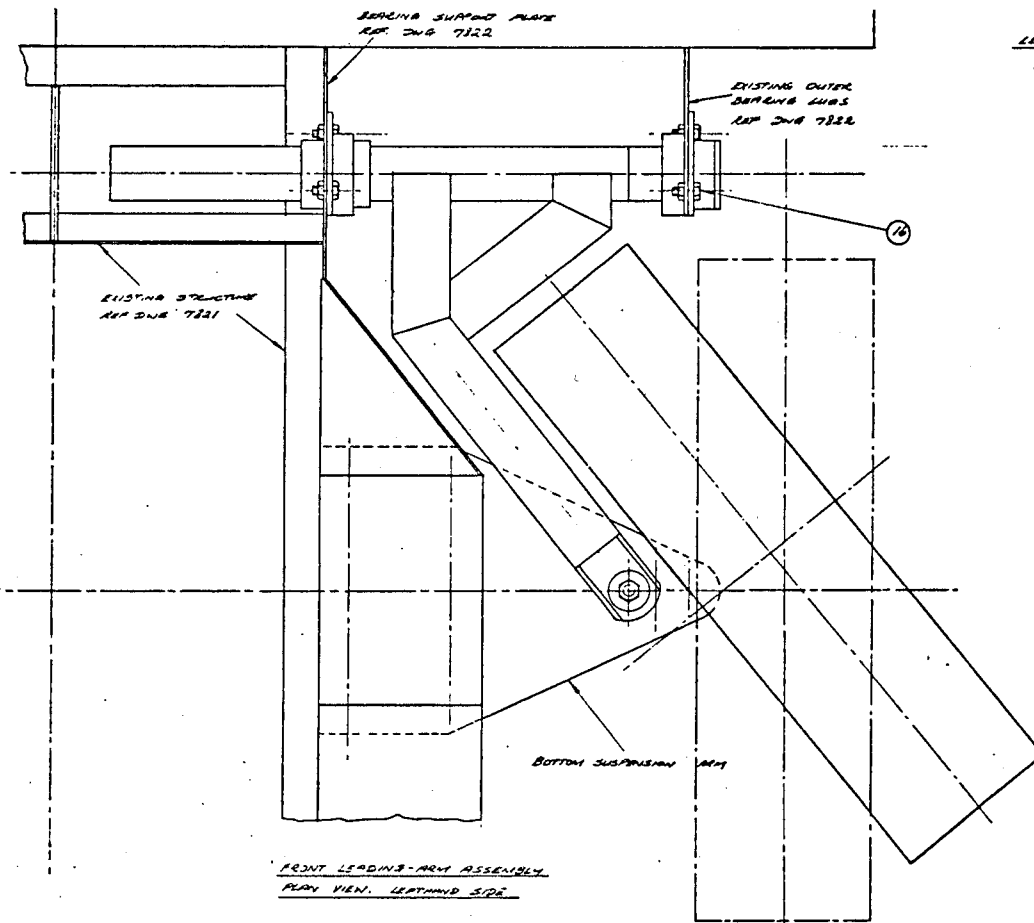


FRONT LEADING-ARM BEARING  
ASSEMBLY DETAIL

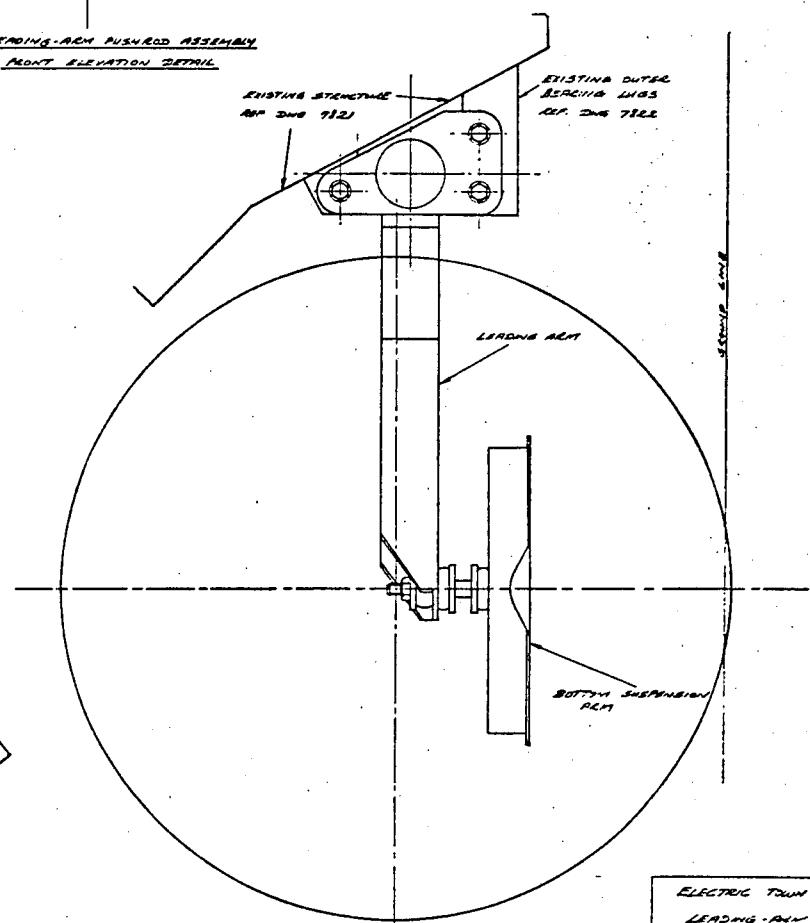


LEADING-ARM PUSHROD ASSEMBLY  
FRONT ELEVATION DETAIL

ITEM	DESCRIPTION	QTY	REF. FIG.
1	LEADING-ARM CROSS-TUBE	2	"101"
2	INNER BEARING HOUSING	2	"102"
3	INNER BEARING HOUSING	2	"103"
4	BEARING HOUSING HOUSING	2	"104"
5	INNER BEARING HOUSING	2	"105"
6	OUTER BEARING HOUSING	2	"106"
7	OUTER BEARING HOUSING	2	"107"
8	OUTER BEARING HOUSING	2	"108"
9	BEARING HOUSING PLATE	2	"109"
10	BEARING HOUSING PLATE	2	"110"
11	MR. HOUSING	2	"111"
12	MR. HOUSING	2	"112"
13	MR. HOUSING	2	"113"
14	MR. HOUSING	2	"114"
15	MR. HOUSING	2	"115"
16	MR. HOUSING	2	"116"

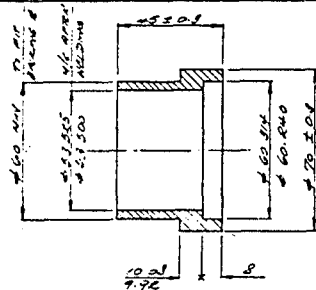


FRONT LEADING-ARM ASSEMBLY  
FRONT VIEW, LEFT HAND SIDE

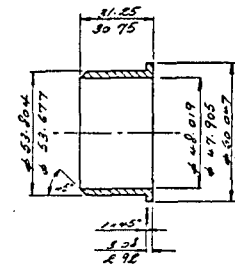


FRONT LEADING-ARM ASSEMBLY  
ELEVATION, RIGHT HAND SIDE

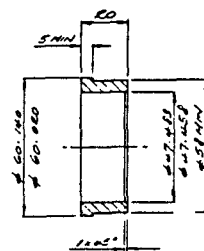
ELECTRIC TOWN CAR  
LEADING-ARM  
ASSEMBLY DETAILS  
DATE: 12/1/51  
SCALE: 1/2" = 1'-0"



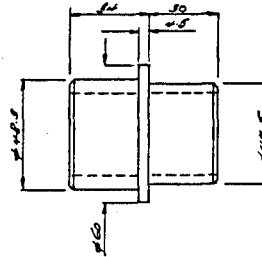
② INNER BEARING HOUSING  
REQD. 4 OFF  
MTRL. - 675 HS BLACK



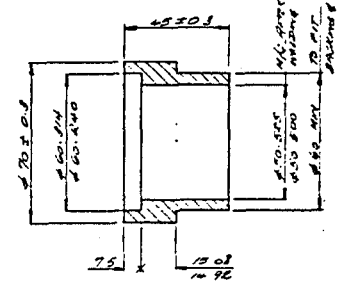
③ INNER BEARING BUSH  
REQD. 4 OFF  
MTRL. - 675 HS BLACK



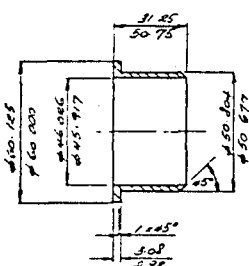
⑤ INNER BEARING SHOULDER  
REQD. 4 OFF  
MTRL. - 675 HS BLACK



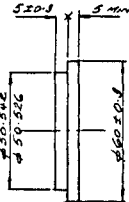
⑥ EXISTING IN HOUSING  
REQD. 4 OFF  
MTRL. - 675 HS BLACK



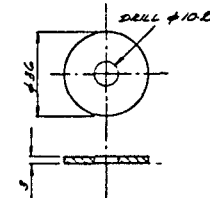
⑦ OUTER BEARING HOUSING  
REQD. 4 OFF  
MTRL. - 675 HS BLACK



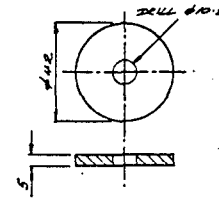
⑧ OUTER BEARING BUSH  
REQD. 4 OFF  
MTRL. - 675 HS BLACK



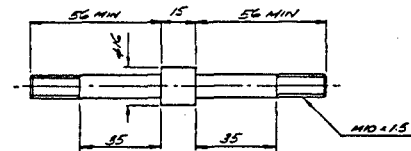
⑩ BEARING HOUSING CAP  
REQD. 4 OFF  
MTRL. - 675 HS BLACK



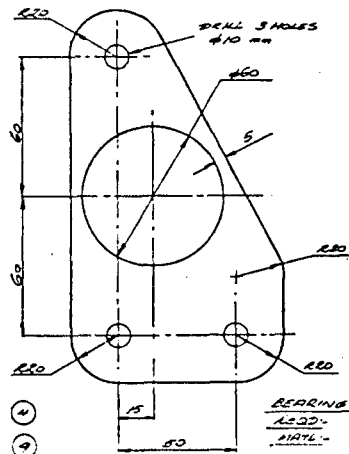
⑫ 1mm WASHER  
REQD. 4 OFF



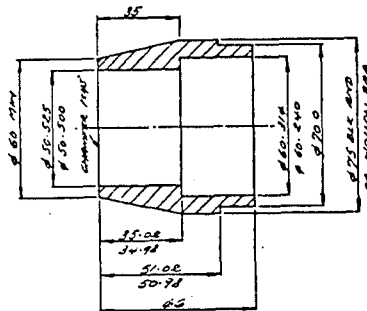
⑭ 5mm WASHER  
REQD. 4 OFF



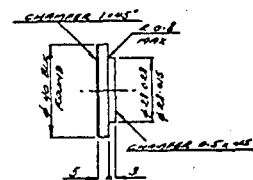
⑮ PUSHROD  
REQD. 2 OFF  
MTRL. - 675 HS BLACK



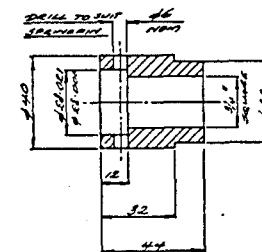
⑨ BEARING SUPPORT PLATE  
REQD. 4 OFF  
MTRL. - 675 HS BLACK



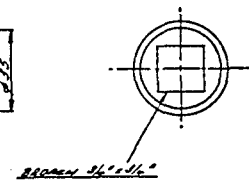
⑪ REQD. OUTER BEARING HOUSING  
REQD. 2 OFF  
MTRL. - 675 HS BLACK



⑪ HOUSING CAP  
REQD. 2 OFF  
MTRL. - 675 HS BLACK



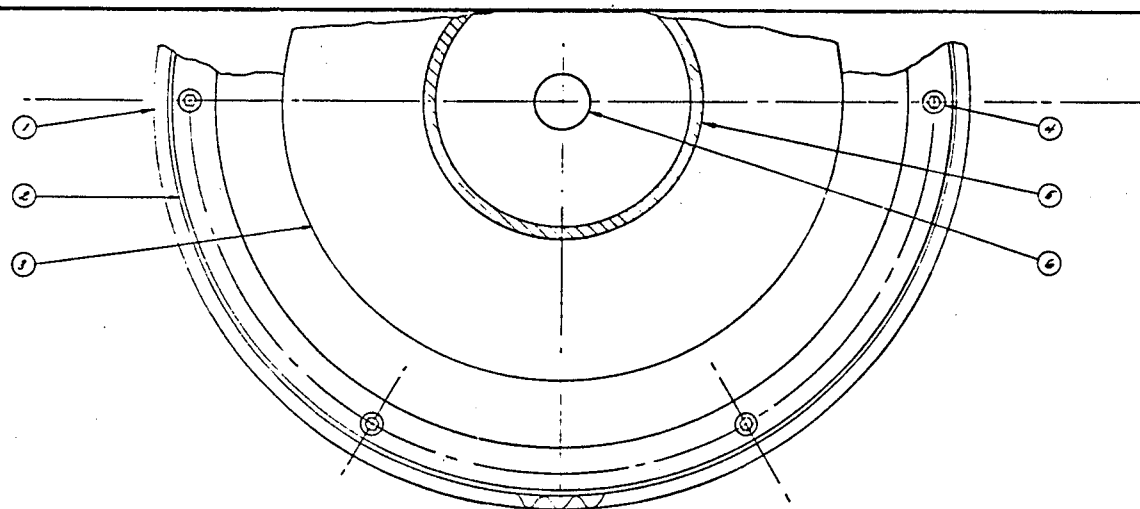
⑱ OUTER HOUSING FOR AUXILIARY TORSION BAR  
REQD. 2 OFF  
MTRL. - 675 HS BLACK



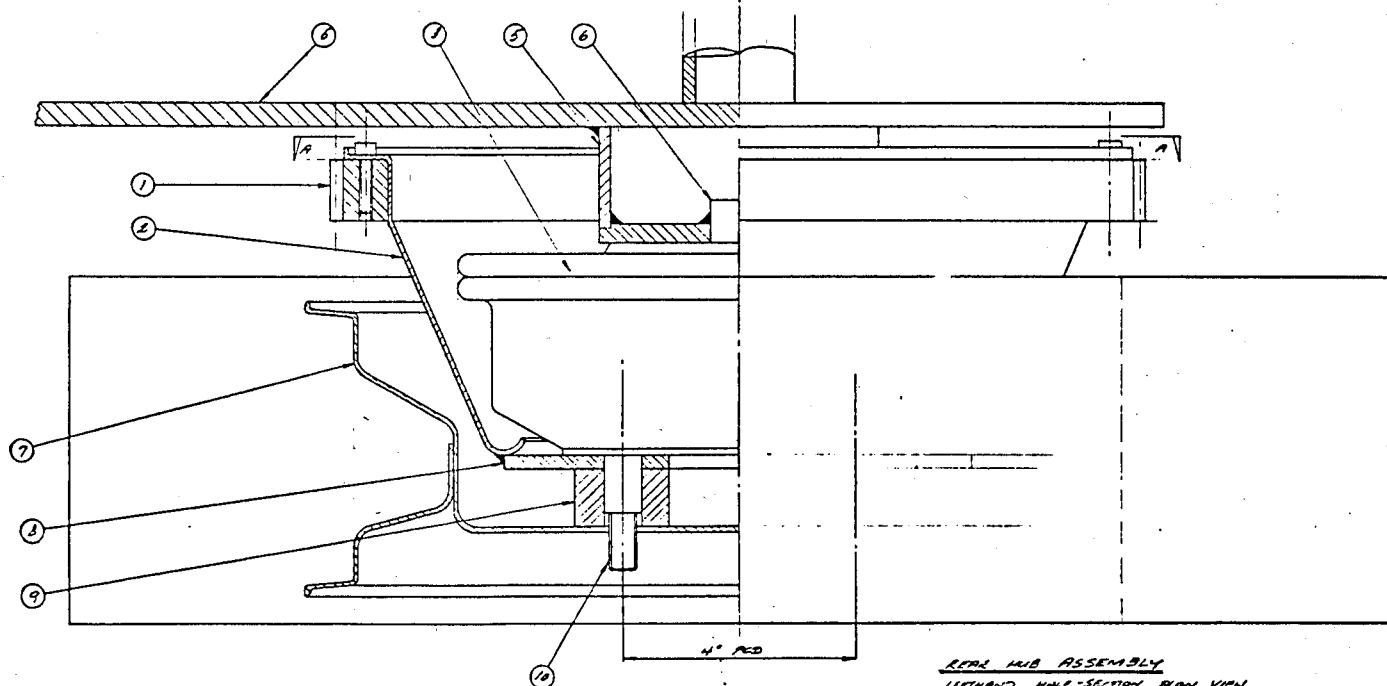
REV. 11-1-79  
ELECTRIC TOWN CAR  
COMPONENT DETAILS  
DATE: 11-1-79  
BY: P. S. K. 7901/11







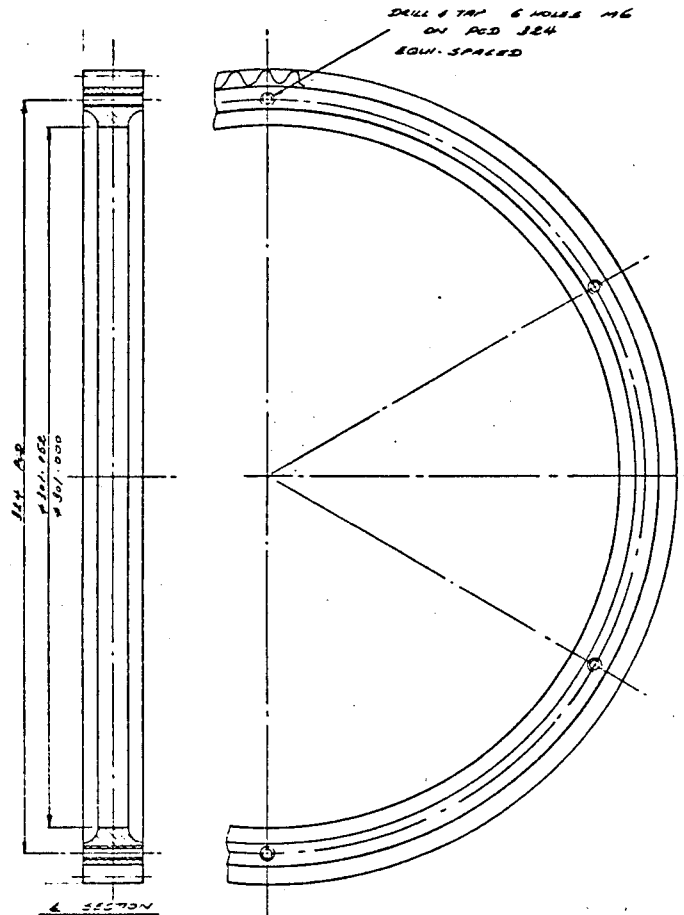
SECTION A-A



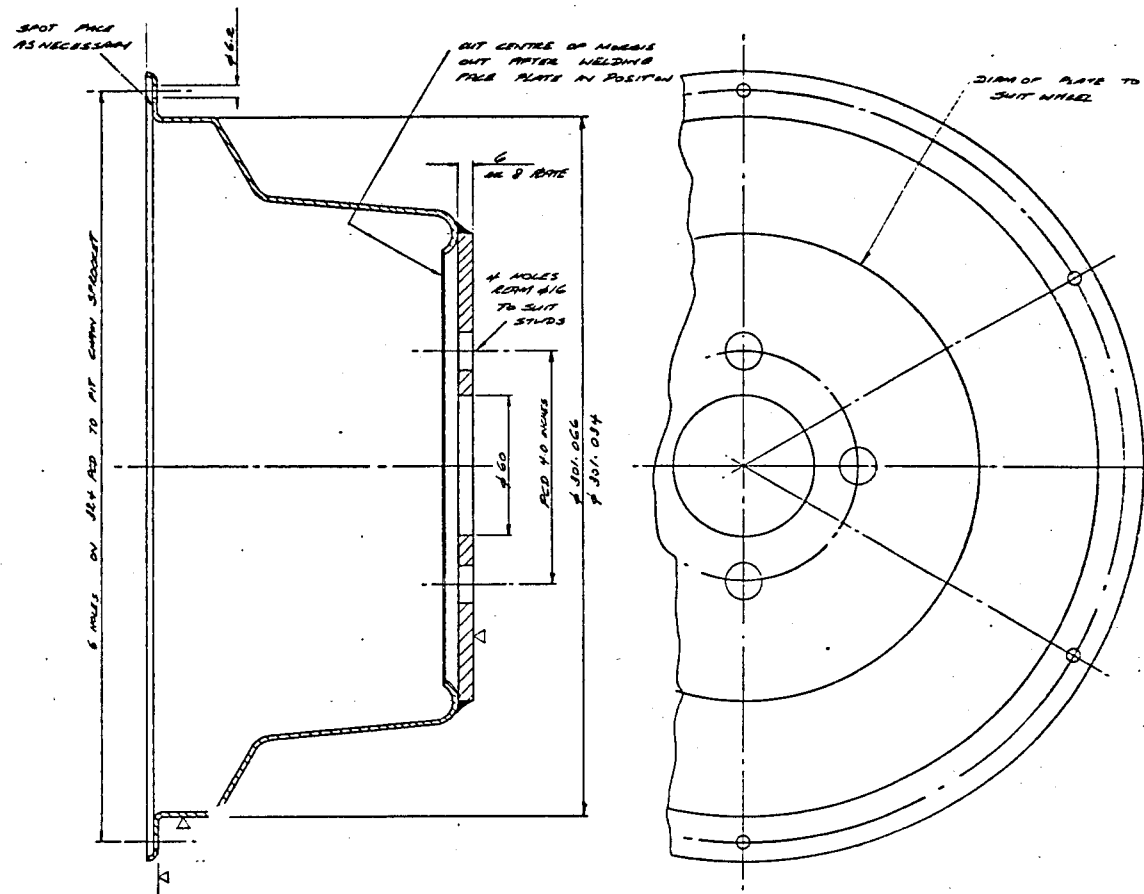
REAR HUB ASSEMBLY  
LEFT-HAND HALF-SECTION PLAN VIEW  
LATH BUILD NOT SHOWN

ITEM	DESCRIPTION	QTY
1	1. Outer flange	1
2	2. Hub flange	1
3	3. Hub flange (3/4\"/>	1
4	4. Hub flange (3/4\"/>	1
5	5. Hub flange (3/4\"/>	1
6	6. Hub flange (3/4\"/>	1
7	7. Hub flange (3/4\"/>	1
8	8. Hub flange (3/4\"/>	1
9	9. Hub flange (3/4\"/>	1
10	10. Hub flange (3/4\"/>	1

ELECTRIC TOWN CAR  
REAR HUB ASSY.  
DATE: 11/1/79  
BY: FS  
DWG NO: 205 7009



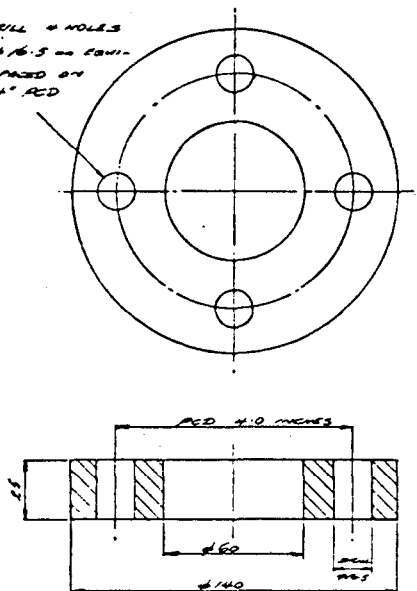
① 3-1/2-3 CHAIN SPROCKET  
 QQQ 2 OFF



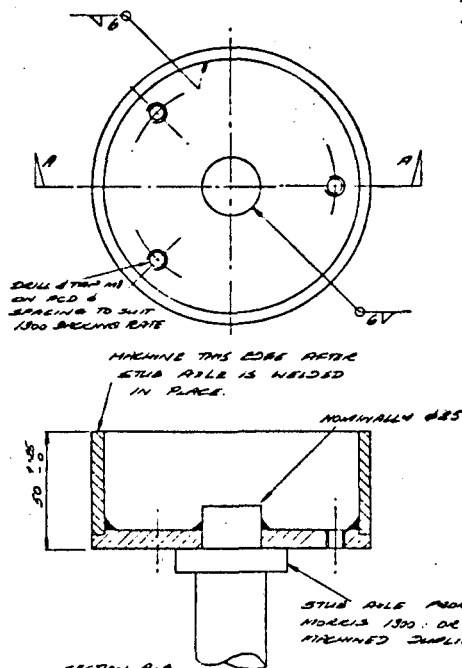
② ③ 100 WHEEL AND FACE PLATE DETAIL  
 QQQ 2 OFF  
 MATL: FACE PLATE IN 3 RATE

ELECTRIC TRAIN CAR  
 CHAIN WHEEL DETAILS  
 200-12114 200-12114  
 SCALE: FS 200-12114

DRILL 4 HOLES  
Ø 16.5 mm EQUI-  
SPACED ON  
4" PCD

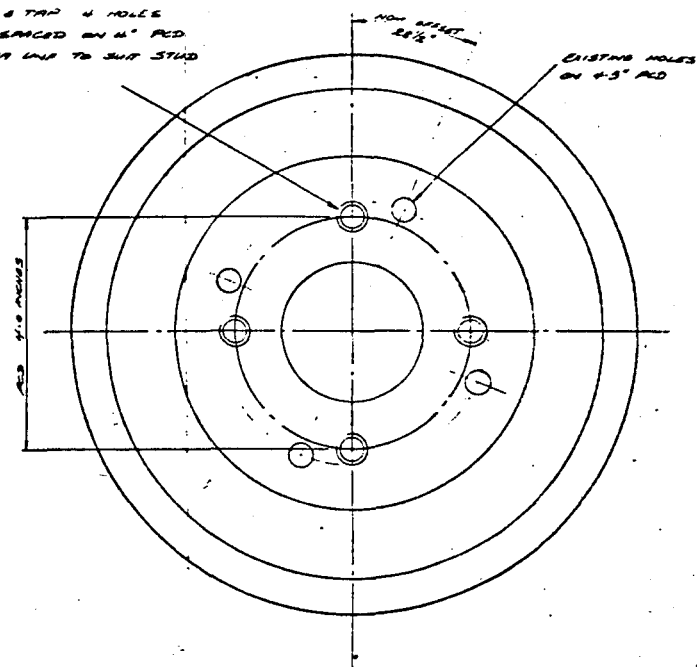


④ 25mm ALUMINUM SPACER  
REQD: 2 OFF  
MTRL: 25mm ALUMINUM PLATE

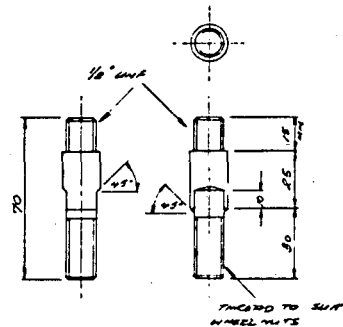


SECTION A-A  
⑤ CORE SUSPENSION FROM STUD HOLE EXTENSION  
REQD: 2 OFF  
MTRL: SEE COMPONENT DRAWING BELOW

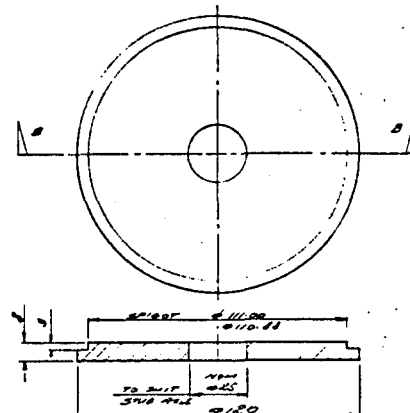
DRILL 8 TAP 4 HOLES  
EQU-SPACED ON 4" PCD  
1/2" DIA LINE TO SUIT STUD



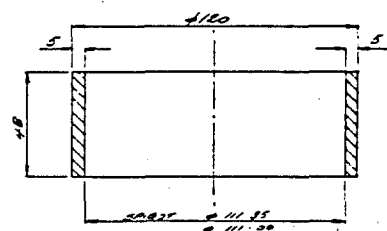
⑥ DRILLING DETAILS FOR MORRIS 1908  
REQD: 2 OFF  
MTRL: ROLLER SCALE MISC.



⑩ 1/8" STUDS  
REQD: 2 OFF  
MTRL: 1/8" ALUMINUM

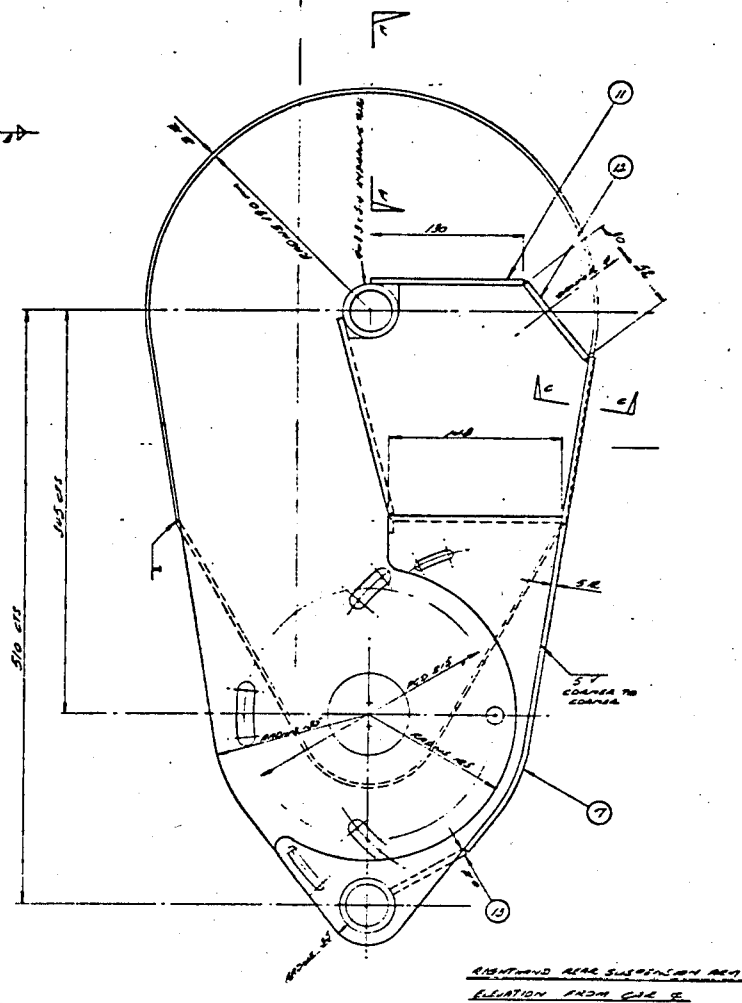


SECTION DD. STUD HOLE EXTENSION DETAIL  
REQD: 2 OFF  
MTRL: 2mm MS PLATE



SECTION DD. STUD HOLE EXTENSION DETAIL  
REQD: 2 OFF  
MTRL: ROLLER SCALE MISC.

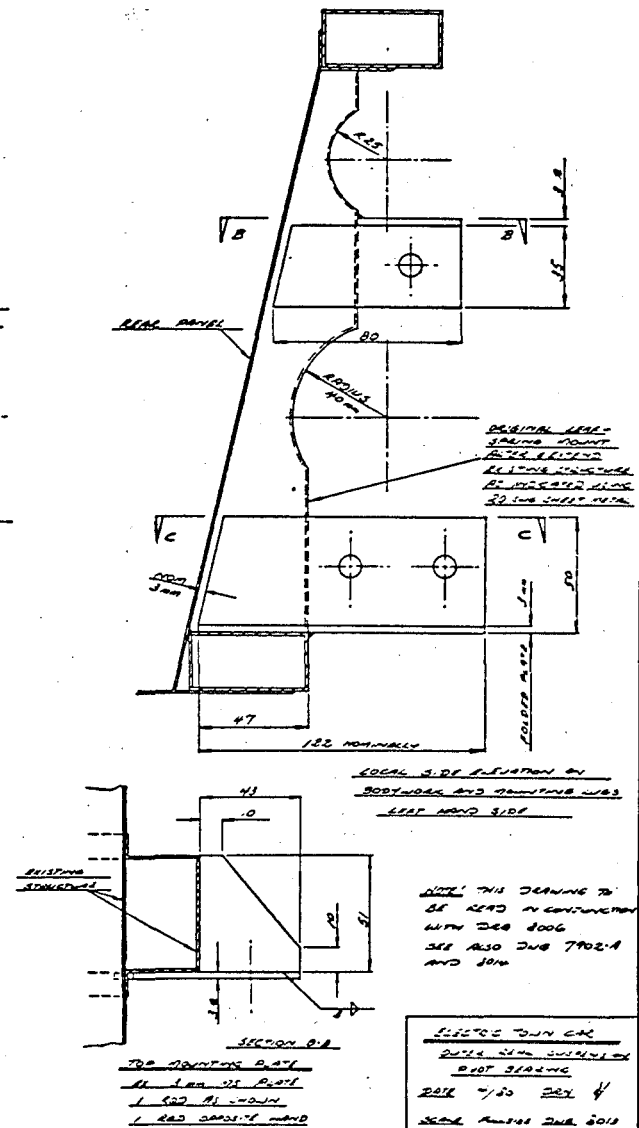
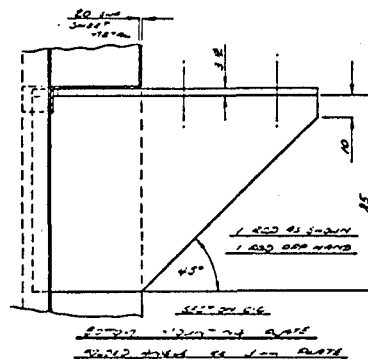
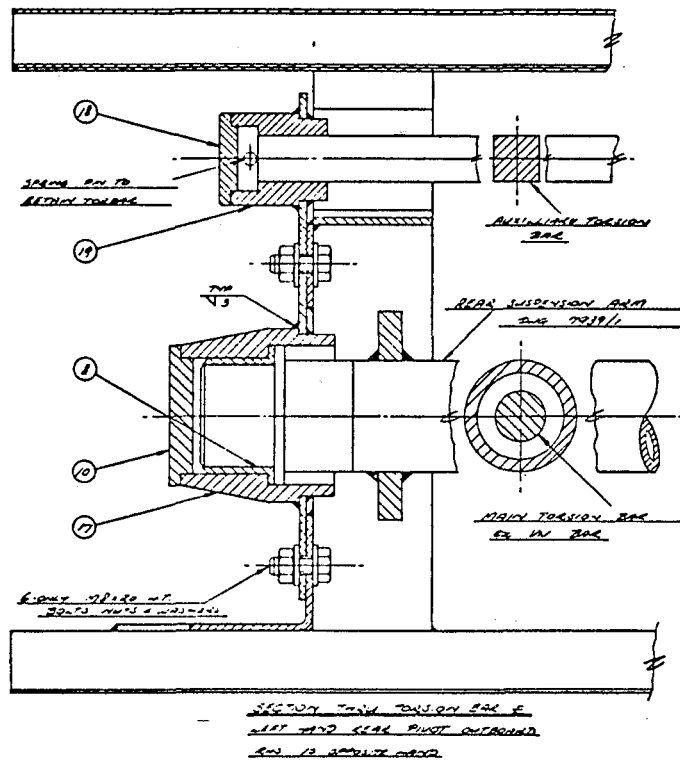
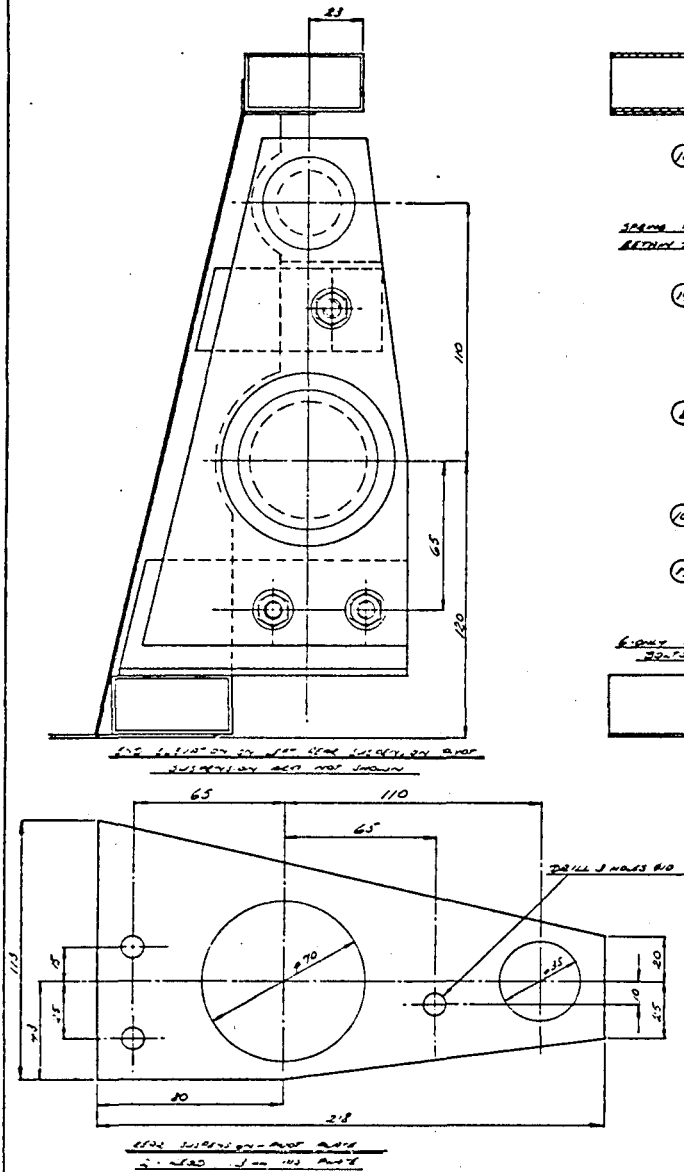
ELECTRIC TOWN GPC  
REQD: 2 OFF  
MTRL: ROLLER SCALE MISC.

208

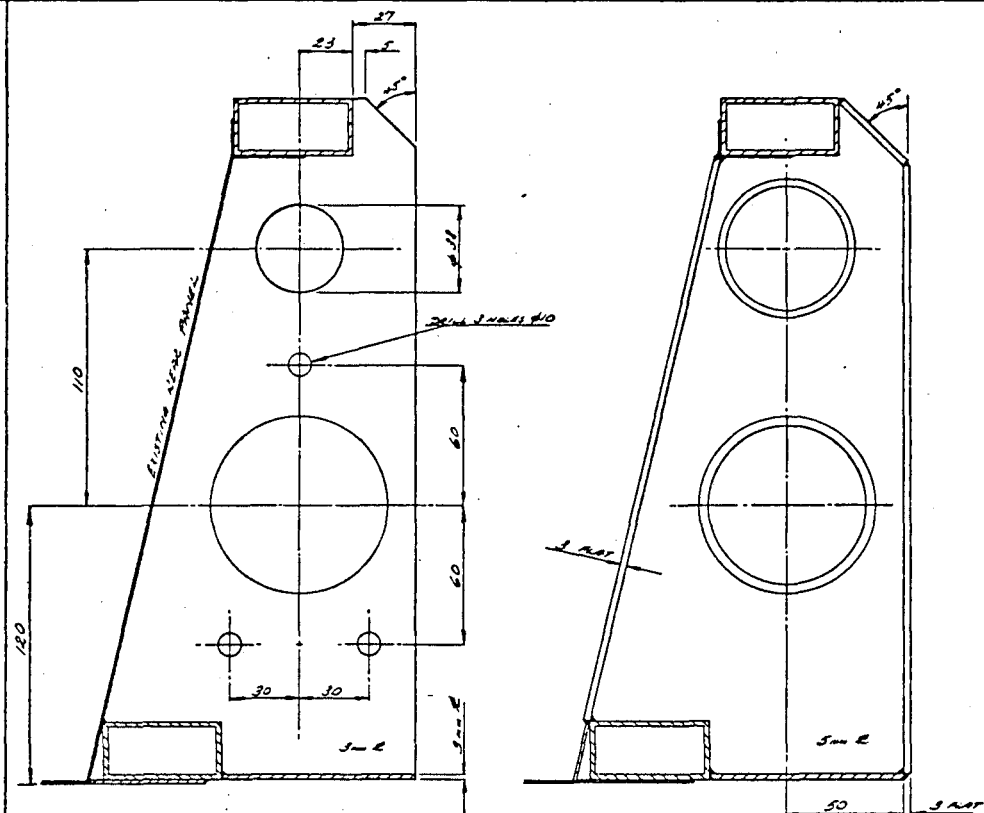




② DETAILS OF CIRCLED NUMBERS  
SEE DMS 7902-A

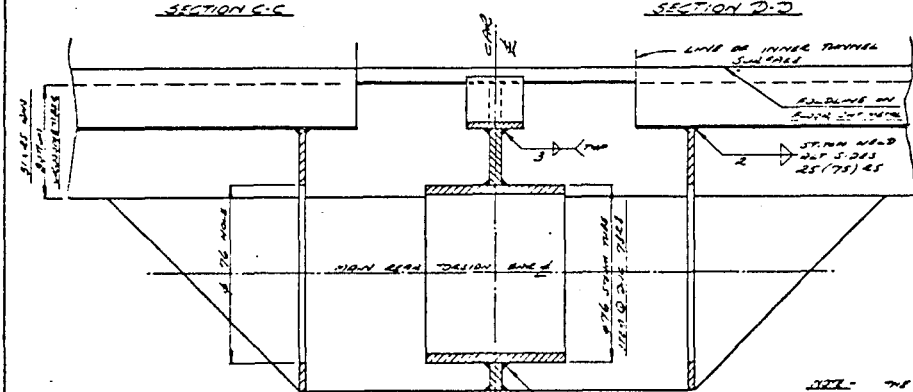






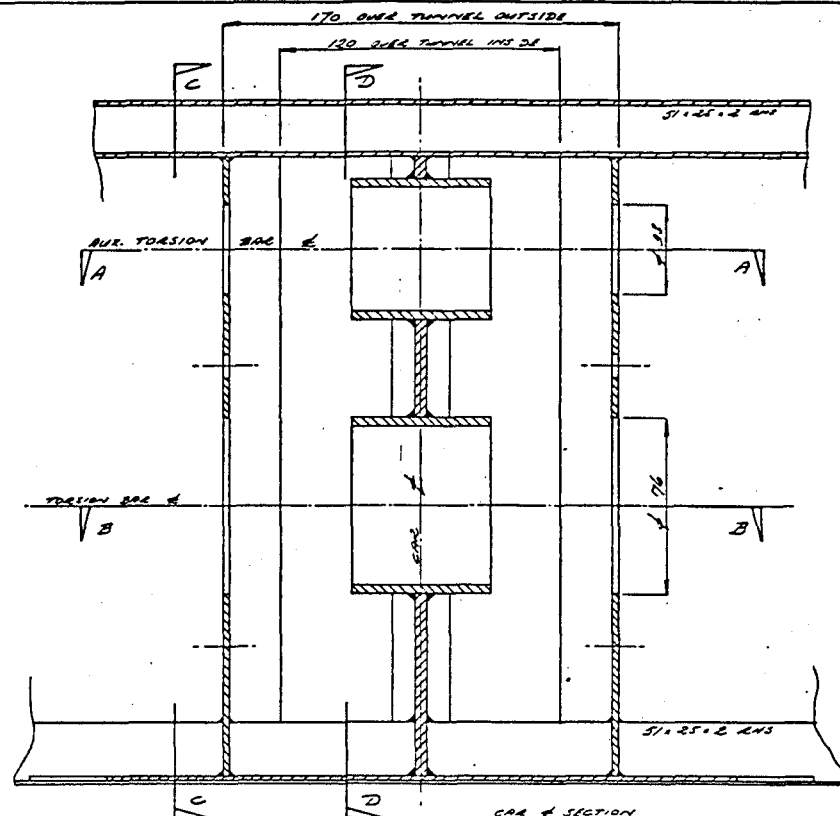
SECTION C-C

SECTION D-D

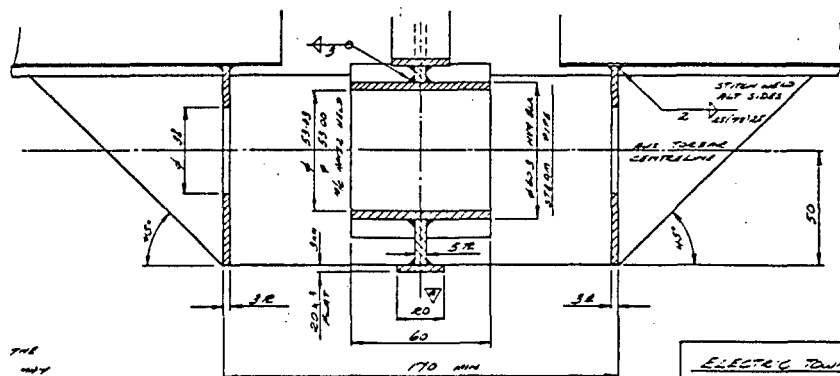


SECTION B-B

NOTE - THE RADIUS OF THE  
"5000" LINE PANEL MAY  
NOT BE CORRECT. DRAWING  
PANEL 1 DRAWN @ 15' TO 160'.

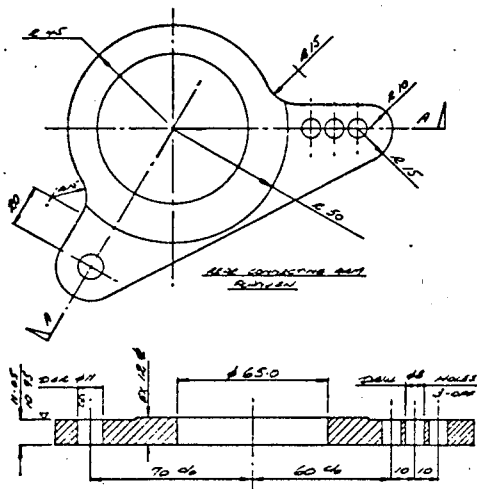


SECTION E-E  
REAR ELEVATION AT TORSION BAR 6

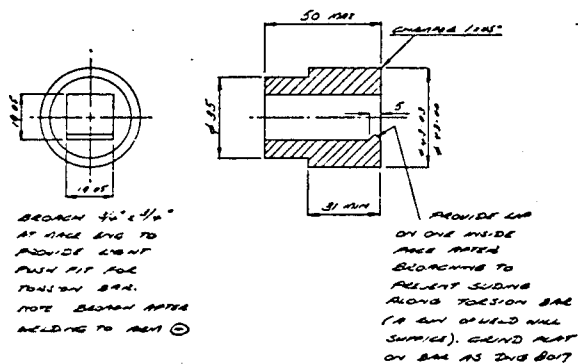


SECTION A-A

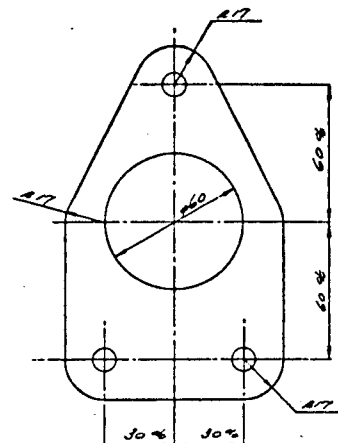
ELECTRIC TOWN GAS  
CENTRAL PART OF LINE  
SUSPENSION & TOWER  
200' H. 10' DIA.  
SCALE: 1/4" = 1' DIA. 80' H. 10' DIA.



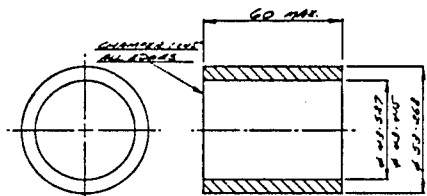
① BEARING CONNECTING ARM  
SECTION A-A  
LEAD:- 1.00 AS UNKNOWN  
1.00 OPPOSITE END  
MATE:- 12mm MS PLATE



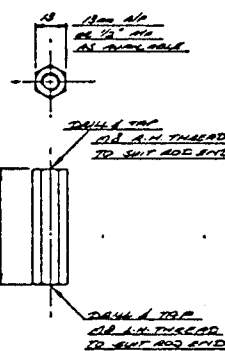
② AXIAL AND TENSION BAR SPINDLE  
LEAD:- 2.00  
MATE:- #50 ON BAR END



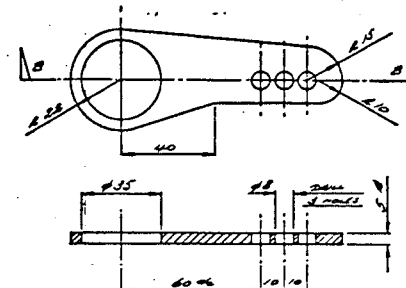
③ BEARING PLATE AND LINE SUSPENSION AND OTHER PLATE  
LEAD:- 2.00  
MATE:- 3mm MS PLATE



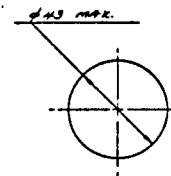
④ AXIAL TENSION BAR RUSH  
LEAD:- 1.00  
MATE:- ON ON PVD BEARING MATERIAL (CARBIDE PLATES)



⑤ CONNECTING TIE ROD  
LEAD:- 2.00  
MATE:- MILD STEEL



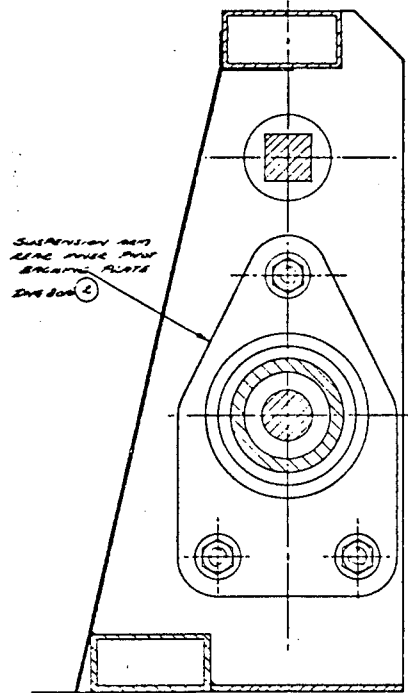
⑥ CONNECTING ARM TO HORIZONTAL LINE  
LEAD:- 2.00  
MATE:- 5mm MS PLATE



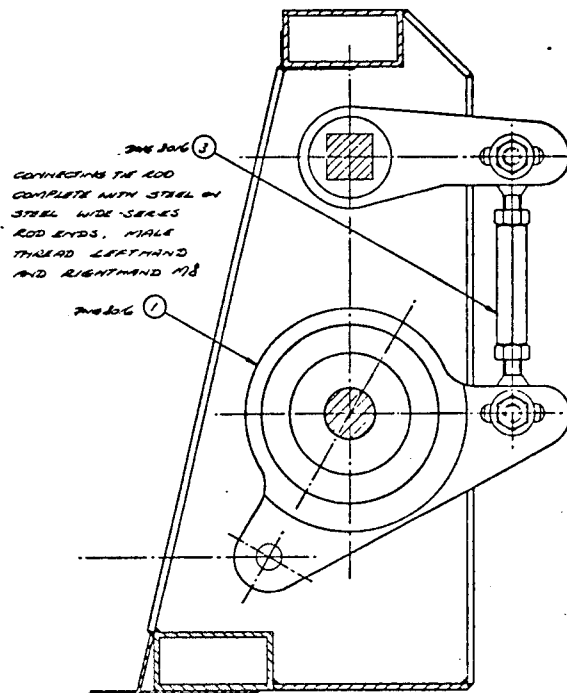
⑦ SEPARATING DISC  
LEAD:- 1.00  
MATE:- 3mm POLYETHYLENE

TO BE USED WITH 2017

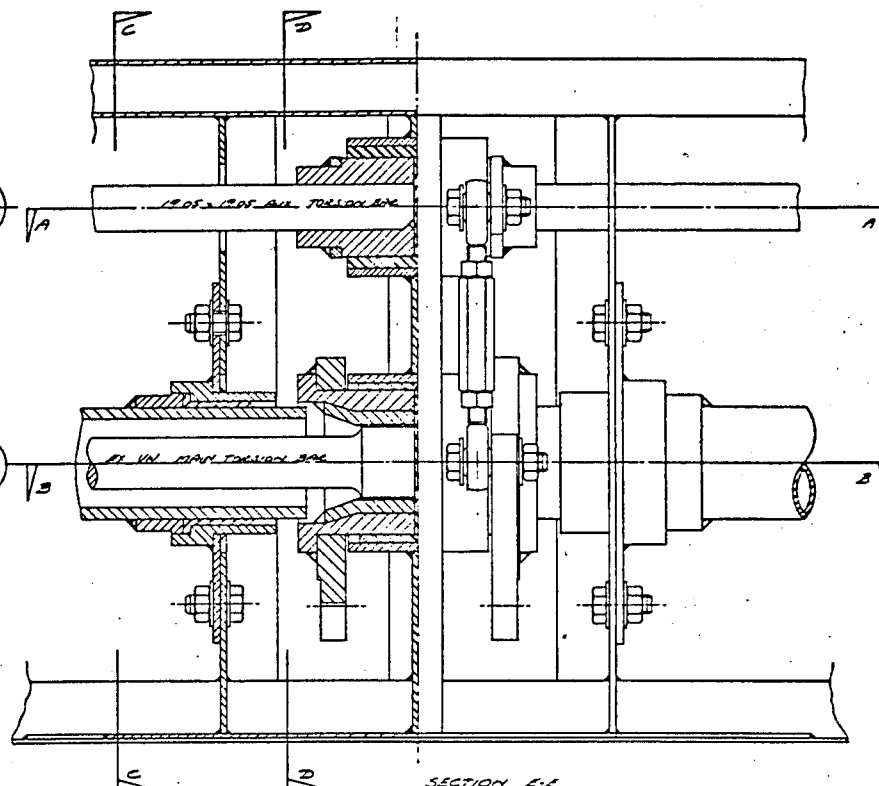
ELECTRIC TWIN CAR  
COMPONENTS AS PER  
POSITION AND PARTS  
SCALE: 1/20 DIA: 1/4  
SCALE: 1/2 DIA: 1/4



SECTION C-C

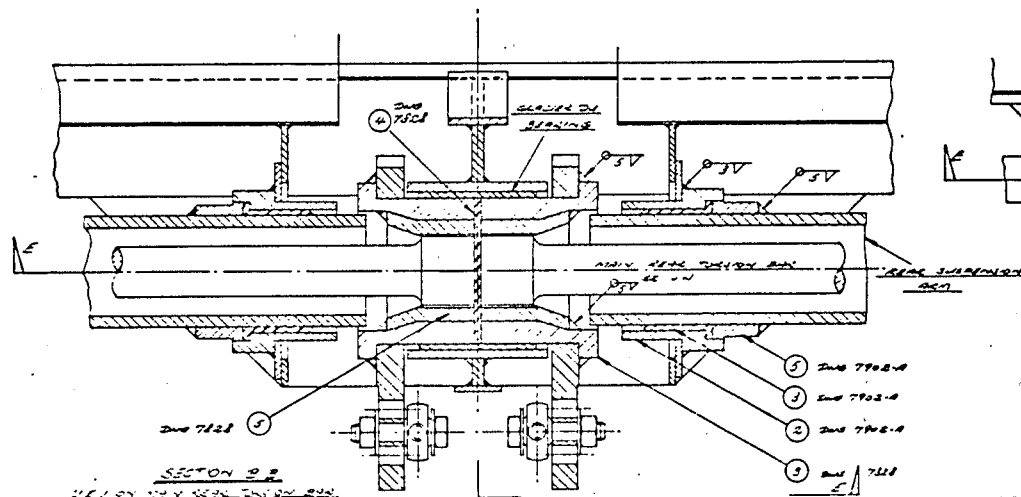


SECTION D-D

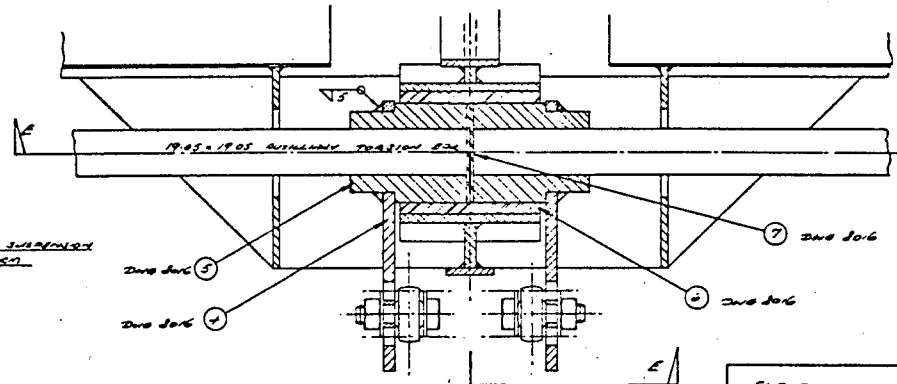


SECTION E-E

VIEW SHOWING MISCELLANEOUS TENSION BAR MOUNTING DETAILS



SECTION F-F



SECTION G-G

VIEW ON BALL JOINT TIES BY 226

ELECTRIC TOWN CAR  
CENTRE FRONT ASSEMBLY  
REAR SUSPENSION  
DATE: 4/16/44  
DRAWN BY: J.B. 226 4/17



